Harmonic Distortion at 400 kV due to Undergrounding of the 132/150 kV Grid

Kaleb Notevik Christensen, Mads Lundsgaard Jensen
& Mathilde Jul Sørensen

Energy Technology, EPSH4-1034, May 29, 2020

Master's thesis

STUDENT REPORT
AALBORG UNIVERSITY

The following programs have been used throughout the report: MATLAB®, DIgSILENT PowerFactory, Python™.

AALBORG UNIVERSITET
STUDENTERRAPPORT

Second year of Msc at the Technical Science Faculty
Energy Technology
Pontoppidanstræde 111
9220 Aalborg Ø
http://www.tnb.aau.dk

Title

Harmonic Distortion at 400 kV due to Undergrounding of the 132/150 kV Grid

Theme

Master's Thesis

Project Period:

04/02/20 - 29/05/20

Project Group:

EPSH4-1034

Participants:

Kaleb Notevik Christensen
Mads Lundsgaard Jensen
Mathilde Jul Sørensen

Supervisor:

Filipe Miguel Faria da Silva

Pages: 144 pages
Appendix: 28 pages
Electronic Files: 4
Submission date: 29-05-2020

Aalborg University, May 2020

Abstract

In the Danish transmission system, the impact on the harmonic distortion on 150 and 400 kV from the upcoming undergrounding of 324 km lines at the 150 kV is unknown. The analyses made in this report are based on the PowerFactory model: *Power System Model for Resonance Studies* which is based on a grid made by Oscar Lennerhag. The model contains the voltage levels 130 and 400 kV. Therefore, this report contains a study of the changes in harmonic propagation, when 130 kV OHLs are replaced by UGCs in both a radial and meshed system in PowerFactory. A literature study regarding the state of the art of propagation of harmonics is described and used as a basis for studies conducted in this report.

Analyses are made in a radial system in order to obtain knowledge about the harmonic propagation in a simple system, when line types are changed. In the radial system analyses, the system is analysed with and without a transformer. The analysis with a transformer is done to analyse the impact of having different voltage levels in a system when analysing the harmonic propagation. From this analysis it is found that when a power system consists of multiple voltage levels, the impedance is transformed from one side to the other due to the per unit conversion factor. Hence, observed from the HV-side, the impedance of the LV-side is multiplied by the conversion factor. Oppositely, observed from the LV-side, the impedance of the HV-side is divided by the conversion factor. Additionally, it is shown that the propagation of harmonic voltage can be obtained from the off-diagonal impedance between two busses from the frequency scan. The harmonic voltage propagation from one voltage level to an other can either be amplified or attenuated depending on the system characteristic and harmonic order.

In the meshed system, analyses are performed where the line types are changed. Here it is found that line type changes made in a system primarily affect the harmonic impedance at the voltage level where the changes are made. Additionally, line type changes made at higher voltage levels has a larger effect on the lower voltage level impedance than opposite. These findings are explained based on the transformer impedance and the conversion factor and is supported by additional case studies. Furthermore, the harmonic propagation between voltage levels is analysed utilising the off-diagonal impedance, when line types are changed on the 130 kV level. Here it is shown that when changing the line types, the changes in harmonic distortions mainly appears at the 130 kV level. Lastly, an exploratory study of mitigation of harmonic distortions are analysed. From the specific case analysed, it was found that the optimal filter location was not always at the location of the harmonic injection, but at the bus with the largest impedance characteristic at the harmonic order to be decreased.

Kaleb N. Christensen

Kaleb Notevik Christensen

Mads L. Jensen

Mads Lundsgaard Jensen

Mathilde Jul Sørensen

Summary

This master's thesis is made to answer the following problem statement.

How does the undergrounding of 132/150 kV lines impact the harmonic propagation at the 132/150 and 400 kV levels?

Until now, undergrounding lines at the 132/150 kV level in the Danish transmission system has not shown any harmonic distortions above the limits. However, with the upcoming undergrounding of 324 km lines at 150 kV in Denmark, the impact on the harmonic distortion and propagation at 150 and 400 kV is unknown. A literature study regarding the state of the art of propagation of harmonics was described, and used as a basis for studies conducted in this report. The analyses in this study was conducted utilising the power system simulation tool PowerFactory. Analyses was performed in both a radial and a meshed system.

Radial System Analyses

First, harmonic propagation studies were analysed in a radial system with three busses at a voltage level of 400 kV. It was analysed and shown, that the more UGCs installed, the more the resonances were shifted towards lower frequencies. Hereafter, it was shown that using the off-diagonal impedance from the frequency scan, the harmonic voltages in the busses, different from where the harmonic current was injected, could be obtained without performing a harmonic penetration study. Moreover, it was shown that the harmonic voltages, currents and phase angles could be visualised utilising a circle, since the propagation followed the norm of a sine wave. Additionally, the influence of the location, number of harmonic current sources and angle of injection was analysed in the radial system. Here it was analysed when multiple harmonic current sources were implemented with the same angle of injection. From this it was found that the voltage distortion was increased at low harmonic orders and decreased at high harmonic orders. If the angle of injection was different for the two sources, this characteristic changed according to the different angles.

Next, a transformer was implemented in the radial system. By introducing a 410/410 kV transformer the resonances was shifted to lower frequencies compared to the system without a transformer, due to the additional inductive element. From the introduction of the 410/410 kV transformer two circles were necessary in order to describe the harmonic propagation in the system utilising the circle theory, as the transformer introduced a voltage difference across it. From the circles it was observed that the voltage difference could either be an increase or decrease. This could be explained from the phase difference between the voltage and current and the current magnitude. Whether the voltage difference across the transformer was a decrease or increase could also be obtained from the frequency

scan. This was done utilising the relation between the off-diagonal impedance from the bus of injection to the two busses where the transformer was connected.

Furthermore, by introducing a 410/145 kV transformer the first parallel resonance was shifted to a higher frequency compared to the system without a transformer. It was found that when observing the impedance of another voltage level through the transformer, the impedance was changed by the per unit conversion factor. When a power system consists of multiple voltage levels, the impedance is transformed from one side to the other utilising the per unit conversion factor. In the 410/145 kV system, the conversion factor was $\frac{(410kV)^2}{(145kV)^2} \approx 8$. Hence, observed from the HV-side, the impedance of the LV-side was multiplied by the conversion factor. Oppositely, observed from the LV-side, the impedance of the HV-side was divided by the conversion factor. Analysing the harmonic propagation in the 410/145 kV radial system, the circles had to be represented utilising two ellipses. The ellipses followed the same principles as the circles. An analysis was performed on the 410/145 kV system when the line types were changed. The off-diagonal impedance relation were utilised to obtain knowledge about when the voltage across the transformer would increase or decrease in these analyses. It was found that the harmonic impedance relation across the transformer was only determined by what was on the opposite side of the transformer from where the harmonic current was injected.

Meshed System Analyses

The analyses performed in the radial system was also performed in a meshed system with the voltage levels: 400 kV and 130 kV. The meshed system analysed was based on the *Power System Model for Resonance Studies* from PowerFactory, originally made by Oscar Lennerhag. In the system an impedance analysis was made, investigating the influence of replacing OHLs with UGCs and opposite on both voltage levels. From the impedance analysis of the meshed system the main findings were:

- Changes made to the system primarily affect the harmonic impedance at the voltage level where the changes are made
- Changes made at higher voltage levels has a larger effect on the lower voltage level impedance than opposite

These findings was explained by the transformer impedance and the conversion factor. When changing at the 400 kV level, the impedance at the LV-side is multiplied by the conversion factor, hence this impedance is large. The large impedance of the LV-side seen from the HV-side and the transformer impedance, results in the path of least impedance being primarily on the 400 kV level. When changes are made to the 130 kV level, the HV-side impedance is divided by the conversion factor, however, the path of least impedance is primarily at the 130 kV level due to the transformer impedance. This was supported by three case studies: Changing the turns ratio of the transformer, removing the transformer impedance and increasing the line lengths on the LV-side to have the same total line length as the HV-side.

Hereafter, the propagation of harmonic voltages between voltage levels was analysed. Here it was shown that the propagation through the transformer was mainly affected by what was changed on the opposite side of the transformer from where the harmonic current was injected, as in the radial system. Furthermore, the harmonic voltages were analysed when changing the line types at the 130 kV system, when injecting at either the LV- or HV-side. From this analysis it was found that the differences in harmonic voltages were mainly observed at the 130 kV, when the 130 kV system was changed. This was the case both when the harmonic current injections were at the LV- or HV-side. However, larger harmonic voltage differences were observed at the 130 kV busses, when the injection were at the LV-side, compared to harmonic voltage differences observed at the 400 kV busses, when the injection were at the HV-side. This was explained from the fact that the injections were closer to where the line type changes were made.

Lastly, an exploratory study of mitigation of harmonic voltages was made in the meshed system. In the reference case it was observed, that no mitigation was required on the HV-side. Therefore, the meshed system was changed to only contain OHLs on the 400 kV level. One OHL at the 400 kV level was replaced by an UGC in order to analyse where the filter should be placed if one change was made in the system, which increased the harmonic voltages. The system was analysed, to investigate the optimal filter location, depending on where the harmonic current was injected. From the analyses made, no clear tendency was observed, regarding the optimal filter location from different locations of harmonic current injection. However, it was observed that the optimal filter location was not always in the bus of injection, which is the normal procedure. In several cases, the optimal filter location, was in the bus with the largest impedance characteristic before a filter was installed for the harmonic order of injection. Additionally, it was observed that if injections was on the LV-side, the filter location was most optimal when placed on the LV-side. When the injections was on the HV-side, the optimal filter location could be at both the LV- or the HV-side dependent on where the harmonic current was injected on the HV-side. The filter analysis was not the main scope of this report, hence the observations were not analysed in detail.

Based on the findings, the impact on the harmonic propagation in the 400 kV system will be insignificantly affected when undergrounding lines in the 132/150 kV system. Additionally, the change in the harmonic propagation from the 132/150 kV to the 400 kV system will change slightly from the undergrounding. The harmonic propagation in the 132/150 kV system itself will be significantly impacted when undergrounding the lines in the 132/150 kV system.

Preface

This master's thesis was written by the group EPSH4-1034, at the 4^{th} semester of a Master of Science program with specialisation in Electrical Power Systems and High Voltage Engineering at Aalborg University, Denmark. This report was developed from the 4^{th} of February 2020 to the 29^{th} of May 2020, during the corona pandemic. This report was made under the supervision of Filipe Miguel Faria da Silva. The authors would like to offer their gratitude to Troels Jakobsen from Energinet for the cooperation and help during this master's thesis.

Reading Guide

This report is build up chronologically, meaning that the chapters, sections and subsections appears as numbered. The chapters, sections and subsections are listed as they appear in the report in the table of content.

The citations in this report are displayed as numbers in square brackets for example [1]. The citations are numbered based on the appearance in the report. In the bibliography the citations are listed in numeric order with details regarding the individual citations.

The figures, equations and tables presented in the report are numbered numeric according to appearance in the chapter in where they appear. For example, the third figure in chapter 2 will be referred to as Figure 2.3. Below each figure and above each table a caption will be present describing the content of the element.

The indexes utilised in the report are listed in a nomenclature. For every index the nomenclature includes a small description and the corresponding SI-unit. The abbreviations utilised in the report are listed below the nomenclature.

In the beginning of each chapter, a introduction describing the content of the chapter will be present. At the end of each chapter, a summary and discussion of the results presented in the chapter will be present.

DIgSILENT PowerFactory has been used for the power system simulations performed in this project. Moreover, as several case studies are conducted, a Python™ script has been developed to simulate and collect data. Additionally, MATLAB® has been used for data processing. The models in DIgSILENT PowerFactory and the Python™ script have been attached as electronic files.

Nomenclature List

Special Symbols and Denotations

Symbol	Description	SI-Unit
B	Susceptance	S
C	Capacitance	F
$\mathcal{C}$	Capacitance	F/m
f	Frequency	Hz
$\mathcal{G}$	Conductance	S/m
I	Current	A
l	Length	m
L	Inductance	H
$\mathcal{L}$	Inductance	H/m
N	Number of turns	-
n_{res}	Tuning order	-
P	Active power	W
a	Per unit conversion factor	-
Q	Reactive power	VAr
QF	Quality factor	-
R	Resistance	Ω
$\mathcal{R}$	Resistance	Ω/m
t	Time	s
TDD	Total demand distortion	%
THD	Total harmonic distortion	%
V	Voltage	V
v	Velocity	m/s
X	Reactance	Ω
Y	Admittance	S
Z	Impedance	Ω
γ	Propagation constant	s^{-1}
λ	Wavelength	m
ω	Angular frequency	rad/s
ϕ_i	Current angle	rad
ϕ_v	Voltage angle	rad
ϕ_{vi}	Phase angle between voltage and current	rad
ϕ_z	Impedance angle	rad

Acronyms

Acronym	Abbreviation of:
AC	Alternating current
DC	Direct current
G	Grid
HV	High voltage
L	Load
LCC	Line commutated converter
LV	Low voltage
OHL	Overhead line
RES	Renewable energy sources
RMS	Root mean square
TSO	Transmission system operator
UGC	Underground cable

Contents

1 Introduction

In an effort to reduce greenhouse gas emission, the power generation is changing to renewable energy sources (RES). With the implementation of RES, additional power electronic converters are added to the power systems. One disadvantage of power electronic converters is that they are sources of harmonic distortions. As an example, power electronic converters at transmission level are utilised at high voltage DC (HVDC) connections. The amount of HVDC connections are increasing in order to ensure the security of supply with the fluctuating nature of RES. Moreover, an increased amount of high voltage AC (HVAC) cables are installed. With the implementation of HVAC cables, the resonance frequencies of the power system are shifted to lower frequencies. This happens because of the higher capacitance compared to overhead lines (OHLs). As a result, low-order harmonic distortion are susceptible to be amplified. [1]

Harmonic distortions are usually an undesired side effect of an equipment's main function. Harmonic distortion occur as a multiple or sub-multiple of the nominal system frequency. When harmonic distortions are present in a power system the power quality is impacted. The larger the harmonic distortion in a system, the worse the power quality. Hence, limits are defined and applied to obtain an acceptable power quality at each voltage level in a power system. [1]

1.1 The Danish Transmission System

The transmission system in Denmark consists primarily of 400 kV and 132/150 kV voltage levels. The Danish power system consists of two asynchronous networks referred to as DK1 and DK2. The 132 kV level is utilised on Zealand (DK2) and the 150 kV level is utilised in Jutland and Funen (DK1). The Danish system is composed of both underground cables (UGCs) and OHLs. The transmission system operator (TSO) in Denmark is Energinet. Energinet is responsible for the coordination of the overall power quality in the transmission system in Denmark. To coordinate an acceptable power quality, Energinet has adopted limits from IEC 61000-3-6. These limits applies to the harmonic distortion from new connections and the amplification of existing harmonics in the transmission system. [2]

In November 2008 the Danish government decided that new 132/150 kV connections should be installed as UGCs. Furthermore, the existing 132/150 kV OHLs should be replaced by UGCs over a time period of approximately 30 years. This was done as a beautification of the Danish landscape. The decision regarding the existing 400 kV OHLs was, that they should be kept as OHLs with the possibility of beautification projects such as new types of transmissions towers and underground cabling of specific sections. These guidelines are referred to as the *Kabelhandlingsplan*. [3]

Later the *Kabelhandlingsplan* was revised and the present guidelines for the 132/150 kV system are as presented in [4] from 2016. The guidelines for new 132/150 kV connections are unchanged, and should therefore still be installed as UGCs. The revised guidelines states that the existing 132/150 kV OHLs should remain as OHLs. However, at specific sections through nature and urban areas, the 132/150 kV OHLs should be replaced by UGCs. Regarding new 400 kV connections, they should be installed as OHLs with the possibility of installing specific sections as UGCs. Moreover, as a compensation for new 400 kV OHLs, nearby existing 132/150 kV OHLs can be replaced by UGCs. [4]

Such a beautification project was done in Vejle-Ådal as a result of the decision made in 2008. Here two 8 km 400 kV OHLs were replaced by UGCs [5]. The Vejle-Ådal cable section is encircled in Figure 1.1 with green. When the 400 kV line with the two new cable sections was energised in July 2017, an amplification of the existing harmonic distortion were observed at the 400 kV substations in Trige and Fraugde, encircled with blue in Figure 1.1. Geographically the distances from Vejle-Ådal to Trige and Fraugde are approximately 90 and 80 km, respectively. Hence, the replacement of 8 km 400 kV OHLs with UGCs impacted the power quality in remote locations. This phenomenon was not predicted in the simulation studies performed by Energinet. The experiences from the Vejle-Ådal UGCs proves that extensive harmonics studies are needed in the planning of cabling 400 kV lines. [2]

A new 170 km 400 kV connection from the German border to Endrup and from Endrup to Idomlund has been approved by the Danish government. The connection is marked with orange in Figure 1.1. The amount of UGCs in the new line is limited by the allowable harmonic distortion in the power system. A study made by Energinet showed that 15 % of the new 400 kV connection can be implemented as UGCs, while the rest of the line has to be implemented as OHLs. To compensate for the new 400 kV OHLs, 324 km of the existing 150 kV OHLs near the new 400 kV OHLs will be replaced by UGCs. [6]

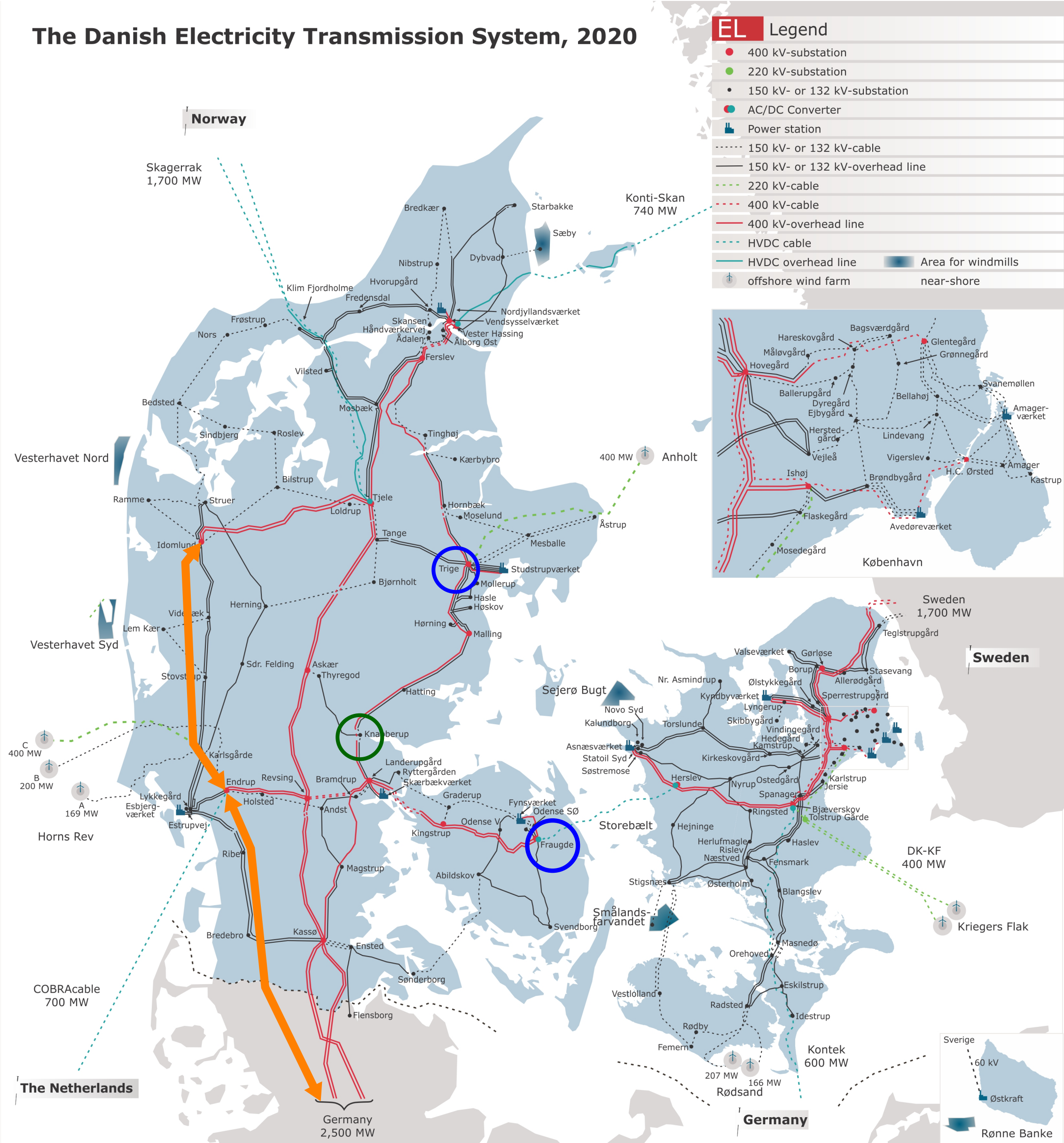

Figure 1.1: Schematic of the Danish transmission system. The 400 kV cable section in Vejle-Ådal is encircled by the green circle. Trige and Fraugde substations are encircled by the blue circles. The new 400 kV connection on the west coast from Idomlund to Endrup and from Endrup to Germany is marked with orange. [7]

Until now, the replacement of 132/150 kV OHLs with UGCs has not shown any significant increase of harmonic distortions in meshed systems [8]. At 400 kV, harmonic distortion is especially undesired, due to to cost of equipment. Additionally, a high power quality is crucial at 400 kV in order to maintain security of supply. As the power mostly propagate down from high to low voltage levels, so will the harmonic distortion. As a result, high harmonic distortion at 400 kV will affect the harmonic distortion at lower voltage levels. However, the opposite can also occur. Therefore, with the upcoming 324 km UGCs at 150 kV, the impact on the harmonic distortion and propagation at 150 and 400 kV should be analysed.

1.2 Problem Statement

Based on the previous analysis, the following problem statement has been formulated:

How does the undergrounding of 132/150 kV lines impact the harmonic propagation at the 132/150 and 400 kV levels?

To answer the problem statement the following objectives are formulated:

Objectives

- Investigate the state of the art regarding harmonic propagation
- Describe and explain the behavior of harmonic propagation between voltage levels
- Analyse the harmonic propagation in an example grid with different levels of UGCs and harmonic current injection at different voltage levels
- Investigate the optimal filter location at different voltage levels in a meshed system

1.3 Methodology

In this thesis, the objectives are utilised to answer the problem statement. The objectives are therefore used as headlines in the structure of the methodology.

Investigate the state of the art regarding harmonic propagation

In Chapter 2 a literature study is conducted and the state of the art regarding the propagation of harmonics are described. In this chapter, the basic theory of harmonics as well as the analysis methods of harmonic propagation in power systems are elaborated. As the harmonic propagation studies are dependent on the system, the modelling of basic power system equipment is analysed. Additionally, the state of the art of mitigation of harmonic distortions in a power system is elaborated to gain knowledge about the different filter solutions.

Describe and explain the behavior of harmonic propagation between voltage levels

Chapter 3 and 4 are made to answer this objective. First, harmonic propagation studies are analysed in a radial system at one voltage level in Chapter 3. Throughout this chapter, the basic principles of harmonic propagation is analysed, for different line types, placements of harmonic current sources and angle of harmonic current injections. This analysis is made to obtain a basic understanding of the propagation of harmonics. Next, harmonic propagation studies are analysed in the radial system with a transformer implemented in Chapter 4. In this chapter, the influence of different voltage levels on the propagation of harmonics is analysed. Thereby, the harmonic propagation through a transformer is analysed. The findings in this chapter is obtained, by simulating several cases and analysing the results using theoretical expectations. This is the inductive method, which means that the conclusions are based on several observations, which has been theoretical explained.

Analyse the harmonic propagation in an example grid with different levels of UGCs and harmonic current injection at different voltage levels

To investigate this, Chapter 5 is conducted. In this chapter, the harmonic propagation between voltage levels is analysed in a meshed grid. The influence of changing line types on both voltage levels is analysed. Additionally, the turns ratio, transformer impedance and line lengths on the LV-side are analysed in the system, to validate the results when changing the line types. Furthermore, the harmonic propagation in lines and through transformers are analysed in the meshed system. The study includes the harmonic voltage differences, when changing line types in the LV-system. This is analysed when injecting harmonic currents at either voltage levels. Similar to the previous chapter, the inductive method is used and the findings have been obtained by simulating several cases and analysing the results using the theoretical expectations.

Investigate the optimal filter location at different voltage levels in a meshed system

To answer this objective, Chapter 6 is written. In this chapter, the harmonic mitigation is analysed. Only one filter type is utilised and analysed in the meshed system. The filter is installed at two different voltage levels to analyse tendencies regarding the placement of the filter. To analyse the tendencies, several simulations are performed for different harmonic current injection and filter locations in the meshed system.

1.4 Delimitation

The focus of this study is to describe the harmonic propagation and the tendencies of harmonic propagation between voltage levels, and not the magnitude of the harmonic voltage distortion. Therefore the harmonic voltage magnitudes are not considered in terms of the practical limits. The focus of this study is on the effects of permanent line type changes in a system. Therefore, only steady-state analyses are performed.

Moreover, balanced operation is used throughout this report. In doing so, only the positive sequence values are used. Therefore, even though the frequency scan method shows the impedance for every frequency, the results obtained is still missing some details. In power systems, both the negative- and zero-sequence components and the coupling between sequence components will influence the results [9]. Therefore, unbalanced simulations would be required for accurate results. However, the balanced operation can be used to observe tendencies regarding harmonic propagation.

In this report, the modelling of the components are performed using detailed models, but with a simplified modelling of asymmetries. Therefore, the phases of OHLs are modelled with perfect transposition and the sheath of the UGCs are modelled as cross-bonded. As the transposition of phases in OHLs in Denmark is not performed, the modelling of perfect transposition lacks some details of the asymmetries in the system. However, transposition is not done in Denmark since the lines are often short and as the asymmetries does not have a significant effect. Therefore, this assumption does not have a large impact on the results. Regarding the modelling of UGCs, different ways of modelling, can lead to large differences in results [10]. Therefore, the results obtained in this report could be significantly different with another type of bonding. However, the focus of this report is on tendencies and not on specific results for a specific bonding type. Hence, by modelling the UGCs as cross-bonded, general tendencies are observed. Moreover, the UGCs in this study are modelled in trefoil formation due to symmetry.

The harmonic orders of interest are up to the 50^{th} harmonic order. This is chosen based on recommendations from IEC 61000-3-6. [11].

State of the Art 2

In this chapter a literature study regarding harmonic propagation is conducted. First the theoretical background of harmonics will be described, where the waveform and measurement of harmonic distorted signals will be explained. Furthermore, the sources of harmonic generation and the effect of harmonic distortion in a power system will be explored. This study focuses on balanced operation, hence the harmonic phase sequence will be investigated in order to investigate the harmonic orders of interest. The methods utilised in harmonic propagation studies of power systems will be explained. Additionally, the mitigation of harmonics will be investigated in terms of active and passive filters. Furthermore, the equipment modelling required for harmonic studies will be explained. The mitigation of harmonic voltages is also described in terms of active and passive filters.

2.1 Harmonics

Ideally the waveforms of AC voltages and currents follows a pure sinusoidal. In reality, this is rarely the case. Often the waveforms have periodically distortions referred to as harmonics. A waveform can be measured in the time-domain, where the amplitude is measured at each time instant. Therefore, the measured signal contains all distortions, which can be separated when transformed to the frequency-domain. An example of this can be seen in Figure 2.1, where a 3D plot shows a measured disturbed signal, shown in blue.

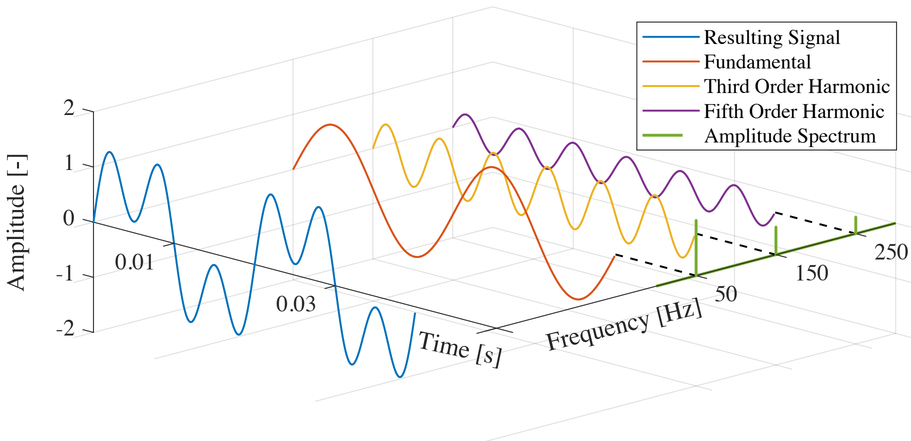

Figure 2.1: 3D plot of harmonics in time- and frequency-domain.

The orange curve is oscillating at 50 Hz, which in this case is the fundamental frequency. The yellow and purple waveforms are the third and fifth order harmonics respectively, which means that they are a multiple of the fundamental frequency. On the frequency axis, the amplitude of the frequency components are shown. This fragmentation of the frequency components are shown with its corresponding amplitudes in the frequency-domain. [12]

As power systems mainly operates with AC, which has halfwave symmetry. A waveform has halfwave symmetry if $x(t) = -x(t + T/2)$. A waveform with halfwave symmetry only contains odd harmonics (1^{st}, 3^{rd}, 5^{th} ...). Hence, harmonics in power systems are usually odd. [12]

The total harmonic distortion (THD) can be utilised to measure the harmonic voltage distortion in a power system utilising Equation 2.1. THD is equal to the RMS of all the harmonics as percentage of the fundamental. [12]

$$THD = \frac{\sqrt{\sum_{n=2}^{N} V_n^2}}{V_1} \tag{2.1}$$

Where N is the maximum harmonic order considered.

THD is normally used to express the harmonic distortion on voltage. For harmonic currents the THD is not representative. since during light load, the harmonics are large compared to the fundamental. Therefore, total demand distortion (TDD) is commonly used to measure the harmonic distortion for current. The TDD is calculated from the RMS of all harmonics as a percentage of the rated current, I_{rated}, as seen in Equation 2.2. [12]

$$TDD = \frac{\sqrt{\sum_{n=2}^{N} I_n^2}}{I_{rated}} \tag{2.2}$$

Analysis of harmonic distortion is typically performed for voltage, as the power system is dependent on a sinusoidal voltage waveform. However, harmonic distortion of the voltage is often the outcome of a distorted current. When a non-sinusoidal current is flowing through the system impedance, a non-sinusoidal voltage drop occurs, which creates harmonic distortion in the system. [12]

Harmonic Sources

Before the introduction of power semiconductors, harmonics were generated in electric arc furnaces, fluorescent lamps, electrical machines and transformers. Today, power electronics are used for several applications to control the power in both domestic appliances, HVAC-HVDC transformation and generation of electrical energy from RES. The switching of power electronics is what generates the harmonics. [12]

There is a distinction in the produced harmonics, which are steady state distortion and transient effects. Steady state distortion deals with excitation of system resonance, by harmonic injections from active devices such as converters. The active devices are normally controlled to produce a continuous power, hence creating a steady state harmonic distortion. An example of this is an inverter for photovoltaics, which generate steady state distortions during injection of power to the grid. Transient effects deals with components, which are transient in nature because of non-linearity. Therefore, these transient harmonics are only temporary, and occurs when changes appears in the system. An example of this is a saturated transformer. [1]

Effects of Harmonics

Harmonics in a power system are undesired, which can be explained by the following four effects. The first effect is that harmonics reduce the efficiency of generation, transmission and consumption of electricity. When harmonic currents are present, the ohmic losses in the transmission system increases. As an example, the ohmic losses are increased by skin- and proximity-effects, which increases with frequency. The second is that harmonics decreases the life time of insulation in electrical equipment. As an example, harmonic distortions in a cable increases the dielectric stress, which decreases the lifetime and increases the number of faults. The third effect is that harmonic distortion affects the system voltage. Therefore, equipment which are very dependent on system voltage can experience malfunctions. The fourth effect of harmonic distortion is that system resonances can be excited from harmonic emissions. Thereby, harmonic distortion is amplified, which cause over-voltage and over-current at parallel and series resonances respectively. Resonance occurs between a inductor and capacitor, when their reactance is equal in magnitude, as shown in Equation 2.3. [12]

$$\omega_0 L = \frac{1}{\omega_0 C} \qquad \Leftrightarrow \qquad f_0 = \frac{1}{2\pi\sqrt{LC}} \tag{2.3}$$

Where L is the inductance, C is the capacitance, ω_0 is the resonance angular frequency and f_0 is the resonance frequency.

In Figure 2.2 series and parallel LC circuits are visualised with the impedance as a function of frequency. Here it is shown that at the series resonance zero impedance is present and at a parallel resonance an infinite impedance is present, as no resistance is in the circuit. Therefore, if a voltage is applied to a series resonance circuit, amplified currents will flow and if a current is injected to a parallel resonance circuit an amplified voltage will appear.

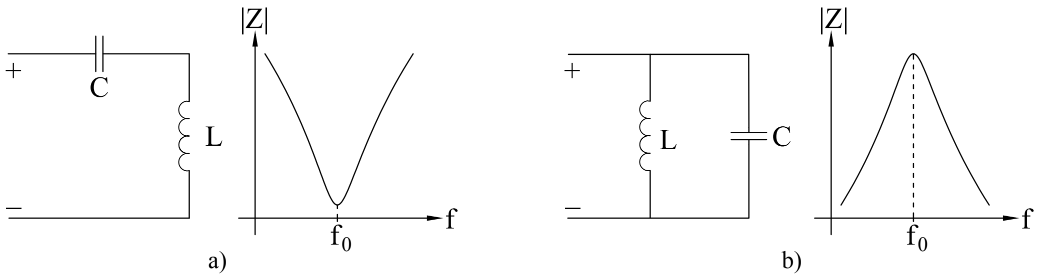

Figure 2.2: Series (a) and parallel (b) LC circuits with impedance as a function of frequency showing the resonance points.

Harmonic Phase Sequences

The sequence components of the harmonics for a balanced system of order $3 \cdot n + 1$ are positive sequence, where n is an integer from zero to infinity. The harmonics of order $3 \cdot n - 1$ are negative sequence and the harmonics of order $3 \cdot n$ are zero sequence. The phase sequence of the harmonics from order 1 to 7 are shown in Table 2.1. The harmonic sum of the positive sequence is zero due to the symmetry. The same applies for the negative sequence. However, zero sequence harmonics add in the neutral, resulting in three times larger harmonics. [13]

Table 2.1: Sequence components of harmonic orders.

Harmonic order	**Phase A**	**Phase B**	**Phase C**	**Phase sequence**
1	$0°$	$-120°$ or $240°$	$120°$	$+$
2	$2 \cdot 0° = 0°$	$2 \cdot 240° = 480° = 120°$	$2 \cdot 120° = 240°$	$-$
3	$3 \cdot 0° = 0°$	$3 \cdot 240° = 720° = 0°$	$3 \cdot 120° = 360° = 0°$	0
4	$4 \cdot 0° = 0°$	$4 \cdot 240° = 240°$	$4 \cdot 120° = 120°$	$+$
5	$5 \cdot 0° = 0°$	$5 \cdot 240° = 120°$	$5 \cdot 120° = 240°$	$-$
6	$6 \cdot 0° = 0°$	$6 \cdot 240° = 0°$	$6 \cdot 120° = 0°$	0
7	$7 \cdot 0° = 0°$	$7 \cdot 240° = 240°$	$7 \cdot 120° = 120°$	$+$
...	...	...	...	...

In [14], measurements of harmonic voltages showed that the sequences of harmonics does not follow the pattern in Table 2.1 completely. In Figure 2.3, measurements of harmonic voltages at Trige substation are shown as sequence components. An example of the deviations is the third harmonic, which is naturally a zero sequence component. However, the measurements show that the positive sequence component is dominant in the Trige substation.

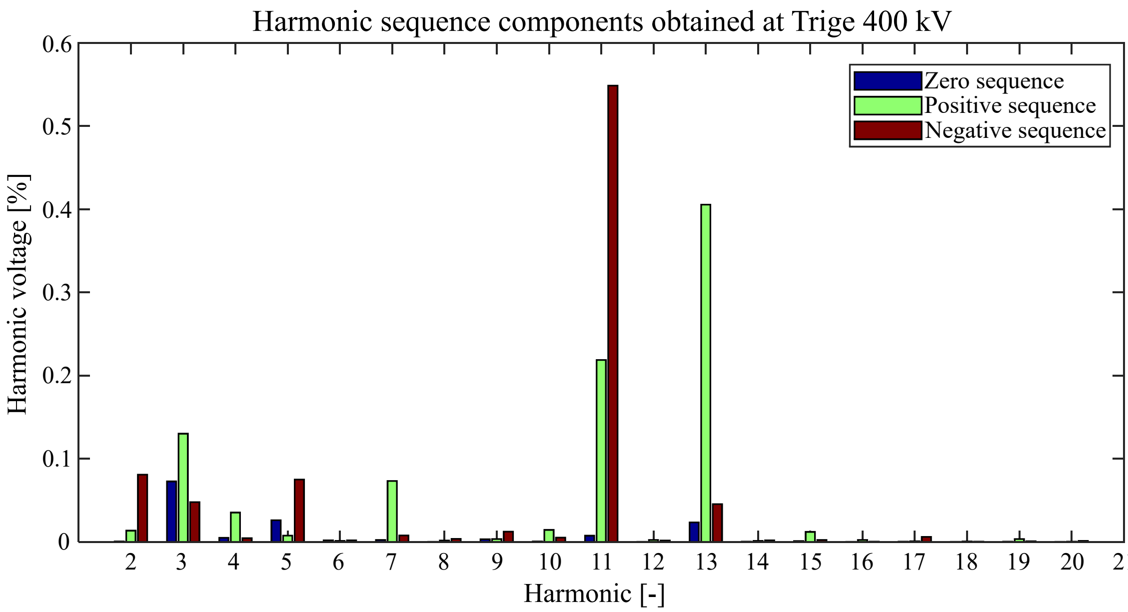

Figure 2.3: Measured harmonic voltages as sequence components at Trige 400 kV substation. [14]

Usually, power systems are unbalanced, because of asymmetries in the system such as UGCs and OHLs in flat formation. This asymmetry creates inter-sequence coupling. The inter-sequence coupling can have a considerable effect especially at frequencies near the resonance points. Asymmetries are the reason that the measured sequence components in Figure 2.3 does not follow the pattern in Table 2.1 completely. In [14], a detailed modelling and analysis was performed on this system. In Figure 2.4(a), the impedance of each phase seen from Trige substation is shown. Here it is visualised that the impedance is asymmetric. In Figure 2.4(b) an ideal positive sequence voltage is applied for each integer harmonic order from the 2^{nd} to the 20^{th} in the 400 kV Trige substation and the voltage is simulated and plotted for the Anholt offshore substation. Here it is visible, that a positive sequence voltage energise negative and zero-sequence components, especially at the resonance points due to asymmetries. [14]

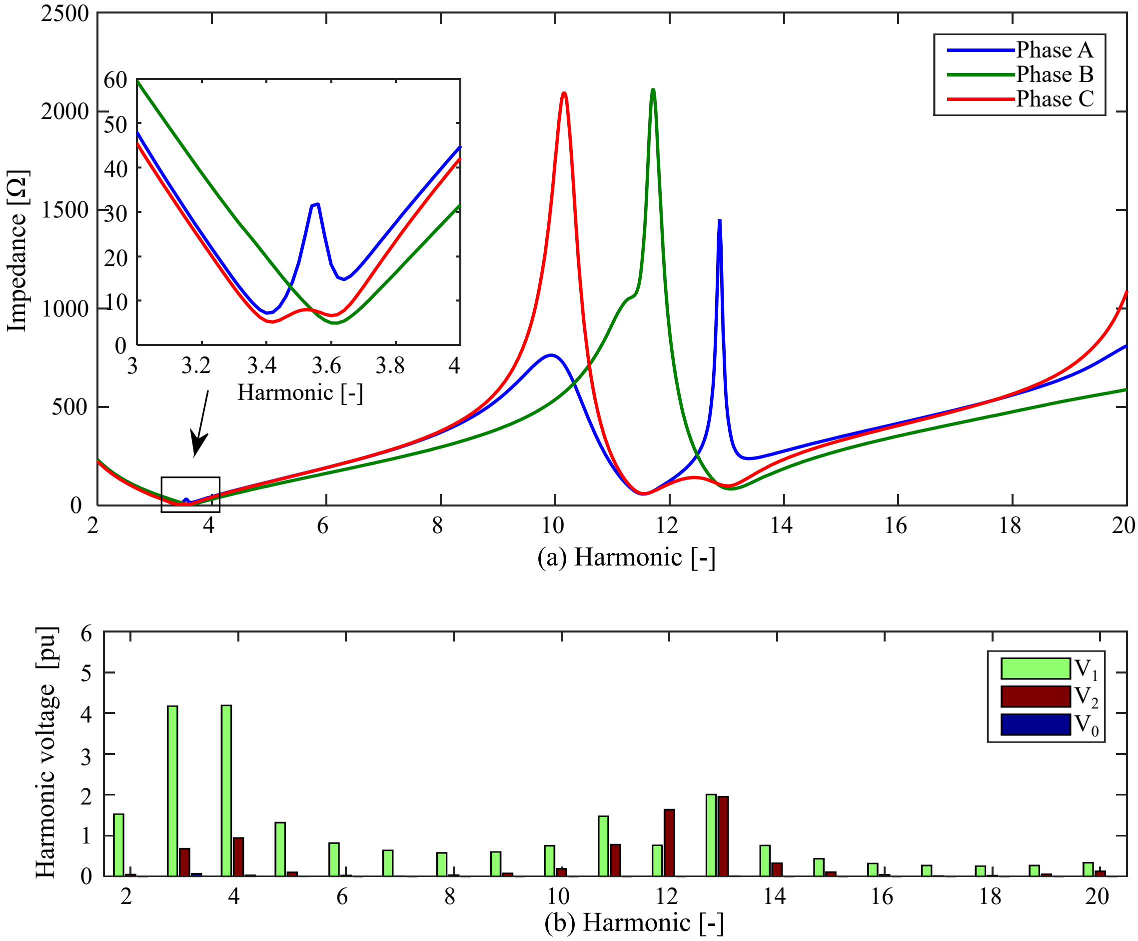

Figure 2.4: Phase impedance of each harmonic order seen from Trige (a) and simulated harmonic voltage at Anholt offshore substation, shown as sequence components (b). [14]

In order to conduct a thorough analysis of harmonics, frequency dependent phase-domain models of power system components must be used [14]. This modelling process is complex and time consuming, and the data needed is not easily obtained. Additionally, the simulation speed is slow due to the detailed modelling. Therefore, power system equipment is often modelled as decoupled sequence components, although this method can lead to errors.

2.1.1 Harmonic Propagation

Harmonic propagation in a system is in this report referred to how the harmonic voltages and currents spread in the system. Harmonic propagation in a power system can be studied in the time- or frequency-domain. The time-domain is utilised for transient analysis, such as energisation of a transformer. The frequency-domain is utilised for steady state analysis and will be the focus in this report. The steady state harmonic injections from converters are not captured in the frequency-domain, due to the control of the converter. However, the scope of the study is the tendencies of harmonic propagation, which can be analysed in steady state utilising the frequency-domain.

The frequency-domain studies can be categorised based on the objective. The two general approaches are network impedance calculations and voltage and current harmonic calculations as seen in Figure 2.5. The calculation methods are frequency scan, harmonic penetration and harmonic load flow. The frequency scan method calculates the network impedance, while harmonic penetration and harmonic load flow calculates voltage and current harmonics. Furthermore, harmonic penetration can be done using both an iterative and a direct solver. The above mentioned methods can all be utilised for both balanced or unbalanced system analysis.

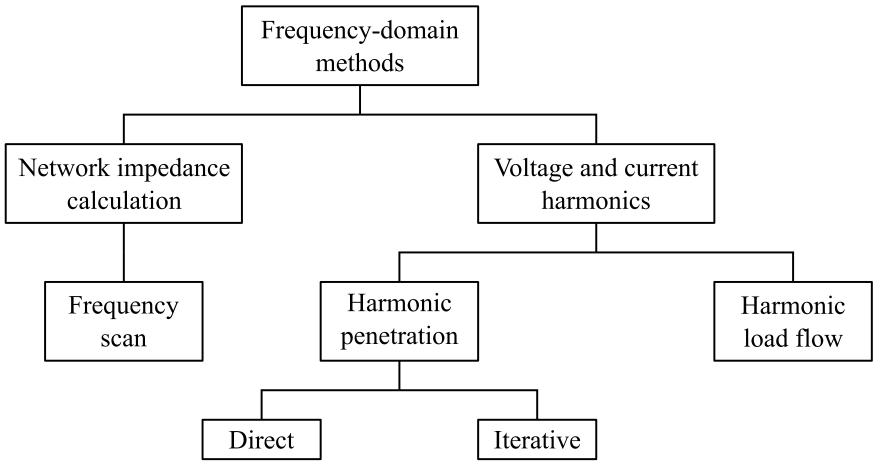

Figure 2.5: Overview of frequency-domain methods, based on [1].

In the frequency-domain non-linearities, such as magnetisation of transformers or surge-arresters, are neglected. As well as harmonic injection by converters, which utilise time-domain for control. If the non-linearities are relevant, studies should be performed in the time-domain.

Frequency Scan

Frequency scan is the simplest of the methods and it is used to determine the impedance of nodes in a power system as a function of the frequency. Therefore, it is typically the first method used in harmonic studies in the planning stage. The admittance of the system changes as a function of the frequency and is calculated for each frequency step within the desired range. By injecting a current, the harmonic voltage can be calculated using Equation 2.4. [1]

$$\mathbf{I_h} = [\mathbf{Y_h}] \cdot \mathbf{V_h} \tag{2.4}$$

Where $[\mathbf{Y_h}]$ is the admittance matrix, while the vectors $\mathbf{V_h}$ and $\mathbf{I_h}$ contains the harmonic nodal voltages and currents. In the frequency scan method, one harmonic current is injected at a time in order to determine the harmonic voltages. Hence, only one element in the current vector is different from zero and the process requires recalculation for each harmonic of interest. The method can be performed in either the phase- or sequence-domain. [1]

The admittance matrix can be divided into self-admittance and mutual admittance. The self-admittance is the diagonal in the admittance matrix as seen in Equation 2.5, while the mutual admittance are in the off-diagonal.

$$\begin{bmatrix} I_1 \\ I_i \\ I_j \\ \vdots \\ I_n \end{bmatrix} = \begin{bmatrix} y_{11} & -y_{1i} & -y_{1j} & \dots & -y_{1n} \\ -y_{i1} & y_{ii} & -y_{ij} & \dots & -y_{in} \\ -y_{j1} & -y_{ji} & y_{jj} & \dots & -y_{jn} \\ \vdots & \vdots & \vdots & \ddots & \vdots \\ -y_{n1} & -y_{ni} & -y_{nj} & \dots & -y_{nn} \end{bmatrix} \begin{bmatrix} V_1 \\ V_i \\ V_j \\ \vdots \\ V_n \end{bmatrix} \tag{2.5}$$

The individual self- and off-diagonal admittances can be calculated utilising Equation 2.6.

$$y_{ij} = \left.\frac{I_i}{V_j}\right|_{I_k=0} \qquad k = 1 \dots n \tag{2.6}$$

A current injection of 1 pu simplifies the impedance calculation to Equation 2.7. Since non-linearities are neglected, the system impedance does not depends on the magnitude of the injected current. [1]

$$\mathbf{V_h} = [\mathbf{Y_h}]^{-1} = [\mathbf{Z_h}] \tag{2.7}$$

Similar to the admittance matrix, the impedance matrix consists of a self- and off-diagonal impedance. The self-impedance z_{ii} is the diagonal value. The voltage in bus i can be calculated utilizing z_{ii} and the current injected in bus i. The off-diagonal impedance z_{ji} can be utilised to calculate the voltage in a bus different from the current injection. As an example the voltage in bus j, when injecting a current in bus i, can be calculated utilizing z_{ji}.

Harmonic Penetration and Harmonic Load Flow

Harmonic load flow and harmonic penetration are very similar. In fact, harmonic penetration is often referred to as harmonic load flow in simulation software and is the most common method used to analyse harmonic voltages and currents in power systems. The main difference between the two methods is that harmonic penetration does not consider interactions between harmonics, while harmonic load flow does. As the interaction between harmonics is complex to model and calculate, the harmonic load flow is rarely used. The interaction between harmonics will impact the magnitude of the harmonics in the system. However, the harmonic propagation will not be influenced. Hence, the harmonic load flow will not be used in this report. Harmonic penetration is used to determine the harmonic distortion at specific nodes in the power system. The determined harmonic distortion can then be used to determine if the harmonic disturbance is within the required limits.

Harmonic penetration is performed by solving linear equations either using direct- or iterative-solvers. Both solvers utilises the conventional load flow at the fundamental frequency [15]. In the direct method, the admittance matrix is recalculated for each of the frequencies considered. The injected harmonic current is considered and Equation 2.4 is solved directly. The RMS voltages and currents are calculated for each harmonic order of interest. The voltages and currents are obtained by adding the result of the conventional load flow at the fundamental frequency with the results from the direct method. The iterative method solves Equation 2.4 iteratively. [1]

Both the direct- and iterative methods can be applied for balanced or unbalanced operation. The system can be studied in balanced operation if there is no inter-sequence coupling at the frequencies of concern. Thereby, the system can be studied using a single phase, simplifying the analysis. [1]

Power systems are usually asymmetric mainly from lack of transposition and coupling between phases. Therefore, more accurate results can be obtained by performing unbalanced harmonic penetration analysis. Unbalanced studies are performed by injecting an unbalanced harmonic current and studying the effect on each phase. Additionally, in the unbalanced harmonic penetration study, the conventional load flow can be performed for balanced or unbalanced operation. The most accurate result is obtained when utilising unbalanced operation. However, the computational time can be extensive for large systems. [1]

2.2 Mitigation

Ideally, all negative effects caused by harmonics should be eliminated. However, this is not economically and technically realistic. A realistic approach is to try and mitigate the harmonics to a level within specified limits. Since the power system mainly consist of voltage sources and not current sources, the harmonic limits are based on voltage and not current. [12]

Harmonic voltage mitigation can be done by designing nonlinear devices so that they emit a low level of harmonic distortion to the power system. An example of this is phase shifting of transformers, which is utilised in an HVDC 12-pulse line commutated converter (LCC). By phase shifting the transformers by 30°, the 5^{th} and 7^{th} harmonic are eliminated. Other options are utilisation of modular multilevel converter and active wave-shaping techniques. Another possibility is to install harmonic filters at the terminals, which can be either active or passive. [12]

2.2.1 Active Filters

Active filters mitigate the harmonics by utilising power electronic devices. The basic principle of the active filter is that a harmonic distortion, equal to the distortion in the power system in magnitude, but opposite in polarity, is injected into the system. Hence resulting in a sinusoidal waveform. An example of this is a non-linear load drawing a square wave current, the active filter injects a compensating current as shown in Figure 2.6 and as a result, the source current is sinusoidal. [16]

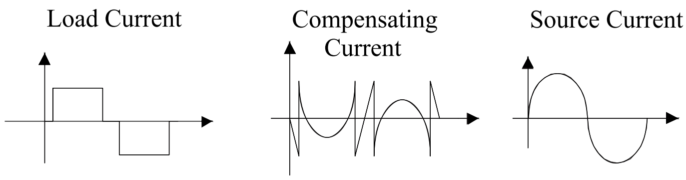

Figure 2.6: Load current, compensating current from active filter and the filtered source current.

Active filters with high power rating for high voltage applications are however not cost effective. This is due to the limited availability of high frequency switching devices with high voltage and power ratings. [17]

Moreover, it is stated in [2], that no active filter based solution is implemented in the world today to mitigate harmonics at transmission system level in a meshed grid. With this in mind, the active filter is not elaborated further in this report.

2.2.2 Passive Filters

A passive filter is constructed from the passive circuit components: inductors, capacitors and resistors. When utilised for harmonic mitigation, the passive filter is commonly of the shunt type. A shunt type filter is tuned to provide a low impedance path for the specific harmonics, hence mitigating the specific harmonics in the system. The low impedance is obtained by utilising capacitors and inductors to achieve a resonance point. [16]

The quality factor (QF) of a filter defines the sharpness of the tuning. The higher the QF, the sharper the tuning and opposite. In this report the tuned and damped filter types will be explored. The tuned filter has a high QF, while the damped filter has a low QF. [12]

Tuned Filters

The schematic of single-, double- and triple-tuned filters are shown in Figure 2.7.

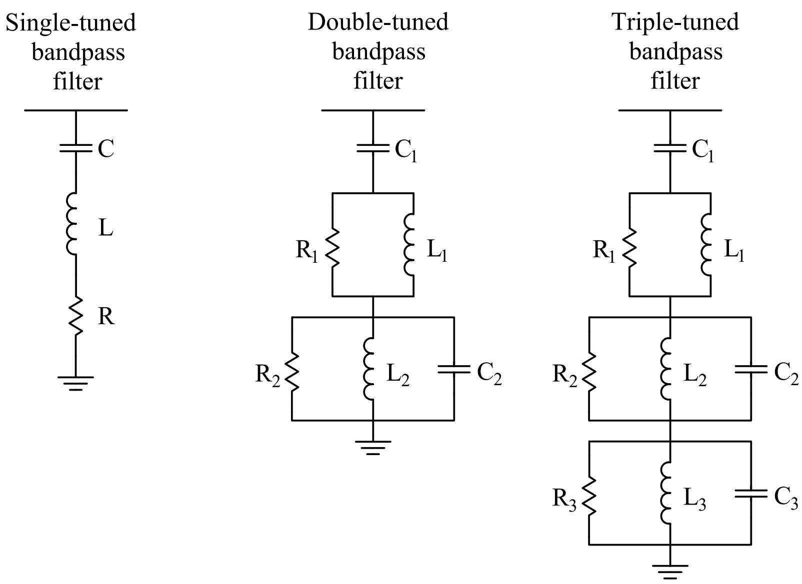

Figure 2.7: Circuit schematic for tuned filter types. Inspired by [12].

A single-tuned filter is tuned to provides a low impedance path for one harmonic frequency. A double- and triple-tuned filter is tuned to filter two and three harmonic frequencies respectively. The frequency scan of the single- and double-tuned filter types are shown in Figure 2.8, where f_1 and f_2 are the tuned harmonic frequencies.

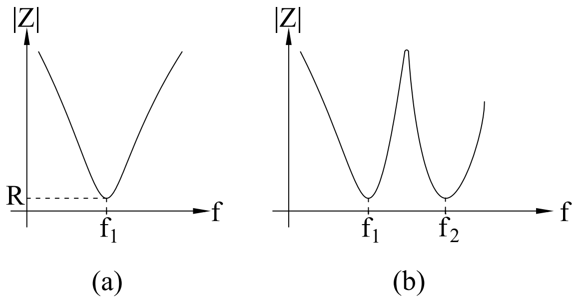

Figure 2.8: Frequency scan for a single-tuned (a) and double-tuned (b) filter types. Inspired by [12].

An advantage of tuned filters is, that they have low losses at the fundamental frequency. Moreover, tuned filters are more effective at the tuned frequency compared to damped filters. The disadvantages of tuned filters are, that they are not easily adapted to change. The characteristics of inductors and capacitors can change, due to aging and temperature effects, referred to as de-tuning effects. These effects reduces the effectiveness of the filter, since the actual harmonic frequency might be outside the designed tuning frequency. Another disadvantage of the tuned filter is, that a parallel resonance between the filter and the system arises, which is below or between the tuning frequencies. [16]

Damped Filters

Damped filters differs from tuned filters, as they are designed to mitigate a wide spectrum of harmonics. The schematic of a first-, second- and third-order high-pass damped filter is shown in Figure 2.9. A fourth type called a C-type high-pass damped filter is also shown in Figure 2.9.

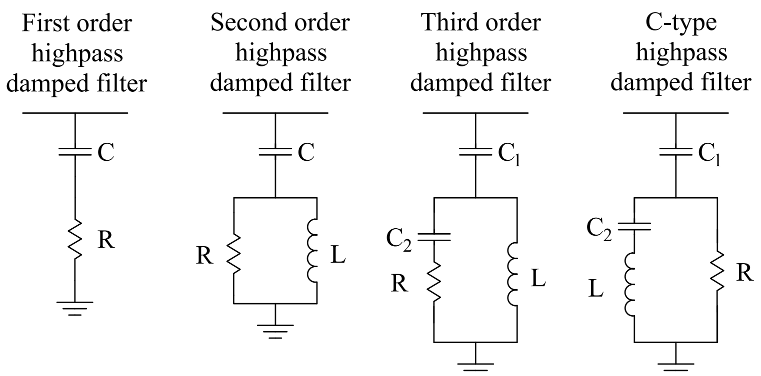

Figure 2.9: Circuit schematics of damped filter types. Inspired by [12].

The frequency scan of a damped filter has a flatter characteristic compared to the tuned filter. The frequency scan of a second order damped filter is shown in Figure 2.10.

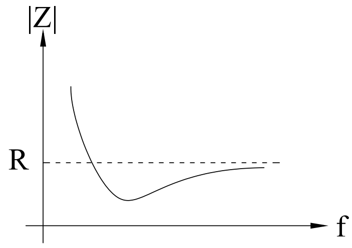

Figure 2.10: Frequency scan for a second order damped filter. Inspired by [12].

The first order filter is not commonly used, since a large capacitor is required. Additionally, the losses at the fundamental are excessive. The second order filter performs the best filtering. However, it also has higher losses at the fundamental frequency compared to a third order filter. The performance of the C-type filter is a compromise between the performance of the second- and third-order filters. At the fundamental frequency, the capacitor C_2 and the inductor L creates a series resonance resulting in a low impedance path bypassing the resistor R. This means, that at the fundamental frequency, the impedance is determined by C_1. Hence, the losses at the fundamental frequency are low. [16]

The advantages of utilising damped filters over tuned filters are, that they are less sensitive to the de-tuning effects as the low impedance spectrum is wider. Moreover, damped filters does not give rise to a significant parallel resonance frequency with the system. However, when a damped filter is installed in a power system, a shift in the existing system resonance frequencies will happen. The disadvantages of damped filters compared to tuned filters are, that to achieve the same amount of filtering, the fundamental VA rating should be higher, due to the higher current. Moreover, the losses are higher in the damped filters compared to the tuned filters at the fundamental frequency. [12]

2.3 Equipment Modelling

In the analysis of harmonic propagation, the modelling of equipment can have a significant influence on the results. Therefore, different modelling approaches for transmission lines and transformers will be presented and elaborated.

2.3.1 Transmission Lines

Transmission lines consist of the distributed parameters: Series inductance, series resistance, shunt capacitance and shunt conductance. The inductance and capacitance are related to the magnetic and electrostatic conditions, whereas the resistance and conductance cause ohmic losses. The parameters can be calculated using the geometry and conductor data of the line. The simplest representation of a line is the nominal π-model and is easy to analyse. This model is made using the series element, and half of the shunt admittance at the sending and receiving end. The nominal π-model is shown in Figure 2.11, where $Z_n = R + j\omega L$ and $Y_n = G + j\omega C$. [12]

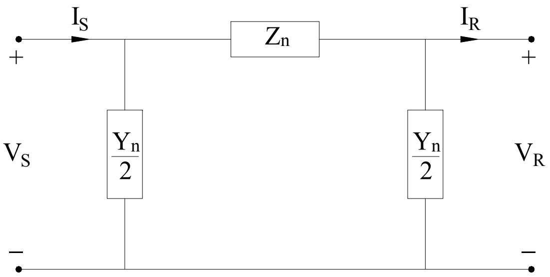

Figure 2.11: Nominal π-model of a transmission line.

The nominal π-model is only valid for short lines and at low frequencies, due to the accuracy of the model. Therefore, the nominal π-model is not a good representation of a line for harmonic studies. Additionally, the model only contains one resonance peak, which is inaccurate. A way of overcoming this is to divide the line into several sub lines, using cascaded nominal π-sections. The cascaded nominal π-sections contain resonance peaks equal to the number of sections. [12]

A line is commonly modelled using the equivalent π-model, which take into account the distributed parameters. This model is derived from equations describing the wave propagation of transmission lines. In this way, the model distributes the parameters along the line with the distance l, using hyperbolic equations. In Figure 2.12 the equivalent π-model is visualised.

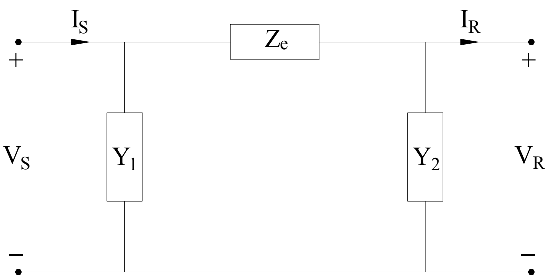

Figure 2.12: Equivalent π-model of a transmission line.

The impedance and admittance Z_e, Y_1 and Y_2 are as expressed in Equation 2.8 and 2.9. The characteristic impedance, Z_0, is expressed in Equation 2.10 and the propagation constant, γ, is expressed in Equation 2.11.

$$Z_e = Z_0 \cdot sinh(\gamma \cdot l) \tag{2.8}$$

$$Y_1 = Y_2 = \frac{tanh(\gamma \cdot l)}{Z_0 \cdot 2} \tag{2.9}$$

$$Z_0 = \sqrt{\frac{\mathcal{R} + j\omega\mathcal{L}}{\mathcal{G} + j\omega\mathcal{C}}} \tag{2.10}$$

$$\gamma = \sqrt{(\mathcal{R} + j\omega\mathcal{L}) \cdot (\mathcal{G} + j\omega\mathcal{C})} \tag{2.11}$$

Where $\mathcal{R}$, $\mathcal{L}$, $\mathcal{G}$ and $\mathcal{C}$ are the resistance, inductance, conductance and capacitance per unit length.

By analysing the impedance characteristics of an equivalent π-model in open circuit, it is shown in [12], that resonance occurs at a frequency interval of a quarter wavelength. The wavelength can be calculated as shown in Equation 2.12.

$$\lambda = \frac{v}{f} \tag{2.12}$$

Where the velocity v of a travelling wave can be calculated using Equation 2.13. The velocity of a travelling wave in free space is $3 \cdot 10^8$ m/s, while it is approximately $1.8 \cdot 10^8$ m/s and $2.8 \cdot 10^8$ m/s for UGCs and OHLs respectively. [18]

$$v = \frac{1}{\sqrt{\mathcal{L}\mathcal{C}}} \tag{2.13}$$

The wavelength frequency of a line can be calculated by v divided by the length of the line. To illustrate the resonance at each quarter wavelength frequency an example of a 25 km UGC with the parameters in Table A.4 in Appendix A.2 is used. The wavelength at 50 Hz of this UGC type is 2444.9 km, and the wavelength frequency is 4889.7 Hz. The impedance magnitude and angle characteristics of the UGC in open- and short-circuit are shown in Figure 2.13. [12]

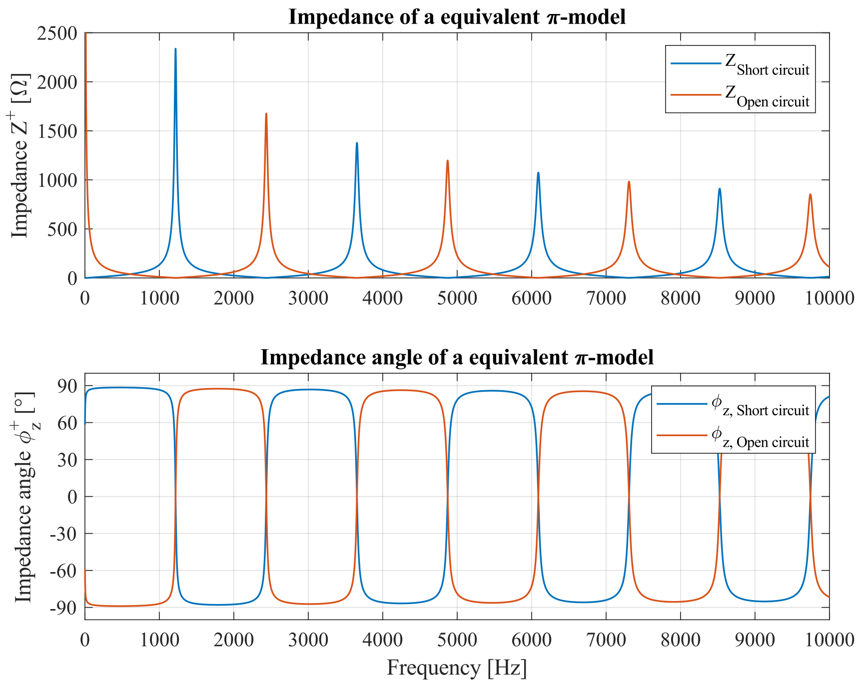

Figure 2.13: Impedance magnitude and angle as a function of frequency of an open- and short-circuited equivalent π-model with skin effect included.

It is visible that the natural occurrence of resonance points is at every quarter of the wavelength frequency. The resonance points rotates between series and parallel resonance. The parallel and series resonances are shifted one quarter of the wavelength frequency between the open and short circuit. Additionally, it can be seen that the resonance peaks are gradually reduced with frequency. This is due to the fact, that resistance increase with frequency, which damps the magnitude at the resonance frequency [12]. One effect causing increased resistance is the skin effect. The skin effect causes the current to be distributed near the surface of the conductor, which increases with frequency. With the current distributed at the surface, the effective cross sectional area is reduced, hence increasing the resistance [18]. The skin effect also reduces the internal inductance. Due to this, the resonance frequencies gets slightly shifted. [1]

To obtain accurate results of a line, a frequency dependent model using the Bessel functions can be used. This modelling approach is geometry based and includes skin effect for both the resistance and inductance. Additionally, for high frequencies and long lines, distributed line models should be used for accurate results. [12]

A comparison of the different line models from [19] can be seen in Figure 2.14. Here a nominal π-model, an equivalent π-model and a Bessel equivalent π-model are evaluated for the impedance characteristic as a function of frequency of the line. The nominal- and equivalent π-model are analysed both with and without skin effect.

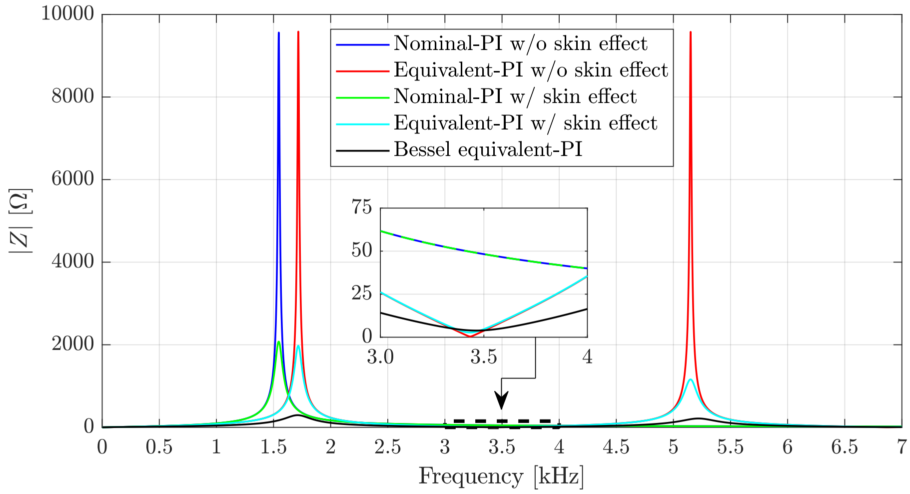

Figure 2.14: Comparison of impedance as a function of frequency of the different line models. [19]

It is visible that the nominal π-model only has one resonance peak. The inaccuracy of the nominal π-model can be seen since the resonance peak is located at a different frequency compared to the other models. Furthermore, the reduction of the impedance at the resonance peak, by including the skin effect can be seen. The Bessel equivalent π-model has a lower impedance at the resonance peak at the parallel resonance. Additionally, the Bessel equivalent π-model has a slightly higher impedance at the series resonance compared to the other models as seen in the zoom. This is due to a higher resistance in the Bessel equivalent π-model. Additionally, it can be seen, that at higher frequencies, the resonance frequency is shifted in the Bessel equivalent π-model.

In the analysis of harmonic propagation, the parameters of lines can have a significant influence on the resonance frequencies in power systems. The difference between OHLs and UGCs is the inductance and capacitance. The inductance is larger for OHLs compared to UGCs, due to the larger distance between the phases. In OHLs the inductance is approximately four times larger than the inductance in UGCs [20]. The capacitance is larger in UGCs compared to OHLs, due to both the short distance between the phase conductor and ground and the permittivity of the insulation material. The capacitance of UGCs is approximately 20-50 times larger than the capacitance of OHLs [20].

Because of the higher capacitance, the resonance frequencies appears at lower frequencies for UGCs compared to OHLs. This is the case as the resonance frequency in Equation 2.3 is lower for UGCs compared to OHLs due to a larger LC-term.

2.3.2 Power Transformers

Power transformers are common components in power systems. A transformer is an inductive component at the frequencies of interest, which in this report is from the nominal frequency and up to the 50^{th} harmonic. Therefore, the transformer creates either series or parallel resonances with cables and capacitor banks. Accurate modelling of transformers will give a more accurate estimation of the resonance frequencies in the system. [1]

Transformers can be modelled either in the frequency- or time-domain. With a frequency-domain model, the propagation on the primary and secondary sides are modelled. Hysteresis and eddy currents are often ignored in a frequency-domain model. With a time-domain model, the non-linearities in the core can be modelled. The non-linearities contains saturation, hysteresis and eddy currents. [17]

Since the analysis in this report will be made in the frequency-domain as described in Section 2.1.1, only frequency-domain transformer models are considered. A single phase equivalent model of a transformer is shown in Figure 2.15.

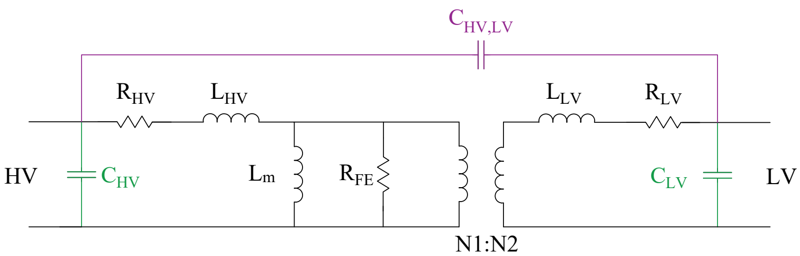

Figure 2.15: Transformer single phase equivalent model circuit schematic. [1]

In Figure 2.15, the high- and low-voltage winding impedance, R_{HV}, L_{HV}, R_{LV} and L_{LV}, are shown. The magnetising branch, composed by L_m and R_{FE} are included. The transformer stray capacitances are also included. The capacitance between the high- and low-voltage windings, $C_{HV,LV}$, is shown with purple and the capacitance between the windings and the core, C_{HV} and C_{LV}, are shown with green.

In [1], five different frequency-domain models are presented and analysed. Common for the five models is, that the stray capacitances in the transformer are neglected. This is done as the capacitance has a negligible influence at the frequency of interest. As a guideline, the stray capacitance should be considered for frequencies higher than 4 kHz. Additionally, the magnetising branch is neglected during normal operation, as the core operation lies in the linear region of the B-H curve. The simplified transformer equivalent model schematics for the five models are shown in Figure 2.16. [1]

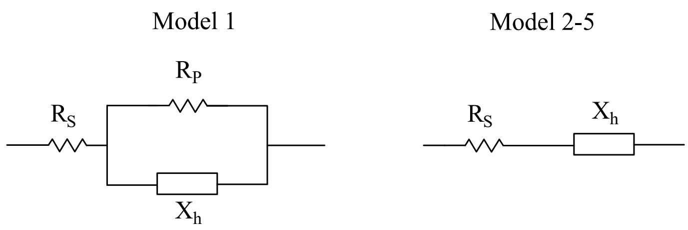

Figure 2.16: Model circuit schematics of the five models described in [1].

In model 1, the transformer is represented by an impedance, which is composed by a resistor, R_S, in series with a parallel connection of a reactance, X_h, and a resistance, R_P. Transformer models 2-5 are all represented by a series impedance composed by R_S and X_h. The models all assume a constant leakage inductance of the transformer in the frequency range of interest. This means, that the resonance frequency is the same for all the models. However, the modelling of the resistances are all different. Hence, the magnitude of the harmonic impedance is different. [1]

Three different power transformers, with measurements available, were tested with the five different transformer models in [1]. The analysis showed, that even the best fitting transformer models requires modifications to follow the measurements. Model 1 proved to have the highest losses in all three cases. Model 4 had the lowest losses and model 5 had losses in the middle range. Model 1, 4 and 5 are also compared in four different nodes in [1] in a system representing the transmission grid in Ireland. The results are shown in Figure 2.17, where the relevant frequency range is shown for each node.

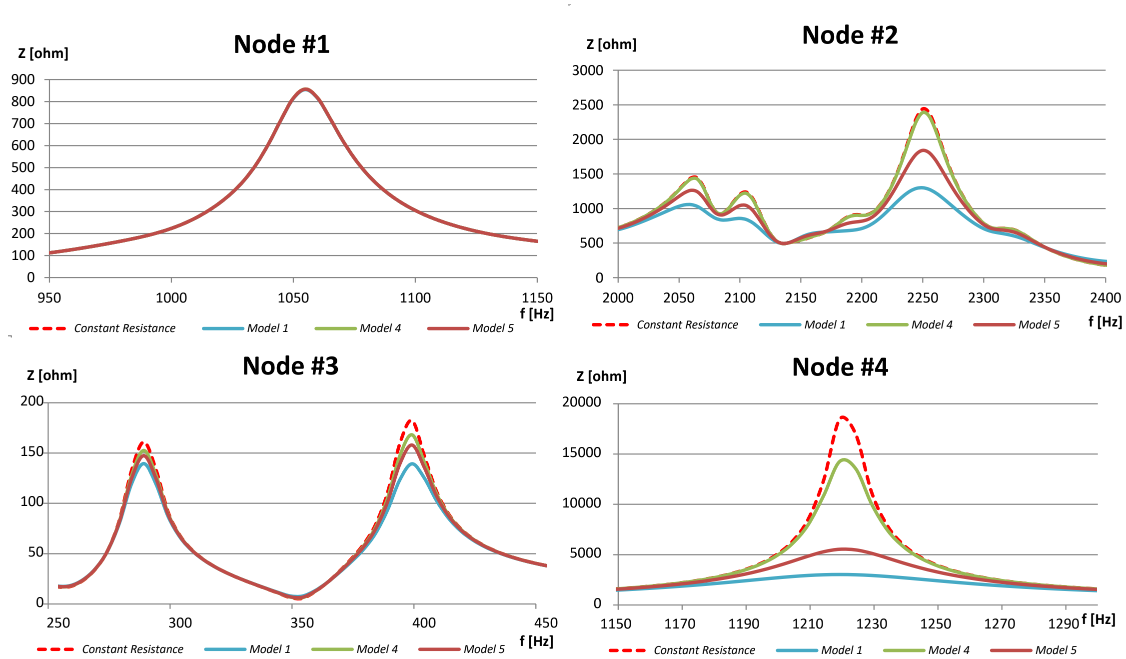

Figure 2.17: Impedance as a function of frequency with model 1, 4 and 5 utilised in a power transmission system at four different nodes. [1]

Node #1 is remote from large transmission transformers. Therefore, the impact from the transformer model has no impact on the impedance in this node.

Node #2 is a distribution level node placed one node from two large transmission stations with two transformers each. Here, the losses in the transformer model has an impact on the impedance magnitude from 2 to 2.4 kHz.

Node #3 has two transformers and several insulated cable connections. In this node, the transformers impact the impedance from 250 to 450 Hz.

Node #4 is not part of the transmission system, but has been introduced to create a parallel resonance at 1220 Hz between a transformer and a cable.

The tendency from this analysis is, that all three models has a higher damping at the parallel resonances than if the resistance were considered constant. Model 1 provides the lowest impedance, while model 4 provides the highest in nodes 2-4. At higher resonance frequencies, the difference between the models are greater. Moreover, if the analysed node is far from the transformer, the type of model does not matter. Model 5 is the recommended transformer model for harmonic studies, based on [1].

An important measure to include, when modelling transformers, is the transformer vector group. The winding connection will for example impact the zero-sequence harmonic current flow. A delta connection will trap the zero-sequence currents. In a grounded connection, the zero-sequence currents will add up, which can lead to operation of the protection relay.

Summary

For harmonic propagation studies, the frequency scan and harmonic penetration methods will be utilised in this report. The frequency scan will be utilised to calculate the harmonic impedances, while the harmonic penetration will be utilised to calculate the harmonic voltages and currents.

When mitigation studies will be conducted, the C-type high-pass damped filter will be utilised in this report. This filter type will be utilised, since it has low losses at the fundamental frequency and does not give rise to a significant parallel resonance with the system.

The equipment modelling theory will be utilised as a guideline, when making decisions in the modelling of the harmonic propagation studies. The lines will be modelled with equivalent models for most accurate results. The transformers will be modelled using model 5 of the Cigré technical brochure, since it is recommended by Cigré.

Radial System Analysis 3

In this chapter, a three bus radial system with one voltage level at 400 kV is analysed utilising the frequency scan and harmonic penetration methods in PowerFactory. First, the modelling of the radial system will be described. Afterwards, impedance analysis is conducted utilising the frequency scan method. This analysis is performed in order to understand how adjustments in the radial system, changes the harmonic impedance. In addition to this impedance analysis, the impact of replacing an OHL with an UGC is analysed in regards to harmonic impedance.

The harmonic propagation from the harmonic penetration method is compared to the impedance from frequency scan method. Hereafter, the harmonic penetration through the lines in the radial system are analysed according to harmonic voltage, current and angle between the voltage and current.

Lastly, the impact of the placement of the harmonic current source and the angle of injection of the harmonic currents is analysed. Additionally, the harmonic injection angles are an unknown factor in a power system, hence tendencies regarding these are analysed.

3.1 Radial System Description

The system analysed in this report is based on a model in PowerFactory called *Power System Model for Resonance Studies*, originally modelled by Oscar Lennerhag [21]. This model will be referred to as *Example grid*. A circuit schematic in PowerFactory of the *Example grid* is shown in Figure C.1 in Appendix C.1.

In the radial system analysis, three busses from the *Example grid* are considered. The three busses, which will be analysed are Bus 1, 5 and 7. The rest of the system is disconnected in the model. A circuit schematic of the radial system is shown in Figure 3.1. To simplify the analysis, the system will be analysed in the balanced sequence domain, for balanced operation. Thereby, coupling between sequence domains are missing as well as the zero sequence domain. However, the tendencies will still appear using the balanced sequence domain. As this study focuses on the tendencies rather than the actual values, the balanced operation is utilised to simplify the analyses.

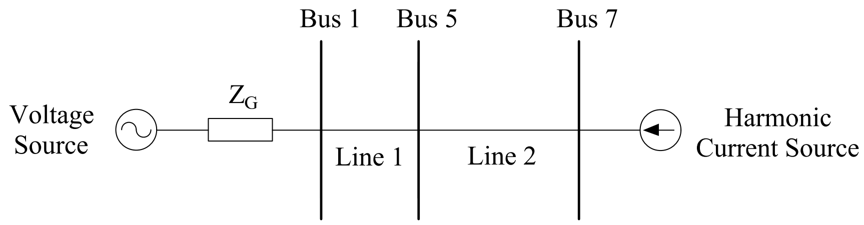

Figure 3.1: Circuit schematic of the radial system.

An external grid, represented as a voltage source and grid impedance Z_g, is connected to Bus 1. Normally for harmonic studies, the grid is modelled utilising several R, L and C elements, which introduces harmonics. However, as the focus of this report is on the study of harmonic propagation through lines, a detailed model of the grid is unnecessary for this study. Therefore, the grid is modelled as a simple series R-L element. The short circuit power of the external grid is the original value from the *Example grid* of 3807 MVA [21]. At Bus 7 a harmonic current source is connected. In a power system, the harmonic currents are normally odd as described in Section 2.1. Since the analysis in this report is made in balanced operation, the zero-sequence harmonics are neglected. Therefore, the injected currents are of the harmonic order $6 \cdot n \pm 1$ with 1 kA and an angle of 0°. The nominal voltage is 400 kV, the base current is 1 kA and the nominal frequency is 50 Hz. Bus 1 and 5 are connected through Line 1, while Bus 5 and 7 are connected through Line 2. Line 1 and 2 are OHLs. The conductor types are different, but the tower and shield type are the same. The parameters of the two OHLs are given in Table 3.1. [21]

Table 3.1: Line 1 and 2 parameters. [21]

Line	**Conductor Type**	**Tower Type**	**Shield Type**	**Length [km]**	**R [Ω/km]**	**L [mH/km]**	**C [μF/km]**	**G [μS/km]**
1	B	A	AA	25.3	0.0144	0.8723	0.0133	0
2	A	A	AA	41.6	0.0186	0.9507	0.0123	0

The line types can either have lumped or distributed parameters in PowerFactory. The distributed parameters are chosen based on the recommendations from the PowerFactory manual for harmonic studies. The conductor, shield wire and tower type parameters are given in Appendix A.

3.2 Impedance Analysis

The frequency scan method is utilised to determine the harmonic impedance of the radial system. First, the system is analysed in open circuit. Hereafter, the system is analysed with the external grid implemented.

3.2.1 Radial System Analysis in Open Circuit

Three cases in open circuit without the external grid and harmonic source are considered as seen in Figure 3.2.

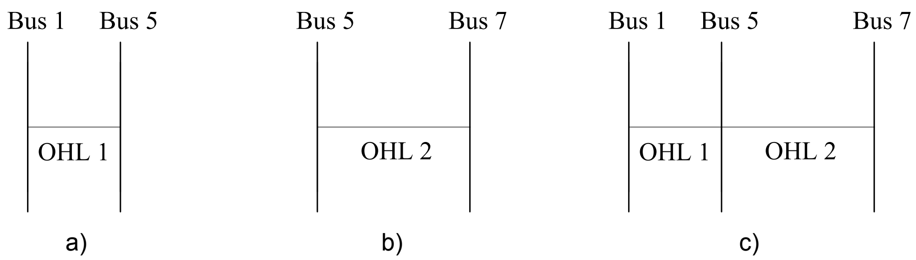

Figure 3.2: Circuit schematics of OHL 1 and 2 separately in a) and b) and the two OHLs combined in c).

The results of a frequency scan seen from Bus 5 in Figure 3.2 a), b) and c), in terms of impedance magnitude and angle as a function of the harmonic order, are shown in Figure 3.2. Since the system is in open circuit, the first resonance point is a series resonance.

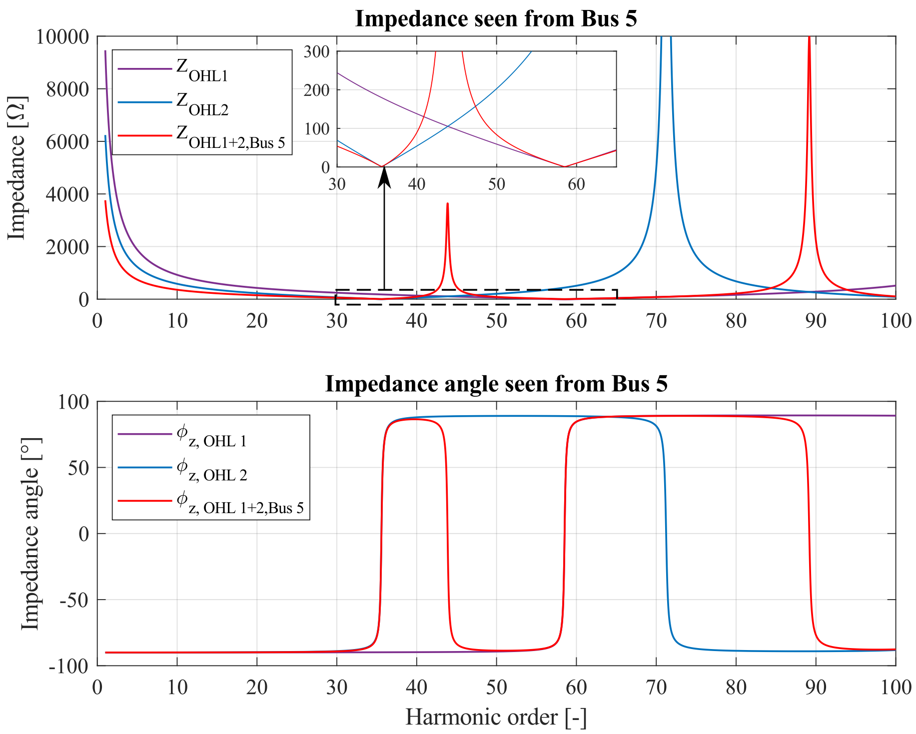

Figure 3.3: Harmonic impedance magnitude and angle, of the three cases, seen from Bus 5.

In Figure 3.3 it is visible that OHL 2 has a lower series resonance frequency (near the 35^{th} harmonic), compared to OHL 1 (near the 58^{th} harmonic), due to a longer line length. Moreover, it can be observed that when a series resonance occurs, the impedance angle goes from $-90°$ to $90°$, and opposite when a parallel resonance occurs.

For case c) where both OHLs are connected, the two OHLs are connected in parallel observed from Bus 5. As the two OHLs are in parallel, the series resonance points appears at the series resonance points of the individual OHLs. This can be seen in the zoom in Figure 3.3. This can be explained from the fact that when one of the OHLs has a series resonance, a low impedance path is created. Therefore, the two series resonance points in case c) are the same as for each of the individual OHLs.

For case c), a parallel resonance point is present at the 43^{rd} harmonic order as seen in Figure 3.3. The parallel resonance occurs when the impedance magnitudes of the two OHLs are equal with opposite impedance angle which can be verified from Figure 3.3. At the 43^{rd} harmonic order OHL 1 has a capacitive impedance angle, while OHL 2 has an inductive impedance angle as seen in the impedance angle plot. Considering the zoom, it can be seen that OHL 1 and OHL 2 intersects at the 43^{rd} harmonic order, which means that the impedance magnitudes are equal.

The reason for this can be explained by simplifying the two lines to a resistive and reactive element, as shown in Figure 3.4.

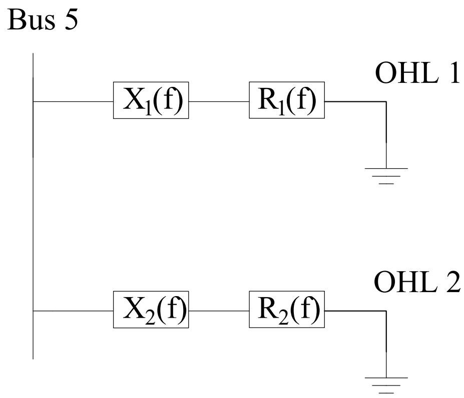

Figure 3.4: Simplified representation of the OHL models seen from Bus 5 in case c).

The parallel impedance of the simplified model is shown in Equation 3.1.

$$Z = \frac{(R_1(f) + jX_1(f)) \cdot (R_2(f) + jX_2(f))}{(R_1(f) + jX_1(f)) + (R_2(f) + jX_2(f))} \tag{3.1}$$

Equation 3.1 can be simplified for a parallel resonance, which occurs when $X_1 = -X_2$. Therefore, at a parallel resonance, the imaginary part of the impedance is infinite. Therefore, the magnitude is determined by the real part of the impedance. The real part of the impedance as a function of frequency can be seen in Equation 3.2.

$$Re(Zpar., resonance) \approx \frac{(X_1(f_0))^2 + R_1(f_0)R_2(f_0)}{R_1(f_0) + R_2(f_0)} \tag{3.2}$$

Here it is visible that the impedance depends on the reactance and resistance at the parallel resonance. For larger reactance values, the impedance is larger, as it rises with the square. Even though the resistance is increasing with frequency due to skin effect, the reactance is still dominating. This is the reason for the parallel resonances are increasing in magnitude with frequency, as seen in Figure 3.3.

Previously, the impedance analysis was performed seen from Bus 5. In order to analyse the impact of which bus the impedance is seen from, a frequency scan is performed on the combined circuit in Figure 3.2(c) in open circuit. The impedance magnitudes and angles as a function of the harmonic order, seen from Bus 1, 5 and 7, are shown in Figure 3.5. Since the system is in open circuit, the first resonance point is a series resonance.

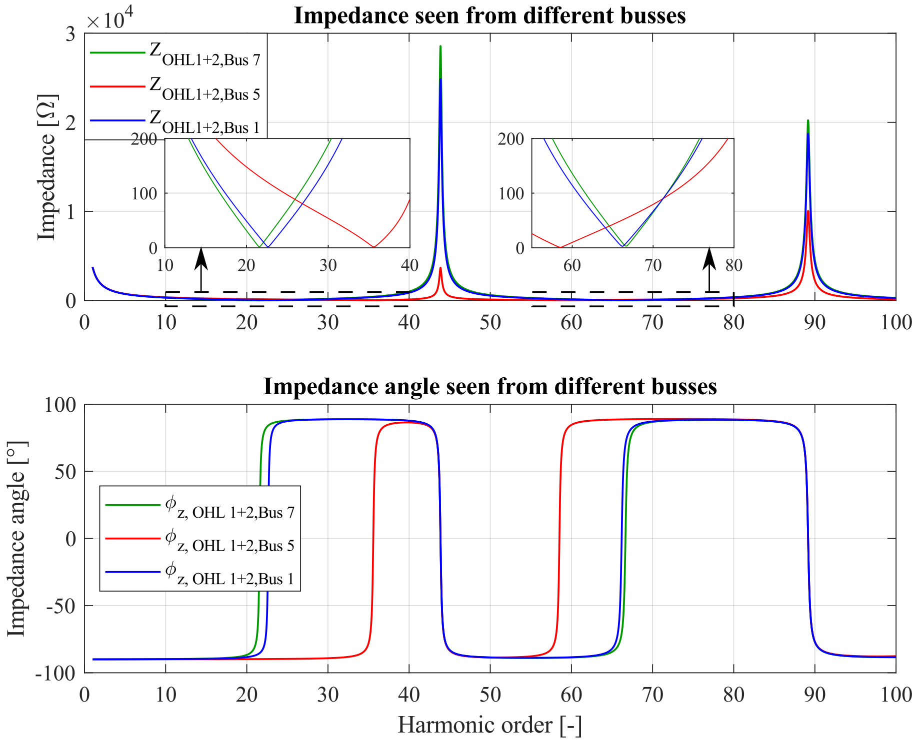

Figure 3.5: Harmonic impedance magnitude and angles as a function of the harmonic order seen from Bus 1, 5 and 7.

From Figure 3.5, it is visible that the impedance characteristics are almost identical seen from Bus 1 and 7. The small difference is due to OHL 1 and 2 being modelled as two different line types and two different lengths. The impedance characteristic seen from Bus 5 has different series resonance points compared to the other busses. However, the parallel resonance points occurs at the same frequencies for the three busses, since it is a radial system. This has been shown mathematically using a nominal π-model in Appendix B. However, this characteristic would change if the system is no longer radial.

3.2.2 Radial System Analysis with External Grid

The frequency scan of the radial system including the external grid seen from Bus 1, 5 and 7 are visualised in Figure 3.6.

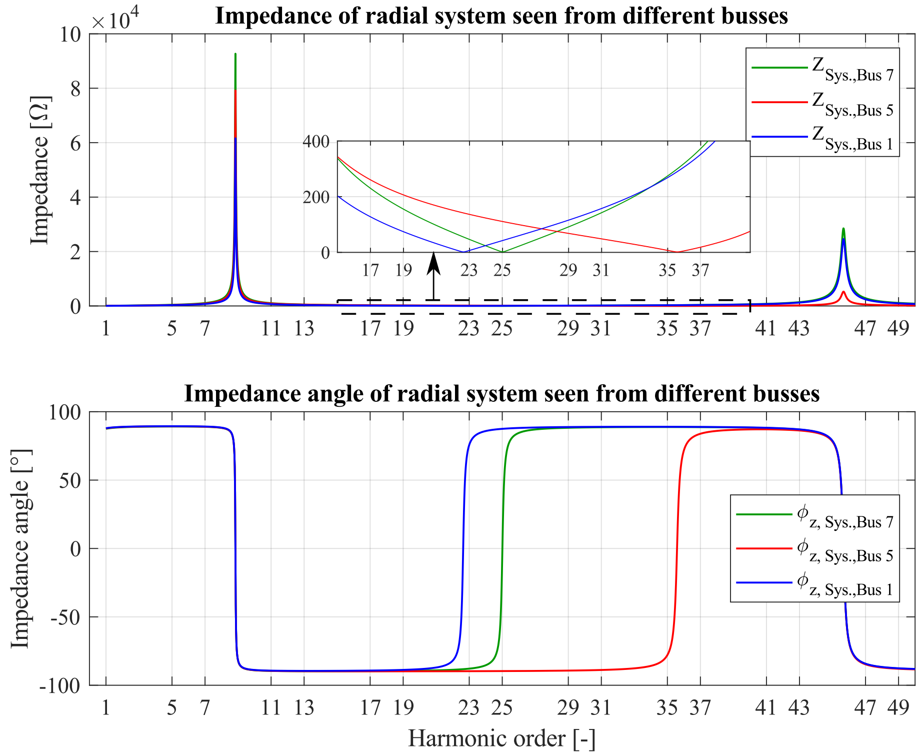

Figure 3.6: Harmonic impedance magnitudes and angles of the radial system including external grid as a function of the harmonic order seen from Bus 1, 5 and 7.

Since the system is no longer in open circuit, the first resonance point is a parallel resonance. Furthermore, the resonance frequencies are shifted to lower orders, due to the grid impedance.

Additionally, it can be seen that the first series resonance seen from Bus 1 is the exact same as in open circuit, whereas the series resonance from Bus 7 has changed. This is explained in Appendix B.2, where it is shown that the series resonance seen from Bus 1 is independent of the grid impedance.

3.3 Underground Cable Analysis

In this analysis, the OHLs in Line 1 and 2 are replaced by UGCs with equivalent lengths of the previous lines of 25.3 km and 41.6 km, respectively. The cable type utilised in both lines is the same, which is a 2500 mm^2 Cu cable with the parameters presented in Table A.3 in Appendix A.2 [21]. The cables are placed in a trefoil configuration and the electrical parameters are given in Table 3.2.

Table 3.2: Electrical parameters of a 2500 mm^2 Cu cable when arranged in a trefoil.

Conductor Type	**Resistance [Ω/km]**	**Inductance [mH/km]**	**Capacitance [µF/km]**	**Conductance [µS/km]**
2500 mm^2 Cu	0.0126	0.3170	0.2111	1.5109

To analyse the impact of replacing OHLs with UGCs, the following scenarios will be analysed:

- Line 1 and 2 as OHLs
- Line 1 is an UGC and Line 2 is an OHL
- Line 1 is an OHL and Line 2 is an UGC
- Line 1 and 2 as UGCs

The frequency scans of the radial system seen from Bus 7 of the cases are compared to the frequency scan of the original system with both lines as OHLs. The frequency scans are shown in Figure 3.7.

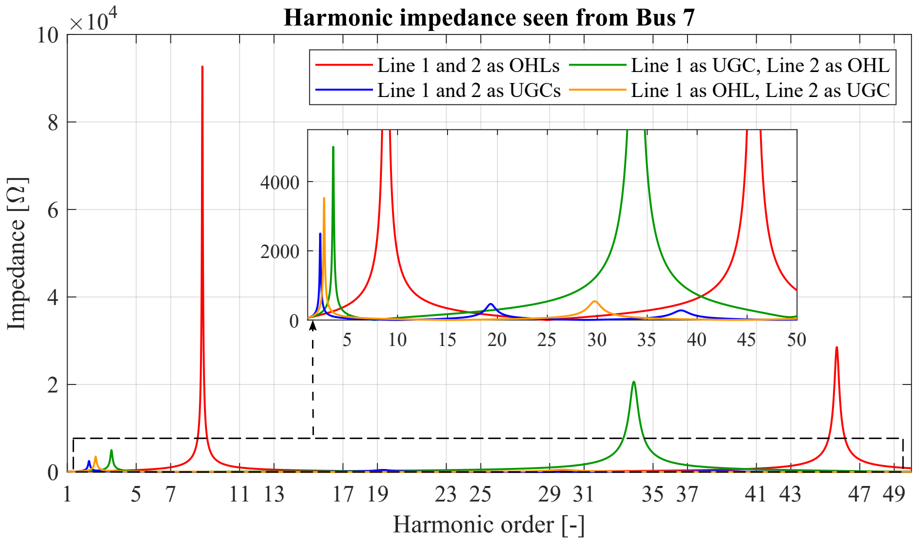

Figure 3.7: Comparison of impedance from frequency scan of the radial system seen from Bus 7, when composed by OHLs, UGCs and a combination of an OHL and an UGC.

From Figure 3.7 it can be seen, that the parallel resonance frequencies are shifted to lower frequencies when introducing UGCs in the system. The largest shift, compared to the system with OHLs, occurs when both Line 1 and 2 are replaced by UGCs. The second largest shift occurs when Line 2 is replaced by an UGC. The smallest shift occurs when only Line 1 is replaced by an UGC. This is expected, as Line 2 is longer than Line 1, hence changing Line 2 to an UGC will have a greater impact than changing Line 1.

Additionally, it can be observed that the first parallel resonance peak impedance gets more damped with an increasing amount of UGCs installed. The first parallel resonance impedance peak magnitude of the system with OHLs is 92.69 kΩ. In the system with both lines installed as UGCs the first parallel resonance peak magnitude is 2500 Ω. This significant damping is due to the electromagnetic behaviour of cables. Due to both circulating currents and induced voltage in the sheath of the cable higher losses occurs, which can be seen as a larger series resistance. [22]

The same significant damping can be observed for the second peak, when both Line 1 and 2 are UGCs and when only Line 2 is an UGC. However, when Line 1 is an UGC and Line 2 is an OHL, the second parallel resonance peak impedance is not significantly damped. This could indicate that the second peak is more dependent on the parameters of Line 2.

This could be explained from the fact that the impedance is seen from Bus 7, which is closer to Line 2 and that Line 2 is longer than Line 1.

3.4 Harmonic Propagation Analysis

The harmonic propagation in the radial system can be analysed utilising the harmonic penetration method. A harmonic current source is required for the harmonic penetration method to work and the results of the method is the harmonic voltages and currents. The system analysed is the radial system with a harmonic current source in Bus 7 as shown in Figure 3.1.

As described in Chapter 2, the frequency scan is normally made, by injecting 1 pu current into the system in order to calculate the impedance. Therefore, if 1 pu current is injected in the associated bus it is expected that the harmonic voltage from harmonic penetration will have same values as the impedance. From the PowerFactory manual, it not clear how the methods are performed. To clarify that the frequency scan and harmonic penetration works as expected, the methods are compared with a harmonic current source in Bus 7. The harmonic current source is injecting 1 kA in Bus 7 for the harmonics specified in Section 3.1. The harmonic voltage and impedance curve seen from Bus 7 are compared as seen in Figure 3.8.

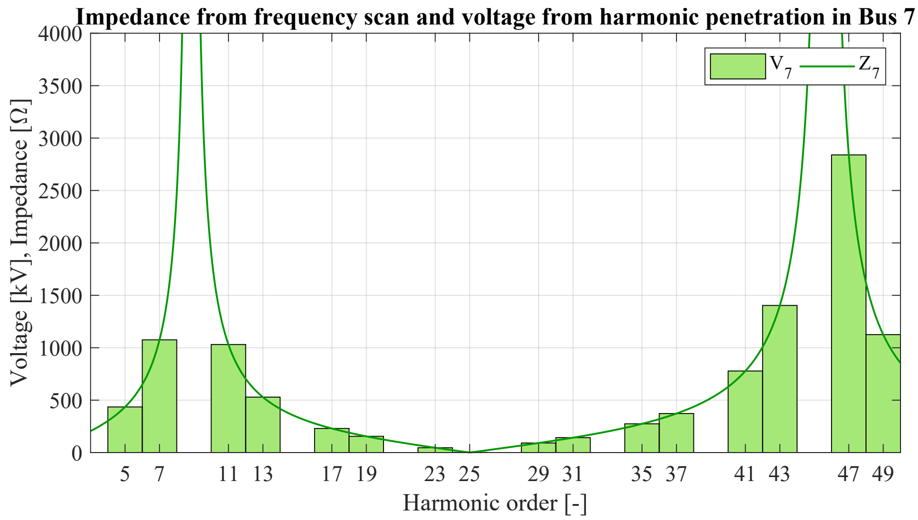

Figure 3.8: Frequency scan and harmonic penetration methods compared in Bus 7 with a harmonic current injected into Bus 7.

From Figure 3.8 it is visible, that the impedance and voltage has the same value on the y-axis in Ω and kV. This shows that the frequency scan in PowerFactory is performed using a current injection of 1 A for each frequency.

The frequency scan and the harmonic penetration only give the same results in the bus, where the harmonic current sources is connected. The harmonic voltages in Bus 1, when injecting the harmonic current in Bus 7 is compared to the harmonic impedance in Bus 1 as seen in Figure 3.9.

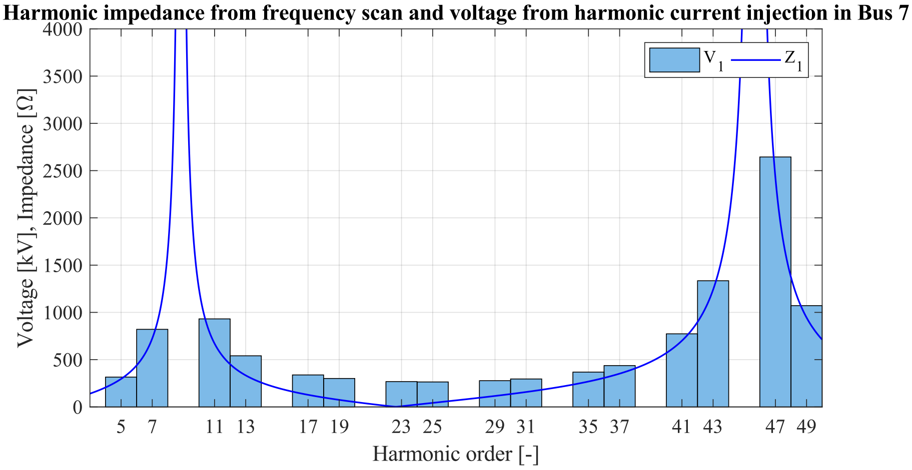

Figure 3.9: Frequency scan and harmonic penetration methods compared in Bus 1 with a harmonic current injected into Bus 7. Where Z_1 is the harmonic impedance in Bus 1.

From Figure 3.9 it is visible, that the voltage no longer follows the impedance characteristic directly at the harmonic orders. However, a tendency between the harmonic voltage and the harmonic impedance can be observed, as the lines have a short electrical distance.

In the impedance matrix shown in Equation 2.7 in Chapter 2, the impedance from a bus (e.g. Z_1) correspond to the self impedance, and the impedance between two busses (e.g. Z_{7-to-1}) correspond to the off-diagonal impedance. Therefore, in order to obtain the exact voltage in a bus different from the bus of injection the off-diagonal impedance has to be used. The off-diagonal impedance is obtained in PowerFactory by selecting the two busses of interest. The off-diagonal impedance can then be defined utilising the mutual data. The harmonic voltages in Bus 1, when injecting the harmonic current in Bus 7 is compared to the off-diagonal impedance from Bus 7 to 1 as seen in Figure 3.10.

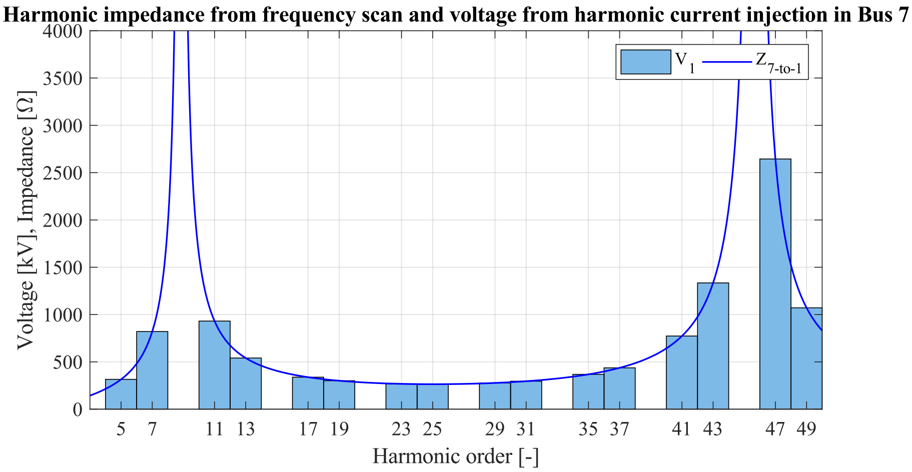

Figure 3.10: Frequency scan and harmonic penetration methods compared in Bus 1 with a harmonic current injected into Bus 7. Where Z_{7-to-1} is the off-diagonal impedance between Bus 7 and 1.

From Figure 3.10 it is visible, that the off-diagonal impedance from Bus 7 to 1, Z_{7-to-1}, corresponds to the harmonic voltage measured in Bus 1, with a harmonic current source connected in Bus 7. This shows that utilising the off-diagonal impedance between busses the harmonic voltage between busses in a radial system can be predicted.

Furthermore, the voltages and currents in the system is analysed using the harmonic penetration method. The harmonic voltages and currents in Bus 1, 5 and 7 are shown in Figure 3.11.

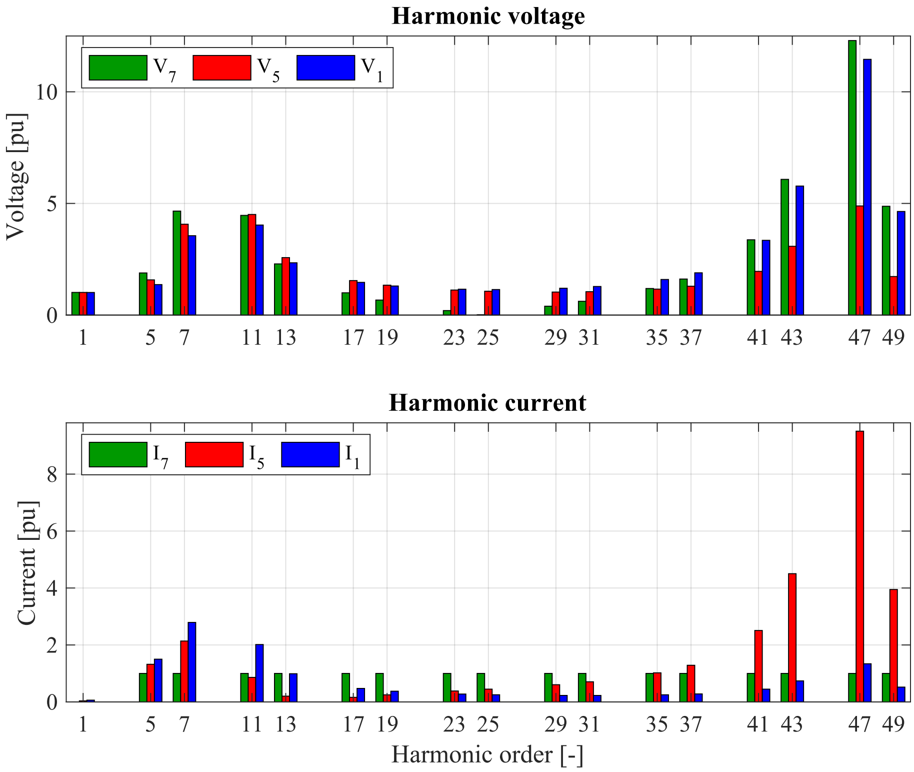

Figure 3.11: Harmonic voltages and currents as a function of the harmonic order, seen from Bus 1, 5 and 7.

The harmonic current source injects 1 pu directly at Bus 7, which determines the harmonic current at Bus 7 for the specified harmonic orders. Additionally, the harmonic currents in Bus 1 and 5 rises with the same tendency as the voltage rise. For example, the currents are generally higher around the parallel resonance frequencies (the 9^{th} and 45^{th}). This is a result of the charging current from the line's capacitance, which increases when the voltage rises and opposite when the voltage decreases.

As seen in Figure 3.11, the harmonic voltage at the 47^{th} harmonic order is higher in Bus 1 and 7 compared to Bus 5. This characteristic can be explained by dividing the OHLs into intersections to measure the voltage and current along the line. The schematic of the system with intersections is shown in Figure 3.12. From Bus 7 to 5, the intersections are named A1 to A9, and from Bus 5 to 1, the intersections are named B1 to B5. The intersections are named based on the harmonic propagation from Bus 7 to 1.

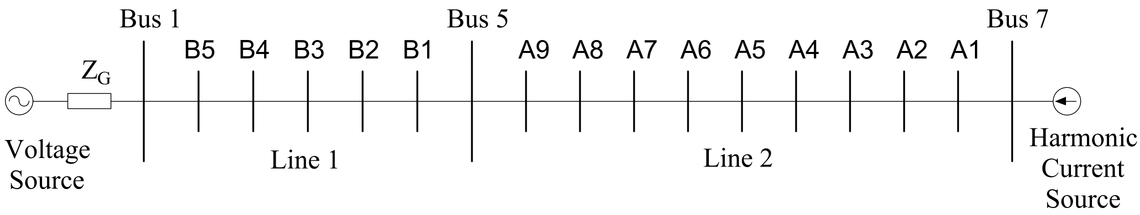

Figure 3.12: Circuit schematic of the radial system with intersections.

In Figure 3.13 the harmonic voltages, currents and phase angles of the intersections between Bus 1 and 7 are visualised. The phase angle measured is the angle between the voltage and current. The harmonic voltage is measured from Bus 7 to 1 to follow the harmonic propagation, since the harmonic current source is connected at Bus 7.

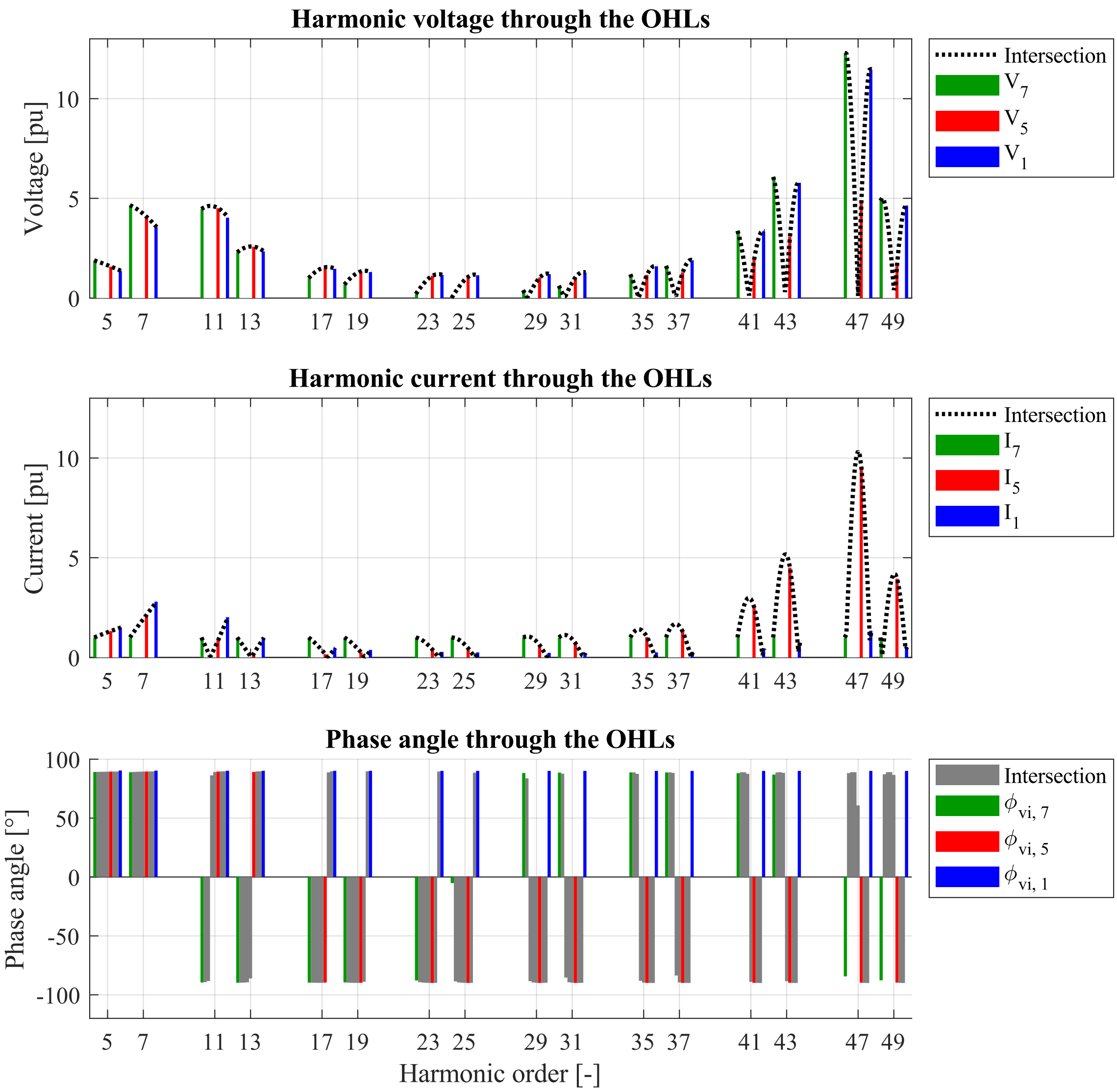

Figure 3.13: Harmonic voltages, currents and phase angles as a function of the harmonic order along the lines from Bus 7 to Bus 1.

From Figure 3.13 it is visible that the voltage and current magnitude through a line follows the norm of a sine wave. However, there is a phase shift between the harmonic current and voltage, which means that when the voltage peaks, the current is at a minimum and opposite. When the voltage or current magnitude crosses the minimum, a phase shift appears. At lower frequencies, the variations through the lines are small, since the wavelength is large. Oppositely, the variations are larger for higher order harmonics as the wavelength is smaller. The voltage is lower in Bus 5 at the 47^{th} harmonic order, since it is close to the minimum of the sine wave, while the voltages in Bus 1 and 7 are close to the peaks. Regarding the current at the 47^{th} harmonic order, the opposite can be observed.

In [23], the harmonic propagation through a line is explained using a circle as shown in Figure 3.14, with current on the x-axis and voltage on the y-axis. The harmonic propagation through a line follows the circumference of the circle in an anticlockwise direction. The concept of harmonic propagation using the circle is new and therefore it is still not completely validated. Additionally, it has only been used in simple radial systems. However, it can help to explain the tendencies of harmonic propagation, thus it will be used to explain harmonic propagation in further analyses in this report.

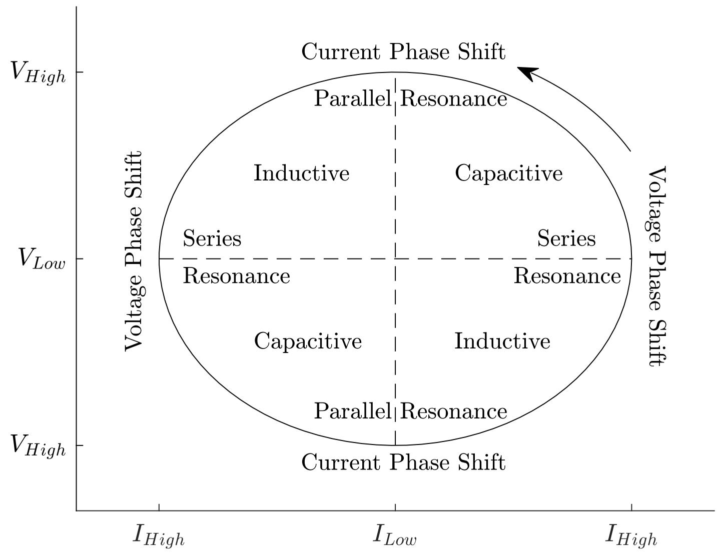

Figure 3.14: Harmonic propagation through a line. [23]

This graphical representation helps visualising the harmonic propagation of voltages and currents through a line, with corresponding phase shifts. The current phase shift occurs when the voltage is high and the current is low. When the current phase shift occurs, the current changes from leading the voltage to lagging, hence changing region from capacitive to inductive. From the impedance angle it is shown that a parallel resonance occurs when changing from capacitive to inductive. The voltage phase shift occurs when the current is high and the voltage is low. Here a series resonance occurs and the system changes from inductive to capacitive.

During this study, a MATLAB script has been developed, which utilises the measured data from PowerFactory to generate a circle representation of a specified harmonic order. The data points are represented on the circle based on the voltage and current magnitudes, as well as the phase angle between voltage and current. Since the harmonic propagation is analysed from Bus 7 to Bus 1, the first data point analysed is Bus 7. If the phase angle between voltage and current is 90°, the bus is located in the inductive region and if the phase angle is -90°, the bus is located in the capacitive region. In this study the initial inductive and capacitive regions are in the 2^{nd} and 3^{rd} quadrant of the circle. The initial quadrant could have been any of the four, but this was a choice that was made to always start on the left side of the circle. Additionally, when a phase shift occurs, a shift in the quadrant of the circle occurs. Since the voltages and currents does not reach the same magnitudes, the data points follows an ellipse. In this study the data is normalized, which means that the ellipsis is turned into a circle with the same width and height. In order to determine the factor required to normalise the data points, Equation 3.3 is utilised, which is the ellipse equation. [24]

$$\frac{I_{data1}^2}{I_{factor}^2} + \frac{V_{data1}^2}{V_{factor}^2} = 1, \qquad \frac{I_{data2}^2}{I_{factor}^2} + \frac{V_{data2}^2}{V_{factor}^2} = 1 \tag{3.3}$$

As seen in Equation 3.3, two data sets containing voltages and currents are utilised. The two equations are then solved in order to determine the normalisation factors for voltage and current respectively. The normalisation factors are used to draw the circle. The circle is made from two measurements, which means that it is possible to utilise two bus terminals, which removes the need for the intersection points along the line. This has a practical application in terms of estimation of over-currents and over-voltages in the lines. However, in this report the intersection points are plotted to showcase the harmonic propagation through the line.

The harmonic propagation of the 47^{th} harmonic order is visualised utilising the circle as seen in Figure 3.15. The busses of the radial system are marked on the circle. From Bus 7 (green) to Bus 5 (red), the nine busses A1 to A9 from Figure 3.12 marked with grey. Likewise, the five busses between Bus 5 (red) and Bus 1 (blue), B1 to B5 is also marked with grey. It is visible how the voltage and current changes through the radial system. Additionally, it can be seen that both a voltage and two current phase shifts appears in the radial system at the 47^{th} harmonic order.

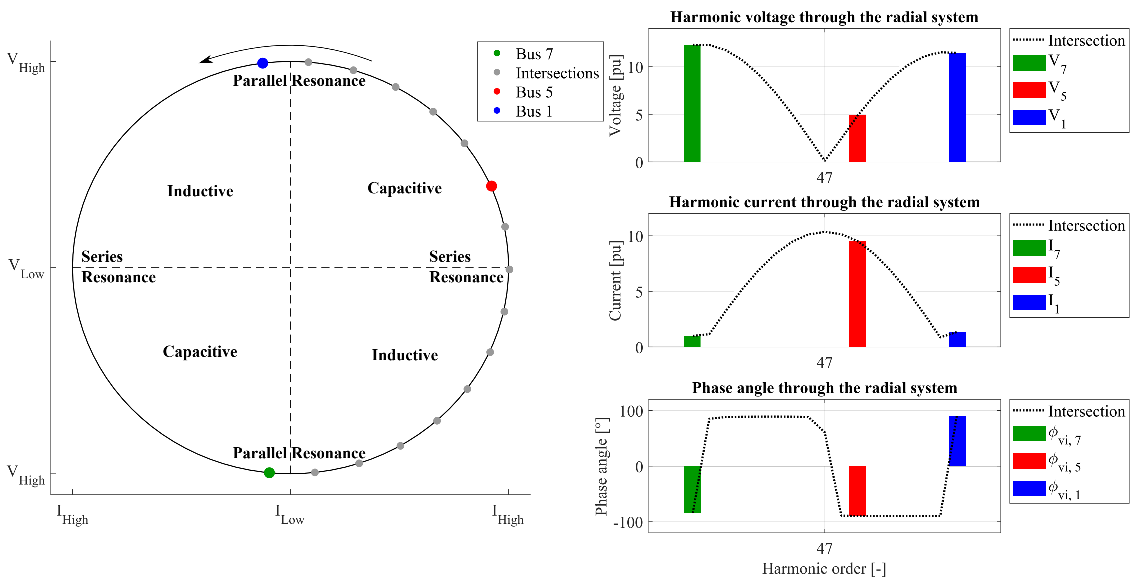

Figure 3.15: Harmonic propagation of the 47^{th} harmonic order through the radial system.

The phase angle between the voltage and current can be utilised to determine what region the busbar is located in. If the phase is negative, the busbar is located in the capacitive region and opposite. As the voltage changes through a line, it is evident that the voltage in a line can be higher than the voltage measured at the bus terminals. Therefore, this should be taken into consideration in the design and analysis of the lines.

To visualise how the resonances appears through the line, the series resonance of the 47^{th} harmonic order is analysed. From Figure 3.15, the series resonance appears at the eight intersection, which is at the intersection A8. To show this, the circuit from A8 to the grid is analysed. The circuit schematic of this system is shown in Figure 3.16.

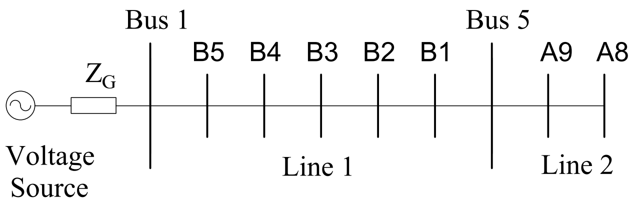

Figure 3.16: Circuit schematic of the radial system from the intersection A8 to the grid.

The harmonic impedance, when performing a frequency scan in A8 in Figure 3.16, can be seen in Figure 3.17. As the frequency scan is made from A8 to the grid, which has a reduced line length compared to the full radial system, the resonance frequency is shifted to higher frequencies. Therefore, the first parallel resonance has shifted from the 9^{th} harmonic order to the 13^{th} harmonic order.

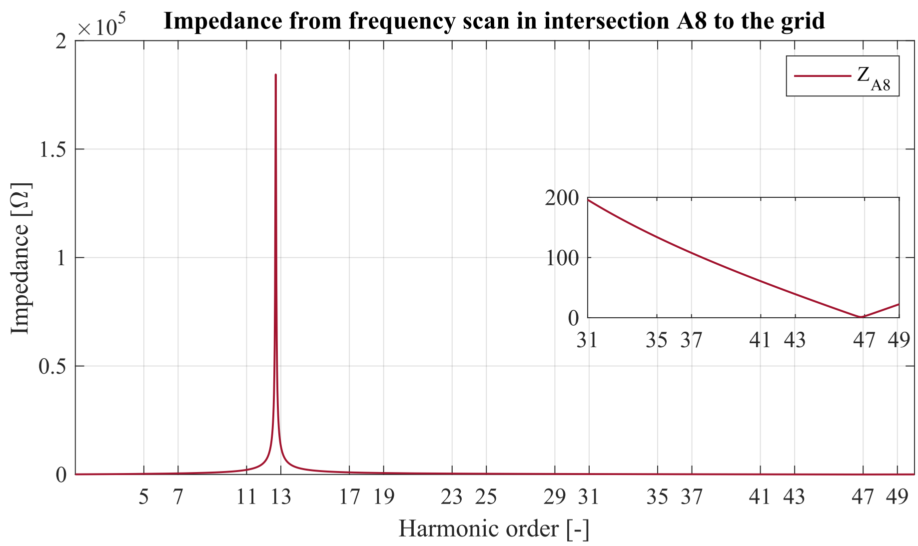

Figure 3.17: Impedance of from A8 to the grid in the radial system.

From Figure 3.17 it can be seen that a series resonance point appears at the 47^{th} harmonic order. Therefore, the harmonic current propagation through the radial system at the 47^{th} harmonic order, will reach a series resonance at intersection A8. Hence a high current and low voltage is observed at the intersection A8. Additionally, it can be seen that a parallel resonance is located close to the 13^{th} harmonic order. Therefore, a high voltage and low current appears at the intersection A8 for the 13^{th} harmonic order.

3.4.1 Underground Cable Analysis

The harmonic propagation of the system with Line 1 and 2 as UGCs is visualised utilising the circle theory. The characteristics of the 47^{th} harmonic order is shown in Figure 3.18.

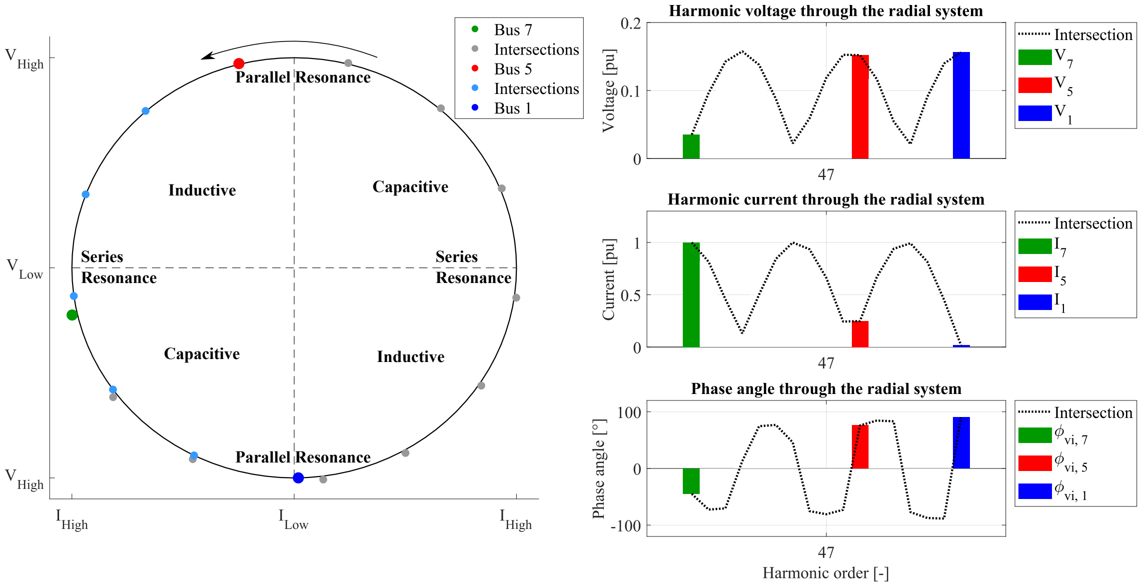

Figure 3.18: Harmonic propagation of the 47^{th} harmonic order through the radial system with Line 1 and 2 as UGCs.

In Figure 3.18 it is visible, that the harmonic propagation of the 47^{th} harmonic order rotates more than one round in the circle. Therefore, the intersections between Bus 7 and 5 are highlighted with grey, while the intersections between Bus 5 and 1 are highlighted with light blue. The large rotation can be explained from the wavelength frequency, which is lower in cables. From this, it can be seen how the voltage in the lines can be greater than the measured voltage in the busses. However, as this is for a the 47^{th} harmonic order, which is a large harmonic order, the voltage of this will be small compared to the more critical lower order harmonics, and the larger voltage along the line for the 47^{th} harmonic order is not critical for the design of the lines. For lower order harmonics, a full rotation does not occur in the circle in this specific system due to a shorter wavelength. If a half circle rotation is obtained, the voltage along the line must reach the maximum of the circle before reaching the receiving end bus. However, for the 7^{th} harmonic order to reach a half round in the circle, the UGCs should be three times the length of the radial system. From this analysis it can be concluded, that the circles in theory can be utilised to estimate the voltage along a line. However, this will only be a problem for very long lines and at higher order harmonics, which have a low magnitude and therefore these are not relevant.

3.5 Harmonic Source Analysis

The influence of the placement of the harmonic current sources in the radial system is analysed. Additionally, the influence of the injection angles of the harmonic current sources on the harmonic propagation is analysed. The harmonic penetration method is used, with the harmonic current source, described in Section 3.1, placed in either Bus 1 or 7. The circuit of the two cases can be seen in Figure 3.19. The cases are referred to as orange and green case and represents which of the harmonic current sources is connected, in the following two scenarios.

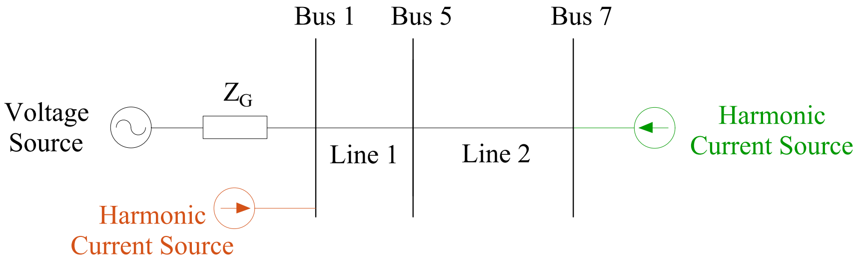

Figure 3.19: Circuit schematic of the radial system with harmonic current source placed in Bus 1 (orange) or in Bus 7 (green).

The harmonic voltage magnitude and phase measured in Bus 7 as a function of the harmonic order for the two scenarios are shown in Figure 3.20. Here it can be seen that harmonic voltages has the same tendency, whether the source is placed in Bus 1 or 7. However, from the 29^{th} harmonic order and above, the harmonic voltage angle has shifted 180°.

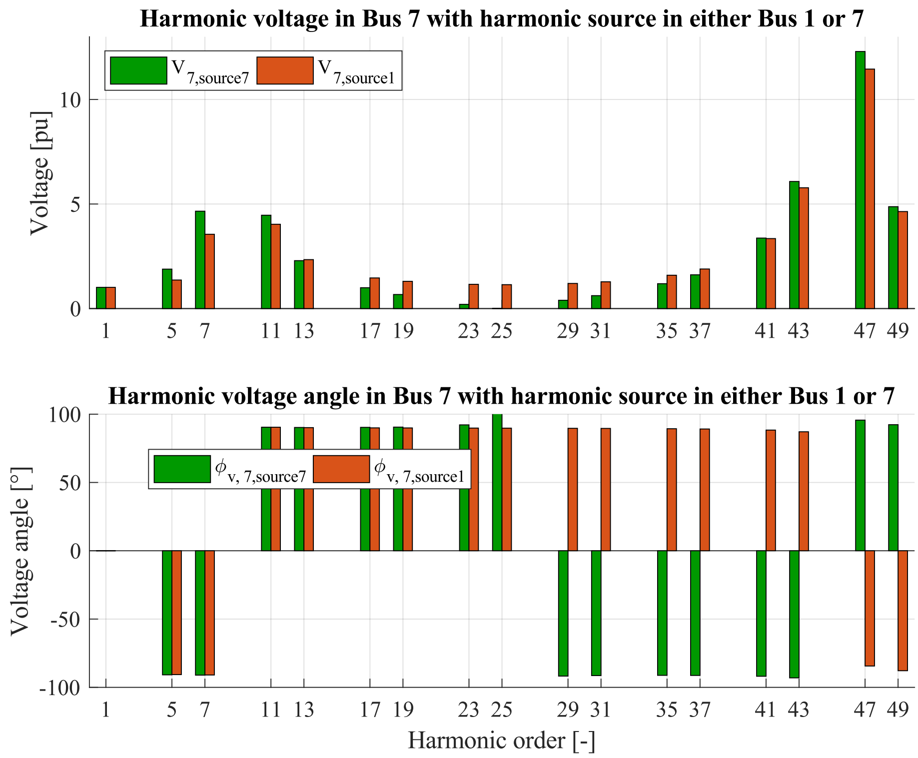

Figure 3.20: Harmonic voltage magnitude and angle in Bus 7, with a harmonic current source placed in Bus 1 (orange) or Bus 7 (green).

The harmonic voltage magnitudes and angles from Figure 3.20 can be converted to phasors. Phasors can help visualise how the harmonics will interact if they are injected in the same system. The phasors of the two individual harmonic voltages are shown in Figure 3.21.

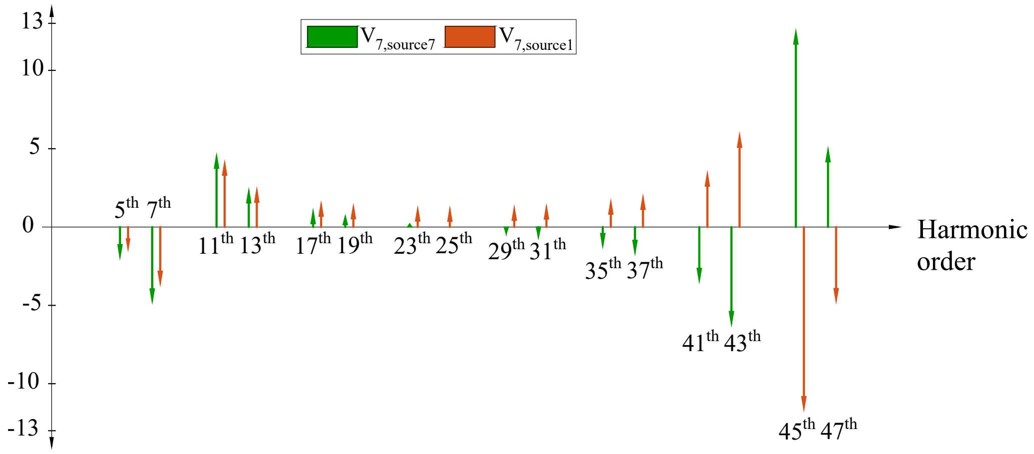

Figure 3.21: Phasors of harmonic voltage measured in Bus 7, with a harmonic current source placed in Bus 1 (orange) or Bus 7 (green).

From Figure 3.21 it is visible that the lower order harmonic voltages are in phase, while the higher order harmonic voltages are 180° out of phase. Therefore, if the two sources both are connected in the system it is expected that lower order harmonic voltages will add up, while the higher order will cancel out.

To verify, that the lower order harmonics will add up and the higher order harmonics will counteract each other, the system has been analysed with a harmonic current source in both Bus 1 and 7. The harmonic voltage magnitudes and phases in this case are shown in Figure 3.22.

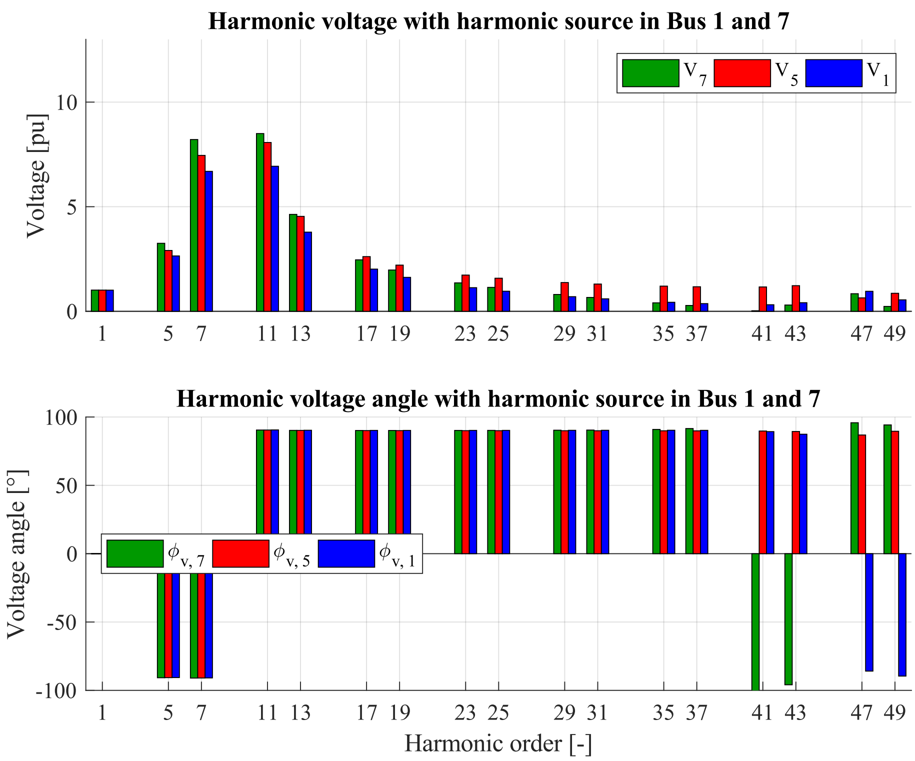

Figure 3.22: Harmonic voltage magnitudes and angles in Bus 1, 5 and 7, with a harmonic current source placed in both Bus 1 and 7.

From Figure 3.22 it is visible that lower order harmonic voltages are increased, while higher order harmonic voltages are decreased, as expected. As an example, the phasors of the 41^{th} harmonic order in Figure 3.21 have the same magnitude, but with opposite polarity when seen from Bus 7. Therefore, when injecting in both Bus 1 and 7 the phasors cancel out seen from Bus 7, which is why the harmonic voltage in Bus 7 at the 41^{th} harmonic order is zero, as seen in Figure 3.22. The harmonic voltage of the system with both sources is equal to the sum of the harmonic voltages of the two systems with one source each. This shows that the superposition principle applies. If non-linear devices was part of the system, superposition principle could not be used.

The influence of having different injection angles is analysed. In the previous analyses, the angle of the harmonic injections was always 0°. In this analysis the harmonic injection is analysed with different angles. Therefore, the previous case with a harmonic current source in Bus 1 and 7 with injection angles of 0° apart from each other is compared to having a harmonic current source in Bus 1 and 7 with injection angles of 45° apart from each other. The harmonic voltage magnitudes from this analysis in Bus 7 are compared for the two cases as seen in Figure 3.23.

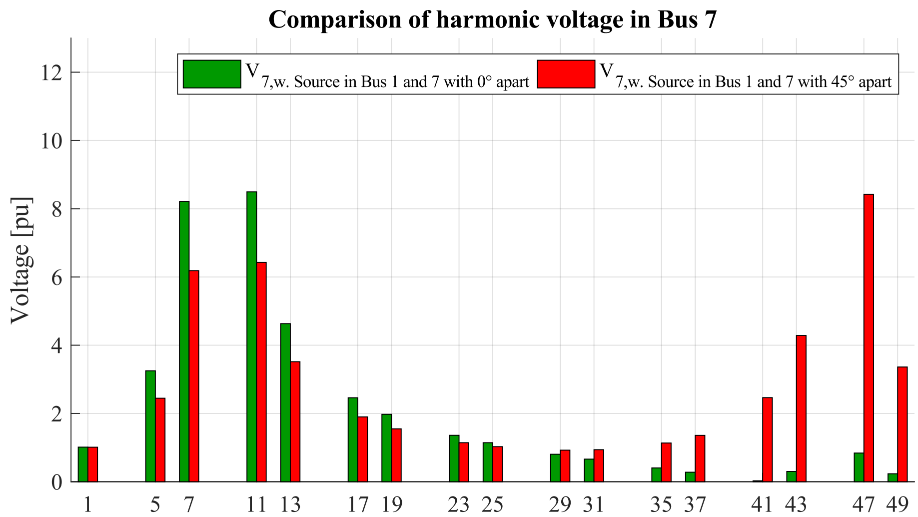

Figure 3.23: Comparison of harmonic voltage magnitude in Bus 7. The harmonic current injection in Bus 1 has an angle of 0°, while Bus 7 has an angle of either 0° (green) or 45° (red).

From Figure 3.23 it can be seen that the lower order harmonics in Bus 7 are decreased, while the higher order harmonics increased. This is a results of the 45° shifting of the harmonic currents in Bus 7, which shifts the point on the sine wave of the voltage. Before the shifting, the voltage from each source was in phase for lower order harmonics and 180° shifted for higher order harmonics. Therefore, a shifting results in a decrease in voltage for the lower order harmonics and an increase for higher order harmonics.

In power systems, the harmonic angles of injection are an unknown factor and no current method exist to measure them precisely. Therefore, in reality some harmonics will unknowingly cancel out and some will add up. From the simulations of the radial system it can be seen that if the harmonic currents are injected with the same angle, the harmonics will add for the lower order harmonics and cancel for the higher orders. This is caused by as the voltage changes through the line. If the angle of one of the sources is changed, the harmonics start to add at higher order harmonics and give a smaller increase for lower order harmonics. However, as the harmonic magnitudes of the harmonics in power systems in general decreases with $\frac{1}{n}$ [25], higher order harmonics will have lower magnitudes. Therefore, the above simulations can be misleading, since 1 kA are injected for each harmonic order. However, when injecting 1 kA for each harmonic order, the results are comparable. From the analysed radial system, it has been observed that the worst case scenario occurs when all harmonic current sources injects harmonic currents with the same angle, which will cause the lower order harmonics to add up. Therefore, all further simulations will be performed with harmonic current sources with an with an angle of 0°, to simulate the worst case.

3.5.1 Off-Diagonal Impedance

The harmonic penetration and frequency scan methods are also compared in the system with both a harmonic current source in Bus 1 and in Bus 7. This comparison is made in order to determine whether one method can be utilised to predict the harmonic voltage in a bus from the other method when having multiple harmonic current sources with different locations. The voltage is measured in Bus 5, V_5, utilising the harmonic penetration method. In order to obtain a voltage from the frequency scan method for comparison, the off-diagonal impedance from Bus 1 to Bus 5, Z_{1-to-5}, is multiplied by the injected harmonic current in Bus 1, resulting in a voltage V_{1-to-5}. The same is done for the off-diagonal impedance from Bus 7 to Bus 5, Z_{7-to-5}, resulting in a voltage V_{7-to-5}. The voltages V_{1-to-5} and V_{7-to-5} are added together in order to get the voltage in Bus 5. When adding the two voltages, the sign of the impedance angle should be taken into account. The absolute value of the addition is then utilised for comparison with the measured voltage in Bus 5 from the harmonic penetration method. The comparison is shown in Figure 3.24.

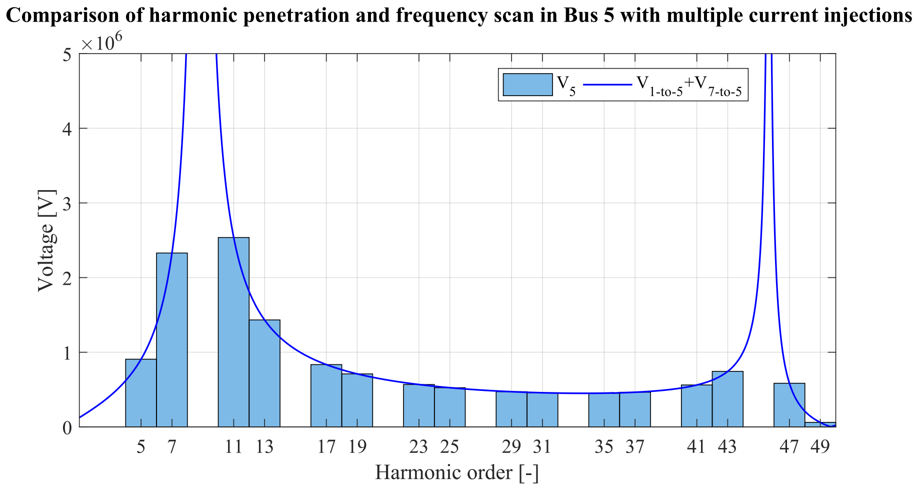

Figure 3.24: Harmonic voltages obtained from a harmonic penetration with harmonic current sources in Bus 1 and 7 compared to harmonic voltages obtained from the frequency scan method.

From Figure 3.24 it is visible, that the voltages follow each other. Hence, utilising the off-diagonal impedance and the magnitude of the injected currents, the frequency scan method can be utilised to predict the harmonic voltages in a bus.

It should be noted, that the harmonic current sources has the same phase angle. Moreover, the magnitude of the injected harmonic currents are 1000 A in Bus 1 and 1647 A in Bus 7. The different harmonic current magnitudes are utilised in order to validate, that the voltages from the harmonic penetration and the frequency scan methods are the same for different harmonic current source injection magnitudes.

Summary and Discussion

In this chapter a radial system with three busses from the *Example grid* was analysed. First a frequency scan was performed on the lines separately and then together in open circuit. This analysis was utilised to understand how the impedance plot changes depending on the line type, the length and the point of observation. Hereafter an external grid was included in the system and an impedance plot of the radial system were obtained seen from Bus 1, 5 and 7. These impedance plots were utilised as a reference, when changing the system throughout the chapter. Additionally, the impact of replacing the two OHLs in the radial system by UGCs was analysed. First one line at a time is replaced by UGCs and then both lines. From this analysis it was observed, that the more UGCs installed, the more the resonances were shifted towards lower frequencies.

Hereafter it was shown, that the off-diagonal impedance between two busses could be utilised to obtain the harmonic voltage in a bus different from where the harmonic current was injected. However, only the harmonic voltages were obtainable from the off-diagonal impedance. Therefore, in order to obtain the harmonic currents and the angle between the harmonic voltages and currents, the harmonic penetration method was utilised. It was observed that the harmonic voltage and current propagation follows the norm of a sine wave, which could be described utilising the circle shown in Figure 3.14.

The influence of replacing the OHLs with UGCs was also analysed regarding harmonic propagation. It was observed, that the circle theory was applicable. However, due to the lower wavelength frequency of UGCs compared to OHLs, the angular velocity in the circle per unit length was faster utilising UGCs.

In practice the circle theory is a tool for visualising the propagation of one harmonic order of the harmonic voltage and current. The circle between two busses can be obtained by doing measurements in the two busses, meaning that the intersection measurements utilised in this chapter are not required. Therefore, in theory for a radial system, two measurement points can be utilised to determine over-voltages in the lines at the harmonic orders of interest. However, for a harmonic order to reach half a round in the circle at lower order harmonics, the lines would have to be very long.

The location and number of harmonic current sources was also analysed. The first analysis conducted was with a harmonic current source in Bus 7, next with a harmonic current source in Bus 1 and lastly with a harmonic current source in both Bus 1 and Bus 7. In all three cases, the injected harmonic current magnitudes were 1 kA with an injection angle of 0°. From the two analyses with one harmonic current source it was observed, that for each harmonic order, the harmonic voltage angles changes through the system. This change is different for each harmonic order, as the wavelength gets shorter as the harmonic order increases. If both harmonic current sources are implemented, it was shown how the harmonic voltages cancelled each other at high order harmonic voltages and added at low order harmonic voltages due to the voltage phase shifting through the lines. Additionally, it was shown that the off-diagonal impedance could be used to determine the voltage in a specific bus with multiple harmonic current injections in the system.

An analysis regarding the harmonic current source angle was also performed, in the radial system with a harmonic current source in both Bus 1 and 7. The angle in the harmonic current source in Bus 7 was changed to 45°, while the harmonic angle in the source in Bus 1 was kept at 0°. This analysis showed, that the low order harmonic voltages were decreased compared to having both sources with an angle of 0° and opposite for the high order harmonics. Since low order harmonics are most critical in a power system the worst case scenario is when the harmonic current sources has the same angle. In reality, the angles of the harmonic emissions are unknown.

In the next chapter, a transformer will be implemented in the radial system analysed in this chapter. The results obtained in this chapter will be utilised as reference in order to analyse the impact of installing a transformer.

Harmonic Propagation through Transformers 4

In this chapter, a transformer is implemented in the radial system from Chapter 3. This is done in order to analyse the harmonic propagation through a transformer and between voltage levels.

An impedance analysis is performed, utilising the frequency scan method. The radial system with a 410/410 kV transformer implemented is analysed first. This is done in order to analyse the impact of implementing a transformer in the system without the influence of different voltage levels. Hereafter, the transformer is changed to a 410/145 kV transformer and an impedance analysis is performed in this system. Line 1 is kept at a voltage level of 400 kV, while Line 2 is changed to have a voltage level of 130 kV. This analysis is performed to analyse the impact on the harmonic impedance, when having different voltage levels in the system.

When the impact of different voltage levels are investigated, the influence of implementing UGCs on the different voltage levels is analysed in regards to the impedance. In order to limit the factors influencing the results, the line length and tower types are kept the same in both lines in order to focus on the voltage levels.

After the impedance analysis, harmonic propagation studies are conducted on the radial systems with a transformer implemented utilising the harmonic penetration method. First the system with the 410/410 kV transformer is analysed to investigate the impact of implementing a transformer on the harmonic propagation through a transformer without different voltage levels. The circle theory from Chapter 3 is applied in order to determine whether it can be applied to a radial system with a transformer. Then the system with the 410/145 kV transformer is analysed through a harmonic propagation study. The circle theory is also applied to determine if it can explain the harmonic propagation in this radial system with different voltage levels.

The harmonic propagation is also analysed in the system with the 410/145 kV transformer with the OHLs replaced by UGCs. This analysis is performed in order to analyse the impact on the harmonic propagation when installing UGCs on the different voltage levels.

4.1 410/410 kV Transformer System Impedance Analysis

The analysis is conducted with Line 1 and 2 as 400 kV OHLs and a 410/410 kV 350 MVA transformer. The voltage base values follows the transformer ratings throughout this chapter.

A transformer creates resonance with itself above 4 kHz [1]. However, since this analysis is performed up to 2500 Hz, this resonance within the transformer will not be visible in the results. Therefore the stray capacitance in the transformer is also not considered. The transformer parameters are based on [21] and shown in Table 4.1.

Table 4.1: Transformer parameters. [21]

Rated power [MVA]	350
Reactance [pu]	0.150
Resistance [pu]	0.00143
Iron core losses [pu]	3500
Magnetisation reactance [pu]	3572.2

An additional bus is implemented referred to as Bus T and the transformer is connected between Bus 5 and Bus T. The circuit schematic is shown in Figure 4.1.

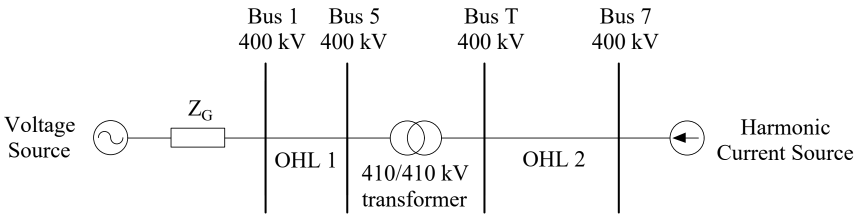

Figure 4.1: Circuit schematic of the radial system with a 410/410 kV transformer implemented between Bus 5 and Bus T.

The transformer model utilised is model 5, as described in Section 2.3.2. The transformer frequency dependent resistance, R_S, is given by Equation 4.1. [1]

$$R_S = R_{f_n}\left(1 + A_R\left(\frac{f}{f_n} - 1\right)^{B_R}\right) \tag{4.1}$$

Where R_{f_n} is the resistance at the nominal frequency, f_n, while A_R and B_R are default values dependent on the transformer size. The transformer frequency dependent inductance, L_S, is given by Equation 4.2. [1]

$$L_S = L_{f_n} A_L \left(\frac{f}{f_n}\right)^{B_L} \tag{4.2}$$

Where L_{f_n} is the inductance at nominal frequency, while A_L and B_L are default values dependent on the transformer size. The default values A_R, B_R, A_L and B_L are listed in Table 4.2 for different transformer sizes.

Table 4.2: Default values utilised to model transformers. [1]

Transformer type	$R_S(f)$		$L_S(f)$	
	A_R	B_R	A_L	B_L
20/0.4 kV, 250 kVA	0.2	1.5	1	-0.03
108/10.5 kV, 40 MVA	0.2	1.4	1	-0.02
220/110 kV, 200 MVA	0.2	1.6	1	≈0

The default values of the 220/110 kV 200 MVA transformer are used for the 410/410 kV transformer as the values of A_R and A_L are the same in the three types, B_R is varying very little and B_L is approaching zero as the transformer increases. Since the value of A_L is one and B_L is zero in the 220/110 kV transformer default values, the inductance is constant.

The transformer resistance factor is plotted as a function of frequency and shown in Figure 4.2.

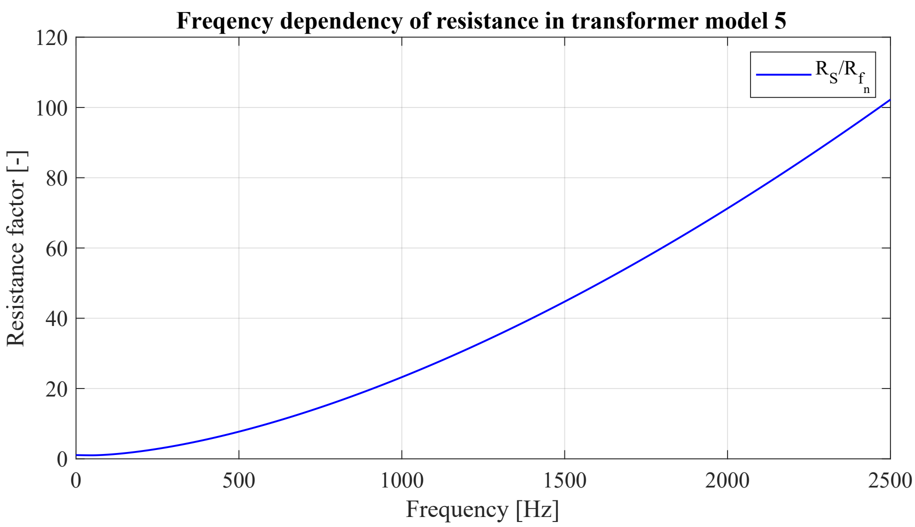

Figure 4.2: Frequency dependent resistance factor.

From Figure 4.2 it can be seen, that the resistance increases with frequency. Hence, the implementation of frequency dependent resistance in the transformer model has a damping effect on the harmonic impedance compared to a constant resistance. The influence of the frequency dependent and constant resistance transformer models are compared utilising the frequency scan of Bus T as seen in Figure 4.3.

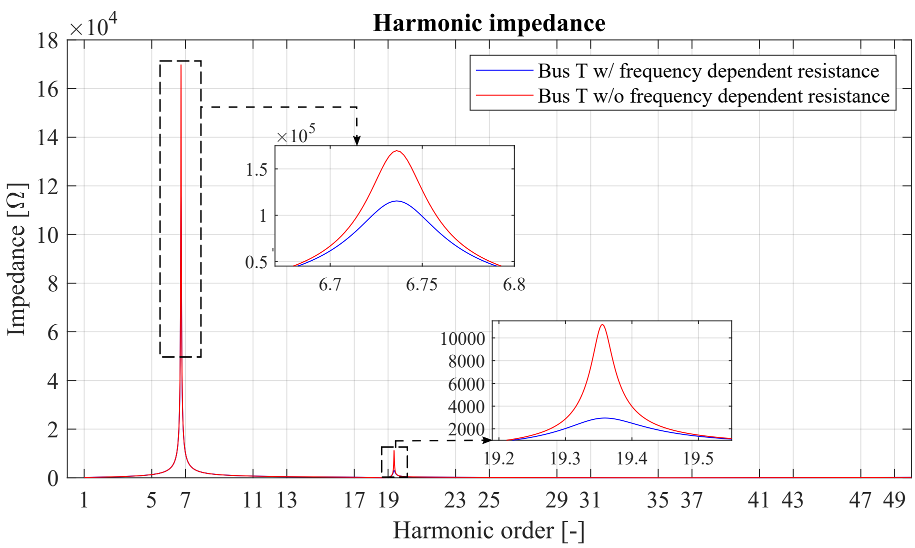

Figure 4.3: Comparison of the impedance as a function of the harmonic order with and without frequency dependent transformer resistance implemented seen from Bus T.

At the parallel resonance point close to the 7^{th} harmonic order, the impedance peak is damped by 34 % compared to the constant resistance. At the parallel resonance point close to the 19^{th} harmonic order, the impedance is damped by 74 %. This shows that the damping increases as the frequency increases which can be explained from the resistance factor in Figure 4.2.

To analyse the influence on the impedance when implementing a transformer in the radial system, two frequency scans, seen from Bus 7, are shown in Figure 4.4. The frequency scans are of the system with and without the 410/410 kV transformer.

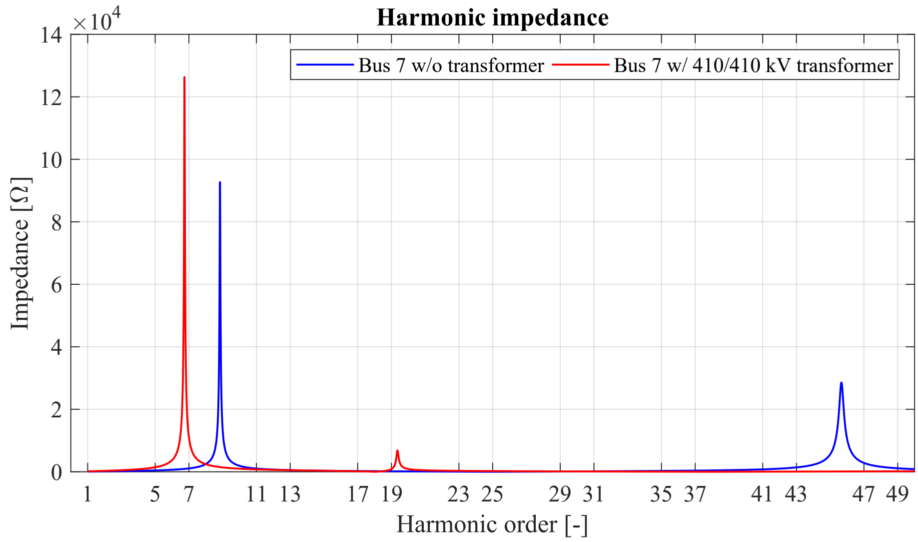

Figure 4.4: Comparison of the frequency scan with and without the 410/410 kV transformer.

From Figure 4.4 it can be seen, that the implementation of the 410/410 kV transformer, shifts the resonance points to lower orders of harmonics. This is due to the additional series impedance of implementing the transformer.

The second parallel resonance peak is significantly shifted to a lower frequency. This can be theoretically shown, by gradually reducing the transformer impedance, until it is zero where the two systems are equal. This is shown in Figure 4.5, where the frequency scan is made for with a transformer with 100 %, 80%, 60%, 40%, 20% and 0% of the transformer impedance.

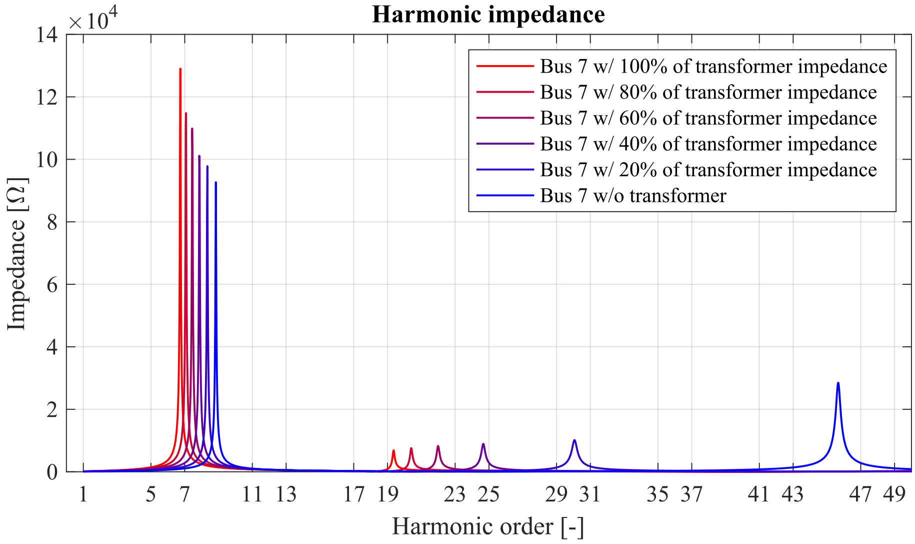

Figure 4.5: Comparison of the frequency scan of having a 410/410 kV transformer with 100 %, 80%, 60%, 40%, 20% and 0% of the transformer impedance.

This shows that the introduction of the transformer has a large influence on the second parallel resonance peak, and a smaller influence on the first parallel resonance peak.

4.2 410/145 kV Transformer System Impedance Analysis

Implementing a 410/145 kV transformer, the impedance observed between voltage levels can be analysed. The circuit schematic of the radial system with the 410/145 kV transformer is shown in Figure 4.6.

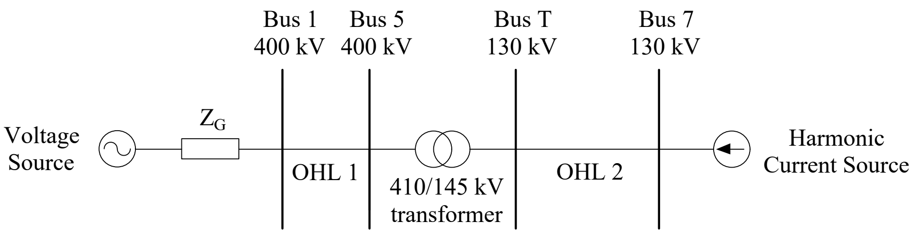

Figure 4.6: Circuit schematic of the radial system with a 410/145 kV transformer implemented between Bus 5 and Bus T.

OHL 1 and OHL 2 are modelled using the same tower types as in the 410/410 kV system with parameters given in Table 3.1. In reality, the same tower type would not be used for both 400 kV and 130 kV. In the *Example grid* the tower type D, shown in Figure A.2, is utilised at 130 kV. However, the assumption is made to make the OHLs in the systems comparable by using same actual values of impedance. The 410/410 kV transformer actual values of the resistance and the reactance are 0.686 Ω and 72.04 Ω, respectively. The transformer actual values of the 410/145 kV transformer are modelled identical to the actual values utilised in the 410/410 kV transformer. The leakage resistance and reactance are distributed equally on each side of the voltage levels. The actual values are implemented in per unit utilising Equation 4.3.

$$Z_{pu} = \frac{Z_{actual}}{(0.5 \cdot Z_{b,HV} + 0.5 \cdot Z_{b,LV})} \tag{4.3}$$

From Equation 4.3, the 410/145 kV transformer parameters are calculated and shown in Table 4.3.

Table 4.3: 410/145 kV 350 MVA transformer parameters.

Rated voltage [kV]	410/145
Rated power [MVA]	350
Reactance [pu]	0.267
Resistance [pu]	0.00254
Iron core loss [pu]	6222
Magnetisation reactance [pu]	6350

The frequency scans seen from Bus 7 of the system with a 410/410 kV and 410/145 kV transformer are compared in Figure 4.7.

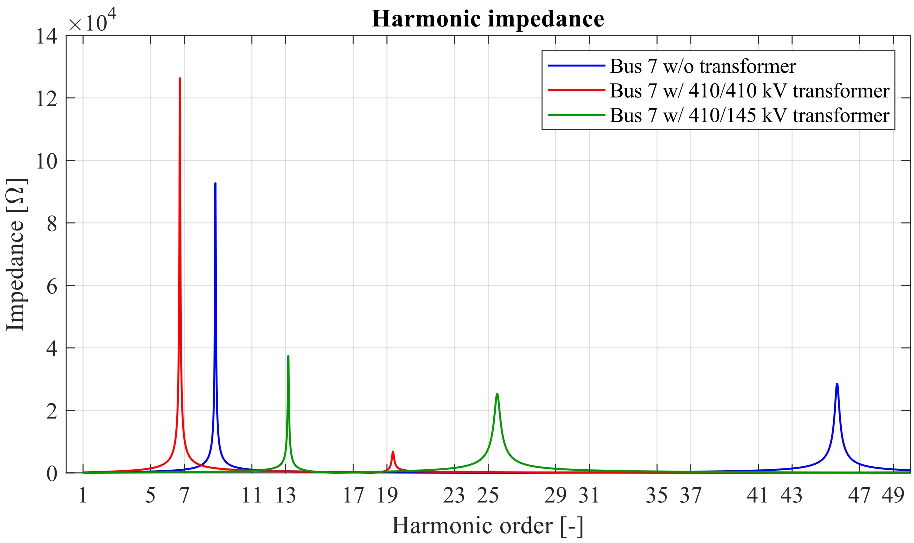

Figure 4.7: Comparison of impedance from frequency scans seen from Bus 7 of the system without a transformer, with a 410/410 kV transformer and with a 410/145 kV transformer.

The first parallel resonance of the system with the 410/145 kV transformer occurs at the 13^{th} harmonic order. In the system with the 410/410 kV transformer, the first parallel resonance appears at the 7^{th} harmonic order. The system without a transformer has the first parallel resonance at the 9^{th} harmonic order. Therefore, the first parallel resonance of the system with the 410/145 kV transformer occurs at a higher resonance frequency compared to the radial system without a transformer, despite of the additional series inductance. This will be analysed and described in the following part.

In the system with the 410/410 kV transformer, the voltage level is the same throughout the system. Therefore, the frequency scan is made using the actual impedance of each component. However, with the 410/145 kV transformer, the frequency scan is calculated using the actual impedance values from the voltage level of the point of observation. In Figure 4.7, the observations are made in Bus 7, which is from the 145 kV side. Therefore, seen from Bus 7, the impedance on the 145 kV side is the actual impedance of each element, while the impedance on the 410 kV side is reduced by the per unit conversion factor, a. The conversion factor in the 410/145 kV transformer is given by Equation 4.4.

$$a = \frac{Z_{b,HV}}{Z_{b,LV}} = \frac{(410\ [kV])^2}{(145\ [kV])^2} \cdot \frac{350\ [MVA]}{350\ [MVA]} = 7.995 \approx 8 \tag{4.4}$$

An illustration of the system parameters in the radial system is shown in Figure 4.8.

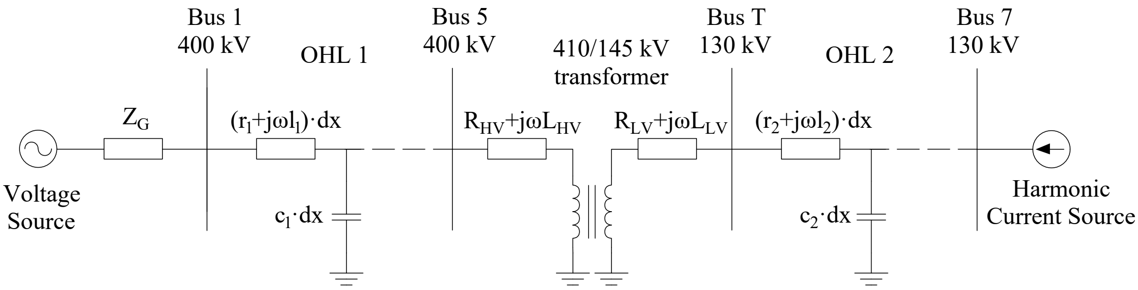

Figure 4.8: Circuit schematic of the radial system with a 410/145 kV transformer.

The system parameters, when seen from either the HV- or LV-side, are listed in Table 4.4.

Table 4.4: System parameters with the per unit conversion factor.

Seen from HV-side										
Z_G	r_1	l_1	c_1	R_{HV}	L_{HV}	$a \cdot R_{LV}$	$a \cdot L_{LV}$	$a \cdot r_2$	$a \cdot l_2$	$\frac{c_2}{a}$

Seen from LV-side										
$\frac{Z_G}{a}$	$\frac{r_1}{a}$	$\frac{l_1}{a}$	$a \cdot c_1$	$\frac{R_{HV}}{a}$	$\frac{L_{HV}}{a}$	R_{LV}	L_{LV}	r_2	l_2	c_2

To show the influence of the conversion factor, the parameters of OHL 1 are changed to consider the conversion factor of eight. By doing this, the 410/410 kV and 410/145 kV transformer systems should have identical impedance plots. However, when utilising the tower type models it is not possible to just change the length of the line to account for the conversion factor. This is due to the resistance, inductance and capacitance of the tower type all increases with the line length. However, to account for the conversion factor, the resistance, inductance and capacitance have to be modified separately. The resistance and inductance have to be be increased by a factor of the conversion factor, while the capacitance has to be decreased by a factor of the conversion factor. In order to achieve this, a nominal π-model is used to demonstrate the principles.

Therefore, OHL 1 is replaced by a nominal π-model in the systems with the 410/410 kV and 410/145 kV transformer. In the system with the 410/410 kV transformer, the nominal π-model is modelled using OHL 1 parameters at the fundamental frequency. Since OHL 2 is located on the side of observation it is not necessary to change the modelling of this.

In the system with the 410/145 kV transformer, the nominal π-model is modelled considering the conversion factor. This is done by increasing the increasing the inductance and resistance in external grid and OHL 1 by a factor of eight and the capacitance is decreased by a factor of eight, compared to the values utilised in the system with the 410/410 kV transformer. The frequency scans of the systems with OHL 1 modelled as π-models are compared in Figure 4.9.

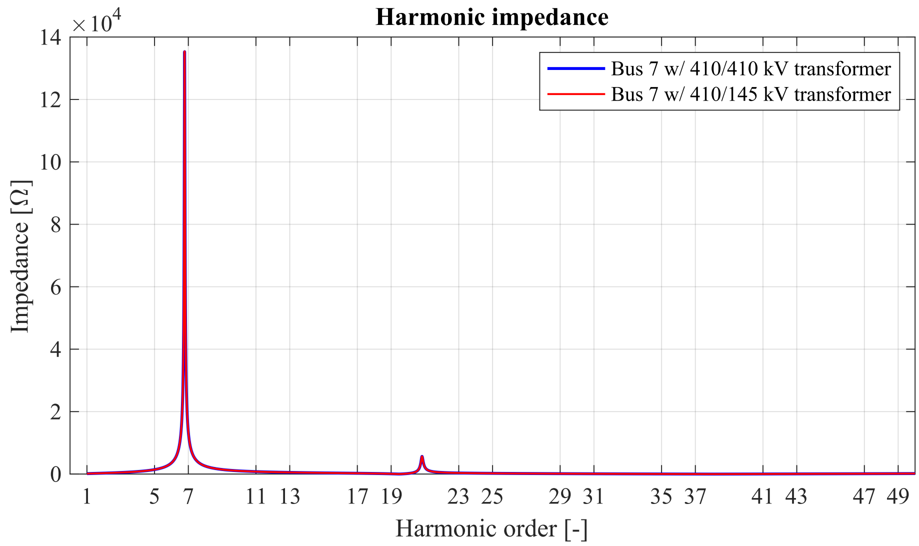

Figure 4.9: Comparison of frequency scans of the systems with a 410/410 kV and a 410/145 kV transformer. The impedance parameters in the 410/145 kV transformer system are modified on the 410 kV side to consider the conversion factor.

As expected, the frequency scans in Figure 4.9 are identical. Hence, it is validated that the frequency scan considers the impedance of the components with respect to the voltage level from the point of observation. From this analysis, it can be concluded, that the impedance of each element is lower on the HV-side, when observed from the LV-side, and opposite. Therefore, the following findings are listed:

- Between voltage levels, the capacitance will always be the conversion factor larger on the HV-side compared to the LV-side
- Between voltage levels, the inductance will always be the conversion factor larger on the LV-side compared to the HV-side

Therefore, the capacitance seems to have a greater effect on the HV-side, independently of the observed voltage level. Oppositely, the inductance seems to have a greater effect on the LV-side, independently of the observed voltage level. Usually, the resonance frequencies are given by $\frac{1}{\sqrt{LC}}$, which has a linear relation between inductance and capacitance. Therefore, this could lead to the assumption that if the capacitance is multiplied by eight and the inductance is divided by eight, the resonance frequencies would be unchanged. However, as shown mathematically in Appendix B.3, the inductance and capacitance have different influences on the resonance frequencies in the radial system. This is why the 410/145 kV system has its first parallel resonance at a higher frequency compared to the system without a transformer.

From the observations it could indicate that implementing UGCs, which has a higher capacitance, on the HV-side of the transformer would have a great impact seen from the LV-side. In Denmark this has not been observed to have a critical impact on the voltage distortion at the 150 kV level. However, it is not a subject which has been significantly analysed and measured. The influence of implementing UGCs on either the HV- or LV-side of a transformer will be investigated in Section 4.3.

The objective of this section was to analyse the impact of the impedance between voltage levels. Therefore, the same actual values of the two transformer were used. From this point on, the same per unit values of the transformer impedance for both the 410/410 transformer and the 410/145 kV transformer will be used. Hence, from this point on, the impedance values in per unit of the two transformers will be as given in Table 4.1.

4.3 Underground Cable Impedance Analysis with 410/145 kV Transformer

The scenarios simulated in Section 3.3 are simulated with the 410/145 kV transformer implemented. However, to make the scenarios comparable, Line 1 and 2 are modelled with the same length in all simulations, and the tower type of the OHLs will be the same. This is done in order to analyse the influence of having different voltage levels. The scenarios simulated are therefore:

- Line 1 and 2 as OHLs
- Line 1 is an UGC and Line 2 is an OHL
- Line 1 is an OHL and Line 2 is an UGC
- Line 1 and 2 as UGCs

The UGC and OHL parameters utilised in the analysis in this section are presented in Table 4.5.

Table 4.5: Line parameters. [21]

Line Type	**Conductor Type**	**Tower Type**	**Shield Type**	**Length [km]**	**R [Ω/km]**	**L [mH/km]**	**C [μF/km]**	**G [μS/km]**
OHL	B	A	AA	25.3	0.0144	0.8723	0.0133	0
UGC	2500 mm^2 Cu			25.3	0.0126	0.3170	0.2111	1.5109

The length of the lines will be 25.3 km as this is the length of Line 1 in the *Example grid*. The tower type utilised is the same as utilised in the *Example grid* in Line 1.

The frequency scan of the four different systems seen from Bus 7 at the 130 kV side are shown in Figure 4.10.

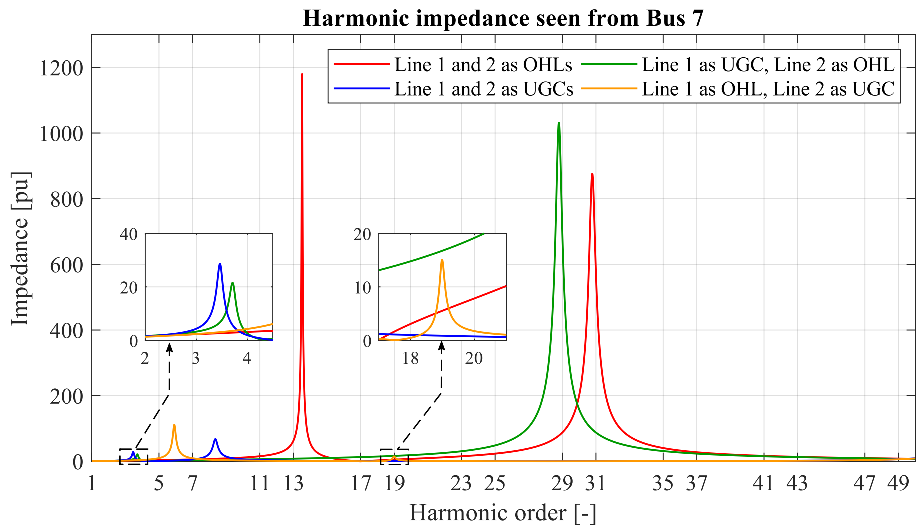

Figure 4.10: Comparison of impedance from frequency scan of the radial system seen from Bus 7, when composed by OHLs, UGCs and both an OHL and an UGC.

From Figure 4.10 it is visible, that the system configuration with UGCs in both lines shifts the resonance frequencies to the lowest order of harmonics, at the harmonic order 3.5. When having an UGC in Line 1 at the 400 kV side, the first parallel resonance occurs at the harmonic order 3.7. Opposite implementing Line 2 as an UGC at the 130 kV side, the first parallel resonance occurs at the harmonic order 5.9. From this, it can be seen that when replacing OHLs by UGCs on the 400 kV side, the resonance points are shifted to lower frequencies when seen from the 130 kV side, compared to replacing OHLs with UGCs on the 130 kV side. This can be explained from the previous finding, that capacitance on the HV-side is the conversion factor higher than on the LV-side. Therefore, when installing an UGC, which has a higher capacitance compared to an OHL, on the HV-side, the impact is greater compared to installing the UGC on the LV-side.

If Line 2 is an OHL, the second parallel resonance peak magnitude is greater than when Line 2 is an UGC. This is analysed further by observing the system from the HV-side.

The frequency scan of the four different systems seen from Bus 1 at the 400 kV side are shown in Figure 4.11.

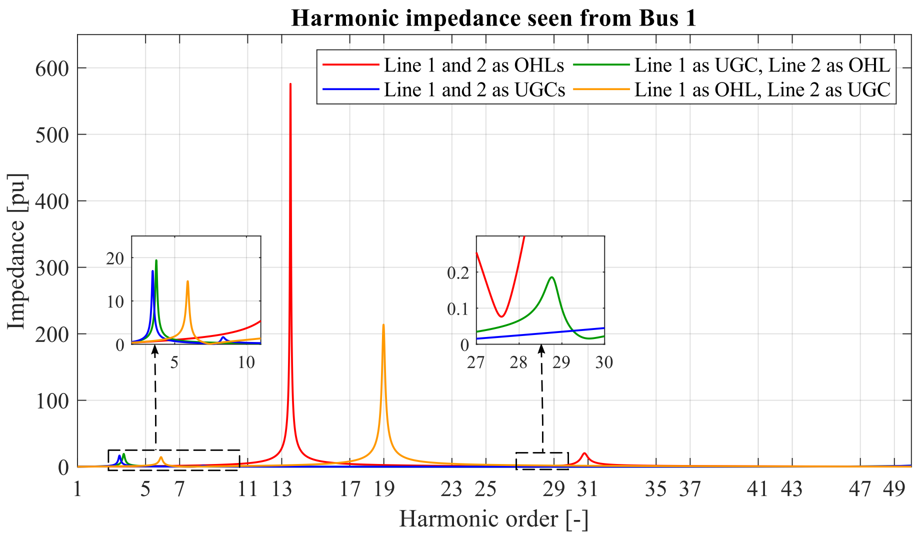

Figure 4.11: Comparison of impedance from frequency scan of the radial system seen from Bus 1, when composed by OHLs, UGCs and both an OHL and an UGC.

From Figure 4.11, it is visible that the parallel resonances occurs at the same harmonic orders in the four scenarios seen both from Bus 1 and Bus 7. However, the magnitude of the parallel resonance peaks are different. The largest difference is seen in the two systems, when only Line 1 or Line 2 is implemented as an UGC. When seen from Bus 1, the second parallel resonance peak is significantly damped when Line 1 is an UGC and Line 2 is an OHL compared to when seen from Bus 7. Oppositely, the second parallel resonance peak is significantly larger for the system where Line 1 is an OHL and Line 2 is an UGC compared to when seen from Bus 7. This indicates, that the magnitude of the second parallel resonance peak is strongly determined by if the line is an UGC or OHL on the side from where the system is observed. When an OHL is present on the side of observation, the second parallel peak magnitude is higher than compared to if it is an UGC.

4.4 Harmonic Propagation Analysis of 410/410 kV Transformer System

In this section, the harmonic propagation in the 410/410 kV transformer is analysed. The harmonic propagation through the 410/410 kV transformer in the radial system is shown in Figure 4.1 and analysed utilising the harmonic penetration method. The transformer parameters are specified in Table 4.1 and the harmonic current source is placed in Bus 7 with the specified harmonic orders. The harmonic voltage and current through the system are shown in Figure 4.12.

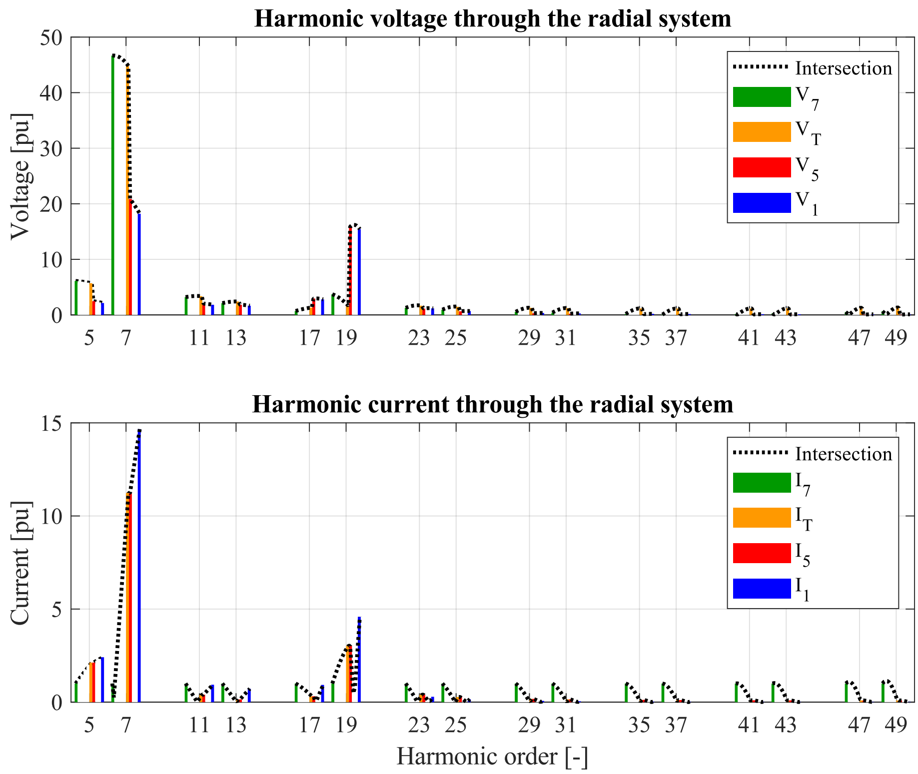

Figure 4.12: Harmonic voltage and current through the radial system with a 410/410 kV transformer implemented between Bus 5 and Bus T.

The harmonic voltages and currents follows the tendency of the impedance characteristics shown in Figure 4.4, which have peaks at approximately the 7^{th} and 19^{th} harmonic orders. From Figure 4.12, it is visible that there is a voltage difference between Bus T and Bus 5 in the transformer. Depending on the harmonic orders the voltage difference from Bus T to Bus 5 can either be an increase (e.g. the 17^{th}) or a decrease (e.g the 7^{th}). Additionally, the current is constant in Bus T and Bus 5, since the transformer can be seen as a series element, since the shunt impedance is much larger than the series element.

The harmonic propagation in the radial system with a transformer can be represented utilising the circle theory as in Chapter 3. Since the current is constant through the transformer, two circles are required to represent each side of the transformer. The harmonic propagation using of the 7^{th} harmonic order using the circle are visualised in Figure 4.13.

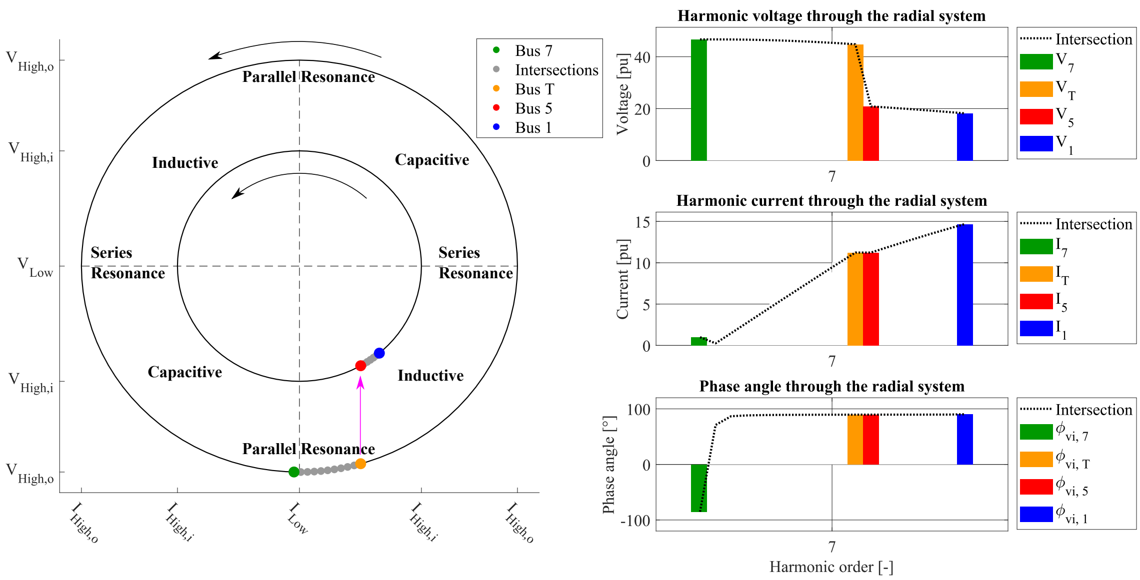

Figure 4.13: Harmonic propagation of the 7^{th} harmonic order through the radial system with a 410/410 kV transformer implemented.

The outer circle in Figure 4.13 represents the relation between the harmonic voltage and currents between Bus 7 and Bus T. The outer circle follows the axes denoted $I_{High,o}$ and $V_{High,o}$. The purple arrow visualise the voltage difference from Bus T to Bus 5. The inner circle represents the relation between the harmonic voltage and currents between Bus 5 and Bus 1. The inner circle follows the axes denoted $I_{High,i}$, $V_{High,i}$. Both circles have a minimum at the same placement on the x- and y-axis. It can be seen that both Bus T and Bus 5 are located in the inductive region and the voltage magnitude decreases from Bus T to Bus 5. The voltage difference can be calculated utilising Equation 4.5.

$$V_{difference} = \sqrt{3} \cdot I_t \cdot Z_t \tag{4.5}$$

Where I_t is the harmonic current through the transformer and Z_t is the leakage impedance of the transformer at the specific harmonic order. The voltage difference depends on the transformer impedance and the current. Therefore, it can be theoretically shown that the voltage differences can be reduced by reducing the transformer impedance. However, it should be noted that this will also change the resonance frequency.

The voltage difference can be explained utilising the phasor diagram of the 7^{th} harmonic order seen in Figure 4.14.

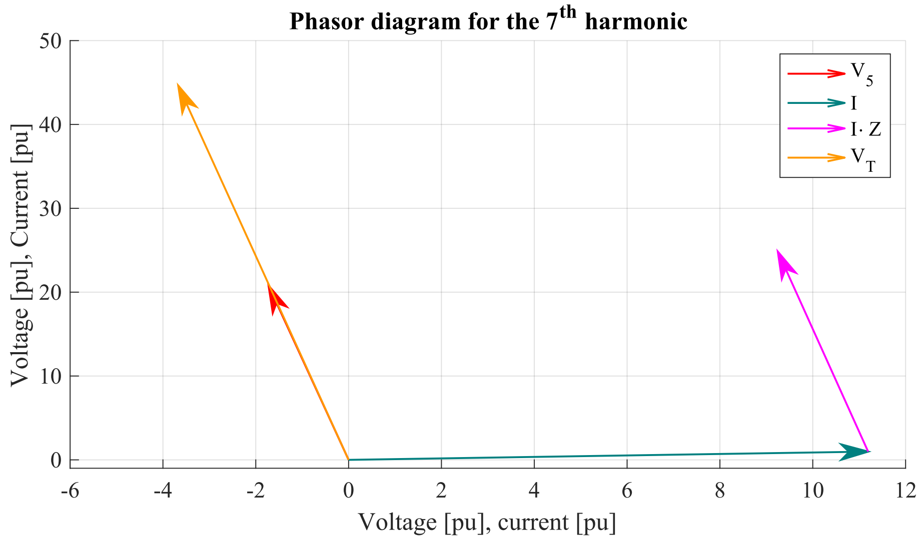

Figure 4.14: Phasor diagram for the 7^{th} harmonic order.

As seen in Figure 4.14, the current is lagging the voltage and the transformer impedance will cause a voltage drop from Bus T to Bus 5.

To analyse the increasing voltage through the transformer, the voltages, currents and phase angles of the 17^{th} harmonic order are considered. The harmonic propagation of the 17^{th} harmonic order using the circle is plotted in Figure 4.15.

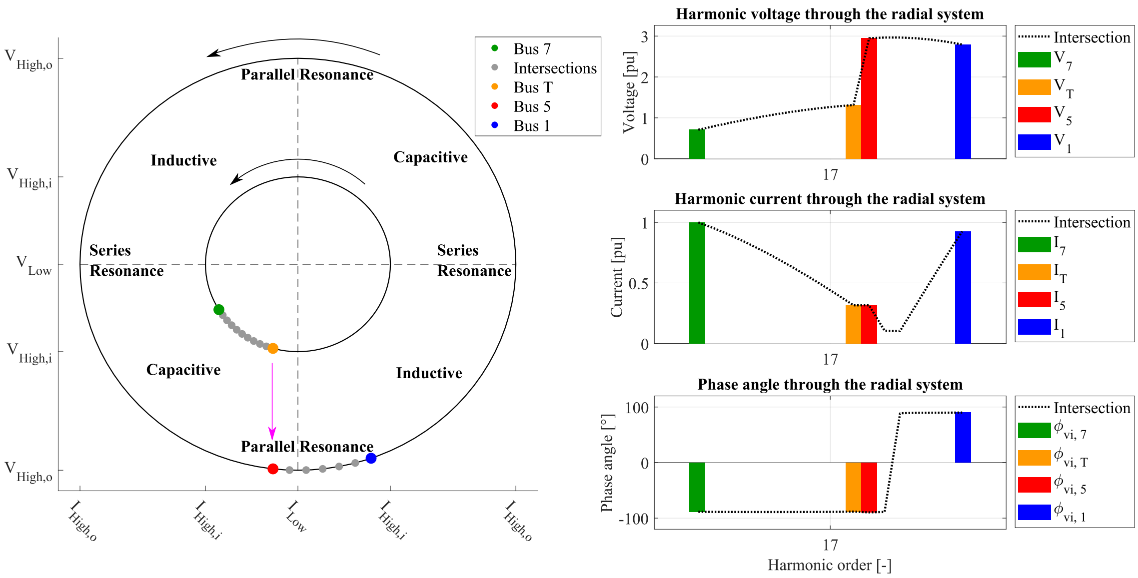

Figure 4.15: Harmonic propagation of the 17^{th} harmonic order through the radial system with a transformer implemented.

It can be seen that both Bus T and Bus 5 are located in the capacitive region and the voltage magnitude increases from But T to Bus 5. Additionally, the voltage difference can be explained utilising the phasor diagram of the 17^{th} harmonic order as seen in Figure 4.14.

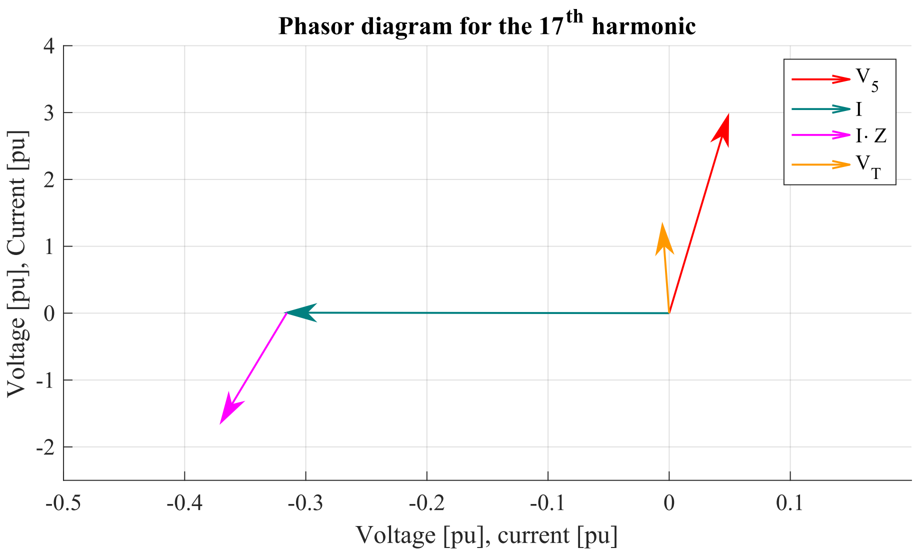

Figure 4.16: Phasor diagram for the 17^{th} harmonic order.

As seen in Figure 4.16, the current is leading the voltage and the transformer impedance will cause the voltage to rise from Bus T to Bus 5.

It is also possible for Bus T and Bus 5 to be located in different regions. However, it is only possible when Bus T is located in the inductive region and Bus 5 is located in the capacitive region, due to the rotation of the circle and the constant current.

An example of the two busses located in different regions is visualised utilising the harmonic propagation of the 19^{th} harmonic order using the circle, as shown in Figure 4.17.

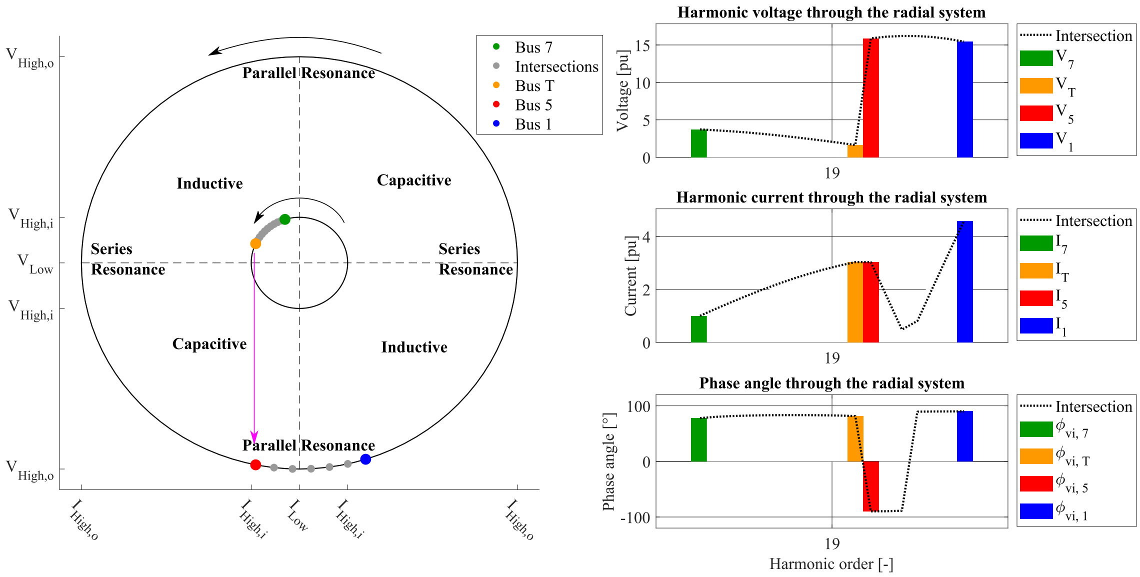

Figure 4.17: Harmonic propagation of the 19^{th} harmonic order through the radial system with a transformer implemented.

It can be seen that Bus T is located in the inductive region, while Bus 5 is located in the capacitive region. Additionally, the voltage magnitude increases from Bus T to Bus 5.

Due to the location of the busses in the specific regions, the current is lagging the voltage in Bus T and leading the voltage in Bus 5. In the case where the two buses are located in different regions, the current magnitude has to be considered to determine if the voltage magnitude between Bus T and Bus 5 will increase or decrease. The phasor diagram of the 19^{th} harmonic order seen in Figure 4.18 visualises the correlation between the two voltage magnitudes.

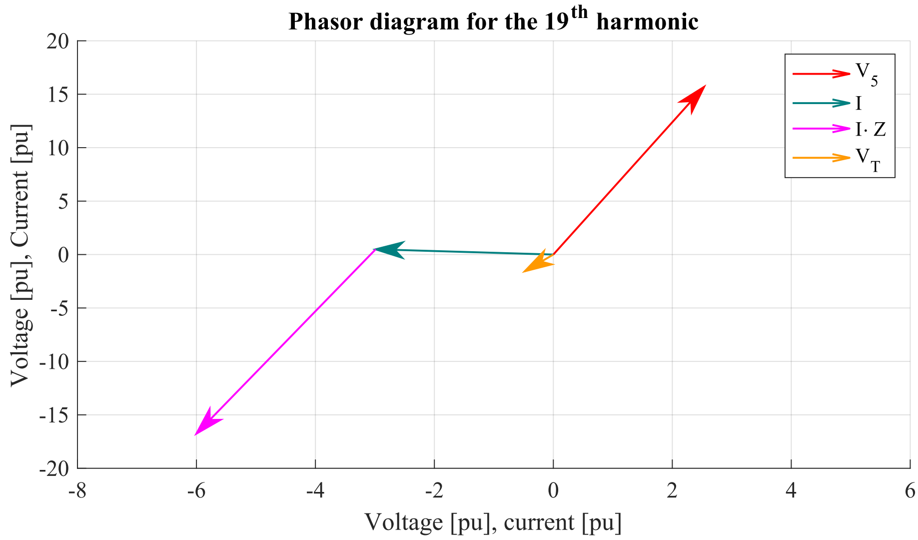

Figure 4.18: Phasor diagram for the 19^{th} harmonic order.

As seen in Figure 4.18, the voltage increase is the difference between the voltage magnitude of Bus T and Bus 5. The voltage drop of the transformer impedance from Bus 5 to Bus T is larger than the voltage magnitude of Bus 5. Therefore, a phase shift occurs for Bus T, which is now leading the current.

The influence of the current can be analysed theoretically by plotting the voltage difference as a function of current, while keeping the Bus 5 voltage constant, as seen in Figure 4.19. It should be noted that the values depends on the harmonic order, the system configurations and the voltage in Bus 5. The harmonic voltages are displayed in absolute values, since the voltage magnitude is of interest and not the angle.

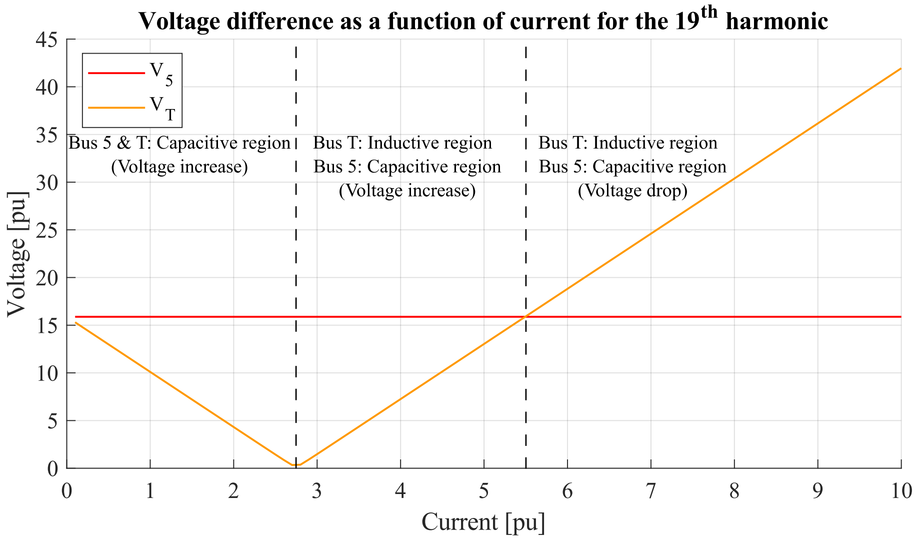

Figure 4.19: Voltage difference as a function of current for the 19^{th} harmonic order. Depending on the current magnitude, Bus T is located in either the capacitive or inductive region. The intervals where voltage increase and decrease from Bus T to Bus 5 are highlighted.

From Figure 4.19 it is visible that below 2.7 pu current, both busses are located in the capacitive region and a voltage increase from Bus T to Bus 5 will occur. The measured harmonic current of the 19^{th} harmonic order is approximately 3 pu, which results in a voltage increase from Bus T to Bus 5, as seen in Figure 4.17.

As seen in Figure 4.19, with current magnitudes larger than 5.5 pu, the voltage drops from Bus T to Bus 5. With increasing current, the voltage drop increases linearly.

The same theoretical analysis can be performed for harmonic orders which have a lagging current. The voltage difference of the 7^{th} harmonic order as a function of current can be seen in Figure 4.20.

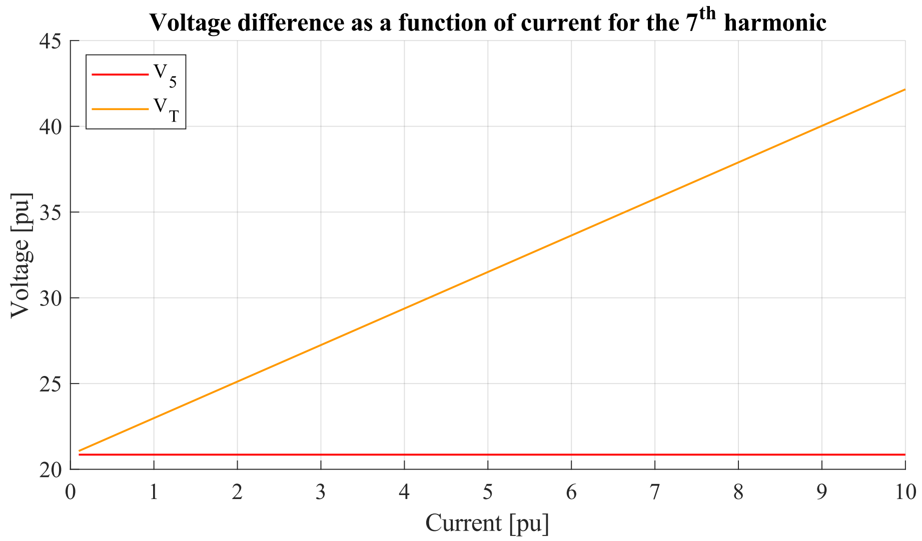

Figure 4.20: Voltage difference as a function of current for the 7^{th} harmonic order. The voltage of both busses are leading the current and the busses are therefore in the inductive region.

From Figure 4.20, it can be seen that no matter the current magnitude there will always be a voltage drop from Bus T to Bus 5. The only exception is when the current is 0 pu, since no voltage drop will occur. From the previous analyses, it can be concluded that the harmonic voltage difference depends on if the terminals are located in the inductive or capacitive region. The following findings are listed:

- If both terminals connecting the transformer are in the inductive region, a decrease in the harmonic voltage occurs from the sending to the receiving end
- If both terminals connecting the transformer are in the capacitive region, an increase in the harmonic voltage occurs from the sending to the receiving end
- If the sending end terminal of the transformer is in the inductive region and the receiving end of the transformer is in the capacitive region either an increase or decrease in the harmonic voltage occurs dependent on the current magnitude

The voltage drop across the transformer can also be described utilising the relation between the radiuses, r_{HV} and r_{LV}, of the two circles as seen in Figure 4.21.

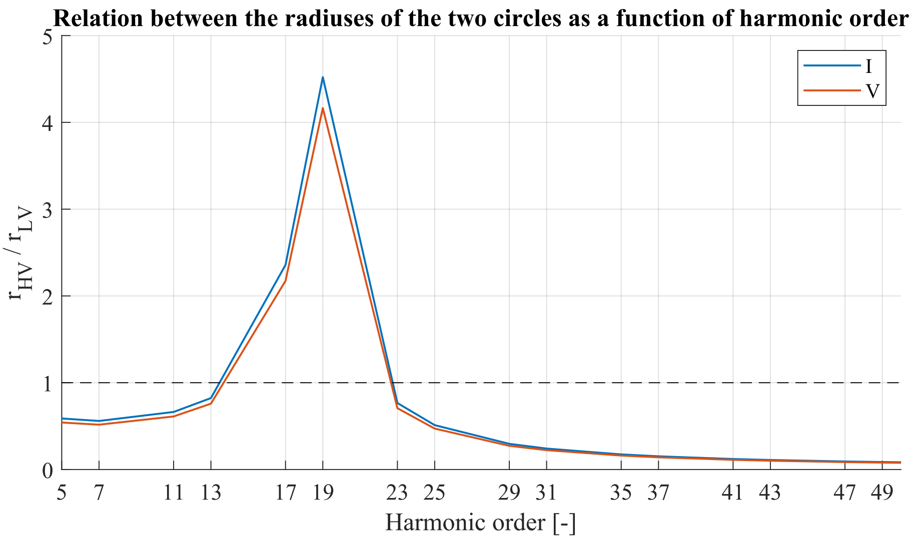

Figure 4.21: The relation between the radius of the two circles representing the HV- and LV-side can be utilised to describe the voltage drop. When the curve is above the black dashed line, a voltage increase from Bus T to Bus 5 occurs.

As seen in Figure 4.21, a voltage drop from Bus T to Bus 5 occurs from the 5^{th} to the 13^{th} harmonic order, since the relation is below the black dashed line. In the circle representation this means that the circle representing the LV-side of the transformer is larger than the circle representing the HV-side. Additionally, it can be seen that a voltage increase from Bus T to Bus 5 occurs at the 17^{th} and 19^{th} harmonic order. For the 23^{rd} harmonic order and up, it can be seen that the relation stays below 1 and decreases with frequency. This means that a voltage drop always occurs from Bus T to Bus 5 and that the HV-circle will stay inside the LV-circle. Since, the relation decreases, the HV-circle will be smaller and smaller compared to the LV-circle at high harmonic orders.

To obtain the circle relations shown in Figure 4.21, the circle for each harmonic order should be determined from the harmonic voltage, current and phase angle between the voltage and current. Therefore, it is analysed if a simpler method can be utilised to obtain the tendency of the relation between the circles and thereby obtain knowledge about the voltage difference across the transformer.. When a harmonic current is injected in Bus 7, the harmonic voltage in a specified bus can be obtained from the frequency scan method utilising the off-diagonal impedance from Bus 7 to the specified bus as described in Section 3.4. Therefore, the relation between the off-diagonal impedances from Bus 7 to Bus T and 5 can be utilised to describe the relation between the harmonic voltage in Bus T and 5. The off-diagonal impedance relations are compared to the circle relations in Figure 4.22 to validate this approach. The impedance relation is shown for the 1^{st} harmonic order to the 49^{th}. The voltage and current relations of the circles are shown from the 5^{th} to the 49^{th} harmonic order.

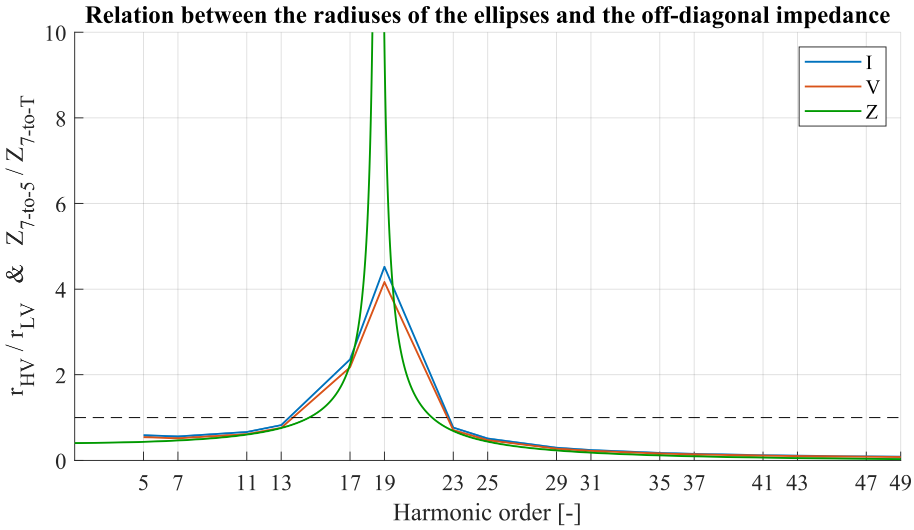

Figure 4.22: The relation between the radius of the two circles representing the HV- and LV-side and the relation between the off-diagonal impedances from Bus 7 to 5 and T. When the curve is above the black dashed line, a voltage increase from Bus T to Bus 5 occurs.

From Figure 4.22 it can be seen, that the off-diagonal impedance relation has the same tendency as the relations from the circles. The voltage increases from Bus T to Bus 5 in the 17^{th} and 19^{th} order harmonic and decreases in the rest of the other harmonic orders of interest. The impedance relation follows the voltage relation close except for at the 19^{th} harmonic order. Here the impedance relation is above the voltage relation. The difference is due to the fact that the voltage relation is the difference between the maximum voltage in the HV- and LV-circles. However, the actual voltage might not reach the maximum voltage in the circles. Therefore, the voltage and impedance relation is not identical in magnitude, but the tendency is still the same.

The current relation can not be obtained from the frequency scan method. In this example, the current relation follows the voltage relation, however this might not always be the case. Since, power systems are voltage controlled, the voltage relation across the transformer is the most important.

4.5 Harmonic Propagation Analysis of 410/145 kV Transformer System

The harmonic propagation through the system with the 410/145 kV transformer is analysed utilising the harmonic penetration method. A harmonic current source is placed in Bus 7. In the previous studies, the harmonic current source injected 1 pu current with a base of 1 kA. Therefore, the harmonic current source magnitude is multiplied by the transformer turns ratio to maintain a harmonic current injection of 1 pu. Hence, the actual values of harmonic injections on the LV-side is 2.83 kA. The harmonic voltages and currents through the system with a harmonic current source placed in Bus 7 are shown in Figure 4.23.

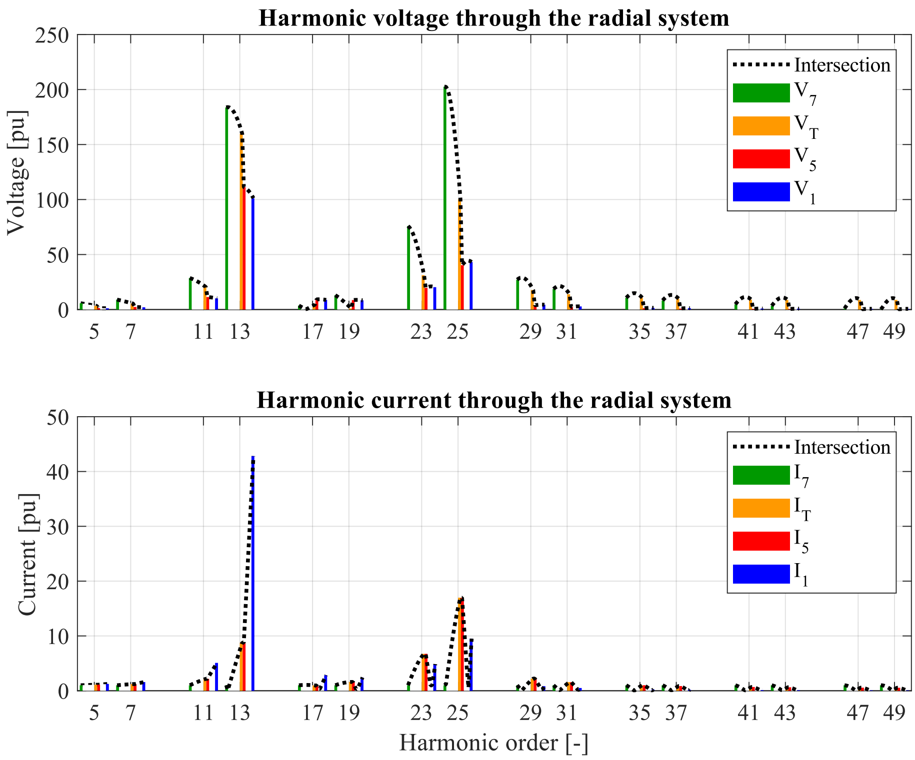

Figure 4.23: Harmonic voltage and current through the radial system with a 410/145 kV transformer implemented between Bus 5 and Bus T and a harmonic current source in Bus 7.

From Figure 4.23 it is visible, that the harmonic voltage differences between Bus T and Bus 5. For some harmonic orders, the voltage is increasing (e.g. the 19^{th}) and for others the voltage decreases (e.g. the 13^{th}). Hence, the same tendencies of the voltage differences occurs when installing a 410/145 kV transformer compared to the 410/410 kV transformer. The harmonic current is constant through Bus T and Bus 5 in per unit. The 13^{th} harmonic order voltage and current are visualised utilising the circle theory. The the harmonic propagation of the 13^{th} harmonic order using the circle is shown in Figure 4.24 along with the harmonic voltage, current and the phase angle.

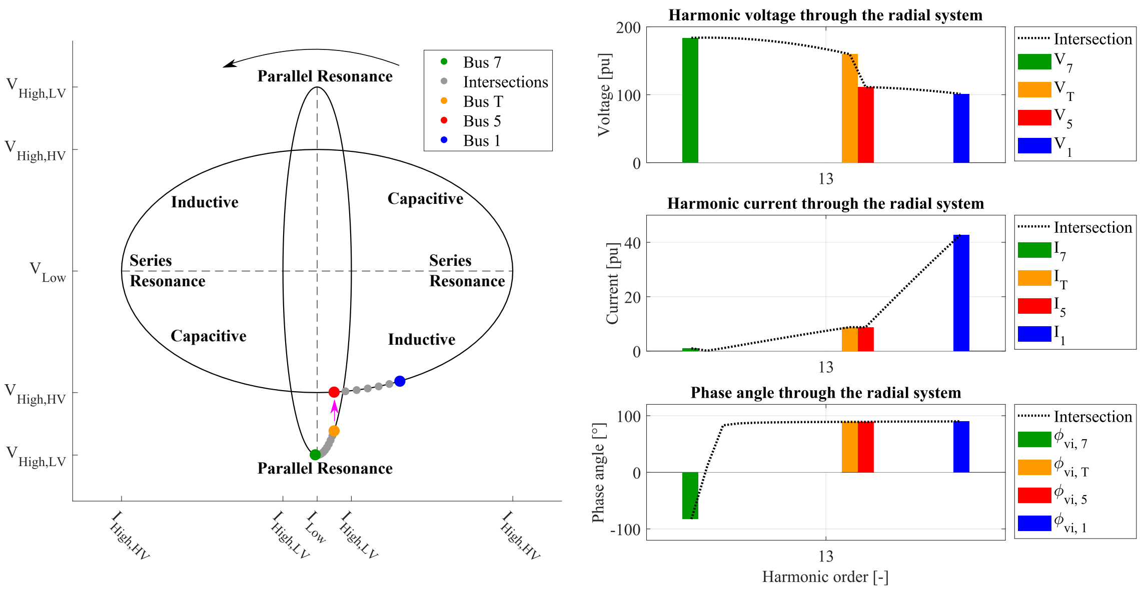

Figure 4.24: Harmonic propagation of the 13^{th} harmonic order through the radial system with a 410/145 kV transformer implemented.

From Figure 4.24 it can be seen, that the characteristics of the harmonic voltage as a function of current no can be normalised to the same type of circles as for the 410/410 kV transformer. Considering the turns ratio of the transformer, the current on the HV-side is divided by the turns ratio, while the voltage is multiplied by the turns ratio. Therefore, it is not possible to normalise into two comparable circles. Instead, the harmonic voltage as a function of current follows two ellipses, due to the different voltage levels of the transformer. One ellipse describes the harmonic propagation on the LV-side and the other the HV-side.

The ellipses follows the same principles as the theory utilised in the normalised circles. The rotation is anti-clockwise, the capacitive and inductive regions are the same and the series and parallel resonances occurs at the same positions. Considering the ellipses in Figure 4.24, it can be seen that from Bus 7 to Bus T the voltage initially increases and then decreases. Opposite, the current initially decreases and then increases. Hence, a shift from the capacitive to the inductive region occurs, which can also be seen in the narrow ellipse representing the LV-side. Between Bus T and Bus 5 a voltage decrease occurs due to both busses being in the inductive region. The voltage difference caused by the transformer is shown by the purple arrow in Figure 4.24. The current between Bus T and Bus 5 is constant as the plots are in per unit. From Bus 5 to Bus 1, the voltage is decreasing and the current is increasing. Hence, the two busses remains in the inductive region.

In Figure 4.24, the highest voltage in per unit is observed at the LV-side, while the highest current in per unit is observed at the HV-side. An analysis of the ellipses configuration with respect to each other is made for all harmonic orders. From this analysis it is observed, that the ellipse relation changes at the 35^{th} harmonic order for this system as shown in Figure 4.25.

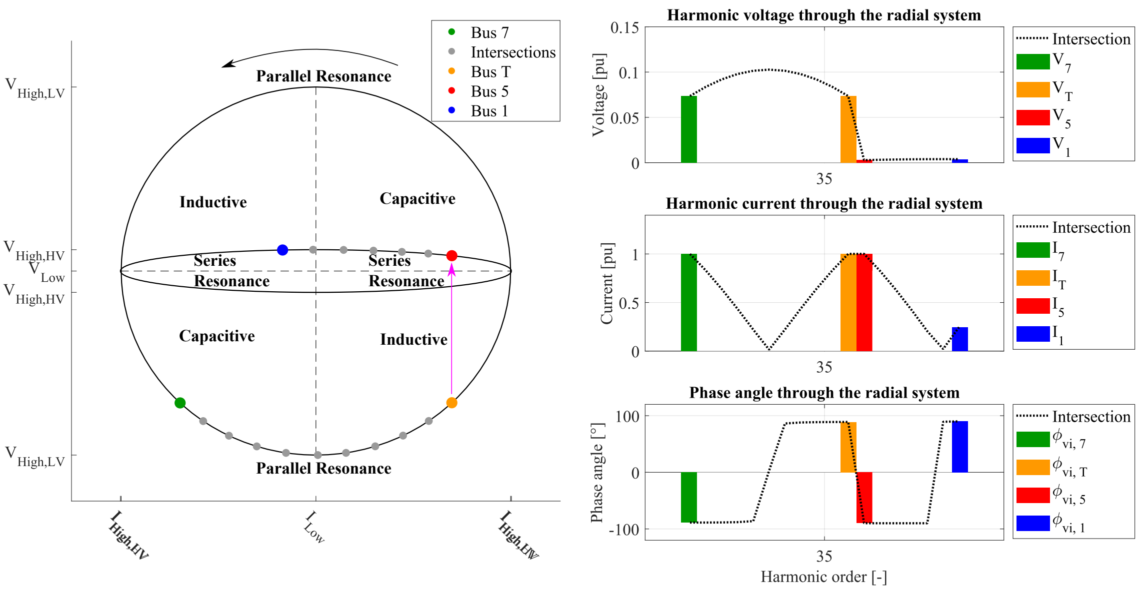

Figure 4.25: Harmonic propagation of the 35^{th} harmonic order through the radial system with a 410/145 kV transformer implemented.

At the 35^{th} harmonic order the HV-side ellipse is inside the LV-side ellipse at all points. This tendency continues up to the 49^{th} harmonic order, which is the frequency range of interest in this study. Hence, from the 35^{th} harmonic order and up, the voltage difference can only decrease from Bus T to Bus 5. It should be noted that this change at the 35^{th} harmonic order is only valid in this specific system. The ellipse relation can be explained from the transformer impedance, which increases with frequency. Therefore, for high harmonic orders, a voltage drop will always occur as described in Section 4.4.

The ellipse relations can also be described from the relation between the HV- and LV-ellipses as a function of the harmonic order as seen in Figure 4.26. The current relation is the width of the ellipses and the voltage relation is the height. Additionally, the relation between off-diagonal impedance from Bus 7 to Bus 5 divided by the off-diagonal impedance from Bus 7 to Bus T in per unit is included.

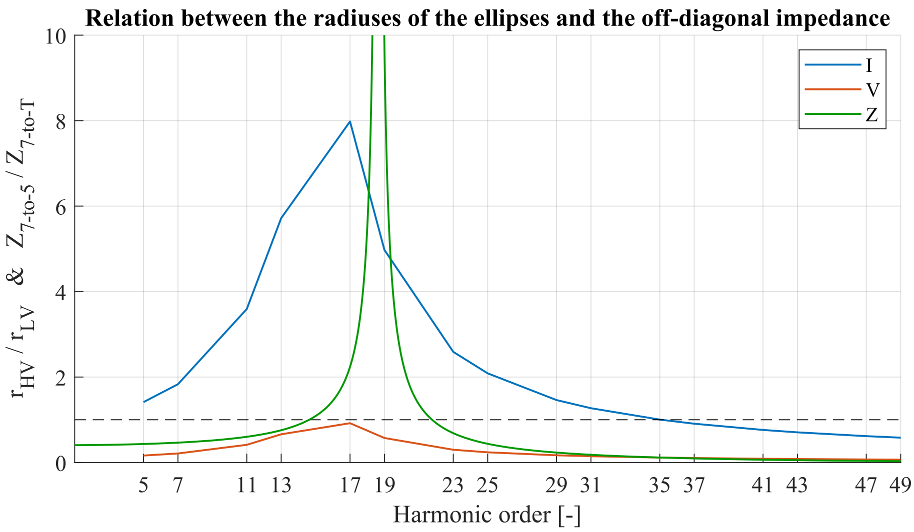

Figure 4.26: The relations between the height and width of the HV- and LV-ellipses and the relation of the off-diagonal impedance from Bus 7 to Bus 5 and T.

The black dashed line represents if the width or height of the HV-ellipsis exceeds the LV-ellipsis. Moreover, if the relation of the off-diagonal impedance is above the dashed line, the harmonic voltage from Bus T to Bus 5 is increasing. As seen in Figure 4.26, the voltage and off-diagonal impedance relations do not follow the same relation as was the case in the 410/410 kV system. Therefore, the tendency observed between the voltage relation and the impedance relation is that they peak at approximately the same harmonic order.

The voltage relation stays below the dashed line for all harmonics, hence indicating that the maximum voltage of the LV-ellipse is above that of the HV-ellipse for the harmonic orders. However, as seen from the relation of the off-diagonal impedance, the voltage increases from Bus T to 5 at the 17^{th} and 19^{th} order harmonics. This can also be verified by analysing the ellipses of the 17^{th} and 19^{th} harmonic orders, shown in Figure 4.27.

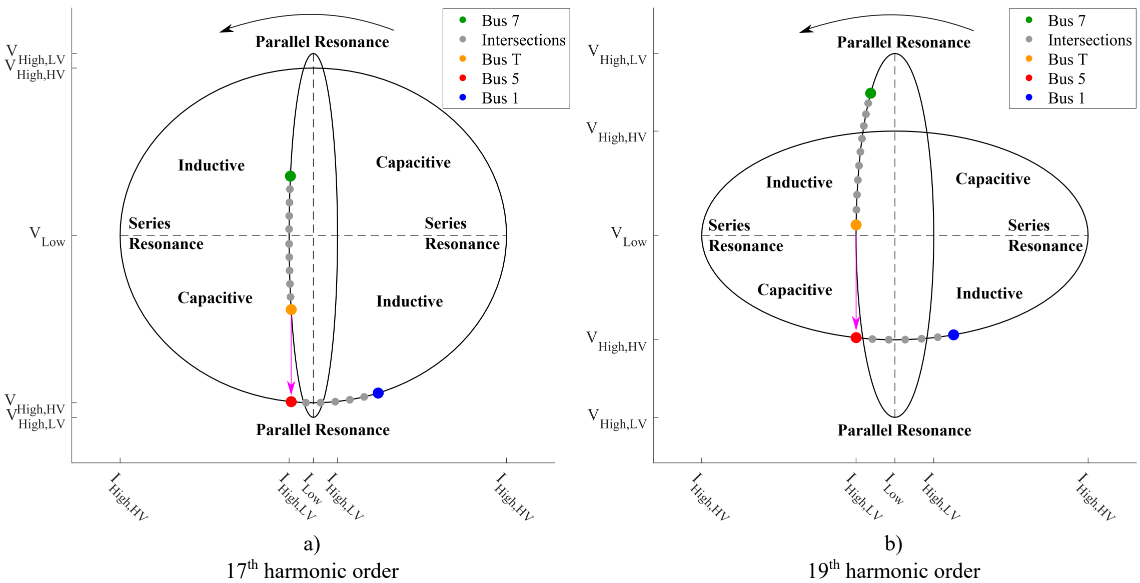

Figure 4.27: Harmonic propagation of a) the 17^{th} harmonic order and b) the 19^{th} harmonic order.

From Figure 4.27 it can be seen why the voltage relation and off-diagonal impedance relations describe different relations for the 17^{th} and 19^{th} harmonic orders in this system. The explanation is that one ellipse does not enclose the other. The off-diagonal impedance relation describes when a voltage increase or decrease across the transformer between Bus T and Bus 5 occurs. The voltage and current relations describes the relation between the two ellipses maximum values on the x- and y-axis. Hence, the voltage will increase or decrease from Bus T to Bus 5, depending on the position of Bus T and Bus 5 on the ellipses.

4.5.1 Underground Cable Analysis

To analyse how the different line types affects the voltage difference across the transformer, UGCs will be implemented in the 410/145 kV radial system. The cable parameters are the same as described in Section 3.3.

UGC on LV- and HV-Side

In this analysis Line 1 and 2 are replaced by UGCs. In Figure 4.28 the harmonic propagation through the system of the 7^{th} harmonic order is shown. Here the harmonic current source is connected in Bus 7.

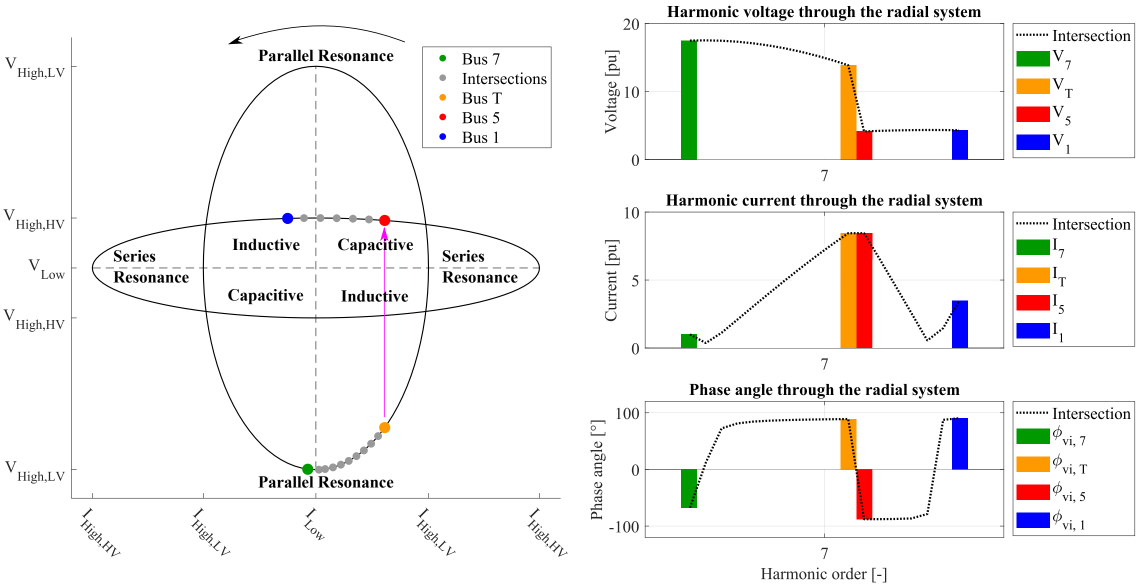

Figure 4.28: Harmonic propagation of the 7^{th} harmonic order through the radial system with a 410/145 kV transformer implemented. Line 1 and 2 are replaced by UGCs.

From Figure 4.28 it can be seen that Bus 5 is located in the capacitive region and Bus T is located in the inductive region. As described earlier, when the two busses are located in different regions, the voltage difference can either be a decrease or an increase from Bus T to Bus 5, dependent on the current. In this case the voltage difference is a decrease.

The voltage difference is analysed by plotting the voltage difference as a function of current, while keeping the Bus 5 voltage magnitude constant, as seen in Figure 4.29.

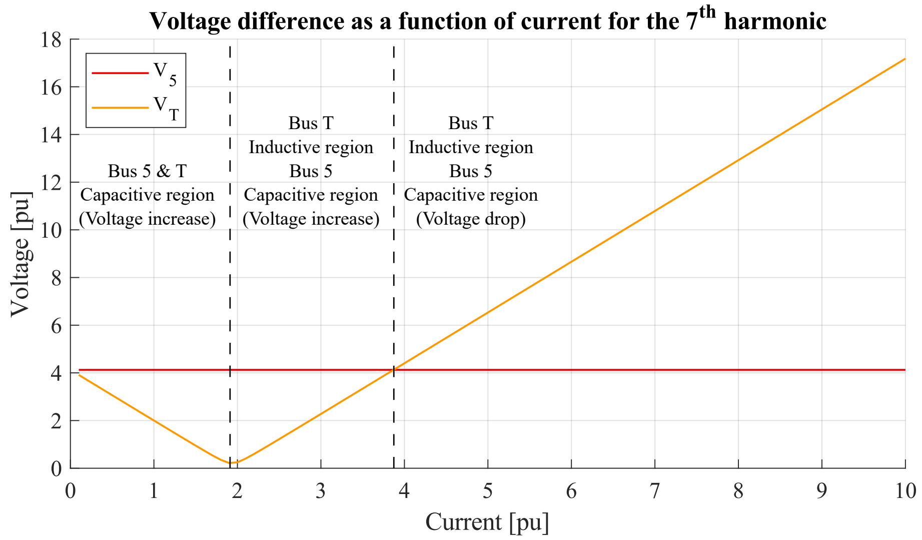

Figure 4.29: Voltage difference as a function of current for the 7^{th} harmonic order. Depending on the current magnitude, Bus T is located in either the capacitive or inductive region. Additionally, the intervals where voltage increase and decrease from Bus T to Bus 5 are highlighted.

From Figure 4.29 it is visible, that the same characteristic shown in Figure 4.19 is present. However, the values are different, that the values are dependent on system parameters. In the case of the 7^{th} harmonic order with both lines as UGCs, the harmonic current is 8.44 pu, which corresponds to a voltage decrease from Bus T to Bus 5, as seen in both Figure 4.28 and 4.29.

In Figure 4.28, the highest harmonic voltage is from the LV-ellipse, while the highest harmonic current is from the HV-ellipse. This ellipse configuration with respect to each other changes from the 11^{th} harmonic order where the LV-ellipse has both the highest voltage and current. The characteristic from the 11^{th} harmonic order continues up to the 49^{th} harmonic order. This means, that in the system with both lines as UGCs, the voltage from Bus T to Bus 5 is always decreasing after the 11^{th} harmonic order. Hence, at the 5^{th} and 7^{th} harmonic orders, due to the ellipse configuration, the voltage across the transformer can either increase or decrease. To analyse whether an increase or decrease occurs, the relation of the maximum voltage and current from the ellipses and the off-diagonal impedance relation are shown in Figure 4.30 as a function of the harmonic order.

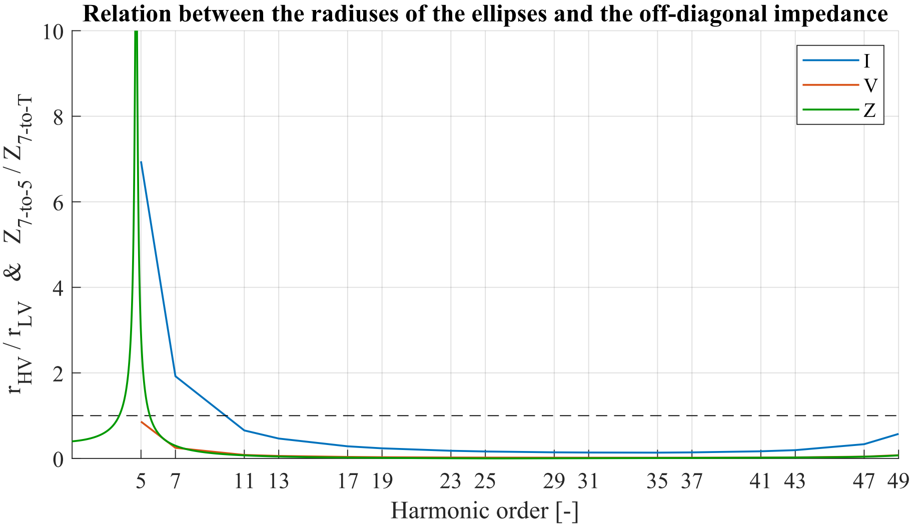

Figure 4.30: The relations between the height and width of the HV- and LV-ellipses and the relation of the off-diagonal impedance from Bus 7 to Bus 5 and T with an UGC in Line 1 and 2.

From Figure 4.30 it can be seen, that the characteristic of the voltage, current and off-diagonal impedance relation follow each other in terms of when they peak and when they are at a minimum. The voltage relation is however below the dashed line for all harmonic orders. Hence, the LV-ellipse voltage max is higher than the HV-ellipse voltage max for all harmonic orders shown. The off-diagonal impedance relation is above the dashed line at the 5^{th} harmonic order. Hence, a voltage increase occurs across the transformer at this harmonic order. In Figure 4.31, the ellipses for the harmonic propagation of the 5^{th} harmonic order are shown.

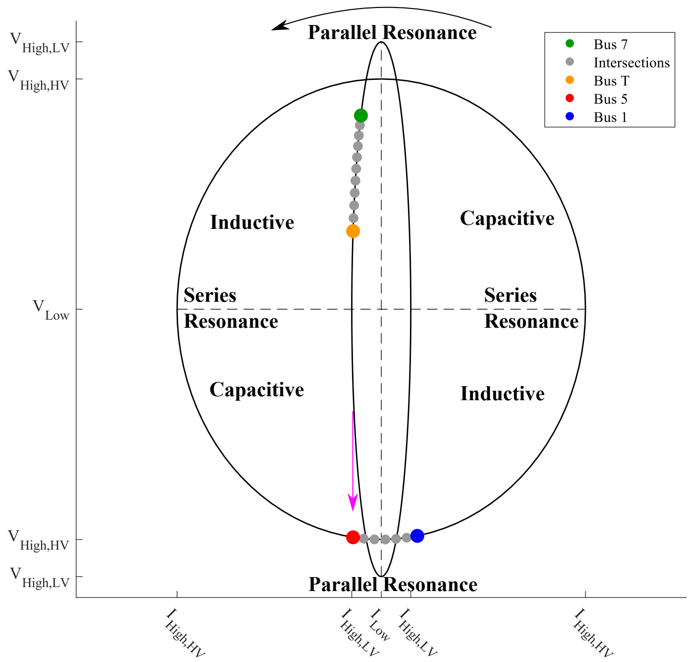

Figure 4.31: Harmonic propagation of the 5^{th} harmonic order through the radial system with a 410/145 kV transformer implemented. Line 1 and Line 2 are UGCs.

From the ellipses it can be seen, that the voltage from Bus T to Bus 5 can either increase or decrease, but for this case, the voltage increase due to the positions of Bus T and Bus 5. For the 7^{th} harmonic order, the voltage decreases from Bus T to Bus 5 due to the placement of Bus T and 5 in the ellipses as shown in Figure 4.28.

UGC on LV-Side and OHL on HV-Side

The system configuration is changed to consist of an OHL in Line 1 and an UGC in Line 2. The ellipses describing the harmonic propagation of the 7^{th} harmonic order in the system with a harmonic current source connected in Bus 7 are shown in Figure 4.32.

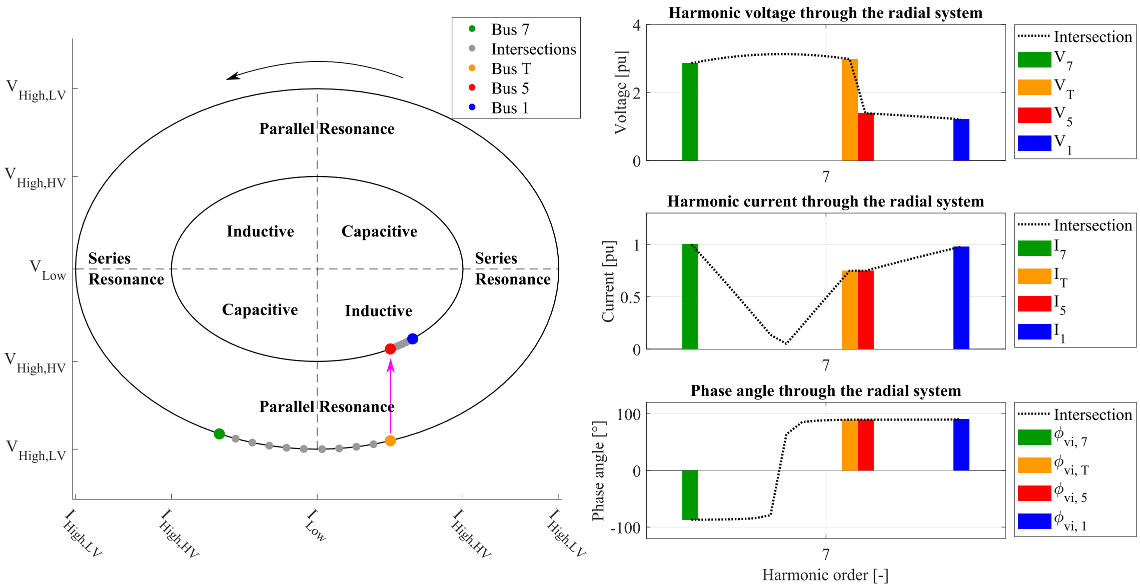

Figure 4.32: Harmonic propagation of the 7^{th} harmonic order through the radial system with a 410/145 kV transformer implemented. Line 1 is an OHL and Line 2 is an UGC.

In Figure 4.32, the LV-ellipse is enclosing the HV-ellipse. This is the case for all harmonic orders except for the 17^{th} and 19^{th} harmonic orders. For these two harmonic orders, the HV-ellipse encloses the LV-ellipse. The relation of the voltages, currents and off-diagonal impedances are shown in Figure 4.33.

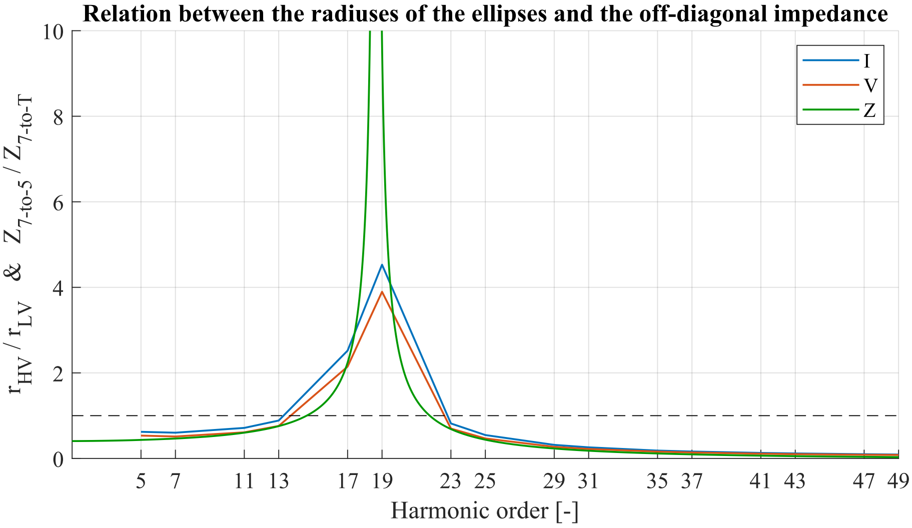

Figure 4.33: The relations between the height and width of the HV- and LV-ellipses and the relation of the off-diagonal impedance from Bus 7 to Bus 5 and T with an OHL in Line 1 and an UGC in Line 2.

The relations all follow the same characteristics, since one ellipsis always enclose the other. Therefore, both the voltage and off-diagonal impedance relations shows, a voltage increase from Bus T to Bus 5 for the 17^{th} and 19^{th} harmonic orders.

OHL on LV-Side and UGC on HV-Side

The system with Line 1 as an UGC and Line 2 as an OHL is also analysed in regards to the impedance, voltage and current relation as shown in Figure 4.34.

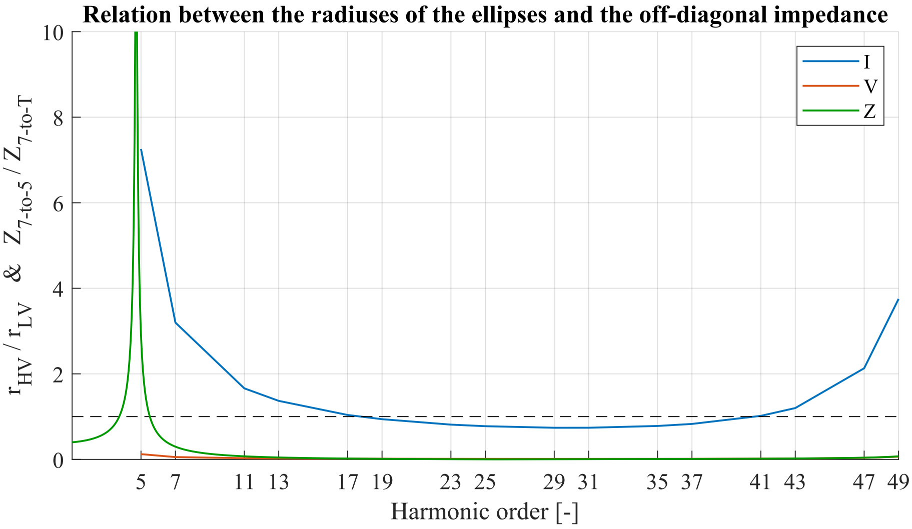

Figure 4.34: The relations between the height and width of the HV- and LV-ellipses and the relation of the off-diagonal impedance from Bus 7 to Bus 5 and T with an UGC in Line 1 and an OHL in Line 2.

From Figure 4.34 it can be seen, that the impedance, voltage and current relation are similar to that of the system with UGCs in both Line 1 and 2 as shown in Figure 4.30.

This shows, that the difference to an UGC on the 400 kV level affects the voltage difference across the transformer, while the change to an UGC on the 130 kV level does not. To verify this, the impedance relations for the case with OHLs on both sides, UGCs on both sides, OHL in Line 1 and UGC in Line 2 and opposite are compared in Figure 4.35.

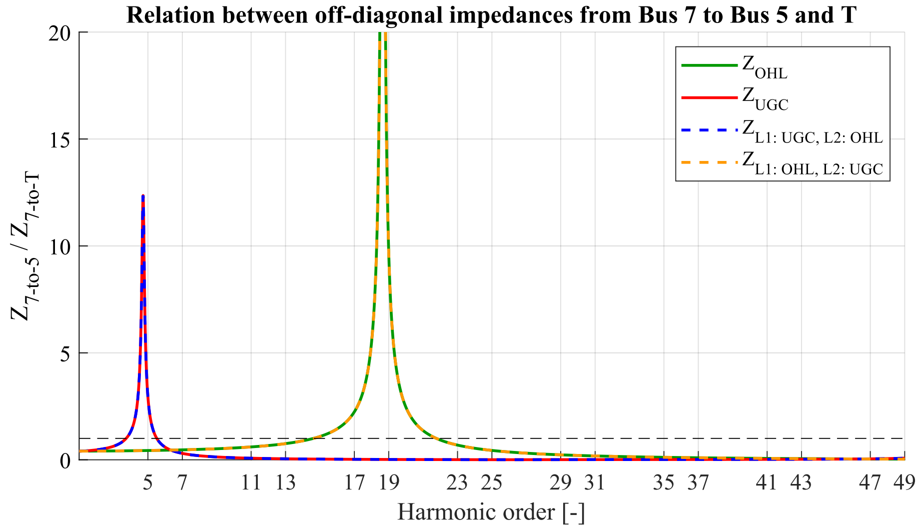

Figure 4.35: The relations between the off-diagonal impedance from Bus 7 to 5 and T.

The impedance characteristics in Figure 4.35 confirms, that the impedance relation only changes when Line 1 is changed on the 400 kV side. As the impedance relation describes the voltage difference across the transformer, it can be concluded, that the voltage difference is only affected by changes on the 400 kV side.

If the same impedance analysis is made with the off-diagonal from Bus 1 to Bus 5 and T, it can be analysed if only changes in Line 2 affects the impedance relation. The result is shown in Figure 4.36.

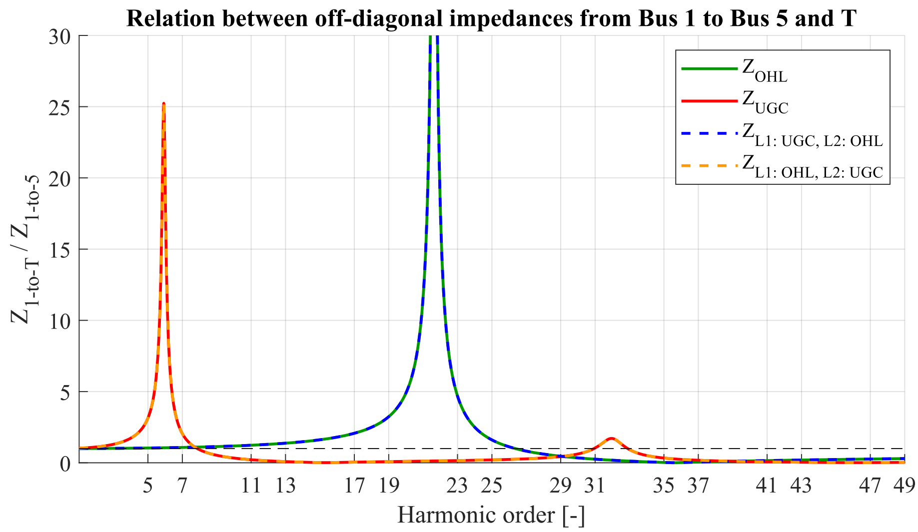

Figure 4.36: The relations between the off-diagonal impedance from Bus 1 to 5 and T.

If the impedance relation in Figure 4.36 is above the dashed black line at 1, an increase in the harmonic voltage occurs from Bus 5 to Bus T. If the impedance relation is below 1, a harmonic voltage decrease occurs. In Figure 4.36 it can be seen, that only changes made in Line 2 affects the impedance relation. From this analysis it can be concluded, that only changes in the system in the direction of the measured impedance relation has an influence on the impedance relation across the transformer.

Summary and Discussion

In this chapter, a 410/410 kV and a 410/145 kV transformer were implemented in the radial system presented in Chapter 3. When implementing the 410/410 kV transformer, it was observed from a frequency scan, that the added inductive impedance from the transformer shifted the resonances to lower frequencies compared to the system without a transformer.

Afterwards, the system with the 410/145 kV transformer was analysed by performing a frequency scan. Here the first resonance was shifted to a higher frequency compared to the radial system without a transformer. The reason for this was found to be due to the different voltage levels in the system. It was shown, that the per unit conversion factor should be considered when analysing the harmonic impedance of a system with different voltage levels. Therefore, observed from the HV-side, the impedance of the LV-side was multiplied by the conversion factor. Oppositely, observed from the LV-side, the impedance of the HV-side was divided by the conversion factor.

The influence on the impedance characteristic when implementing UGCs in the radial system with a 410/145 kV transformer was analysed. The radial system was modified to make the results comparable. The lengths of both Line 1 and 2 were 25.3 km. From this analysis it was observed, that the first resonance was shifted towards lower frequencies when having an UGC on the HV-side and an OHL on the LV-side compared to the opposite scenario. Moreover, it was analysed how the bus of observation impacted the impedance plots. It was observed, that the line type on the side of observation had the greatest impact on second parallel resonance. If an UGC was on the side of observation the second parallel resonance was more damped than if an OHL was present.

After the impedance analyses, the harmonic propagation was analysed. The first analysis was made in the system with the 410/410 kV transformer. The circle theory from Chapter 3 was applied. From the analysis, it was observed, that two circles were necessary to describe the harmonic propagation through a transformer. This was due to the transformer impedance which resulted in a harmonic voltage difference across the transformer. This harmonic voltage difference was an increase for some harmonic orders and a decrease for other harmonic orders. The two circles were utilised to describe three different harmonic orders in order to show the general tendencies of harmonic voltage difference due to the transformer. The following findings were observed:

- If both terminals connecting the transformer are in the inductive region, a decrease in the harmonic voltage occurs from the sending to the receiving end
- If both terminals connecting the transformer are in the capacitive region, an increase in the harmonic voltage occurs from the sending to the receiving end
- If the sending end terminal of the transformer is in the inductive region and the receiving end of the transformer is in the capacitive region either an increase or

decrease in the harmonic voltage occurs dependent on the current magnitude

As the harmonic voltage difference could either be an increase or decrease, the circle configuration in relation to each other changed dependent on the harmonic order observed. For higher order harmonics, it was observed, that the voltage difference always decreased from the LV- to the HV-side. This was found to be due to the impedance of the transformer, which increased with frequency.

It was analysed whether the circle relations were obtainable by utilising the frequency scan method. Here it was observed, that the off-diagonal impedance could be utilised to determine if the harmonic voltage difference from Bus T to Bus 5 was an increase or decrease. This was done by dividing the off-diagonal impedance from the bus of injection (Bus 7) to 5 by the off-diagonal impedance from Bus 7 to T. It was shown, that this impedance relation followed the tendencies of the voltage relation of the circles. The impedance relation could be utilised to obtain the exact harmonic voltage difference across the transformer, which the circles could not.

Hereafter, the harmonic propagation in the system with the 410/145 kV transformer was analysed. When considering the circle in per unit values, the harmonic propagation between voltage levels could no longer be normalised to the same type of circles as was the case with the 410/410 kV transformer. This was due to the current on the HV-side being divided by the turns ratio while the voltage was multiplied. Therefore, two ellipses were utilised to describe the harmonic propagation between voltage levels, which followed the same principles as the circles.

The relation between the ellipses also changed dependent on the harmonic order observed. The ellipse relations were plotted in order to describe the harmonic currents and voltages. The impedance relation was also plotted. Here it was observed, that the voltage and impedance relation followed each other in terms of when a peak occurred. However, the magnitude of the two curves were not equal. In some cases, the voltage relation was observed to not show a voltage increase from Bus T to Bus 5 for harmonic orders, when a voltage increase occurred. This was because the voltage relation was determined based on the maximum of the ellipse, while busses could be far from the maximum. Therefore, in order to determine if the voltage difference across the transformer is a increase or a decrease, the harmonic impedance relation can be utilised.

The harmonic propagation in the system with the 410/145 kV transformer and the OHLs replaced by UGCs was also analysed. First the system with both OHLs replaced by UGCs was analysed. Afterwards, the system with an OHL in Line 1 and an UGC in Line 2 and opposite was analysed. From these analyses, it was observed that when injecting on the LV side, the impedance relation from Bus T to Bus 5 was only affected when the HV line was modified. The same impedance relation analysis were conducted with an injection in Bus 1. For this case, only changes on the 130 kV level affected the impedance relation. Hence, only changes in the system in the direction of the impedance relation has an influence on the impedance relation across the transformer.

In this chapter, the circle and ellipse theories were applied to illustrate the harmonic propagation through a transformer. It was concluded that the circle and ellipse theory was a good tool to visualise the harmonic voltage difference across the transformer. In practice the circles and ellipses are not useful as the harmonic voltages, currents and the angle between these are required. Hence, many measurements should be utilised. Additionally, the relation between the ellipses did not describe the voltage difference across the transformer exactly. The exact voltage difference across the transformer was instead obtained utilising the off-diagonal impedance.

In the next chapter, the tendencies observed in this chapter are analysed in a meshed system.

Meshed System Analysis 5

In this chapter, harmonic analyses for a meshed system are performed. The meshed system analysed in this chapter is based on the *Example grid* from PowerFactory, originally made by Oscar Lennerhag [21]. First the *Example grid* will be presented together with the adjustments made in the model to fit the scope of this study.

The first analysis performed is regarding the harmonic impedance, which is obtained utilising the frequency scan method. An impedance analysis with different line types in the meshed system is performed to investigate the influence of replacing OHLs with UGCs and opposite. The original share of UGCs and OHLs in the *Example grid* is utilised as a reference. This reference is compared to having the entire 400 kV or 130 kV systems implemented as UGCs or OHLs.

In Chapter 4 it was shown that the per unit conversion factor impacts the impedance on the opposite side of the transformer from the bus of observation. This effect is also analysed in the meshed system. This is done by changing the turns ratio of the transformers and increasing the voltage level of the LV-side from 130 kV to 220 kV and 400 kV. Hereafter, the impedance of the transformer is set to 0 Ω. By setting the transformer impedance to 0 Ω, the relation between the HV- and LV-side is independent of the transformer impedance. The last impedance analysis case considered is the impact from the line lengths on the HV- and LV-side. The line lengths on the LV-side are increased to have the same total line length as the HV-side.

Hereafter, harmonic propagation in the meshed system is analysed. In the radial system the circle theory could be utilised to visualise the harmonic propagation in the lines and through the transformer. Therefore, it is analysed if the circle theory is applicable in the meshed system.

In addition to the circle theory analyses, the propagation of harmonic currents in a single bus in the meshed system is analysed. This is done to understand how the currents flow in a meshed system, as the currents can flow in multiple paths. In Chapter 4 it was discovered that a harmonic voltage difference occurred through the transformer. This difference can either be an increase or a decrease. Therefore, it is analysed if the tendencies are still valid in the meshed system. The analysis is performed for the reference meshed system and for the meshed system where the lines in the LV-system are replaced by UGCs. These scenarios are compared to investigate how the harmonic voltage propagation between voltage levels is affected when the 130 kV line types changes.

Besides analysing the harmonic voltage propagation through a transformer, the harmonic voltage in all the busses in the meshed system are analysed. The analysis is performed for the reference system, when the lines in the LV-system are replaced by OHLs and when the lines in the LV-system are replaced by UGCs. This is done to investigate the tendencies of harmonic voltage differences across the transformer in the entire meshed system, when changing the line types.

5.1 Meshed System Model and Adjustments

The original system schematic of the *Example grid* implemented in PowerFactory is shown in Appendix C.1 in Figure C.1. The main voltage levels in the model are 400 kV, 220 kV and 130 kV. Additionally, lower voltage levels in two different networks called urban and rural network are included. Furthermore, there are two network models within the original PowerFactory model. The first is a simplified system model and the second is a detailed system model. The simplified system model has the UGCs bonded ideally by PowerFactory. Moreover, the urban downstream networks are represented by constant power loads. The rural downstream networks are very small and hence not included in the simplified model. For the detailed system model, both of the downstream networks and some of the UGCs are modelled with more details. [26]

The simplified system model will be utilised in this report to simplify the analysis of the harmonic propagation in a meshed system. Adjustments are made in the simplified system model in order to fit the model for the scope of this study. First, the 220 kV system is removed in order to focus on the harmonic propagation between the 400 kV and 130 kV voltage levels. In the original PowerFactory model the transposition of the OHLs are modelled by connecting phase A to phase B, phase B to phase C and phase C to phase A along the OHL. This modelling of the transposition does not provide accurate results for a balanced load flow. Therefore, the transposition of the OHLs are changed to have a perfect transposition in the tower types. Moreover, for simplicity the UGCs are changed to be cross-bonded. The parameters of the tower and cable types utilised in the model are changed to distributed as recommended by PowerFactory for harmonic analyses. The circuit schematic of the adjusted simplified *Example grid* analysed in this chapter is shown in Figure 5.1.

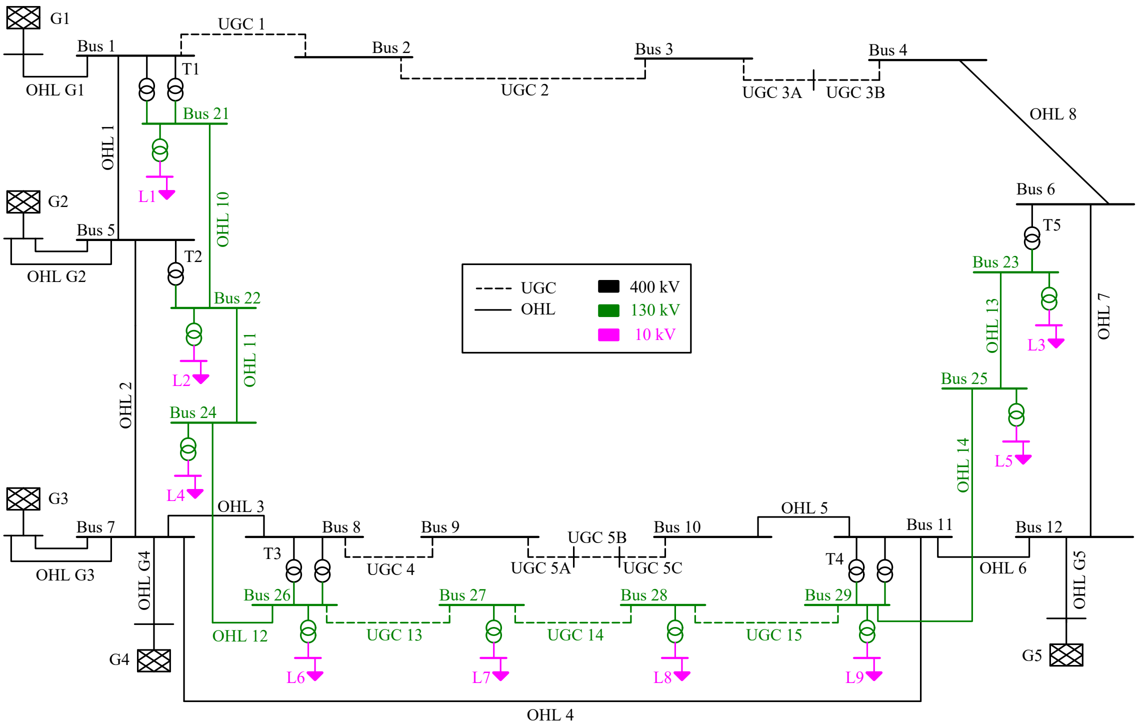

Figure 5.1: Circuit schematic of the adjusted simplified *Example grid* from PowerFactory originally made by Oscar Lennerhag [21].

In Figure 5.1, the elements connected to the 400 kV system are marked with black, while the elements connected to the 130 kV system are marked with green. The 400 kV system has twelve busses denoted Bus 1 to Bus 12. The 130 kV system has nine busses denoted Bus 21 to Bus 29. The loads seen in Figure 5.1 is part of the urban network and the power loads can be seen in Table C.1 in Appendix C.2. The external grids (G1-G5) are connected to the 400 kV system through long lines. The external grids, the equivalent urban load models and the transformer models utilised in the model are the same as utilised in the *Example grid* given in [21]. Additionally, automatic tap-changer is included in the 410/145 kV transformer models. The line types are also the same as utilised in the *Example grid* except for the adjustments mentioned previously. The lengths of the lines in Figure 5.1 are shown in Table 5.1. The UGCs on the 400 kV level are modelled as three lines in parallel.

Table 5.1: Lengths of the lines in the *Example grid*. [21]

OHL 400 kV	**Length [km]**
OHL G1	52.8
OHL G2	85.3
OHL G3	78.5
OHL G4	99.3
OHL G5	76.5
OHL 1	25.3
OHL 2	41.6
OHL 3	47.7
OHL 4	67.2
OHL 5	11.0
OHL 6	8.5
OHL 7	27.1
OHL 8	9.7
Total length	630.5

UGC 400 kV	**Length [km]**
3 x UGC 1	19.2
3 x UGC 2	40.5
3 x UGC 3A	10.8
3 x UGC 3B	15.0
3 x UGC 4	49.2
3 x UGC 5A	13.2
3 x UGC 5B	16.8
3 x UGC 5C	6.9
Total length	171.6

OHL 130 kV	**Length [km]**
OHL 10	28.0
OHL 11	25.0
OHL 12	25.0
OHL 13	20.0
OHL 14	18.0
Total length	116.0

UGC 130 kV	**Length [km]**
UGC 13	25.0
UGC 14	20.0
UGC 15	15.0
Total length	60.0

The line types and configurations of the individual lines are from [21]. At the 130 kV only one UGC type and one OHL type is used. The cable type at 130 kV is 1200 mm^2 Al. The OHL type at 130 kV is a tower type D and conductor type D. Therefore, when a 130 kV line is changed in the analyses these types will be used. At 400 kV several UGC types and OHL types are used. When an UGC at 400 kV is changed to an OHL the line type is changed to a tower type A with shield wire 2xA and conductor type A. When an OHL at 400 kV is changed to an UGC the line type is changed to a single 2500 mm^2 Cu.

The harmonic current sources are not included in the original model of the *Example grid*. Hence, the modelling of the harmonic current source is the same as utilised in Chapter 3. In Appendix C.3 it is shown that there is no tendency between the angle of injection and when the voltages add and subtract, as was shown in the radial system in Section 3.5. Therefore, the harmonic current sources utilised in the meshed system will have a phase angle of 0° and a magnitude of 1 pu.

5.2 Impedance Analysis

The impedance characteristic is analysed for different case studies in order to observe the impact, when changing the lines in the meshed system to OHLs and UGCs at the 400 kV and 130 kV levels. The case studies will be conducted utilising the harmonic impedance from the frequency scan. Two busses will be analysed at both the 400 kV and 130 kV voltage levels. The busses are chosen to represent the system behaviors. The busses chosen are Bus 1 and 11 at the 400 kV system and Bus 21 and 29 at the 130 kV system. They are chosen because they are located far from each other in the *Example grid* and have different line types connected. The busses are chosen to have a direct connection between the voltage levels, where Bus 1 is connected to Bus 21 and Bus 11 is connected to Bus 29. Additionally, the 400 kV busses are chosen so that one is close to the external grid and the other is not.

5.2.1 Case 1: Different Line Types on the 130 kV Side

The first case is performed in order to investigate how the 400 kV system is affected when undergrounding lower voltage levels according to the problem statement in Section 1.2. In the first case study, the lines in the 130 kV system are all changed to OHLs and afterwards to UGCs. The impedance characteristics are compared to the reference system, which contain a mix of OHLs and UGCs. The comparison of the impedance characteristics in Bus 1 and 11 at 400 kV, when the lines in the 130 kV system are changed, can be seen in Figure 5.2.

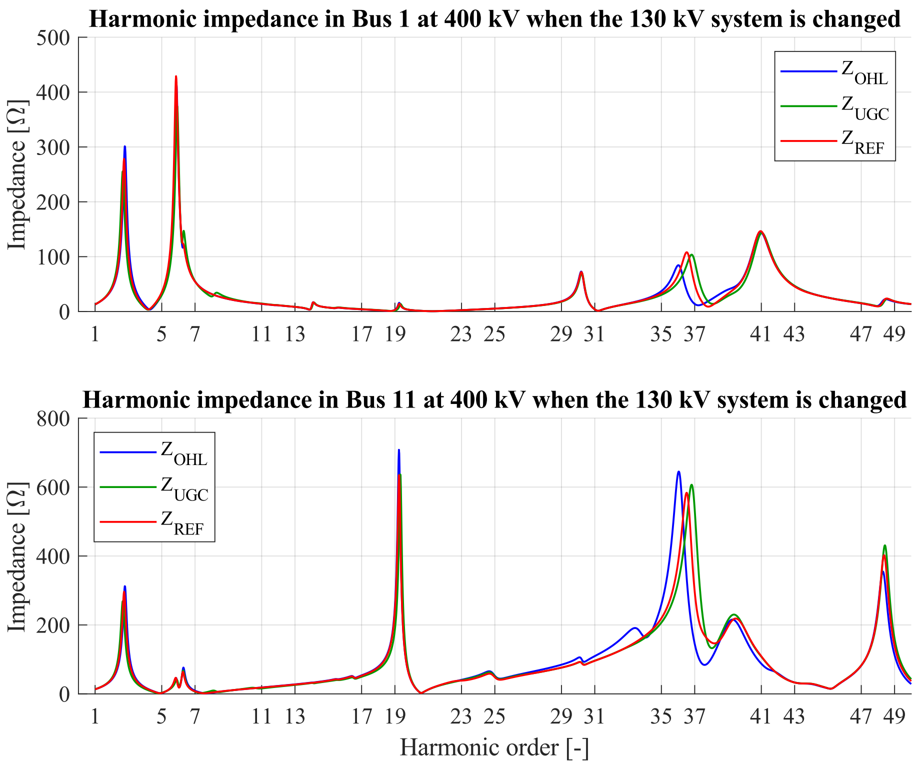

Figure 5.2: Comparison of harmonic impedance in Bus 1 and 11 at 400 kV, when the 130 kV lines are changed.

From Figure 5.2, it is visible that the impedance characteristics in the busses in the 400 kV system are barely affected, when the 130 kV system is changed. At low harmonic orders, a small difference in damping can be observed, while the resonance frequencies are almost constant. The impedance characteristic at high harmonic orders are affected more than the low orders.

The parallel resonance peaks are affected differently, when the 130 kV system is changed to OHLs or UGCs. When implementing OHLs, some of the resonance peaks are shifted to higher orders, while other resonance peaks are shifted to lower orders. The same occurs when UGCs are implemented, but at different harmonic orders. This shows that no clear tendency for when the resonance frequencies are increased or decreased can be observed. This is similar to what was observed in the radial system, where it was observed that each resonance point was affected differently from changes in the system.

The comparison of the impedance characteristics in Bus 21 and 29 at 130 kV, when the lines in the 130 kV system are changed, can be seen in Figure 5.3.

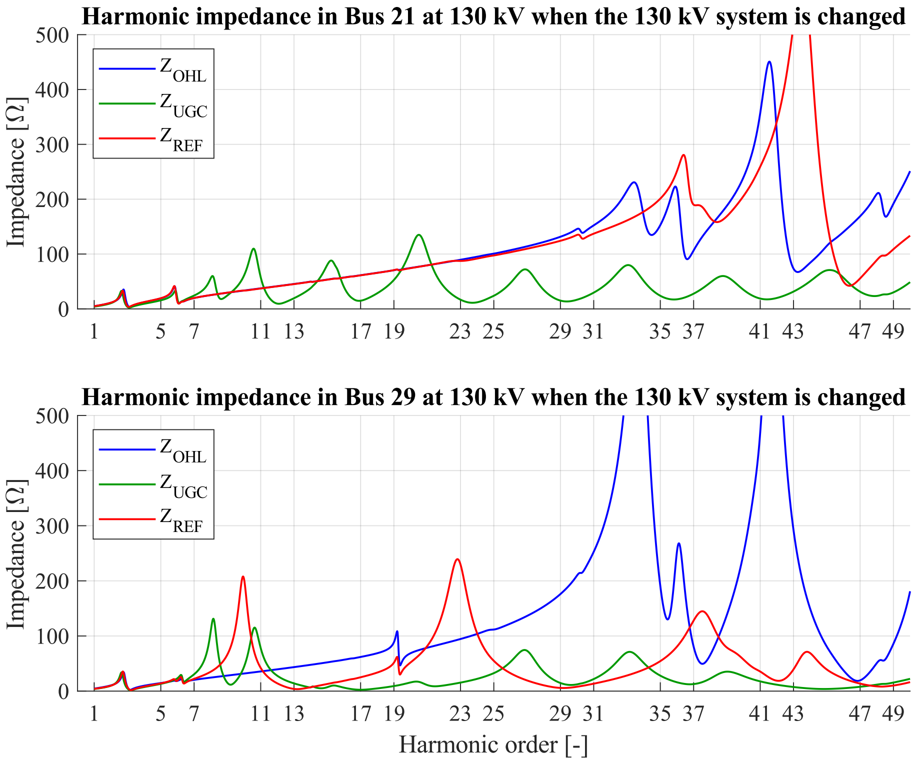

Figure 5.3: Comparison of harmonic impedance in Bus 21 and 29 at 130 kV, when the 130 kV lines are changed.

From Figure 5.3, it is visible that impedance characteristics in the busses at the 130 kV system are significantly affected, when the 130 kV line types are changed. The impedance characteristic in Bus 21 is especially affected, when UGCs are implemented, while the implementation of OHLs has less influence. In Bus 29 the impedance characteristic is significantly affected when OHLs are implemented. The impedance characteristic in Bus 29 is also changed when UGCs are implemented, but not as much as in Bus 21. These changes can be explained from the system configuration seen in Figure 5.1, where Bus 21 is connected to the rest of the 130 kV system through an OHL. Therefore, when the system is changed to UGCs, the line connected directly to Bus 21 is changed, which has a significant impact. When the system is changed to OHLs, the lines that are changed are located far from Bus 21 and therefore less impact is observed. Bus 29 is connected to the rest of the 130 kV system through an OHL and an UGC. Therefore, the impedance characteristic is affected when the system is changed to either OHLs or UGCs, since the lines directly connected to Bus 29 are changed. From this it can be seen that the impedance characteristics are more influenced by the lines close to the point of observation, compared to the lines far away, as was also observed in the radial system.

5.2.2 Case 2: Different Line Types on the 400 kV Side

In Case 1 it was observed that when the system is changed, the harmonic impedance was almost exclusively affected at the voltage level where the changes are made. The second case is performed in order to investigate if this is valid when the changes are performed on the 400 kV system.

In this case study, the lines in the 400 kV system are all changed to OHLs and afterwards to UGCs. The impedance characteristics in Bus 1 and 11 at 400 kV, when lines in the 400 kV system are changed, can be seen in Figure 5.4.

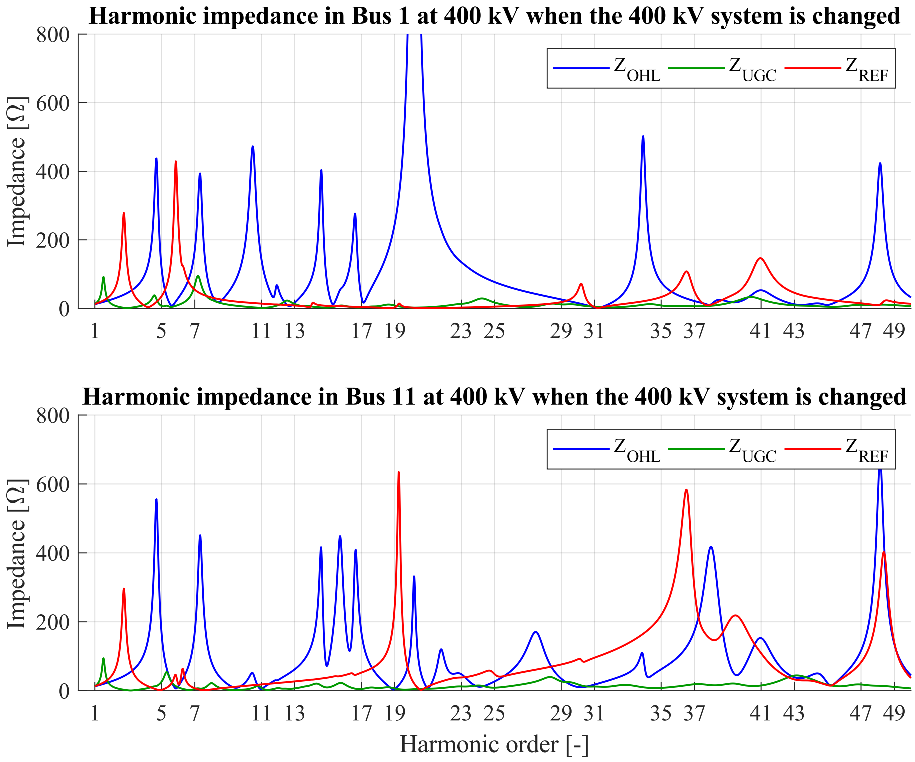

Figure 5.4: Comparison of harmonic impedance in Bus 1 and 11 at 400 kV, when the 400 kV lines are changed.

From Figure 5.4, it is visible that the impedance characteristics in the busses in the 400 kV system are significantly changed, when the 400 kV system is changed. Bus 1 is connected to the rest of the 400 kV system through both OHLs and UGCs. This can explain why the impedance characteristic is significantly changed when the system is changed to either OHLs or UGCs. Bus 11 is connected through OHLs, which can explain why the impedance characteristic is most affected in terms of the magnitude when the lines are changed to UGCs. However, the impedance characteristic in Bus 11 is also significantly affected when the system is changed to OHLs. This can be explained from the short length of OHL 5 of 11 km. Therefore, when the lines in UGC 4 and 5 are changed to OHLs it affects Bus 11. Additionally, UGC 4 and 5 are three lines in parallel, which means that the capacitance is three times larger. As a result, the change from UGCs to OHLs in UGC 4 and 5 has a large effect on the impedance seen from Bus 11.

The impedance characteristics in Bus 21 and 29 at 130 kV, when the lines in the 400 kV system are changed, can be seen in Figure 5.5.

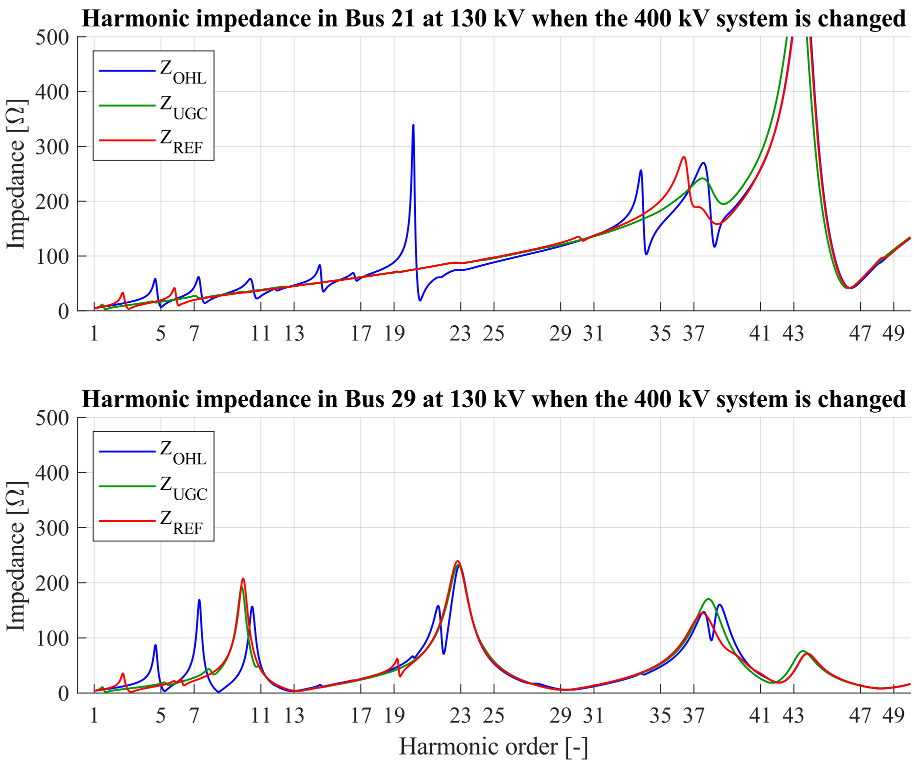

Figure 5.5: Comparison of harmonic impedance in Bus 21 and 29 at 130 kV, when the 400 kV lines are changed.

From Figure 5.5, it is visible that the impedance characteristics in the busses in the 130 kV system are affected when the 400 kV lines are changed. However, the busses at 130 kV are not as affected as the busses at 400 kV when the 400 kV system is changed. This shows that the system is less affected, when changes are made on a different voltage level than where it is observed. This could be explained from the impedance of the transformer, since the other voltage level is observed through the transformer impedance. This will be analysed further in Section 5.2.4. However, the impedance characteristics in the busses at 130 kV are more affected when the 400 kV system is changed than the busses at 400 kV when the 130 kV system is changed. This indicates that the system impedance is more affected when lines at higher voltage levels are changed. The same tendency was observed in the radial system in Section 4.3, where the behaviour was explained from the per unit conversion factor. Therefore, the per unit conversion factor in the meshed system will be analysed in the following sections.

5.2.3 Case 3: Influence of Transformer Turns Ratio

In Case 1 and 2 it was observed that the harmonic impedance was mainly affected on the voltage level where the line changes were performed. Additionally, the LV-system was affected more when the HV-system lines were changed than opposite. This indicates that the voltage levels has an influence, which will be analysed in this case study. The influence on the impedance characteristic from different voltage levels is analysed by changing the voltage levels on the LV-side of the transformers. The system considered follows the *Example grid* shown in Figure 5.1. The system is analysed for three cases where the voltage levels on the LV-side of the transformer (marked with green in Figure 5.1) is 130 kV, 220 kV and 400 kV. The transformer impedance is kept as the per unit values described in Table 4.1. The systems are then compared to when the LV-system is disconnected, which means that only the black elements in Figure 5.1 are connected. This is done in order to investigate the influence of having the LV-system implemented compared to just having the HV-system implemented. The LV-side line types will be kept as the original types for all cases only the voltage level will be changed. The impedance characteristics in Bus 1 and 11 of the three cases compared to when the LV-system is disconnected can be seen in Figure 5.6.

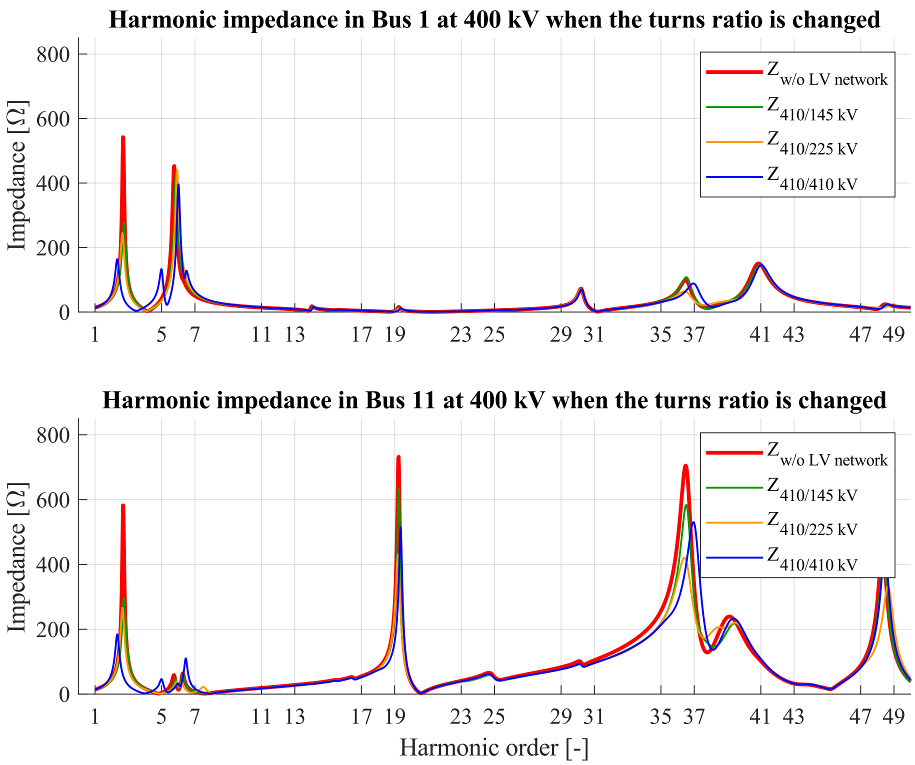

Figure 5.6: Comparison of the influence of the voltage levels of the LV-system on the harmonic impedance in Bus 1 and 11 at 400 kV.

As seen in Figure 5.6 the voltage level changes on the LV-side influence mainly the harmonic impedance magnitude, while the resonance frequencies are almost constant. Additionally, the harmonic impedance in Bus 1 and 11 are the least affected when the 130 kV system is disconnected compared to the other LV-systems. When the voltage levels on the LV-side of the transformer is increased to 220 kV, there is a larger difference compared to the system with the LV-system disconnected. The difference is further increased when the LV-system is changed to 400 kV. The largest differences are observed at lower harmonic orders, which is the worst case for a power system. From this it can be concluded that changes on lower voltage levels has less influence on higher voltage levels in terms of the impedance plot. This could be explained from the per unit conversion factor as in the radial system and will be explored further in the following case study.

5.2.4 Case 4: Influence of Transformer Impedance

In Case 3 it was shown that the voltage levels had an influence on the impact of the harmonic impedance. In order to investigate this further, the system is analysed for the three cases without transformer impedance included.

In this case the analyses are performed for Bus 11 and 29. First the case where the lines on the 130 kV side are changed to UGCs and OHLs, as in Section 5.2.1, are considered with and without transformer impedance. The impedance characteristic in Bus 11 at 400 kV can be seen in Figure 5.7.

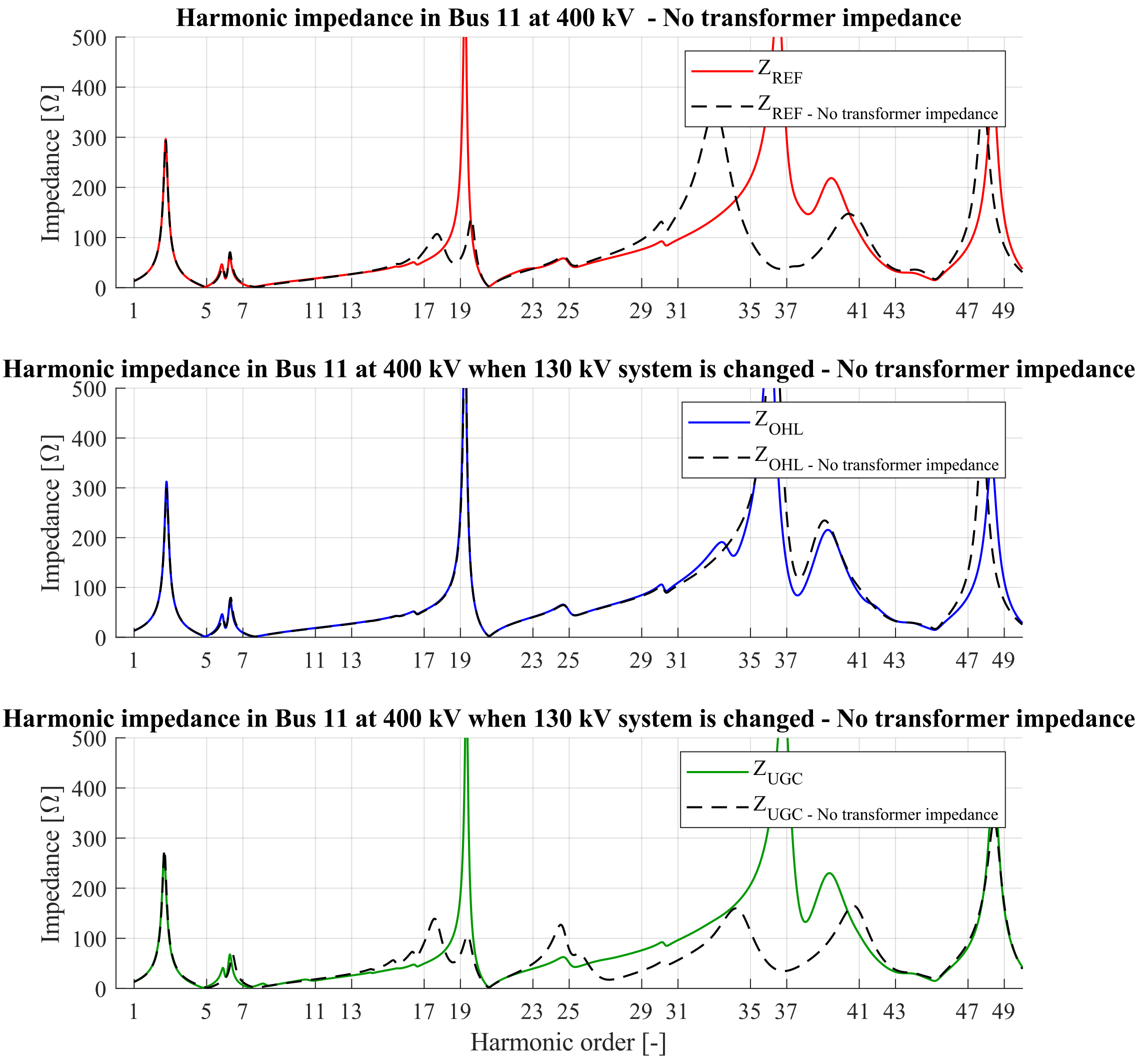

Figure 5.7: Comparison of harmonic impedance in Bus 11 at 400 kV, when the 130 kV lines are changed, with and without transformer impedance.

As seen in Figure 5.7, the impedance characteristic of Bus 11 is affected differently depending on if the 130 kV system consists of UGCs, OHLs or a mix in the reference case. The largest influence of the transformer impedance is observed for the case where the 130 kV lines are UGCs. As previously mentioned, the frequency scan is performed by injecting a current, which is used to calculate the harmonic impedance. Hence, the harmonic impedance is determined by the path of least impedance. In Chapter 4 it was explained that observed from the HV-side, the LV-side impedance is increased by the per unit conversion factor. In order for the current to flow to the 130 kV system, the harmonic impedance has to be much lower at the 130 kV side. The transformer impedance can be considered as a series impedance between the 400 kV and 130 kV system. Therefore, when the transformer impedance is removed the harmonic current might propagate to the 130 kV system at certain harmonic orders which would not be allowed if the transformer impedance was included. However, when the transformer impedance is removed it is possible for the harmonic current to propagate to the 130 kV system for certain setups and harmonic orders. The reason for why the UGC case is more affected when the transformer impedance is removed can be explained from the electric parameters of the UGCs. As explained in Section 3.3, the parallel resonance peak magnitudes of the harmonic impedance are lower for UGCs compared to OHLs. Hence, for certain harmonic frequencies the harmonic impedance of the 130 kV is lower than the 400 kV system and the current prefers to flow at the 130 kV system. At the low harmonic orders the current prefers to flow to the 400 kV system, since that is the path of least impedance. Therefore, the impedance characteristic at low harmonic orders is not affected when the transformer impedance is removed.

To analyse this further the impedance characteristic at the 130 kV system is considered. The impedance characteristic in Bus 29 at 130 kV, with and without transformer impedance, can be seen in Figure 5.8.

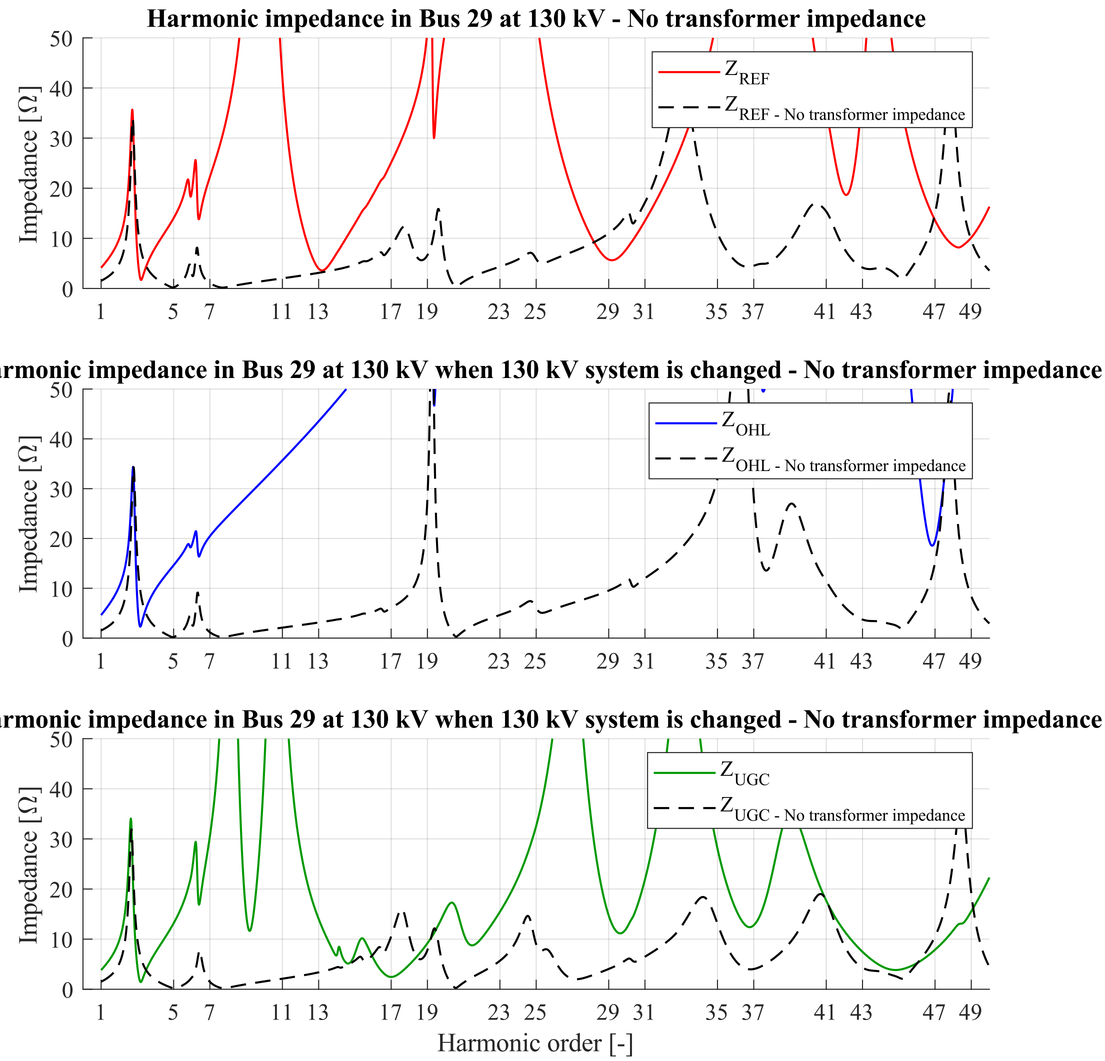

Figure 5.8: Comparison of harmonic impedance in Bus 29 at 130 kV, when the 130 kV lines are changed, with and without transformer impedance.

As seen in Figure 5.8, the impedance characteristic of Bus 29 is very different if the transformer impedance is included or not. As observed in Chapter 4, when observed from the LV-side, the HV-side impedance is divided by the per unit conversion factor. Therefore, when the transformer impedance is removed, the 400 kV system has a lower impedance seen from the 130 kV system than the 130 kV system itself. With the transformer impedance removed the two systems are directly connected. As a result, the harmonic impedance in Bus 11 and Bus 29 follows the same characteristic, but with different magnitudes as seen in Figure 5.9.

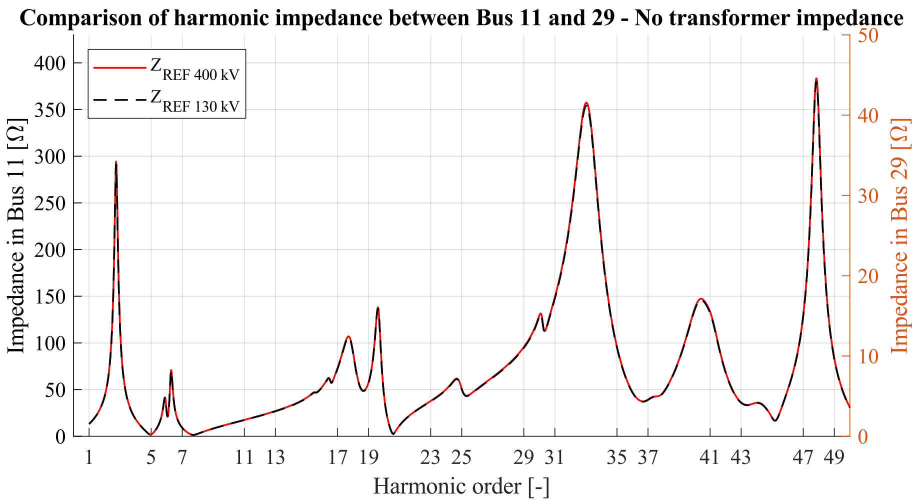

Figure 5.9: Comparison of harmonic impedance in Bus 11 and 29 for the reference case when the transformer impedance is removed.

The two impedance characteristics shown in Figure 5.9 follows two different axes. The 400 kV system follows an axis that is 8.6 times higher than the 130 kV system.

The 8.6 larger axis on the 400 kV side is a result of dividing the LV-side impedance with the HV-side impedance without the transformer impedance. This is shown by the dashed line in Figure 5.10. In the radial system in Chapter 4, the relation between the HV- and LV-side was determined as the per unit conversion factor which was 8. The 8.6 obtained in the meshed system is due to the tap changer in the transformer. Hence, if the tap changer is removed, the relation between the HV- and LV-side in the system without the transformer impedance would be the per unit conversion factor of 8. If the transformer impedance is included, the relation between the HV- and LV-side is not constant. This is shown in Figure 5.10.

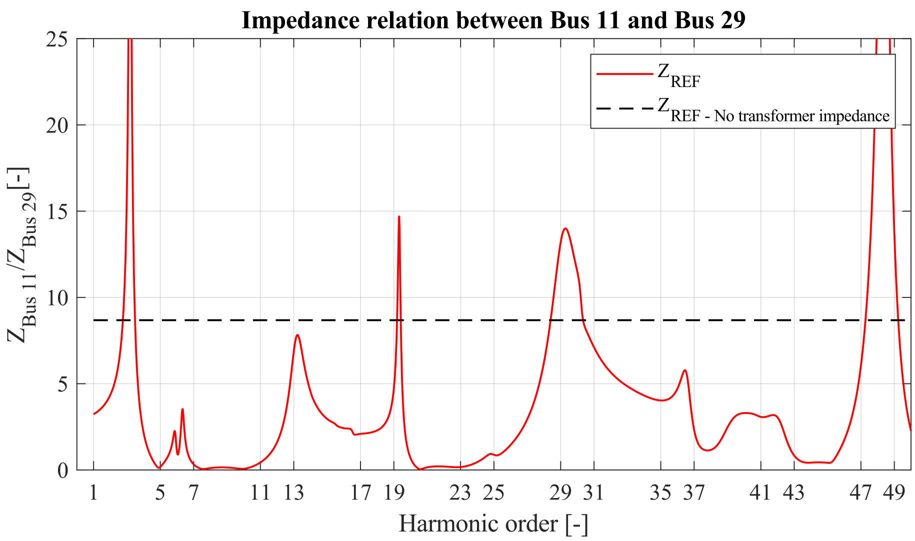

Figure 5.10: Impedance relation in meshed system between Bus 11 and Bus 29, with and without transformer impedance.

The influence of the transformer impedance when the lines on the 400 kV side are changed, as in Section 5.2.2, can be seen in Appendix C.4.1 in Figure C.3 and C.4. The analysis confirms the findings from the previous case, that removing the transformer impedance, highlights the path of least impedance and the conversion factor.

Next the influence of the turns ratio of the transformer as in Section 5.2.3 is analysed. The impedance characteristic in Bus 11 at 400 kV with and without transformer impedance can be seen in Figure 5.11.

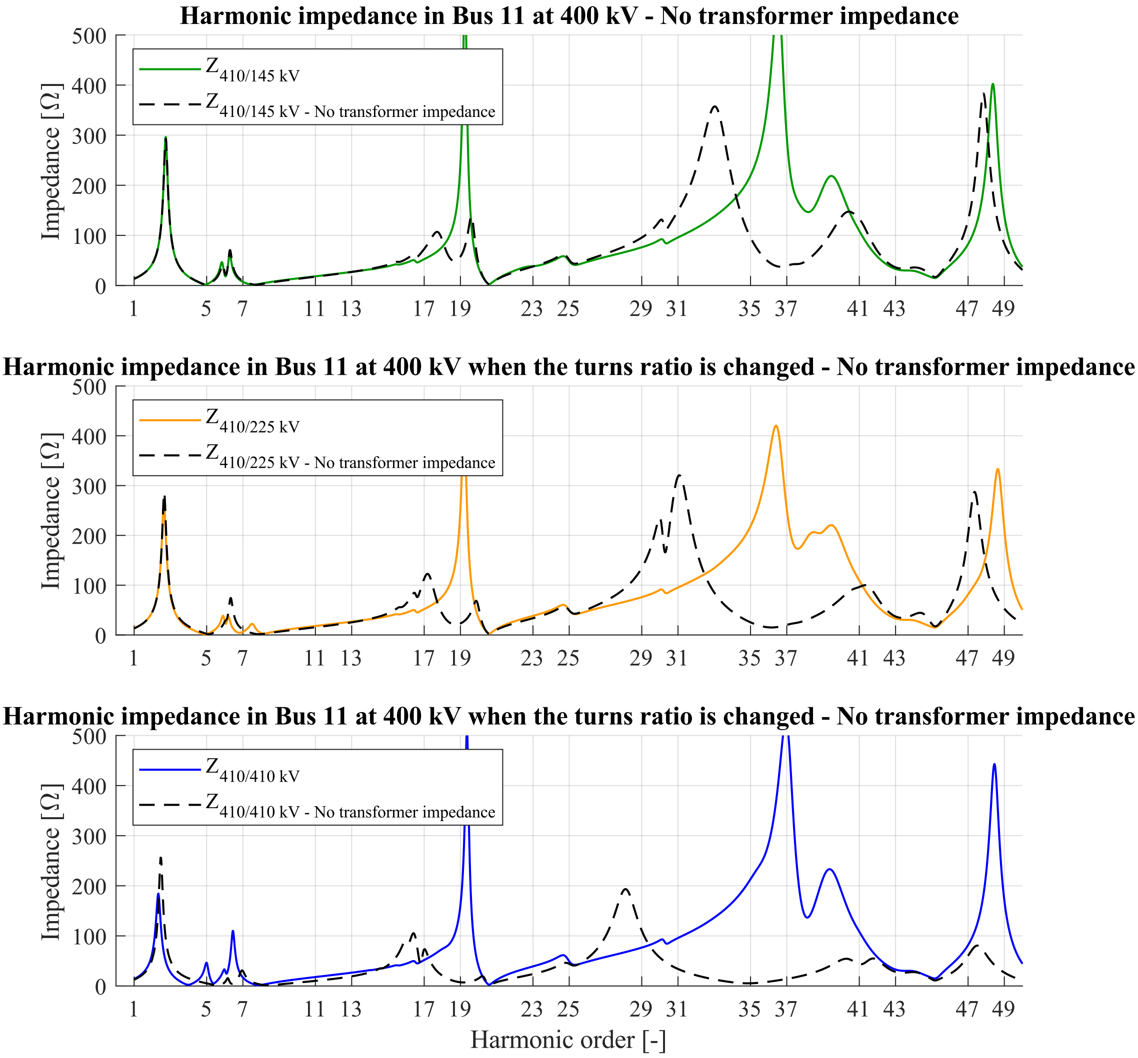

Figure 5.11: Comparison of harmonic impedance in Bus 11 at 400 kV, when the turns ratio is changed, with and without transformer impedance.

As seen in Figure 5.11, the influence of the transformer impedance seen from Bus 11 is largest when the turns ratio decreases, i.e. when the LV-system voltage increases. This can be explained from the conversion factor which will be smaller when the turns ratio decreases. Hence, if the transformer impedance is removed, the 410/410 kV system will have a conversion factor of 1. Therefore, the LV-system is equal to the HV-system, but with different line types.

5.2.5 Case 5: Longer lines at LV system

In the previous cases it was shown that the 400 kV system had the most influence on the harmonic impedance. However, the total line length at the 400 kV system is longer than the total line length at 130 kV. Therefore, the 130 kV lines are made longer in order to investigate the influence of this.

As seen in Table 5.1, the 400 kV system consist of 630.5 km OHLs and 171.6 km UGCs resulting in a total line length of 802.1 km. Additionally, the 130 kV system consists of 116 km OHLs and 60 km UGCs resulting in a total total line length of 176 km. Therefore, the line lengths in the 130 kV system are multiplied by a factor of 4.557 in order to have equal line lengths.

First the case where the lines on the 130 kV side are changed to OHLs and UGCs as in Section 5.2.1, with and without longer lines at the 130 kV system are considered. The impedance characteristic in Bus 11 at 400 kV can be seen in Figure 5.12.

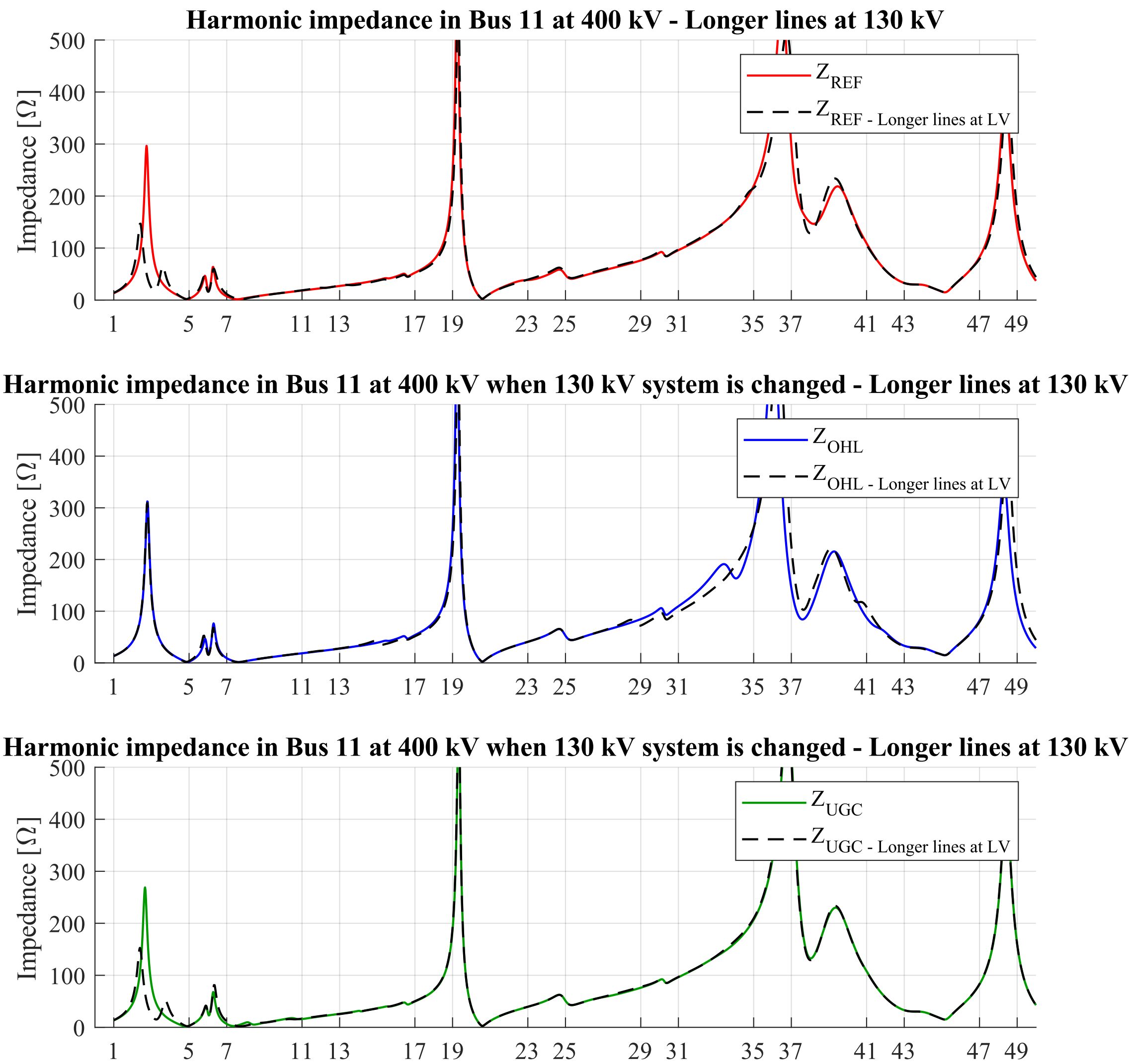

Figure 5.12: Comparison of harmonic impedance in Bus 11 at 400 kV, when the 130 kV lines are changed, with and without longer lines at the 130 kV system.

As seen in Figure 5.12, the impedance characteristic is affected differently for the three cases, when the lines at 130 kV are made longer. In the case where the 130 kV system is replaced by UGCs, the impedance characteristic is slightly changed at the low harmonic orders. In the case where the 130 kV system is replaced by OHLs, the impedance characteristic is slightly changed at the high harmonic orders. The case of the reference system, which has a mix of OHLs and UGCs, has a small difference which can be observed at both the low and high harmonic orders. This can be explained from the fact that Bus 11 is connected with OHLs and UGCs are connected close to Bus 11.

In the case where the lines in the 400 kV system are changed as in Section 5.2.2, when the 130 kV lines are made longer or not can be seen in Appendix C.4.2 in Figure C.5. When the lines in the 400 kV system are replaced by UGCs, the impedance characteristic is not affected. This makes sense, since the harmonic current will stay at the 400 kV system due to the low harmonic impedance of the UGCs. When the lines in the 400 kV system are replaced by OHLs, small differences in the impedance characteristic can be seen.

In the case where the transformer turns ratio is changed as in Section 5.2.3, when the 130 kV lines are made longer or not can be seen in Figure 5.13.

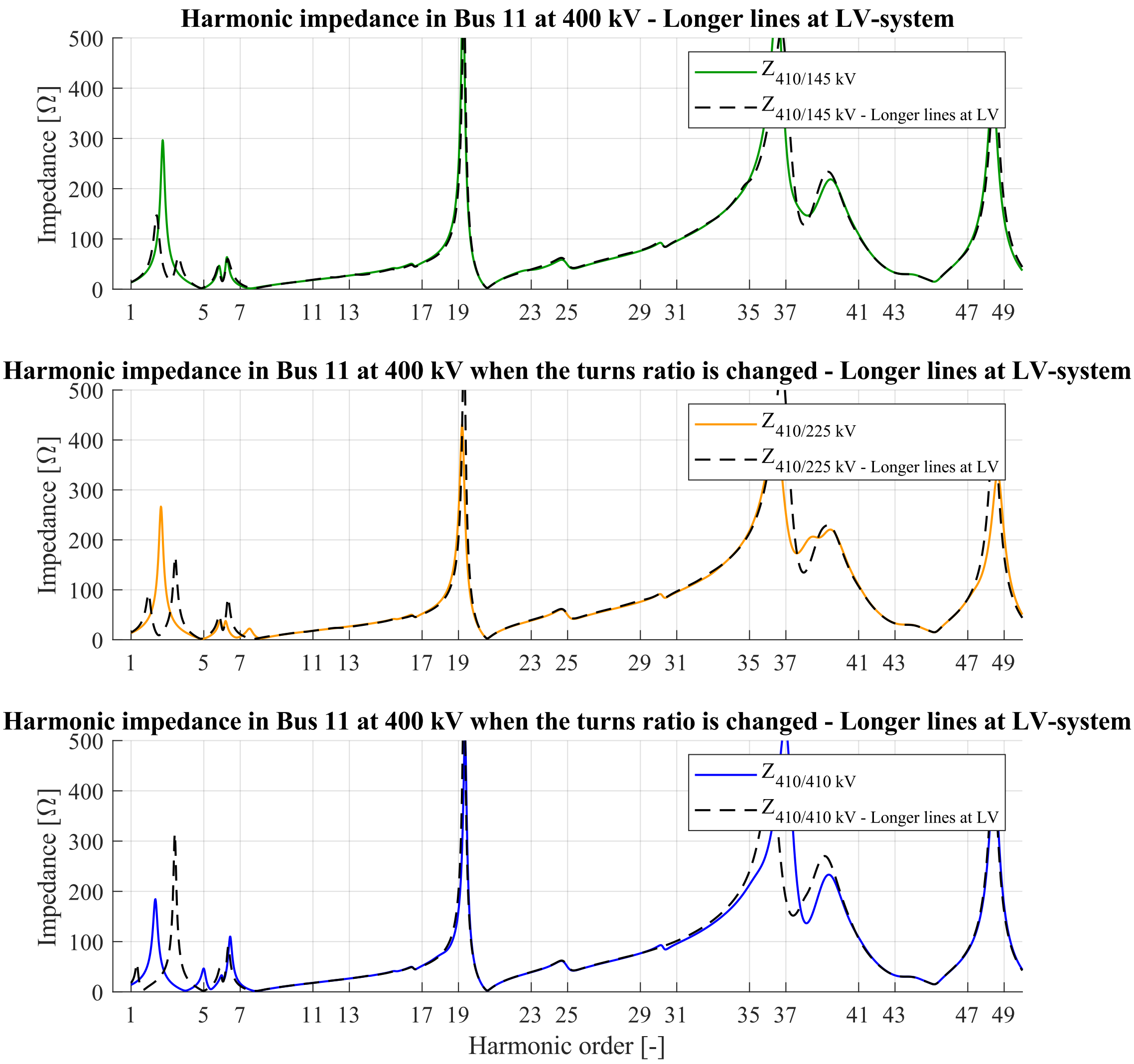

Figure 5.13: Comparison of harmonic impedance in Bus 11 at 400 kV, when the turns ratio is changed, with and without longer lines at the 130 kV network.

The influence of the increased line length at the LV-system is largest when the transformer turns ratio decreases, i.e. when the LV-system voltage increases. This can be explained from the conversion factor, which decreases with the turns ratio squared and observed from the HV-side the LV-side impedance is multiplied by the conversion factor. Additionally, changes to the resonance frequency can be observed at low harmonic orders, when the line length of the LV-system is increased.

5.3 Harmonic Propagation in a Meshed System

In this section, the harmonic propagation between busses and voltage levels will be analysed. To investigate harmonic propagation in the *Example grid*, a harmonic current source is connected in Bus 21. The harmonic current source injects 1 pu at the 130 kV level with the specified harmonic orders as described in Section 3.1. To simplify the analysis, the harmonic propagation study will focus on the propagation from Bus 21 to the nearby busses. The busses of interest are Bus 22, 1, 2, 5 and G1 as well as their connections which are shown in Figure 5.14. The rest of the meshed system in the *Example grid* is still connected. Additionally, the urban networks are disconnected in order to focus on the propagation in the 130 kV and 400 kV systems.

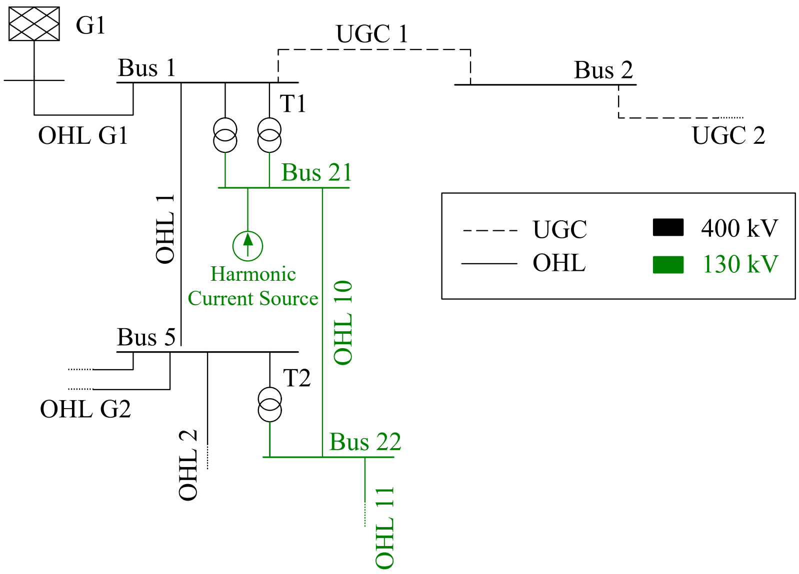

Figure 5.14: Part of the *Example grid*.

5.3.1 Harmonic Propagation Analysis using the Circle Theory

First, the harmonic propagation using the circle theory is analysed in the meshed system. When a harmonic current is injected in Bus 21, part of the current flows through OHL 10. To analyse the harmonic propagation in OHL 10, the line is divided into 12 intersections. In Figure 5.15 the harmonic voltages, currents and phase angles of the intersections between Bus 21 and 22 are visualised.

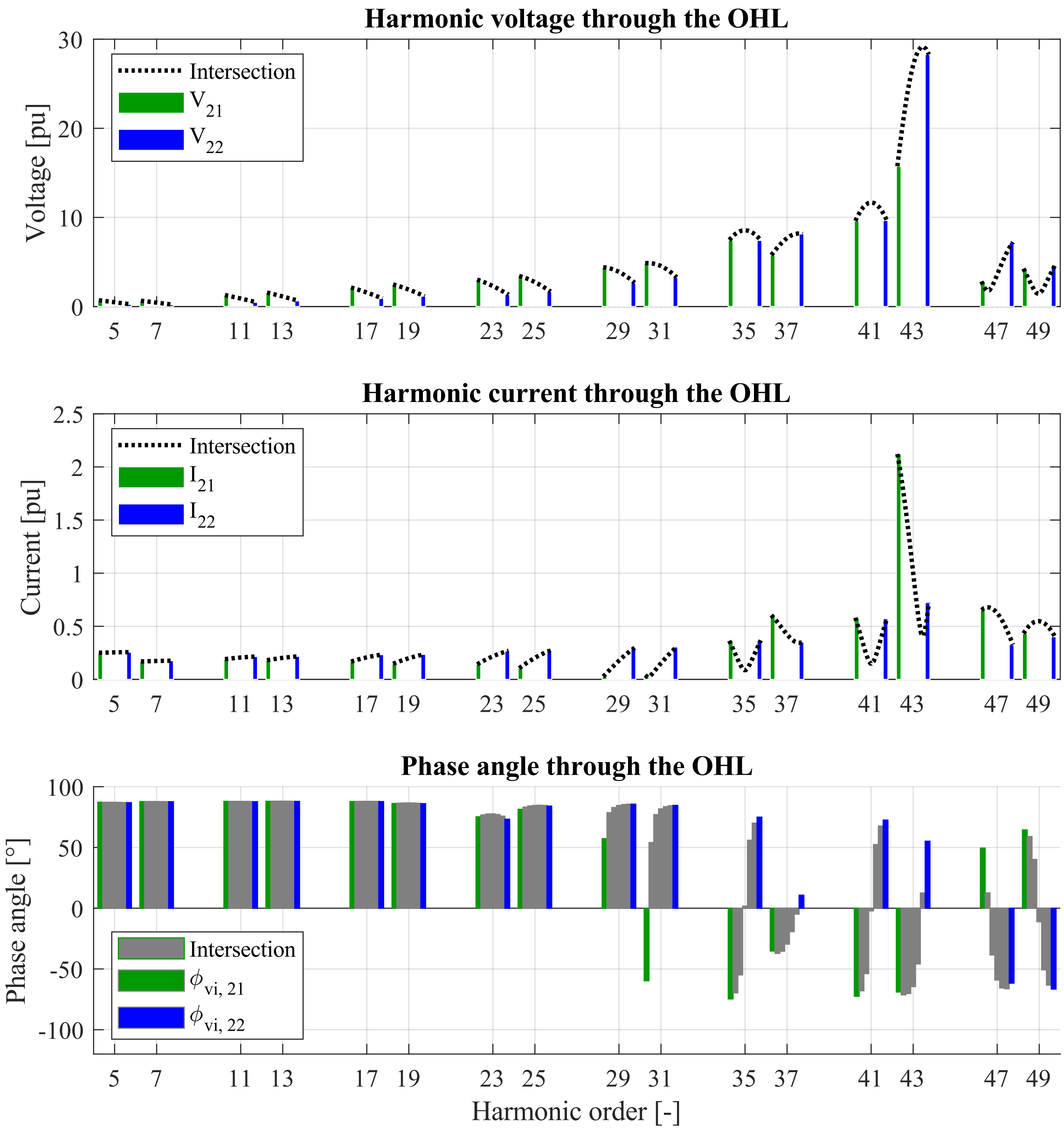

Figure 5.15: Harmonic voltages, currents and phase angles as a function of the harmonic order along OHL 10 from Bus 21 to Bus 22.

From Figure 5.15 it is visible that the voltage and current magnitude through a line in a meshed system still follows the norm of a sine wave. However, compared to the results in Chapter 3 and 4, the phase angles are no longer either 90° or $-90°$ for higher order harmonics. Additionally, the voltage and current does not cross zero during a current or voltage phase shift. This means that the current no longer is purely inductive or capacitive, but contains an active part. The reason for this can be explained by the system being a large meshed grid. In a meshed grid, the resonances occurs between several elements, which means that it is not a simple L, C and R circuit. Due to this, several resistive elements affects the system, causing a larger damping.

In order to investigate if the circle representation can be utilised in the meshed system the 47^{th} harmonic order is considered as seen in Figure 5.16. The circle is made using the current and phase angle in each end of OHL 10, as well as the voltages in Bus 21 and 22.

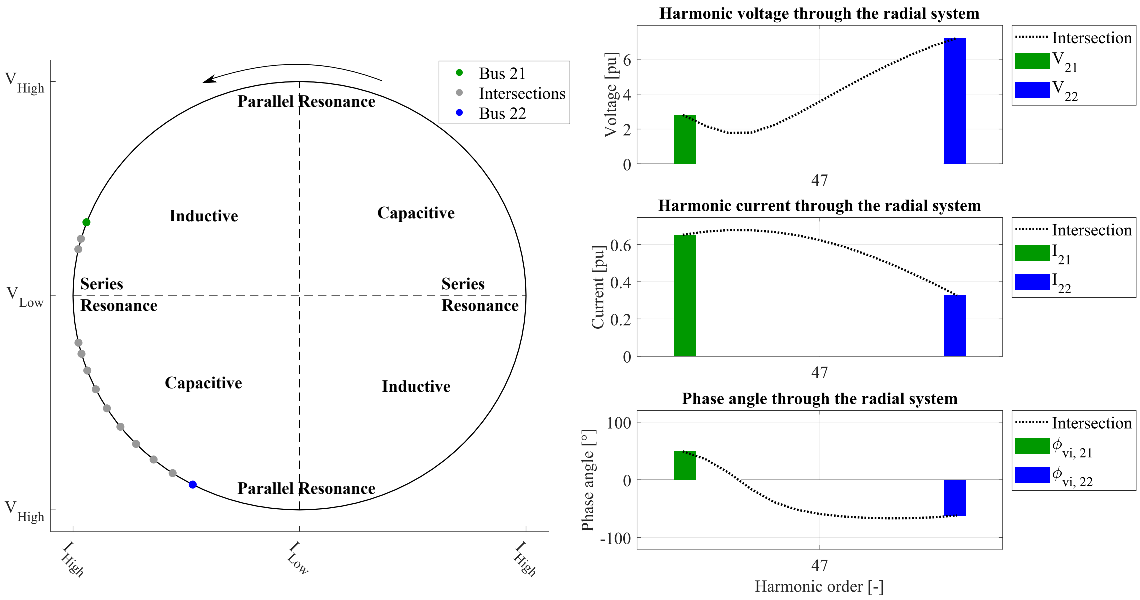

Figure 5.16: Harmonic propagation of the 47^{th} harmonic order through OHL 10.

From Figure 5.16 it can be seen that the measurements of the intersections follows the circumference of the circle. However, as the voltage never reaches zero, a jump on the circumference occurs at the voltage phase shift. This could indicate that the angular velocity of the harmonic propagation is different near the resonance, compared to measurements further away from the resonance points. However, this is not the case, but a shortcoming in the circle representation, due to the voltage and current never reaching zero. This analysis shows that the circle theory is applicable for individual lines between busses in a meshed system, if the currents, voltages and phase angles are available at each end of the line. However, it should be taken into account, that at higher order harmonics or at longer lines it might not be precise around the resonance points.

When analysing the harmonic propagation through the transformer, the ellipses were utilised in the Chapter 4 as a visualisation tool. In the meshed system, three paths are connected in Bus 1. Hence, three HV-side ellipses should be utilised to describe the harmonic propagation with the circle theory. The voltage difference from the LV-side ellipse to the HV-side ellipse will be the same in the three cases. The three HV-side ellipses together with the LV-ellipse are shown in Figure 5.17.

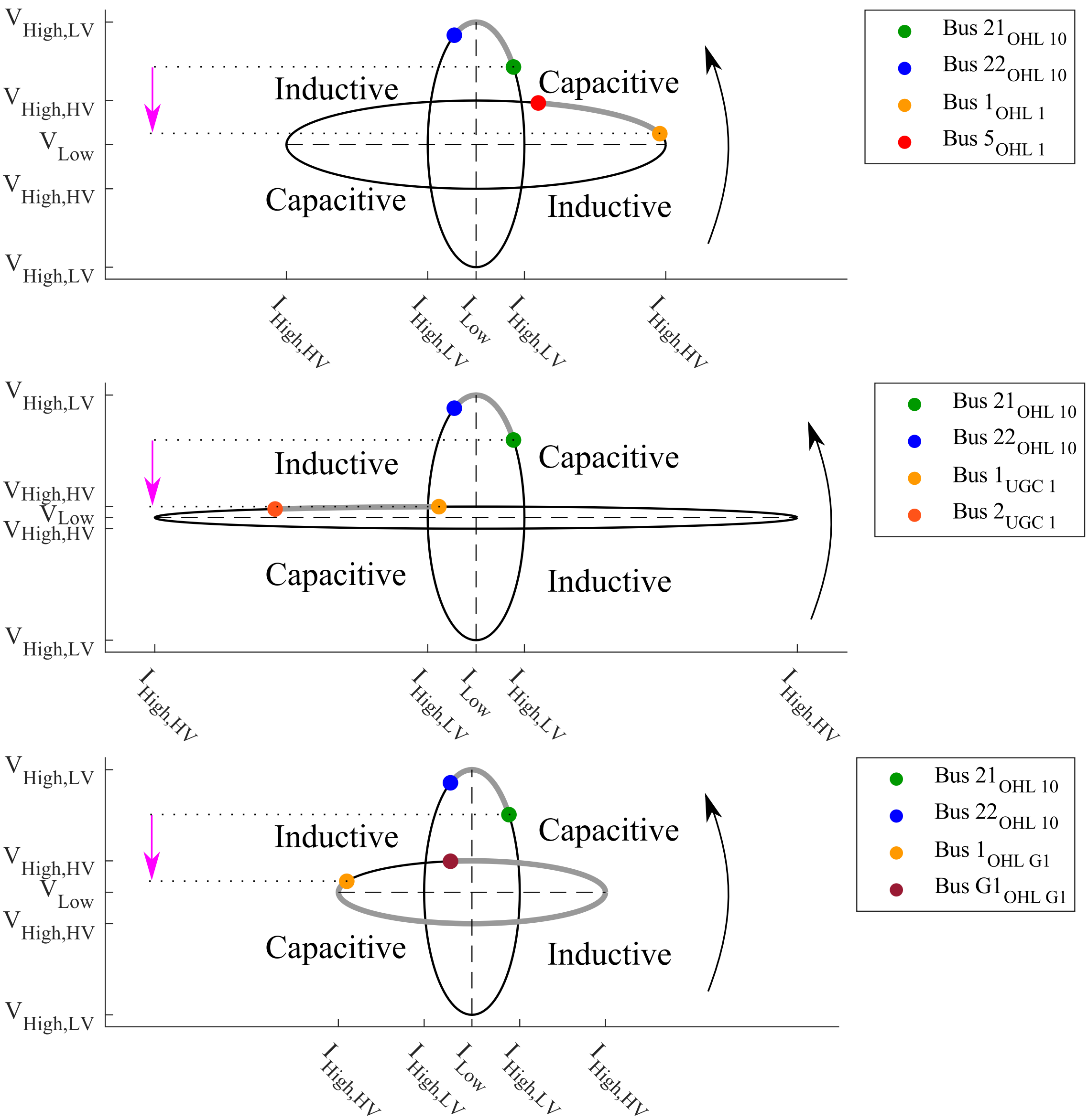

Figure 5.17: Harmonic propagation of OHL 10, OHL 1, OHL G1 and UGC for the 37^{th} harmonic order, illustrated with ellipses.

If multiple connections are present in the LV-side bus these should also be represented by an ellipse. Therefore, utilising the ellipses as a visualisation tool in the meshed system gives a complicated result. Therefore, the concept of utilising the ellipses to visualise the harmonic propagation through a transformer in a clear way is no longer possible in a meshed system. Hence, the propagation of harmonic currents and voltages are analysed separately in the following sections.

5.3.2 Propagation of Harmonic Currents

From Figure 5.14 it can be seen that the injected current in Bus 21 can flow in two directions. A part of the current flows to the 400 kV level through the transformers T1 and the rest of the current flows through OHL 10 at the 130 kV level. In Figure 5.18, the harmonic currents and phase angles are shown for the harmonic current source, the

LV-side of T1 and the sending end of OHL 10.

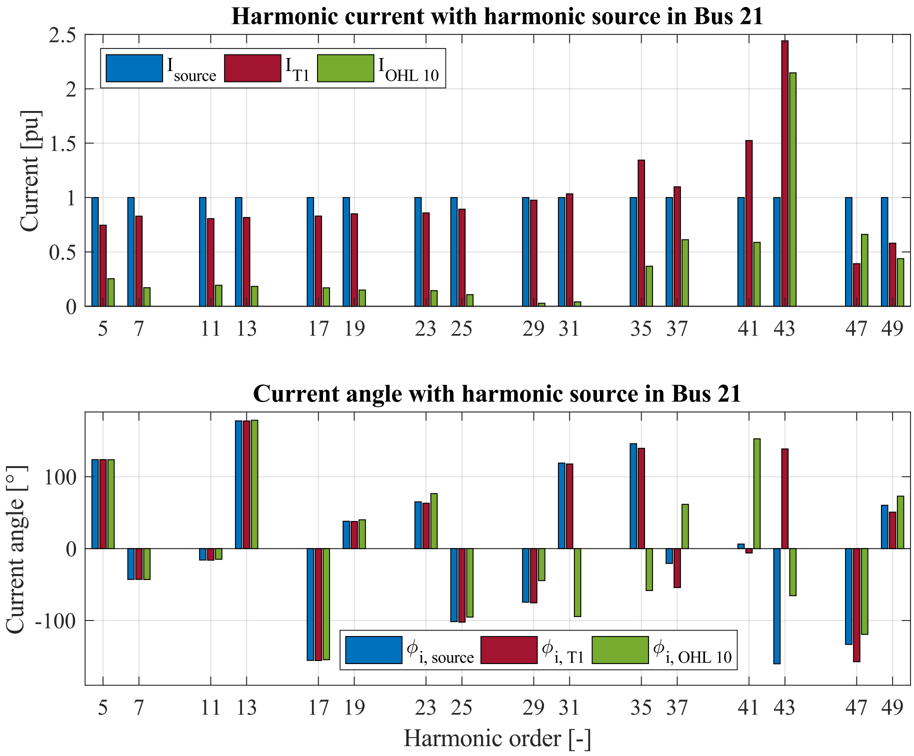

Figure 5.18: Harmonic currents and phase angles shown for the harmonic current source, the LV-side of T1 and the sending end of OHL 10.

From Figure 5.18 it can be seen how much current flows through the transformers and how much flows through OHL 10 for each harmonic order injected. Additionally, it can be seen that for almost every harmonic order, most of the current flows through the transformer to the 400 kV level. However, this does not necessarily result in a high harmonic voltage distortion at 400 kV. This will be analysed further in Section 5.3.4. At the 5^{th} harmonic order 0.75 pu current flows into T1 and 0.25 pu flows into OHL 10. At the 29^{th} harmonic order 0.97 pu current flows into the transformer and 0.03 pu flows into OHL 10. The amount of current flowing in each of the directions is determined by the impedance of the elements as well as the impedance behind the elements. The equivalent impedance of each path is different for each harmonic order. The current through OHL 10 is low at the 29^{th} harmonic order, as the impedance of this path is larger than the impedance path of T1.

The sum of the current magnitudes from the two paths are shown together with the impedance angle for each path in Figure 5.19. The impedance angles are calculated for the frequencies of interest, from the voltage and current angles in each path.

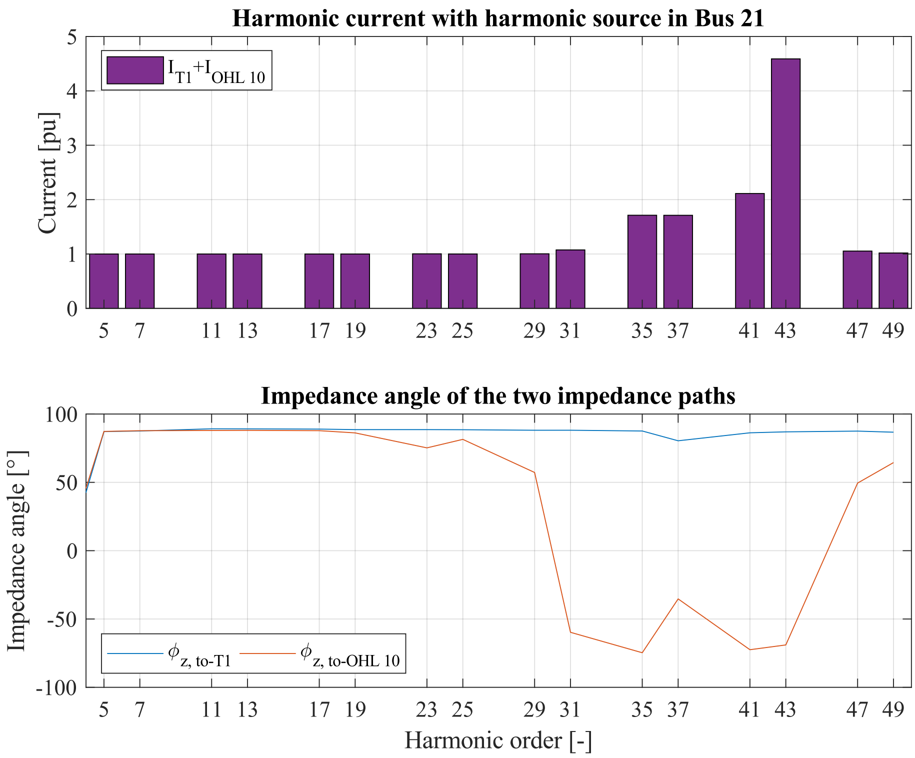

Figure 5.19: Total harmonic current of T1 and OHL 10 and impedance angles for each path.

As seen in Figure 5.19, the sum of the absolute values becomes larger than the injected 1 pu, when the impedance angle of the two paths are different from each other. This is visible from the 29^{th} to the 49^{th} harmonic order. To investigate this, the two paths at the specific harmonic orders can be simplified to two Thévenin equivalent impedances, calculated from the currents and voltages. As an example, the 41^{st} harmonic order is considered. In Figure 5.20, the two impedance paths are shown with their Thévenin equivalent resistance and reactance.

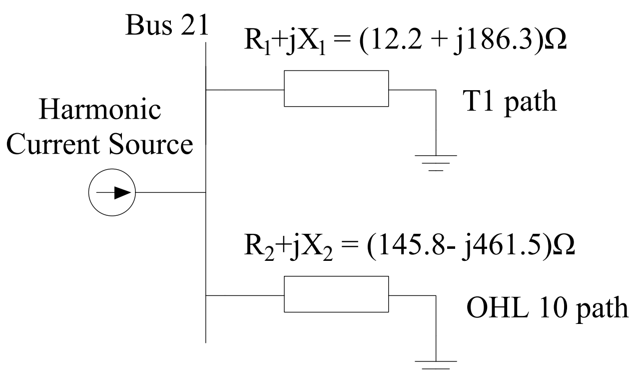

Figure 5.20: Simplified representation of the two impedance paths seen from Bus 21, with the equivalent resistance and reactance for the 41^{st} harmonic order.

From Figure 5.20 it can be seen that the reactance of the two paths have opposite signs. Therefore, the simplified representation of the two impedance paths at Bus 21 can be seen as an inductor and capacitor in parallel. This means that a reactive current is flowing from the capacitive path to the inductive path. In Figure 5.21 the phasor diagram of the 41^{st} harmonic order of the current from the source, T1 and OHL 10 are shown. Additionally, the vector projection of I_{T1} and $I_{OHL\ 10}$ onto I_{source} is shown in Figure 5.21.

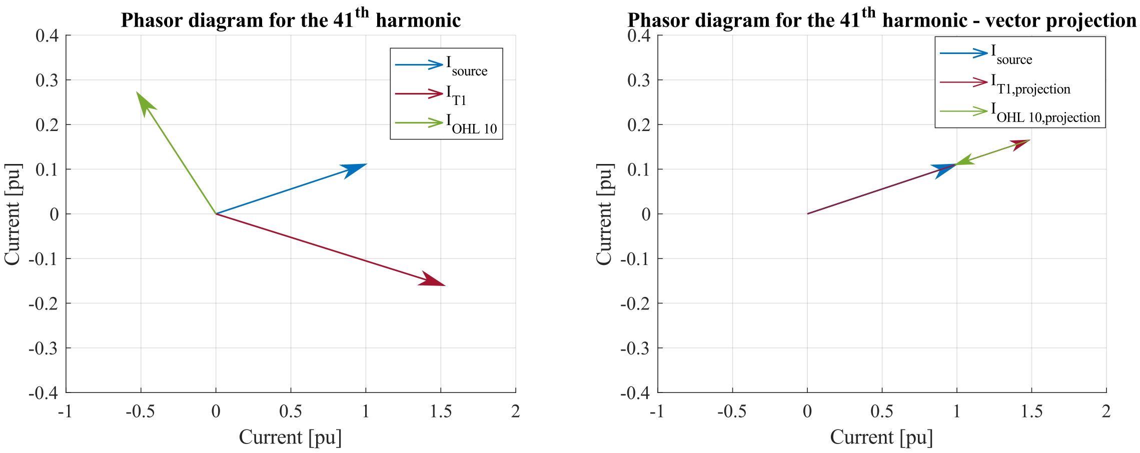

Figure 5.21: Phasor diagram of the currents in Bus 21 for the 41^{st} harmonic order, as well as the vector projection of I_{T1} and $I_{OHL\ 10}$ onto I_{source}.

In Figure 5.21 it is visualised that the current in T1 and OHL 10 are opposite in phase. This is due to the fact that the current from the OHL 10 path is capacitive, hence providing current to the T1 path. Therefore, when the currents are vector projected onto the source current, the current in T1 is positive, while the current in OHL 10 is negative. In order to identify when this occurs in other systems, the Thévenin equivalent impedance for every harmonic order is needed. From the Thévenin equivalent impedances, it can be identified at which harmonic orders the impedance angles are different from each other. This can identify at which harmonic order, the sum of the absolute output currents are larger than the input current. However, the Thévenin equivalent impedance was obtained using the voltage and current from the harmonic penetration method. Therefore, there is no need for calculating the Thévenin equivalent impedance, as the current is available from the harmonic penetration method.

5.3.3 Propagation of Harmonic Voltages through a Transformer

In the radial system it was observed that the off-diagonal impedance from the frequency scan can be utilised to determine the harmonic voltages in the system. An analysis has been made in Appendix C.5 in order to validate that this is also applicable for a meshed system.

With the knowledge that the off-diagonal impedance is applicable in the meshed system, the voltage difference between the HV- and LV-side of T1 is analysed utilising the off-diagonal impedance. In Figure 5.22, the relation between the harmonic voltage on the HV- and LV-side is shown for each harmonic order, from injecting harmonic currents in Bus 1 and in Bus 21. The current injected is 1 pu in both busses.

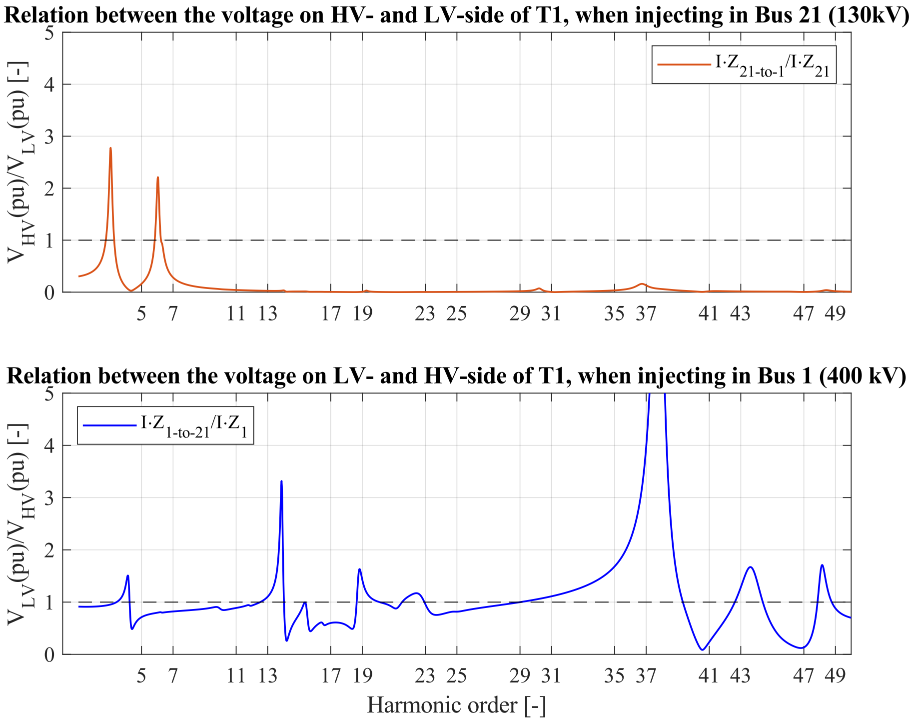

Figure 5.22: Relation between the voltage on HV- and LV-side of T1.

When the relations in Figure 5.22 is above 1, which is marked by the dashed line, the voltage increases across the transformer. In the top plot, a decrease mostly occurs from the LV- to the HV-side and opposite in the bottom plot. Hence, in the top plot in Figure 5.22 it can be seen that a voltage drop from the LV-side to the HV-side occurs for the harmonic orders injected. However, it can be observed that the 5^{th} and 7^{th} harmonic orders are close to a peak. This means that if the impedance and therefore the voltage relation is slightly shifted, due to a new operational scenario, an increase from the LV- to the HV-side could occur. This showcases that even though a harmonic penetration method shows a damping of the harmonic propagation through the transformer, changes in the system could change this behavior. As an example, all the lines in the 400 kV system are changed to OHLs, the impedance characteristic changes, and the harmonic voltages can be amplified through the transformer, as shown in Figure C.8 in Appendix C.6. Therefore, the computation of the voltage relation for every harmonic order utilising the frequency scan, can be important in the study of harmonic propagation through a transformer.

From the bottom plot in Figure 5.22 it can be seen that the voltage both increases and decreases from the HV-side to the LV-side for different harmonic orders. The largest voltage increase appears at the 37^{th} harmonic order and the largest voltage decrease at the 47^{th} harmonic order, for the harmonic orders of injection. From the two plots in Figure 5.22, it is clear that there is a significant difference between the propagation of harmonic voltages between voltage levels. A larger current will flow from the LV- to the HV-side of the transformer when injecting on the LV-side, compared to the current which will flow from the HV- to the LV-side when injecting on the HV-side. With a larger current through the transformer, a voltage drop will occur. Therefore, the harmonic voltages are more likely to be decreased from the LV-side to the HV-side of the transformer, when injecting on the LV-side compared to the opposite. This can be observed in Figure 5.22, where the voltage relation from the LV- to the HV-side (red curve) is small compared to the voltage relation from the HV- to the LV-side (blue curve).

The harmonic propagation through the transformer is also investigated, when replacing the OHLs in the 130 kV system with UGCs. In Figure 5.23, the voltage relation between the HV- and LV-side of T1 is analysed for the reference system and the system with only UGCs on the 130 kV level. The harmonic current source is connected in Bus 21 (130 kV).

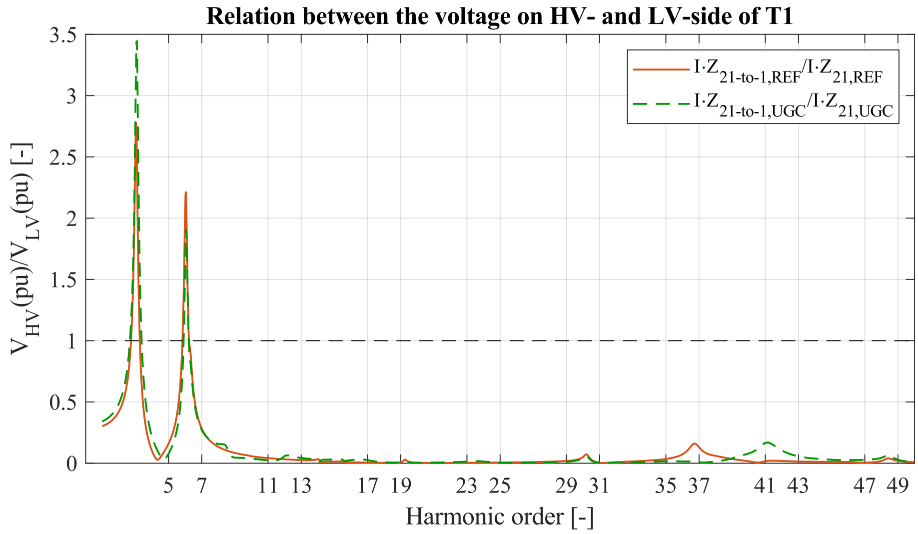

Figure 5.23: Relation between the voltage on HV- and LV-side of T1, when changing the lines of the 130 kV system. The harmonic current source is connected in Bus 21.

From Figure 5.23, it can be seen that the voltage relation between the HV- and LV-side of the transformer at the 5^{th} harmonic order is 0.16 for the reference case and 0.08 for the UGC case. At higher order harmonics, the peak has shifted from the 37^{th} harmonic order in the reference case to the 41^{st} harmonic order in the UGC case. This shows that by replacing OHLs with UGCs in the 130 kV system, only small changes in the harmonic propagation to the 400 kV system occurs. The largest change on the lower orders occurs at the 5^{th} harmonic order, where the harmonic propagation has been halved in the UGC case.

The harmonic propagation through the transformer is also investigated when injecting the harmonic currents in Bus 1 (400 kV). In Figure 5.24, the voltage relation between the LV- and HV-side of T1 is analysed for the reference system and the system with only UGCs on the 130 kV level.

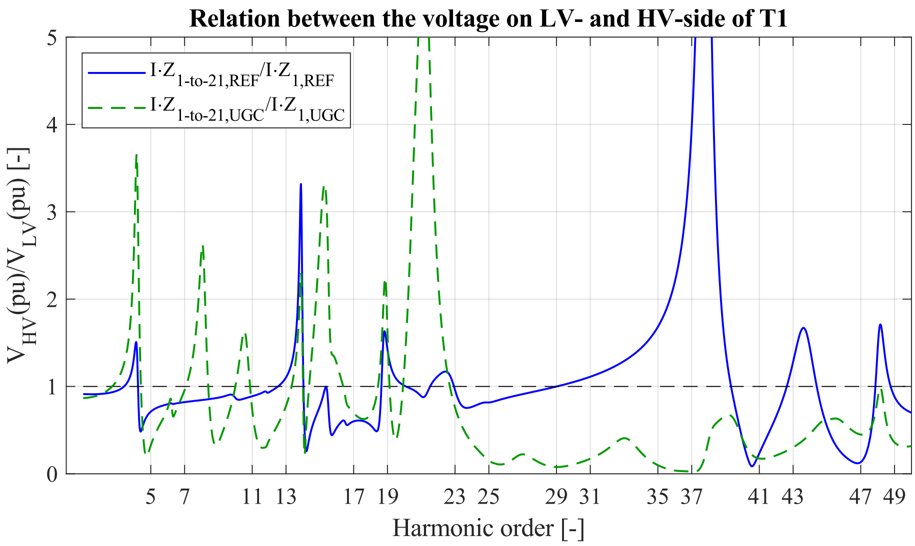

Figure 5.24: Relation between the voltage on HV- and LV-side of T1, when changing the lines of the 130 kV system. The harmonic current source is connected in Bus 1.

From Figure 5.24, it can be seen that the voltage relation in the UGC case has several peaks. These peaks occurs at lower order harmonics. Therefore, when injecting the harmonic current on the HV-side, a harmonic voltage amplification from the HV- to the LV-side of the transformer is more likely to occur at lower order harmonics, when the LV-side lines are UGCs.

The results from injecting on the LV- and HV-side of the transformer, when changing the lines in the 130 kV system to UGCs shows that by injecting on the LV-side, it has almost no effect on the voltage relation. This is similar to the results in the radial system in Figure 4.35, where it was shown that when changing the line on the voltage level of injection, no changes in the voltage relation occurred. However, when changing the line on the opposite voltage level than where the harmonic current is injected, changes occurred in the voltage relation.

5.3.4 Propagation of Harmonic Voltages

Until now, studies with the harmonic penetration method has been on a few selected busses in the meshed system. However, as the harmonic voltages propagate through the system, the voltages are different in each bus. Therefore, all the harmonic voltages are analysed, when harmonic currents are injected in one bus. The harmonic voltages of all busses, when injecting 1 pu harmonic current in Bus 21 are shown in Figure 5.25.

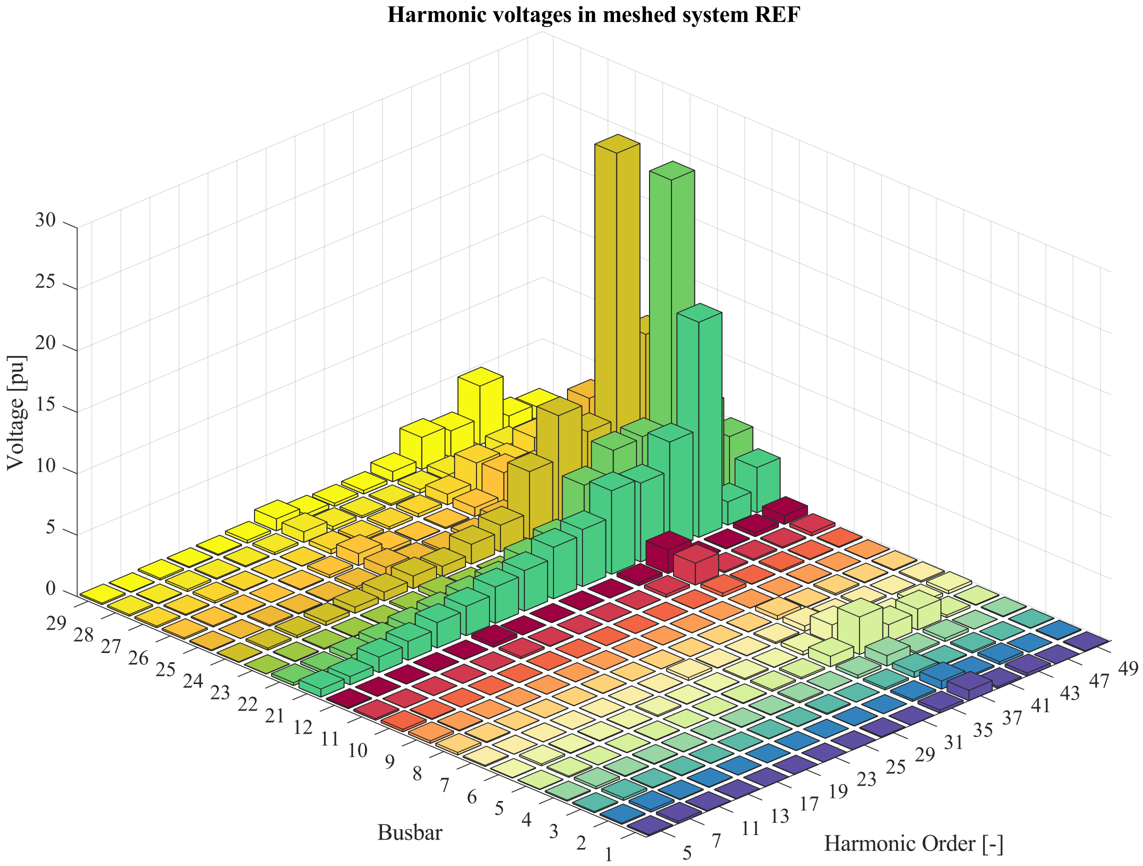

Figure 5.25: Harmonic voltages for each bus in the meshed system with the harmonic currents injected in Bus 21.

From Figure 5.25 it can be seen that the harmonic voltages are significantly lower in the 400 kV busses (1 to 12), compared to the 130 kV busses (21 to 29). This can be explained from the harmonic currents being injected on 130 kV voltage level. Additionally, it can be seen that the harmonic voltages can be larger in other busses, than the bus of injection. This can be seen at 43^{th} harmonic order, where the harmonic voltage is 17.5 pu in the injected Bus 21, while the harmonic voltages in Bus 22 and 24 are 28 pu.

The harmonic voltages in every bus for the case where all lines on the 130 kV are OHLs and the case where all lines on the 130 kV are UGCs are shown in Appendix C.7. To compare the results, the differences in harmonic voltages from the OHL case to the reference case has been plotted for all the busses, for the lower order harmonics. This is shown in Figure 5.26. The bars marked with blue represent a voltage increase, while the bars marked with orange represents a voltage decrease.

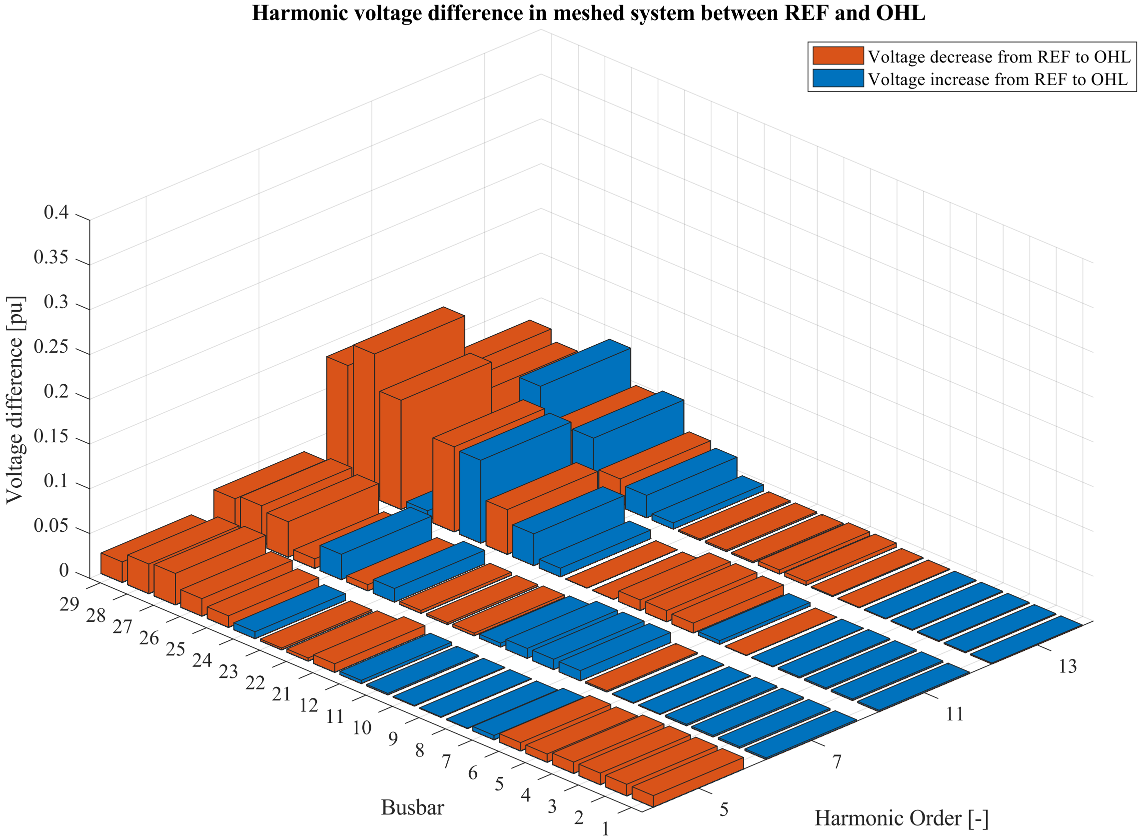

Figure 5.26: Harmonic voltage differences from reference to OHL case, when the 130 kV system is changed for each bus in the meshed system for lower orders of harmonics. The harmonic current source is connected in Bus 21.

From Figure 5.26 it can be seen that the harmonic voltages decrease in most of the busses in the OHL case. It can also be seen that the harmonic voltage differences are largest on the 130 kV level, compared to the 400 kV level. This shows, that changing the lines on the 130 kV level, affects the 130 kV system the most, but still has effects on the 400 kV system.

The differences in harmonic voltages from the UGC case to the reference case has also been plotted for all the busses, for the lower order harmonics. This is shown in Figure 5.27.

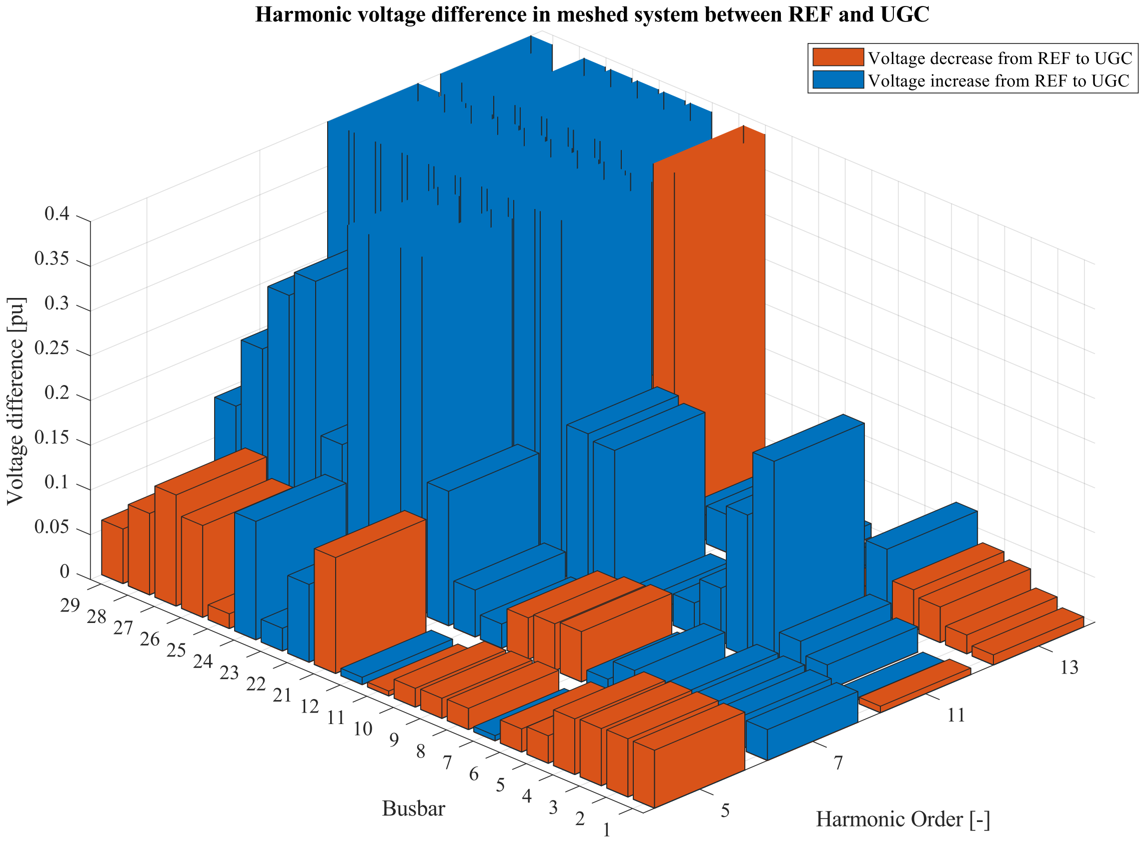

Figure 5.27: Harmonic voltage differences from reference to UGC case, when the 130 kV system is changed for each bus in the meshed system for lower orders of harmonics. The harmonic current source is connected in Bus 21.

From Figure 5.27, it can be seen that the harmonic voltages increases in most of the busses in the UGC case. Moreover, the harmonic voltage differences are largest on the 130 kV level, compared to the 400 kV level as in the OHL case. This supports the statement that line changes made on the 130 kV level, affects the 130 kV system the most. It should be noted that the full magnitude of the bars are not shown in Figure 5.27. The highest harmonic voltage difference occurs at Bus 25 at the 11^{th} harmonic order, with a magnitude of 3.06 pu.

The same analysis has been made, by injecting 1 pu harmonic currents in Bus 1 at 400 kV. In Figure 5.28 the measured harmonic voltages in all busses, in the frequencies of interest are shown.

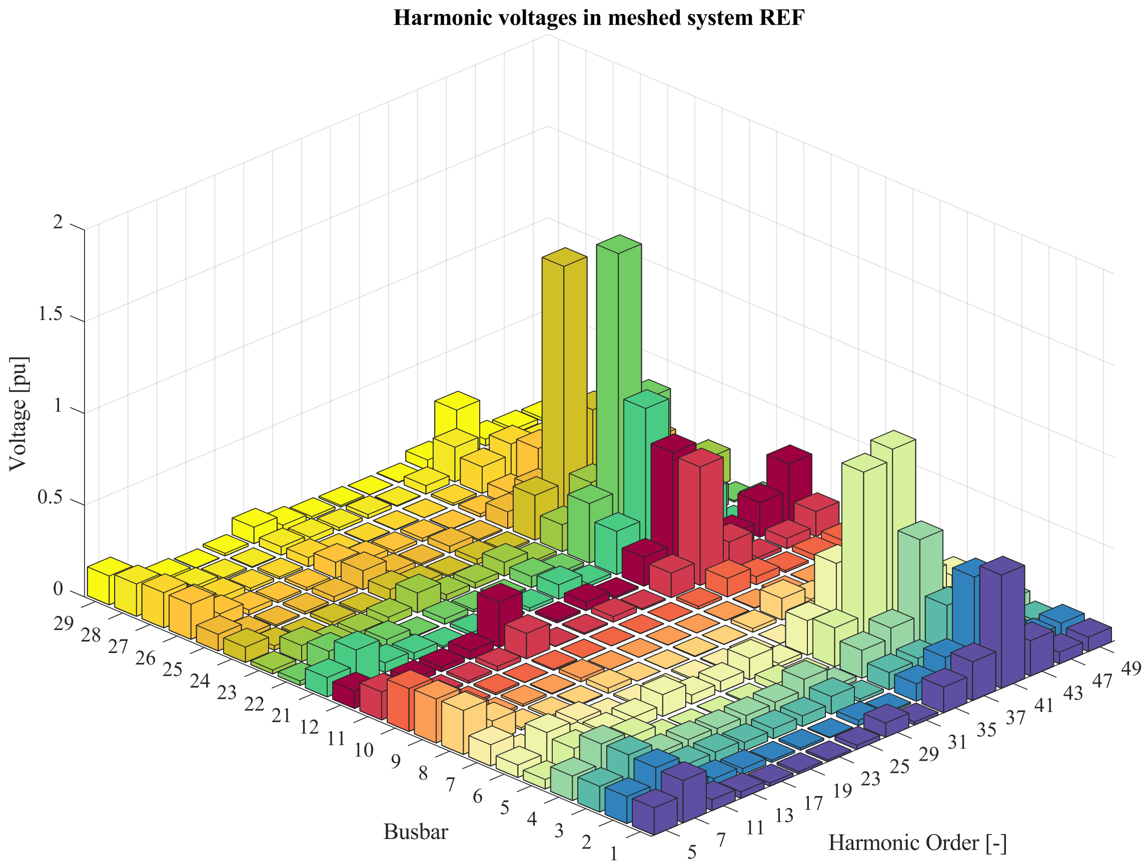

Figure 5.28: Harmonic voltages for each bus in the meshed system for the harmonic orders of interest with the harmonic currents injected in Bus 1.

From Figure 5.28 it can be seen that the harmonic voltages are more equal on both voltages levels compared to injecting in Bus 21, as shown in Figure 5.25. This follows the results from the impedance relation when injecting in Bus 1 shown in Figure 5.22. It should be noted that the harmonic voltages are generally larger, when injecting in Bus 21 compared to injecting in Bus 1. This can be explained from the impedance plots in Figure 5.2 and 5.3. Here it can be seen that the impedance is larger in Bus 21 than Bus 1 for the reference chase at the high harmonic orders where the large voltages are observed.

Next, the differences in harmonic voltage when replacing the lines in the 130 kV system with OHLs and UGCs compared to the reference case are considered. The harmonic voltage differences in the OHL case for all busses, for lower harmonic orders can be seen in Figure 5.29.

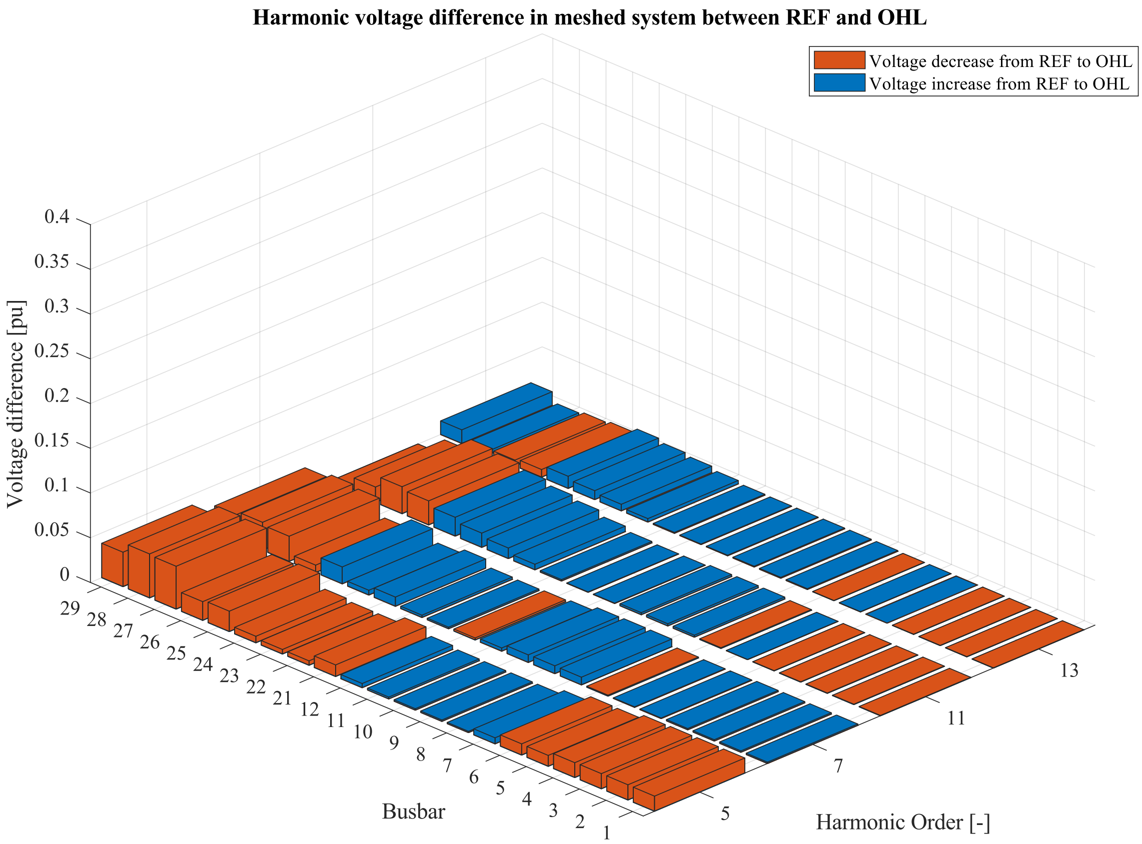

Figure 5.29: Harmonic voltage differences from reference to OHL case, when the 130 kV system is changed for each bus in the meshed system for lower orders of harmonics. The harmonic current source is connected in Bus 1.

From Figure 5.29 it can be seen that differences are lower in the OHL case when injecting in Bus 1 compared to injecting in Bus 21. This can be explained from the fact that the harmonic currents are injected on the opposite voltage level from where the line changes are made. Additionally, the largest differences in the harmonic voltage occurs at the busses on 130 kV. This again confirms that the line changes on the 130 kV system, affects the results on the 130 kV system the most.

The harmonic voltage differences in the UGC case for all busses, for lower harmonic orders can be seen in Figure 5.30.

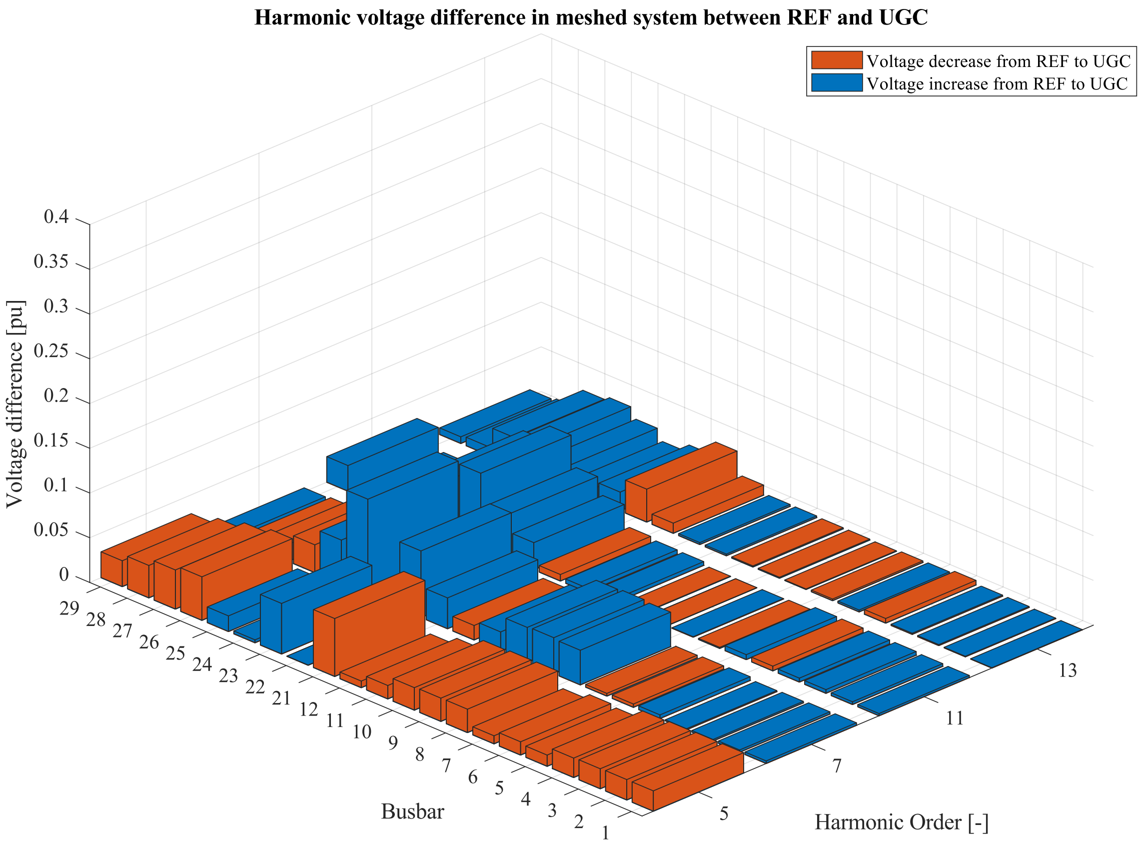

Figure 5.30: Harmonic voltage differences from reference to UGC case, when the 130 kV system is changed for each bus in the meshed system for lower orders of harmonics. The harmonic current source is connected in Bus 1.

From Figure 5.30 it can be seen, that the differences are also lower in the UGC case when injecting in Bus 1 compared to injecting in Bus 21. This is again due to the fact that the harmonic current is injected on the opposite voltage level from where the line changes are made. Moreover, the largest differences are observed in the LV-side lines as in the previous cases.

Summary and Discussion

In the impedance analysis, two main case studies were performed in order to analyse how the impedance characteristics at the 400 kV and 130 kV systems were affected for different scenarios. Three additional case studies were conducted in order to corroborate the findings in the two main studies. The impedance analysis was conducted in two busses at the 400 kV system and two busses at the 130 kV. The analysed busses were as different from each other as possible, both in terms of distance between each other and nearby connections. Therefore, the two busses were representative for the system. However, small differences might be observed in the other busses in the system.

In the first case study, the line types at 130 kV were first changed to OHLs and then to UGCs. From the frequency scan, it was observed that the harmonic impedance at 400 kV was barely affected when changes were made in the 130 kV system. The changes observed at the 400 kV, when the 130 kV system was changed, was primarily in the impedance magnitude. Additionally, small changes to the resonance frequencies could be observed at high harmonic orders. The impedance characteristics of the 130 kV system was significantly affected both regarding resonance frequency and impedance magnitude, when the lines were changed. When the lines were changed to OHLs or UGCs it was shown that the impedance characteristic was most affected, when changes were made close to the bus of observation.

In the second case study, the line types at 400 kV were changed to OHLs and then to UGCs. It was observed that the harmonic impedance at 400 kV was significantly affected, when changes were made at the 400 kV system. The 130 kV system was affected when the 400 kV system was changed, but not as much as the 400 kV system itself. The largest changes were observed when the 400 kV system was changed to OHLs, since a higher impedance was present in the 400 kV system. Additionally, the 130 kV system was affected more when the 400 kV system was changed than opposite. The findings of the two main case studies were:

- Changes made to the system primarily affect the harmonic impedance at the voltage level where the changes are made
- Changes made at higher voltage levels has a larger effect at lower voltage levels than opposite

The influence of the voltage levels was analysed in the third case study by changing the transformer turns ratio, thereby the voltage level of the LV-system. From this case it was observed that changes made on the LV-side have a larger influence on the 400 kV system when the turns ratio was decreased. This showed that the per unit conversion factor also had an influence in the meshed system.

In order to investigate the influence of the conversion factor in the meshed system the transformer impedance was removed in the fourth case. As a result, there was a direct connection between the two voltage levels. From this case it was observed that in some cases the harmonic current propagated different for specific harmonic orders when the transformer impedance was removed. This was especially present when the 130 kV lines were replaced with UGCs. This was explained from the path of least impedance, which at certain harmonic orders were shifted to the 130 kV side. Additionally, a reduction of the impedance at certain harmonic orders was observed at the 400 kV level, when the 130 kV lines were replaced with UGCs. When the 130 kV lines were replaced with OHLs, the transformer impedance did not have an impact, since the harmonics would stay at 400 kV instead of propagating to 130 kV due to the higher impedance magnitude of OHLs.

In the case without the transformer impedance, the impedance characteristics on each side of the transformer followed the same characteristic, but with different magnitudes. This was due to the two sides being directly connected without a transformer impedance between them. As a result, a constant impedance relation of 8.6 was observed, which was larger than the per unit conversion factor of 8. This was explained from the transformer having automatic tap changer and the tap position not being in neutral. If the tap changer was in the neutral position, the conversion factor was 8. The conversion factor was utilised to explain why changes on the 130 kV system had little effect on the 400 kV system. In order for the harmonic current to flow to the 130 kV system from the 400 kV system, the impedance had to be lower at the 130 kV system.

In the *Example grid*, the 400 kV system had 4.557 times longer lines than the 130 kV system. This could explain why the 130 kV system had less influence on the 400 kV system than opposite. Therefore, in the fifth case, the line lengths of the 130 kV system was increased by a factor of 4.557. This case showed slight changes in the impedance characteristics of the 400 kV busses compared to the system with the original line lengths. Hence, the line lengths did not explain why the 130 kV system had less influence on the 400 kV system, than opposite. This verified that it was due to the conversion factor.

Next the harmonic propagation in the meshed system was analysed. Here the harmonic propagation was analysed using the circle and it was shown that the circle theory could be applied for a single line using the voltage, current and phase angle in each end of the line. However, it was shown that the voltage and current never reaches zero for higher harmonic orders. Therefore, a jump on the circumference occurs at phase shifts, which means that the circle was not accurate around the resonance points. This was a shortcoming in the circle representation. Additionally, it was shown that the circle theory could not be used to represent the harmonic propagation between more than two busses in the meshed system, as several lines were connected on each side of the transformers. Therefore, the circle theory was in principle not very useful in a meshed grid.

The harmonic voltage propagation through a transformer in the meshed system was analysed. This was performed using the off-diagonal impedance multiplied by the injected harmonic current. Here it was shown that the propagation of harmonic voltages was larger through the transformer, when injecting on the HV-side than on the LV-side. This was explained from the harmonic currents and the transformer impedance causing a voltage drop. A larger current will flow from the LV- to the HV-side of the transformer when injecting on the LV-side, compared to the current which will flow from the HV- to the LV-side when injecting on the HV-side. With a larger current through the transformer, a voltage drop will occur. Therefore, the harmonic voltages were more likely to be decreased from the LV-side to the HV-side of the transformer, when injecting on the LV-side compared to the opposite. Additionally, it was shown that the harmonic propagation of voltage from the 130 kV to the 400 kV system was barely changed, when the 130 kV line types were changed. However, the harmonic propagation from the 400 kV to the 130 kV system was significantly affected when changing the line types in the 130 kV system.

The harmonic voltage propagation in all the busses in the meshed system were analysed, using the harmonic penetration method. Here it was shown that when injecting a harmonic current on the LV-side, the harmonic voltages stayed mostly at the LV-side with significantly lower harmonic voltages in the busses on the HV-side. When a harmonic current was injected on the HV-side, the harmonic voltages were more or less equal on both voltage levels in per unit. Additionally, it was analysed how the harmonic voltages at low harmonic orders changes, when the lines in the 130 kV system were changed to OHLs and UGCs. These results were compared to the reference system with the original share of OHLs and UGCs. Here it showed that when injecting on the LV-side, the harmonic voltages on both voltage levels increased when the 130 kV system consist of UGCs, but mostly in the busses in the 130 kV system. When the lines on the 130 kV system were replaced with OHLs, the harmonic voltages were barely changed. If the injection were made on the HV-side, the changes in harmonic voltages were much lower with UGCs and OHLs compared to injecting on the LV-side.

6 Harmonic Mitigation

In this chapter, the mitigation of harmonic voltage distortion is analysed in the *Example grid*. The analysis is an exploratory study utilising a C-type high-pass damped filter. In this chapter, only the low order harmonics from the 5^{th} to the 13^{th} order are considered. This is done as the low order of harmonics are the most critical harmonic orders in a power system, hence the need of mitigation is greatest at these harmonic orders. First, the harmonic impedance seen from every bus in the 400 kV and 130 kV systems are analysed in order to have a reference for comparison. Hereafter, the filter is implemented in one bus at a time in all busses.

Furthermore, the meshed system is modified to have a parallel resonance closer to the order of harmonic injection, to see a larger harmonic voltage distortion. Hereafter, one OHL in the modified meshed system is replaced by an UGC to obtain a higher impedance at one of the harmonic orders of interest. This is done to analyse the impact of changing one line in the system and analyse the filter placement according to this change. First six filter placement are analysed in order to determine at which location the largest harmonic voltage decrease is obtained and explain the impact. Afterwards, the harmonic voltage is evaluated for every bus, when bus injections are made in each bus, on at a time, and the optimum filter location of every bus is shown.

The focus of this chapter is on specific case studies. Hence, no deep analyses are performed as in the previous chapters. This is done as the mitigation of the harmonic voltages are not the main scope of the study, hence this is done as an extra study.

6.1 Reference System Impedance and Filter Design

The harmonic voltage distortion, as a result of a harmonic current injection in a given bus, is determined by the harmonic impedance in the specific bus. Therefore, the harmonic impedance seen from all the busses in the meshed system without filters are analysed. The harmonic impedance in the 400 kV and 130 kV busses are shown in Figure 6.1.

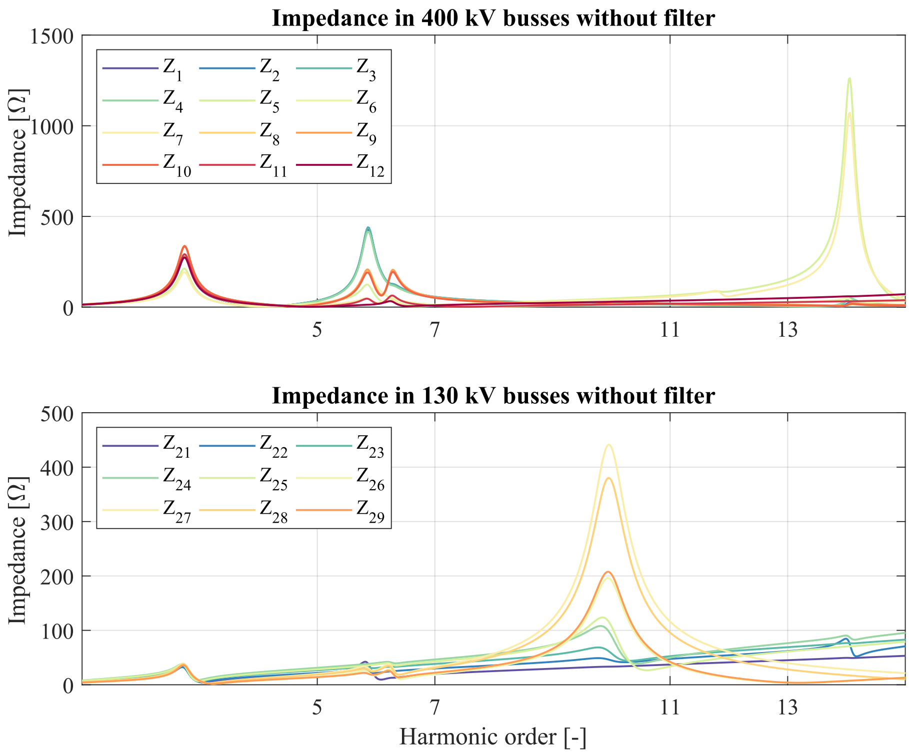

Figure 6.1: Impedance in Bus 1 to 12 and 21 to 29 without filters.

According to Energinet, the tuning order is normally set at critical harmonic orders, such as the 5^{th} or 11^{th} harmonic order. As the frequency scan in the top plot of Figure 6.1 shows a parallel resonance between the 5^{th} and 7^{th} harmonic order, the tuning order is chosen to be at the 5^{th} harmonic order. In PowerFactory a C-type high-pass damped filter can be implemented utilising design or layout parameters. The design parameters are the rated reactive power (Q_{tot}), the tuning order (n_{res}) and the quality factor (QF). The layout parameters are the component values C_1, C_2, L and R. The filter is implemented utilising typical design parameters used by Energinet for harmonic studies. The design parameters are shown in Table 6.1. The same filter design parameters are utilised on the 130 kV side.

Table 6.1: C-type high-pass damped filter design parameters.

Rated reactive power [MVAr]	100
Tuning order	5
Quality factor	2

The size of the filters utilised in this study are 100 MVA on both voltage levels. This is a large filter both on the 400 kV and 130 kV level. However this size is utilised in order to compare the two filters. Additionally, the large filter size allows for an easy observation of general tendencies.

The transfer function of the C-type high-pass damped filter is derived based on the circuit schematic in Figure 2.9 and is shown in Equation 6.1.

$$Z(s) = \left(\frac{\left(\frac{1}{sC_2} + sL\right) \cdot R}{\left(\frac{1}{sC_2} + sL\right) + R} \right) + \frac{1}{sC_1} \tag{6.1}$$

The filter component values are determined based on the design parameters in PowerFactory. The capacitance C_1 is calculated from Equation 6.2. [27]

$$C_1 = \frac{B_{cap}}{2\pi f_{nom}} \qquad \text{where} \qquad B_{cap} = \frac{Q_{tot}}{V_{nom}^2} \tag{6.2}$$

Where f_{nom} is the nominal frequency of 50 Hz, B_{cap} is the susceptance, f_{res} is the resonance frequency and V_{nom} is the nominal voltage. The inductor is calculated utilising Equation 6.3. [27]

$$L = \frac{X_L}{2\pi f_{nom}} \qquad \text{where} \qquad X_L = \frac{V_{nom}^2}{Q_L} \qquad \text{and} \qquad Q_L = Q_{tot}\left(\left(\frac{f_{res}}{f_{nom}}\right)^2 - 1\right) \tag{6.3}$$

Where Q_L is the reactive power of the inductor. The resistance is given by Equation 6.4. [27]

$$R = QF \cdot 2\pi f_{res} L \tag{6.4}$$

The capacitor C_2 and the inductor are tuned at the fundamental frequency. Hence, the capacitor C_2 is given by Equation 6.5. [27]

$$C_2 = \frac{1}{(2\pi f_{nom})^2 \cdot L} \tag{6.5}$$

In Table 6.2 the component values are given for the 400 kV and 130 kV levels.

Table 6.2: Component values for the design parameters utilised.

Voltage level [kV]	C_1 [μF]	C_2 [μF]	L [mH]	R [Ω]
400	1.989	47.746	212.207	666.667
130	18.835	452.038	22.414	70.417

The filter impedance characteristics on the 400 kV and 130 kV levels are shown in Figure 6.2. The impedance characteristics are plotted utilising the transfer function of the filter in Equation 6.1.

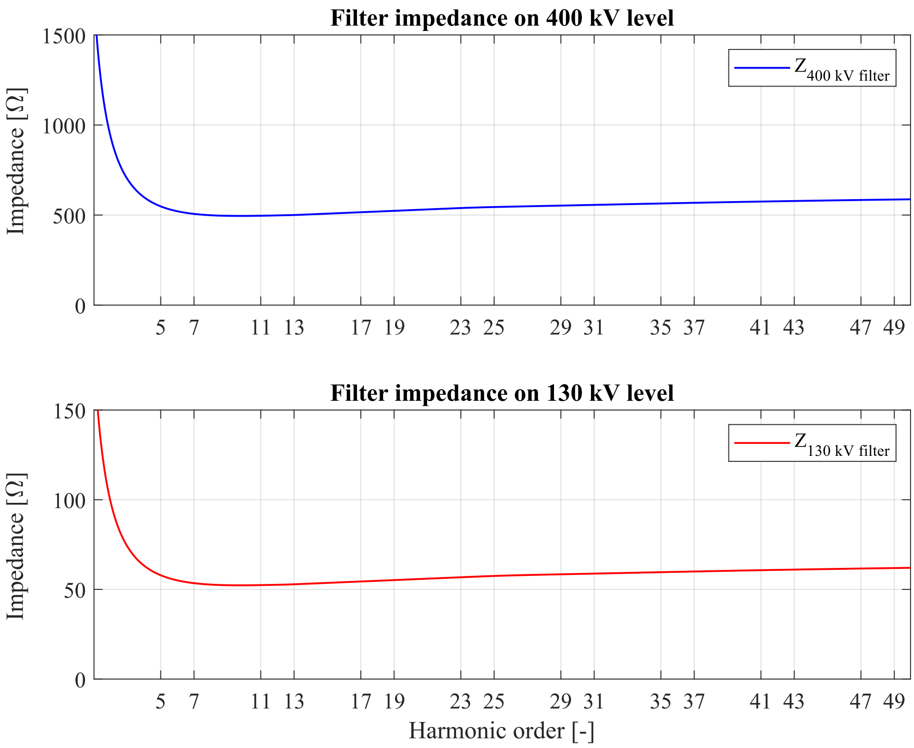

Figure 6.2: Filter impedance for the C-type high-pass damped filter implemented at the 400 kV and 130 kV levels.

6.2 Filter Implementation Analysis

The impedance characteristics of the busses with the filter implemented in the respective bus is shown for all busses in the meshed system in Figure 6.3.

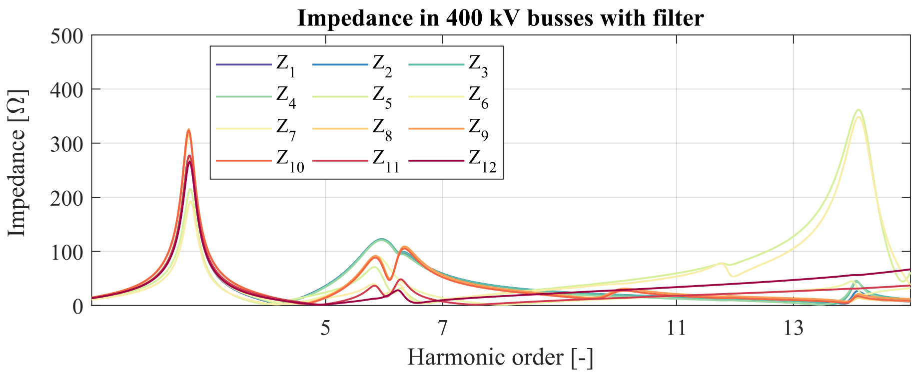

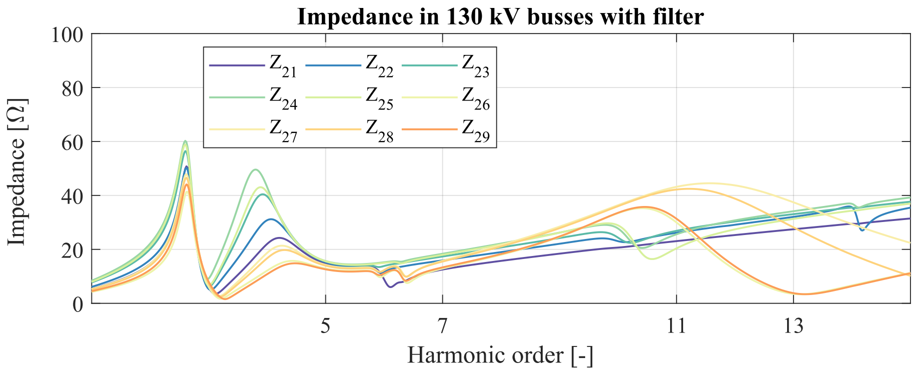

Figure 6.3: Impedance in Bus 1 to 12 and 21 to 29 with one filter implemented in the bus of observation.

From Figure 6.3 it can be seen, that the impedance is damped at both the 400 kV and 130 kV level with the implementation of a filter in the respective bus compared to Figure 6.1. In Figure 6.4 the impedance before and after the filter implementation are shown for Bus 1 and Bus 21 to visualise the damping. Bus 1 is chosen as the parallel resonance peak between the 5^{th} and 7^{th} harmonic order has a high magnitude. The same high magnitude can be seen for Bus 2, 3 and 4. However as none of these busses has a direct connection to the 130 kV system, Bus 1 is chosen. Bus 21 is chosen as this is the bus connected to Bus 1 through transformer T1.

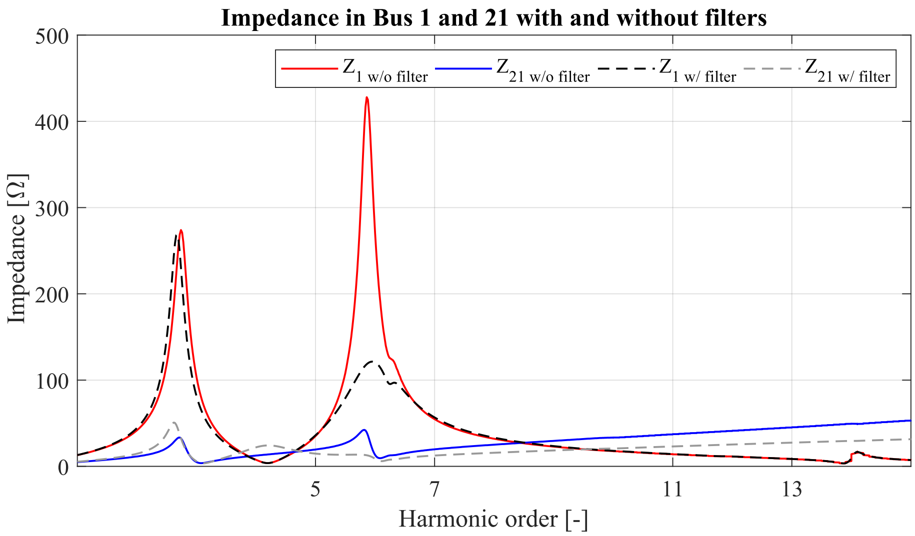

Figure 6.4: Impedance in Bus 1 and 21 with and without filter implemented.

From Figure 6.4 it can be seen that the impedance in both Bus 1 and 21 are damped in the parallel resonance peaks. However at the 5^{th}, 7^{th}, 11^{th} and 13^{th} harmonic orders, no damping of the impedance is observed in Bus 1 when the filter is implemented. In Bus 21, a damping of the harmonic impedance at the 5^{th}, 7^{th}, 11^{th} and 13^{th} harmonic orders can be observed when the filter is implemented. However, since no damping is observed at the HV-side, the line types in the meshed system are changed to obtain an impedance characteristic which has a parallel resonance closer to either the 5^{th}, 7^{th}, 11^{th} or 13^{th} harmonic order in Bus 1.

6.3 Modified Meshed System Filter Analysis

In order to change the parallel resonance frequencies closer the harmonic orders of injection in Bus 1, the UGCs on the 400 kV are replaced by OHLs. This is chosen as the impedance seen from Bus 1 has a parallel resonance close to the 7^{th} harmonic order, as shown in Figure 5.4 in Chapter 5. The impedances seen from Bus 1 and 21 before and after the filter implementation in Bus 1 and 21 in the system with OHLs in the 400 kV system are shown in Figure 6.5.

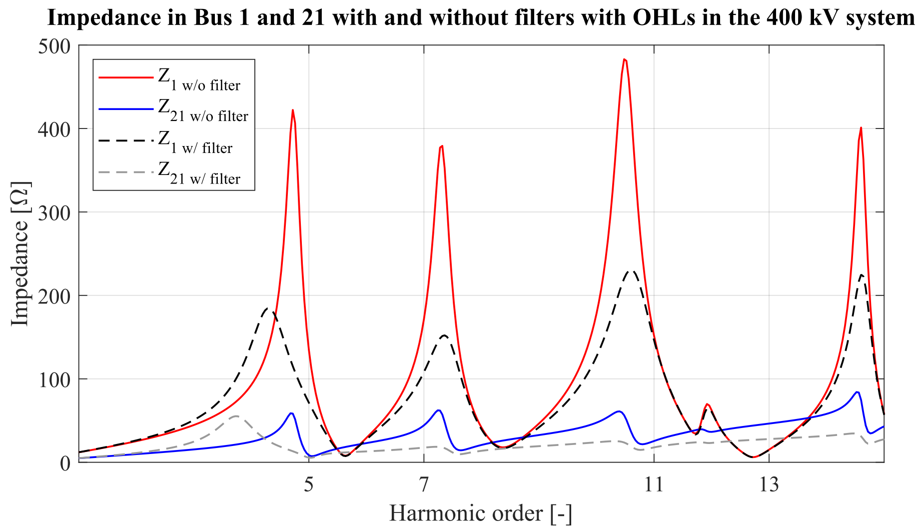

Figure 6.5: Impedance in Bus 1 and 21 with and without filter implemented in Bus 1 and 21 in the system where the UGCs at the 400 kV level are replaced by OHLs.

From Figure 6.5 it can be observed, that at the 7^{th} harmonic order, the impedance is decreased in both cases. At the 11^{th} and 13^{th} harmonic orders, the impedance is unchanged in Bus 1 before and after the filter implementation in Bus 1. For Bus 21 a decrease in impedance is observed at the 11^{th} and 13^{th} harmonic orders when the filter is implemented in Bus 21. Moreover, the impact from the filter is greater in the OHL case compared to the reference case in Figure 6.4 at the harmonic orders of injection.

In this modified meshed system many changes are made at once. Hence, it is difficult to see the influence on the harmonic impedance from a specific line change. Therefore, an analysis is performed in the following section, where only one line on the 400 kV side is changed to an UGC in the system where the entire 400 kV side is composed by OHLs.

6.4 Undergrounding of one Line on the HV-Side

In Chapter 5 it was shown, that changes on the 130 kV level did not significantly affect the 400 kV level. However, when changes were made at the 400 kV level, changes were observed at the 130 kV level. Therefore, it is analysed how one line on the 400 kV side affects the harmonic distortions at the 400 kV and 130 kV sides. Afterwards, the filter location is analysed to determine where the filter would provide the best mitigation. The meshed system only containing OHLs on the 400 kV voltage level is the system which will be modified.

When replacing OHL 8 with an UGC on the HV-side, the parallel resonance close to the 7^{th} harmonic order is shifted closer to the 7^{th} harmonic order. OHL 8 is a short line of 9.7 km connected at Bus 4 and 6. In Figure 6.6 the impedance seen from all the HV- and LV-side busses are shown for this specific case.

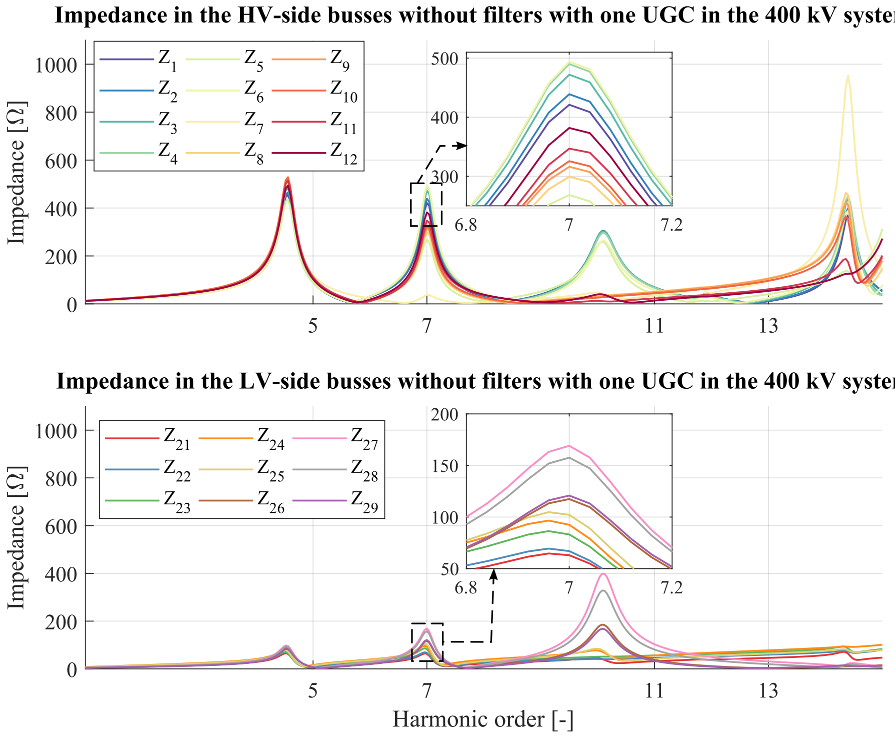

Figure 6.6: Impedance in Bus 1 to 12 and 21 to 29 without a filter implemented in the bus of observation.

From Figure 6.6 it can be seen, that the harmonic impedance at the 7^{th} harmonic order is at a parallel resonance in this system both at the 400 kV and 130 kV voltage level. Furthermore, it can be seen, that at the 7^{th} harmonic order, the largest impedance in the HV-side busses is in Bus 6 and the second largest in Bus 4. Line 8 is connected between these two busses, which is the line that is changed to an UGC. For the LV-side, the largest impedance at the 7^{th} harmonic order is observed at Bus 27. This could indicate that it would be optimal to place a filter in these busses, which will be analysed.

Therefore, the optimal filter location will be analysed, when injections are made in each bus, one bus at a time, using a filter in Bus 6 and 27. Furthermore, a filter will also be evaluated in Bus 23 which is connected to Bus 6 though a transformer. Additionally, filters in Bus 1, 10, and 21 will also be analysed for comparison to the results obtained for the filters in Bus 6, 23 and 27. Since a parallel resonance is present at the 7^{th} harmonic order, only this harmonic order will be analysed in the following section.

6.4.1 Analysis of the Filter Location

In this analysis the filter is evaluated when placed in Bus 1, 6, 10, 21, 23 and 27. The harmonic impedance at the 7^{th} harmonic order before and after a filter is implemented in Bus 1, 6, 10, 21, 23 and 27 are shown in Figure 6.7.

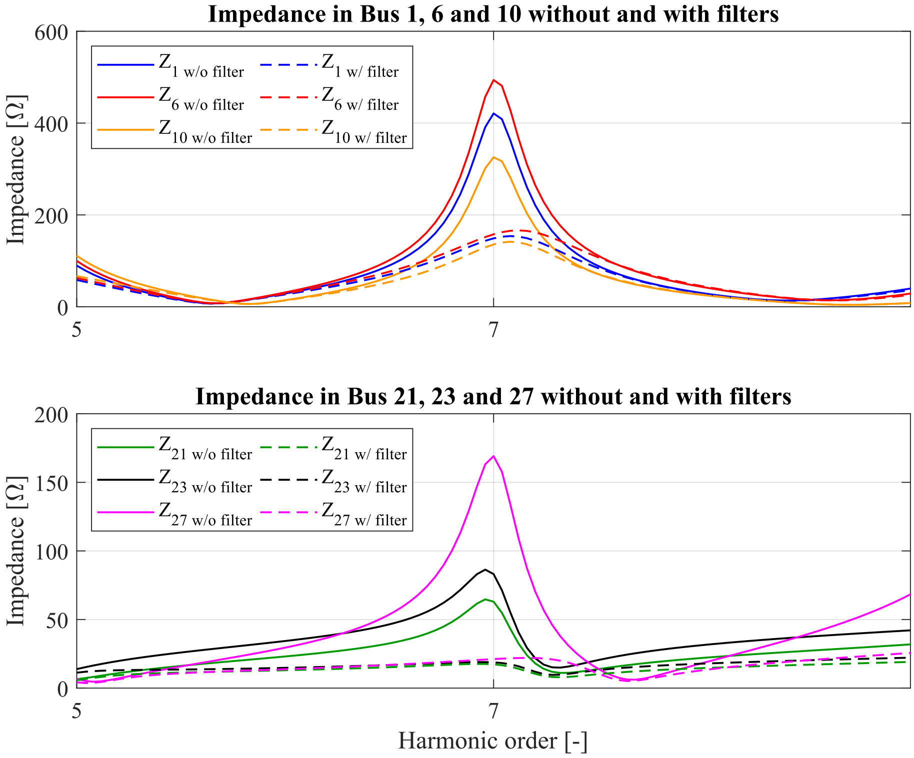

Figure 6.7: Harmonic impedance at the 7^{th} harmonic order before and after a filter is implemented in Bus 1, 6, 10, 21, 23 and 27.

From Figure 6.7 it can be seen, that the harmonic impedance in Bus 1, 6 and 10 are all damped to approximately 150 Ω at the 7^{th} harmonic order. As the impedance peak in Bus 6 is the largest before the implementation of a filter in Bus 6, the largest decrease in harmonic impedance is observed in this bus. For Bus 21, 23 and 27 the harmonic impedances at the 7^{th} harmonic order are decreased to approximately 20 Ω. Again, since the largest impedance is observed in Bus 27, the largest decrease in harmonic impedance occurs after a filter is implemented is in Bus 27.

In the following sections, the harmonic voltage decrease is analysed for the 7^{th} harmonic order between having a filter or not, by injecting an harmonic current in each bus, one at a time. The best filter location will be evaluated based on which of the six filter locations that mitigates the 7^{th} harmonic voltage the most. The harmonic voltage decreases utilised in this analysis is the voltage difference between the system without filter compared to with a filter implemented in either Bus 1, 6, 10, 21, 23 or 27.

Harmonic Voltage Decrease in the HV-Side Busses

The harmonic voltage decreases in the HV-side busses, when the harmonic current is injected in Bus 6 are shown in Figure 6.8. Injection in Bus 6 is chosen, as the largest impedance characteristic appears in this bus.

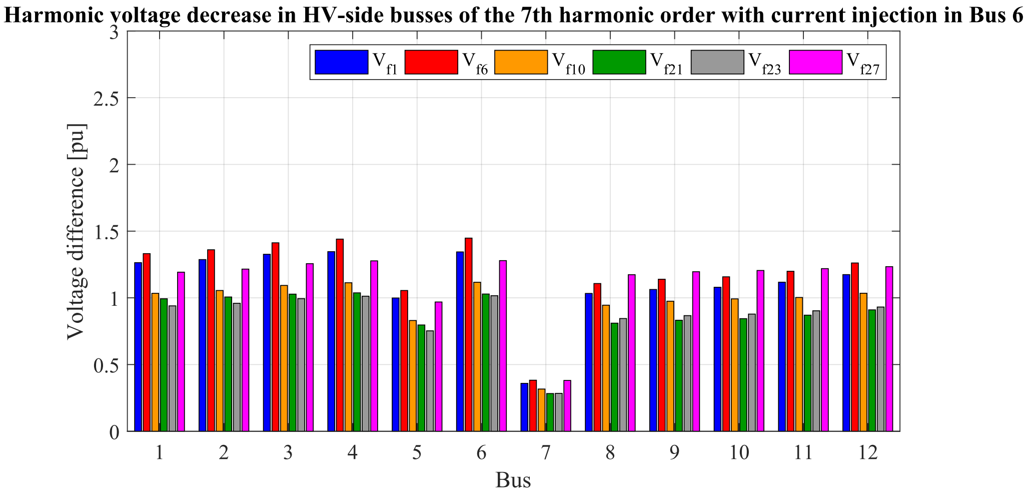

Figure 6.8: Harmonic voltage decrease in the HV-side busses in the system without a filter compared to having a filter in either Bus 1, 6, 10, 21, 23 or 27. The system has OHL 8 replace by an UGC and the harmonic current is injected in Bus 6.

In Figure 6.8, V_{f1}, V_{f6}, V_{f10}, V_{f21}, V_{f23} and V_{f27} represents the harmonic voltage decrease from having no filter compared to having a filter implemented in Bus 1, 6, 10, 21, 23 or 27, respectively. From Figure 6.8 it can be seen, that when having a harmonic current injection in Bus 6, the largest harmonic voltage decrease is observed with a filter in Bus 6 for harmonic voltage decrease in Bus 1 to 7 and Bus 12. However for Bus 8 to 11, the filter mitigating the harmonic voltage the most at the 7^{th} harmonic order is the filter in Bus 27. This could be explained from the fact that Bus 27 is closer to Bus 8 to 11 than the other filter solutions tested except for the filter in Bus 10. The reason for this could be due to the lower impedance in Bus 10, as seen in Figure 6.7. However, this has not been further investigated.

If instead the harmonic currents are injected in Bus 27 at the LV-side, the harmonic voltage decreases of the 7^{th} harmonic order in the HV-side busses are shown in Figure 6.9.

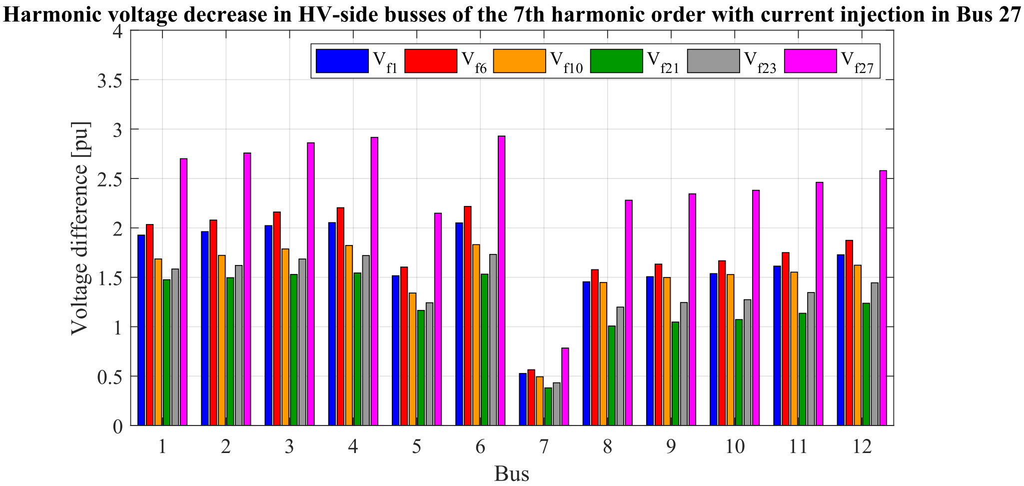

Figure 6.9: Harmonic voltage decrease in the HV-side busses in the system without a filter compared to having a filter in either Bus 1, 6, 10, 21, 23 or 27. The system has OHL 8 replace by an UGC and the harmonic current is injected in Bus 21.

From Figure 6.9 the filter in Bus 27 provides the largest mitigation of the harmonic voltage in all the HV-side busses. This makes sense, as the harmonic current is injected in Bus 27 and a filter implemented in Bus 27 provides a large reduction of the harmonic impedance.

The optimal filter location is further analysed with a filter in every bus in the system one at a time. The analysis is performed with a harmonic current injection in all of the busses in the system one at a time. The optimal filter location is the one that decreases the harmonic voltage the most and the results are shown in Table 6.3.

Table 6.3: Optimal filter location for mitigation in the HV-side busses in the meshed system with OHLs on the 400 kV side where Line 8 is replaced by an UGC with harmonic current injections in all busses.

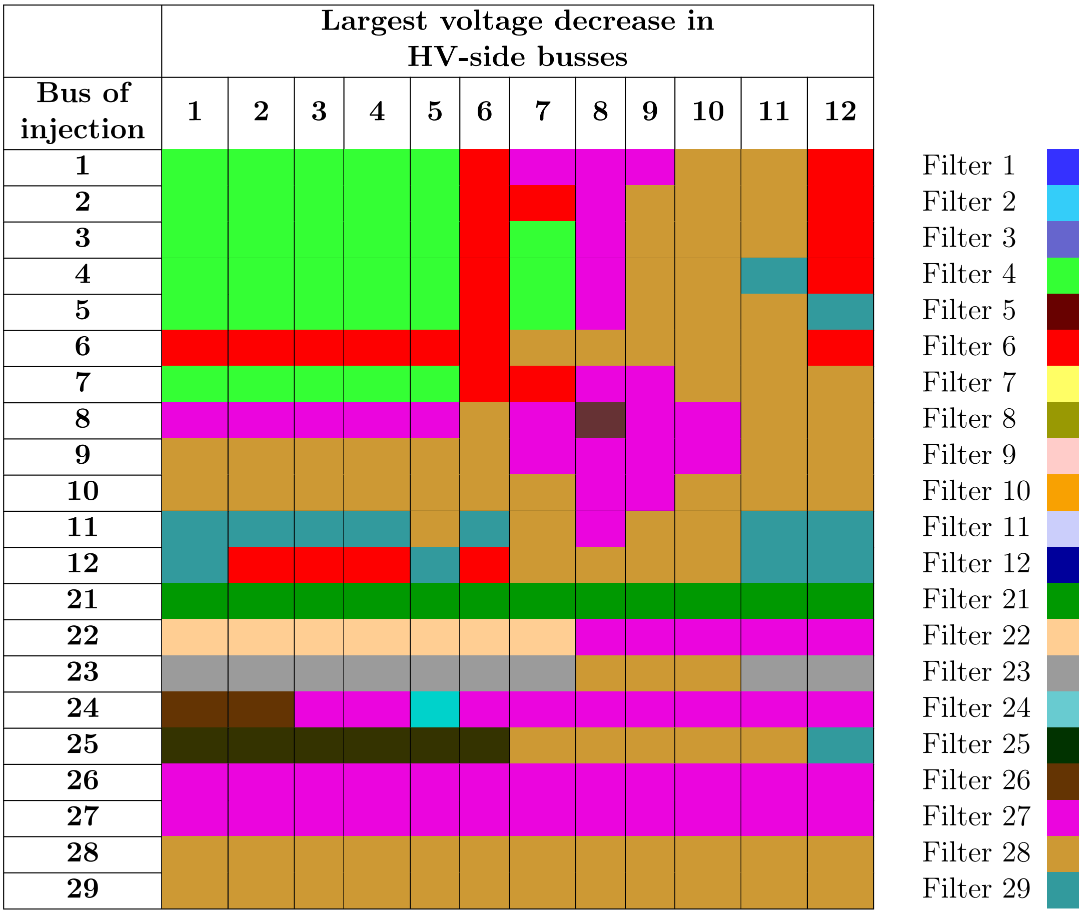

In Table 6.3 the bus where the harmonic current is injected is shown in the first column. The optimal filter location regarding the harmonic voltage decrease in each bus, when the harmonic currents are injected in the associated bus are marked with the corresponding color of the filter.

It can be observed, that the filter in Bus 1, 2, 3, 5, 7, 8, 9, 10, 11 and 12 does not provide the largest mitigation in any case. The filter in Bus 4, 6, 27 and 28 provides the largest mitigation in most of the cases with HV-side current injection. This is due to the impedance in Bus 4 and 6 having the largest impedance on the HV-side before installing the filters as shown in the top plot in Figure 6.6. Additionally, Bus 27 and 28 have the largest impedance on the LV-side before installing the filters as shown in the bottom plot of Figure 6.6. The difference between the harmonic voltage decrease is very small for the filter in Bus 27 and 28 and likewise for the filter solution in Bus 4 and 6. An example of the small difference when injecting a harmonic current in Bus 6 and 27 between the decrease in voltage can be seen in Figure D.1 and D.3 in Appendix D. If injecting in Bus 21, 22, 23 or 25, the better filter location in most cases is in these specific busses.

Harmonic Voltage Decreases in LV-Side Busses

The harmonic voltage decreases in the LV-side busses, when the harmonic current is injected in Bus 6 are shown in Figure 6.10.

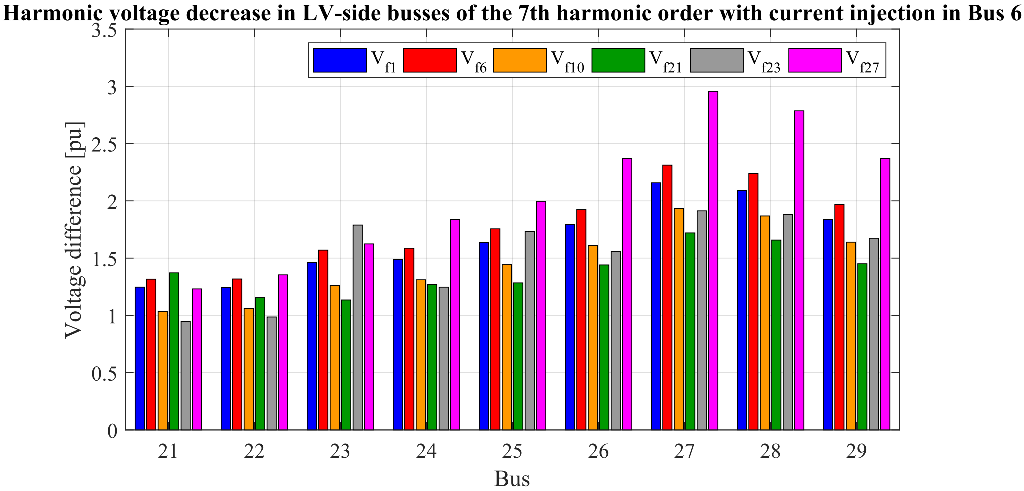

Figure 6.10: Harmonic voltage decrease in the LV-side busses in the system without a filter compared to having a filter in either Bus 1, 6, 10, 21, 23 or 27. The system has OHL 8 replace by an UGC and the harmonic current is injected in Bus 6.

From Figure 6.10 it can be observed, that the filter in Bus 27 provides the most mitigation in almost all of the LV-side busses. The exceptions are in Bus 21 and Bus 23, where a filter in Bus 21 and 23 are the better solutions.

The harmonic voltage decreases in the LV-side busses, when the harmonic current is injected in Bus 27 are shown in Figure 6.11.

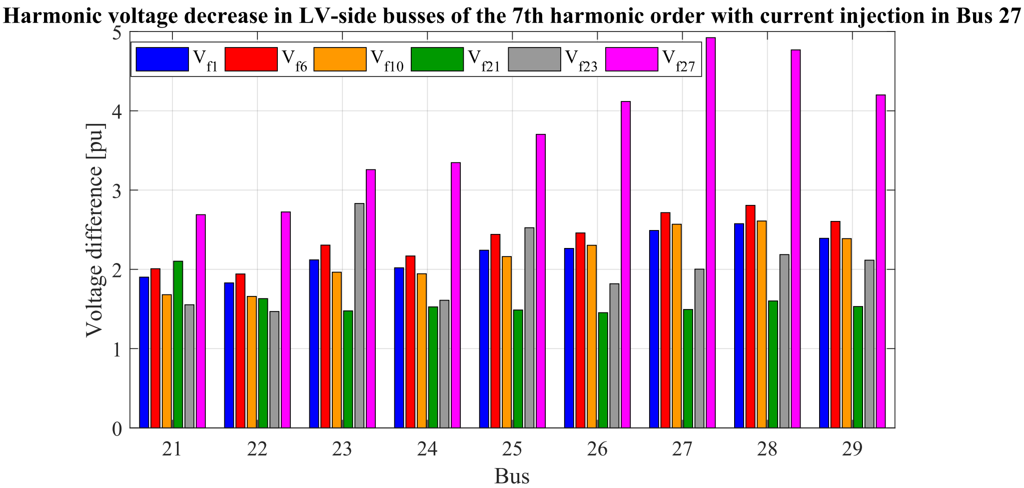

Figure 6.11: Harmonic voltage decrease in the LV-side busses in the system without a filter compared to having a filter in either Bus 1, 6, 10, 21, 23 or 27. The system has OHL 8 replace by an UGC and the harmonic current is injected in Bus 27.

From Figure 6.11 it can be seen, that when injecting in Bus 27, the filter in Bus 27 provides the largest mitigation in all of the LV-side busses.

The optimal filter location to mitigate the LV-side bus harmonic voltages the most is also investigated with harmonic current injections in all of the busses in the system one at a time with a filter placed in all of the busses one at a time. The results are shown in Table 6.4.

Table 6.4: Optimal filter location for mitigation in the LV-side busses in the meshed system with OHLs on the 400 kV side where Line 8 is replaced by an UGC with harmonic current injections in all busses.

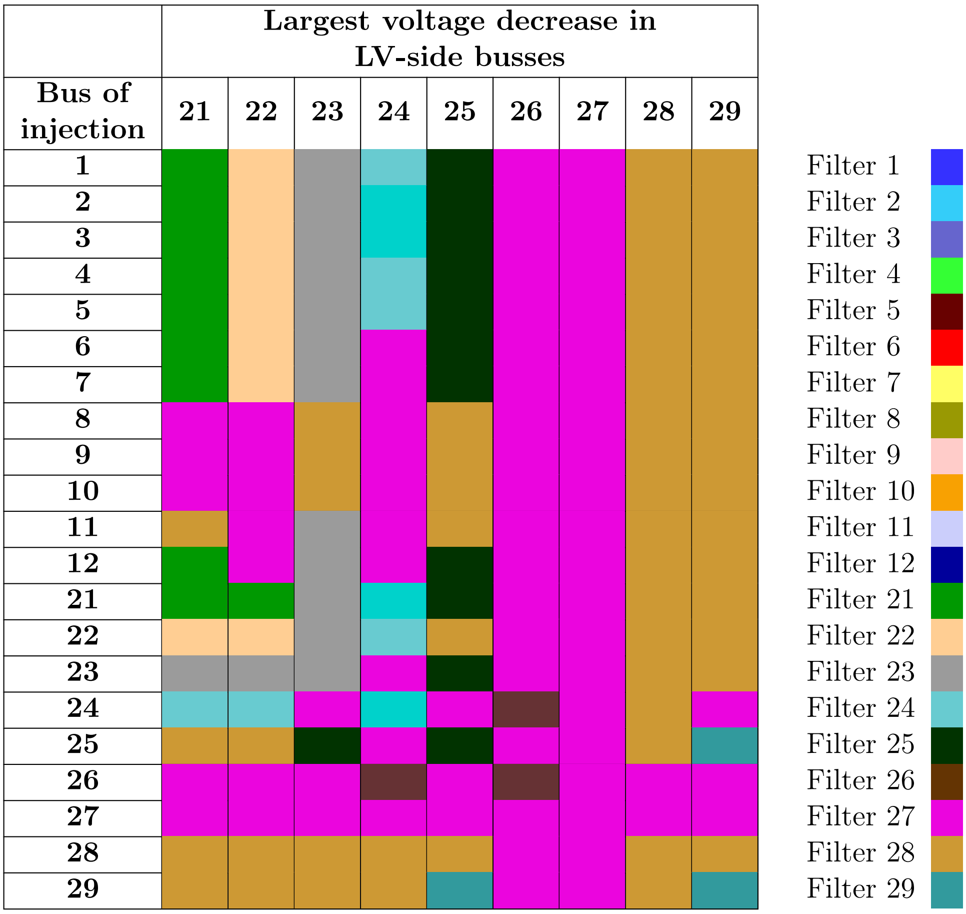

From Table 6.4 it can be seen, that the filter in Bus 27 and 28 provides the largest mitigation of harmonic voltage at the 7^{th} harmonic order in most cases for the LV-side busses. However, if the current is injected in Bus 1 to 7 and 21, the largest decrease in Bus 21, 22, 23 and 25 are observed with a filter in Bus 21, 22, 23 and 25, respectively. When injecting the harmonic current closer to Bus 27 and 28 (Bus 8 to 11 and Bus 24 to 29) the best filter location is in Bus 27 or 28. As with the HV-side busses, the difference between having the filter in Bus 27 or 28 is very small. An example of the small difference with a harmonic current injection in Bus 6 and 27 can be seen in Figure D.2 and D.4 in Appendix D. Hence, in this specific case study, the filter should be placed in the bus with the largest impedance before installing the filter. If the harmonic current is injected in one of the LV-side busses, the best filter location for mitigation in the bus of injection is in this bus. This can be seen in Bus 21 when injecting in Bus 21 and the same for Bus 22 to 29. It should be noted, that no HV-side filter provides the best mitigation in the LV-side busses in this specific case study at the 7^{th} harmonic order.

Sensitivity Study

In the previous mitigation studies, the largest voltage decrease in the busses are used to determine the best filter location. However, in some of the cases, the magnitude of the voltage decreases are very close, which can result in a skewed representation. Therefore, the average voltage decrease that each filter provide in all busses for all busses of injection is calculated. The average is calculated separately for the HV- and LV-busses. The three best filter locations for each bus and each bus of harmonic injection are shown in Table 6.5. In order to show how close the mitigation of the filter locations are, the values of the average harmonic voltage decrease can be seen in the table.

Table 6.5: Top three filter location for mitigation in the HV- and LV-side busses in the meshed system with OHLs on the 400 kV side where Line 8 is replaced by an UGC with harmonic current injections in all busses. The average voltage decrease for all of the busses is noted for the corresponding filter placement.

	Largest voltage decrease in average					
	HV-side busses			**LV-side busses**		
Bus of injection	**Best**	**2^{nd} best**	**3^{rd} best**	**Best**	**2^{nd} best**	**3^{rd} best**
1	1.0942	1.0931	1.0835	1.8965	1.8952	1.8475
2	1.1181	1.1172	1.1059	1.9376	1.9361	1.8877
3	1.161	1.1599	1.1495	2.0114	2.01	1.9601
4	1.1847	1.1837	1.1679	2.0519	2.0489	1.9985
5	0.86721	0.86671	0.85856	1.4947	1.4935	1.4534
6	1.1911	1.1851	1.1682	2.0606	2.0584	2.0082
7	0.31605	0.31544	0.31471	0.55878	0.55742	0.54176
8	0.95372	0.95267	0.94412	1.6542	1.6441	1.592
9	0.97353	0.97249	0.96705	1.6983	1.6906	1.6392
10	0.98525	0.98251	0.98037	1.7227	1.7171	1.6666
11	1.0146	1.0141	1.0072	1.7775	1.7757	1.7293
12	1.0463	1.0445	1.0335	1.8483	1.8471	1.8014
21	1.2808	1.1611	1.1609	2.003	1.9961	1.9913
22	1.2171	1.1824	1.176	1.9098	1.8871	1.8859
23	1.4478	1.4006	1.3932	2.2784	2.2458	2.2159
24	1.5096	1.5074	1.4849	2.3196	2.2939	2.2591
25	1.7032	1.7022	1.6976	2.6645	2.625	2.6022
26	1.9649	1.9375	1.9068	3.0564	2.9883	2.9607
27	2.4285	2.3603	2.2432	3.7477	3.6309	3.4129
28	2.3344	2.2891	2.2173	3.6147	3.5423	3.4031
29	2.0168	1.9982	1.9675	3.1505	3.0997	3.0803

Filter 1
Filter 2
Filter 3
Filter 4
Filter 5
Filter 6
Filter 7
Filter 8
Filter 9
Filter 10
Filter 11
Filter 12
Filter 21
Filter 22
Filter 23
Filter 24
Filter 25
Filter 26
Filter 27
Filter 28
Filter 29

From Table 6.5 it can be seen, that if the harmonic currents are injected in Bus 1 to 6, the best average filter solutions in the HV-side busses are in Bus 3, 4 or 6. The harmonic voltage decrease of these filter solutions are almost the same in per unit. If the harmonic currents are injected in Bus 7 to 12 or 22 to 29, the filters in Bus 27, 28 or 29 are the optimal three filter solutions for mitigation in the HV-side busses.

The optimal filter locations for mitigation in the LV-side busses are either the filters in Bus 27, 28 or 29 independent of the harmonic current injections. This is due to the small difference between the average harmonic voltage decrease between these three busses.

Summary and Discussion

In this chapter the filter placement has been analysed. First the reference case was analysed in terms of the harmonic impedance before and after filter implementation. This analysis showed, that no mitigation was obtained at the 400 kV side in the harmonic orders of interest, since the 400 kV did not require mitigation. On the 130 kV a minor mitigation was observed with the filter implemented.

The 400 kV system was changed to only contain OHLs in order to shift the resonance point closer to the 7^{th} harmonic order and require mitigation. When changing all the 400 kV UGCs to OHLs many changes were made at once. Hence, in order to analyse the impact of changing one line in the system, the OHL in Line 8 was replaced by an UGC. With Line 8 implemented as an UGC, the parallel resonance close to the 7^{th} harmonic order was shifted even closer to the 7^{th} harmonic order. Hence, the harmonic voltage distortion at the 7^{th} harmonic order was increased. The harmonic impedance in all of the busses in the meshed system were analysed. From this analysis it was observed, that the highest impedance at the 7^{th} harmonic order for the HV-side busses was in Bus 6 and 4 where the installed UGC were connected. On the LV-side, the largest harmonic impedance at the 7^{th} harmonic order was observed in Bus 27. Hence, analyses with filters in Bus 6 and 27 were conducted. For comparison, a filter in Bus 1, 10, 21 and 23 were implemented and analysed.

For this specific case study, it was shown, that when the harmonic currents were injected in the HV-side busses, the best mitigation were for most cases obtained when the filter was placed in the bus where the largest impedance on either the HV- and LV-side was observed before the filter implementation. It was shown, that the filter in Bus 27 and 28 provided the largest decrease of harmonic voltages in most cases in the HV-side busses when injecting on the LV-side. However, if the harmonic currents were injected in Bus 21 or 23, the best filter location was in Bus 21 or 23 for most HV-side busses.

The optimal filter placement if mitigation was desired in the LV-side busses was also analysed. From this analysis it was shown, that the filter should be placed in the LV-side bus where the largest impedance was observed before the filter implementation. Exceptions were observed in Bus 21, 22, 23, 24 and 25, where the filter in these busses provided a larger decrease in voltage for injection in some busses.

The tendency observed in this specific case study was, that the filters with the largest impedance characteristic on the LV-side before filter implementation provided the overall best mitigation. The normal procedure is to place the filter at the bus where the harmonic current is injected. In this specific case this was shown to not always be the best solution. The results obtained in this study could indicate, that the best filter placement would be in the bus with the highest impedance, at the harmonic orders to be mitigated. However, this would only make sense if no changes in the system was planned. The reason for the LV-side filters being superior to the HV-side filters in most cases has not been investigated in detail in this study.

Discussion 7

In this chapter, the analyses and the results obtained throughout this report are discussed theoretically and practically. First, the method used in this study to obtain the general conclusions and tendencies is discussed, in order to determine the validity of the results. Next, the conversion factor and the effects of different voltage levels is evaluated. Furthermore, the harmonic propagation in this report is discussed in terms of the circle theory and the off-diagonal impedance. Moreover, the harmonic current injections in power systems are elaborated and discussed. Lastly, the exploratory study of mitigation and the results obtained in the analyses are discussed.

Validity of Results

In this report it is concluded, that changes made on the 130 kV level does not significantly affect the 400 kV level, due to the conversion factor. Therefore, to validate this finding, the model and method utilised in the report is discussed in this section.

Throughout this report, only one power system was used in the meshed system analyses. To verify the tendencies observed in this system, different case studies were made. In the case studies, different line types were installed in the system. However when changing the line types, the types utilised were the same. This makes the results less general since only one type of UGC and OHL is utilised on each voltage level, when changing the line types in the analyses. If the bonding of the cables were different than cross-bonded, different tendencies could be observed. However, for each tendency observed, theoretical explanations are made followed by case studies to verify the statements. As an example, the results obtained regarding changing the line types in the meshed system in Section 5.2, are verified by changing the transformer turns ratio, transformer impedance, and the line lengths. Furthermore, the results in the meshed system are supported by similar tendencies obtained and explained mathematically in the radial system.

Conversion Factor

From the problem statement in this study, both changes in the 132 kV and 150 kV systems are in the scope of this study. The motivation for studying this, is the upcoming undergrounding of lines in the 150 kV system in Denmark. However, the analyses made in this report are performed for a 130 kV system. Based on the per unit conversion factor, the harmonic impedance would be slightly different for a 150 kV system. If the transformer ratings of 410/145 kV would be changed to 410/165 kV, the conversion factor is changed from 8 to 6.2. However, in the analysis made with different turns ratio, it was shown that the changes in the impedance characteristic seen from the 400 kV side when changing the LV-system from 130 kV to 220 kV are low, as shown in Figure 5.6. Therefore, the same tendencies would be valid and the 400 kV system would not be very affected by changes made on a 150 kV system.

In the analyses made in the meshed system in Chapter 5, automatic tap changer was included in the transformers in the PowerFactory model. With this function included, the actual tap position for different simulations is not shown. Therefore, when changes are made in the system, such as line type changes, the transformer tap position could be changed. However, in a real power system, automatic tap changer will be a part of transformers to obtain acceptable voltage levels. The tap changer impact on the results were seen when the transformer impedance were removed. Here it was observed, that the conversion factor was 8.6 and not the theoretical 8. When removing the tap changer, the conversion factor was 8. Therefore, the tap changer might have a minor influence on the harmonic propagation between voltage levels.

Harmonic Propagation

In this report, the circle theory from [23] was analysed and expanded. The theory has been expanded to visualise the harmonic propagation through a transformer in a radial system with different voltage levels. However, for a meshed system, with multiple paths in one bus, the circle could only be applied for a single line between two busses. From the analyses made with the circles, it is shown that the circles is a good visualisation tool, but with limited practical applications. Theoretically, the circle theory can be utilised in a real power system, to estimate the largest voltage and current throughout a line. However, the information will not be very useful, as large deviations will only be visible for high harmonic orders or very long lines. Additionally, as the circles are plotted from both the harmonic voltage and current, it is necessary to implement a harmonic current source and perform a harmonic penetration, to obtain the circle. However, the circle still serves as a good visualisation tool and can help identify tendencies, which is not clear without the visualisation of the circle.

The harmonic voltage difference across the transformer can be obtained utilising off-diagonal impedance from the frequency scan method. The off-diagonal impedance has the advantage that it provides results of every harmonic order compared to the harmonic penetration method. Thereby, resonances in the propagation of harmonic voltages between the harmonic orders of injection can be identified. The disadvantage of the off-diagonal impedance is that the off-diagonal impedance has to be defined for every harmonic current source connected. Furthermore, if the harmonic current sources have different angles, the angles should be taken into account. Additionally, the frequency scan can not indicate anything about the harmonic current, which the harmonic penetration method can. However, as power system are voltage dependent, the harmonic currents are normally not analysed in harmonic studies.

Harmonic Current Source

In the analyses in this report, the harmonic current injected has the magnitude of 1 pu for every harmonic order of injection. However, the harmonic current magnitudes of the injections in power systems in general decreases with $\frac{1}{n}$. Therefore higher order harmonics will have lower magnitudes. This general decrease is only true for some harmonic sources.

From measurements provided by Energinet, it is visible that the largest harmonic voltage distortions are measured at the harmonic orders of $12 \cdot n \pm 1$, which comes from the HVDC LCC systems. Hence, the harmonic voltage distortions at the 11^{th} and 13^{th} harmonic orders are larger than the harmonic voltage distortion at the 5^{th} and 7^{th} harmonic order. Therefore, the harmonic voltage magnitudes obtained in the analyses in this report are not comparable to a real power system. However, by injecting 1 pu for every harmonic order, the results obtained for each harmonic order in this report are more comparable with each other. Hence, the tendencies are more visible.

Harmonic Mitigation

The mitigation of harmonic voltages in this report has been analysed with one harmonic current source in the system at a time. The optimal filter placement, observed in this system, might be different if multiple harmonic current injections are installed. Hence, the results are only valid for one harmonic current injection.

The results obtained in this study could indicate, that the best filter placement would be in the bus with the highest impedance, at the harmonic orders to be mitigated. However, this would only make sense if no changes in the system was planned. The reason for the LV-side filters being superior to the HV-side filters in most cases has not been investigated in detail in this study. However it could be due to the conversion factor, which has not been investigated in the mitigation. The impedance characteristic relation between the the HV- and LV-side filters are 9.5, which is larger than the conversion factor of 8. This might explain why the LV-side filter is optimal in more cases than the HV-side filter.

Additionally, in this specific case study, the HV-side busses with the highest impedance was the busses at the UGC installed. The highest impedances at the LV-side busses were observed in busses, where UGCs were installed. Hence, this could indicate that a correlation between having a high impedance at a low order harmonic and having an UGC connected is present.

Conclusion 8

The scope of this report, was to investigate the impact on the harmonic propagation at the 132/150 and 400 kV levels, when undergrounding lines at the 132/150 kV level.

Harmonic studies were performed in a radial system, a radial system with two voltage levels and a meshed system with two voltage levels. The main objective in the harmonic studies was to analyse how the harmonic propagation changed when the line types were changed. The systems were based on the *Power System Model for Resonance Studies* from PowerFactory, originally made by Oscar Lennerhag, which was referred as *Example grid*.

Radial System

In the radial system analysis it was shown that the harmonic impedance was decreased and the resonances were shifted towards lower frequencies when OHLs were changed to UGCs in the system. This was due to the increased capacitance and resistance of the UGCs compared to the OHLs. The results from the harmonic penetration method, could be visualised utilising a circle, since the propagation followed the norm of a sine wave.

The influence of the location, number of harmonic current sources and angle of injection was analysed in the radial system. From this it was found that when multiple harmonic current sources were implemented, the harmonic voltage distortion was increased for some harmonic orders and decreased for other harmonic orders. This was due to the wavelength decreasing with harmonic order. When two sources were injecting with the same angle of injection in Bus 1 and 7, the harmonic voltage distortion was increased at low harmonic orders and decreased at high harmonic orders. If the angle of injection was different for the two sources, this characteristic changed. Since lower order harmonics are more critical in a power system the worst case scenario is when the harmonic current sources has the same angle.

A 410/410 kV transformer was implemented in the radial system in order to analyse the influence of a transformer. When the transformer was included in the radial system, two circles were necessary in order to describe the harmonic propagation in the system with the circle theory. This was due to the transformer impedance, which caused a voltage difference between the two busses where the transformer was implemented. The voltage difference was an increase or decrease depending on the harmonic order. From the circles it was observed that the increase or decrease of the voltage difference could be explained from the phase difference between voltage and current and the current magnitude. The voltage difference across the transformer could also be obtained from the frequency scan, utilising the off-diagonal impedance from the bus of injection to the two busses where the transformer were connected. The influence of different voltage levels was analysed by changing part of the radial system to 130 kV and implementing a 410/145 kV transformer. From this study, it was found that the first parallel resonance was shifted to a higher frequency compared to the radial system without a transformer. This was explained from the per unit conversion factor. Here it was found that observing from the HV-side, the impedance of the LV-side was multiplied by the conversion factor. Oppositely, observed from the LV-side, the impedance of the HV-side was divided by the conversion factor.

The harmonic propagation in the 410/145 kV radial system had to be represented utilising two ellipses. The ellipses followed the same principles as the circles. The voltage difference could again be obtained by utilising the off-diagonal impedance. An impedance analysis was also performed on the 410/145 kV system when the line types were changed. From this analysis it was concluded, that the impedance relation across the transformer was only determined by what was on the opposite side of the transformer from where the harmonic current was injected.

Meshed System

From the impedance analysis of the meshed system the main findings were:

- Changes made to the system primarily affect the harmonic impedance at the voltage level where the changes are made
- Changes made at higher voltage levels has a larger effect at lower voltage levels than opposite

These findings were a result of the conversion factor explained in the radial system. Additionally, in the meshed system it was possible for the harmonic current to stay at the voltage level where it was injected, unlike in the radial system. Hence, the harmonic current in the meshed system would propagate more between voltage levels if that was the path of least impedance for a specific harmonic order.

The propagation of harmonic voltages between voltage levels was hereafter analysed. From this it was found that the harmonic propagation through the transformer was larger when injecting on the HV-side compared to injecting on the LV-side. Additionally, regarding the impedance relation across the transformer, the same tendency was observed in the meshed system, as in the radial. Hence, more harmonic voltages will propagate down to lower voltage levels, than opposite when line type changes is made.

The harmonic voltages when changing the line types at the 130 kV system was analysed, when injecting at either the LV- or HV-side. From this analysis it was found that the differences in harmonic voltages were mainly observed at the 130 kV, when the 130 kV system was changed, both when the harmonic current injections were at the LV- or HV-side. However, larger harmonic voltage differences were observed at the 130 kV busses, when the injection were at the LV-side. This was explained from the fact that the injections were closer to where the changes were made.

Mitigation

In the study of mitigation of harmonic voltages in the reference case it was observed, that no mitigation was required on the HV-side. Therefore, the meshed system was changed to only contain OHLs on the 400 kV level. One OHL at the 400 kV level was replaced by an UGC in order to analyse where the filter should be placed if one change was made in the system, which increased the harmonic voltages. From the analyses made, no clear tendency was observed regarding the optimal filter location, from different locations of harmonic current injection. However, it was observed that the optimal filter location was not always in the bus of injection, which is the normal filter locations procedure. In several cases, the optimal filter location, was in the bus with the largest impedance characteristic before a filter was installed for the harmonic order of injection. In this specific case study, the HV-side busses with the highest impedance were the busses where the OHL was changed to an UGC. The highest impedances at the LV-side busses were observed in busses, where UGCs are located. Additionally, it was observed that if injections were on the LV-side, the filter location was most optimal when placed on the LV-side. When the injections was on the HV-side, the optimal filter location could be at both the LV- and the HV-side. The filter analysis was not the main scope of this report, hence the observations were not analysed in detail.

Final Conclusions

Based on the findings, it can be concluded that impact on the harmonic propagation at the 400 kV system will be insignificant, when undergrounding lines at the 132/150 kV system. Additionally, the harmonic propagation from the 132/150 kV to the 400 kV system will change slightly. This was found to be due to the conversion factors impact on the LV-side impedance seen from the HV-side. The harmonic propagation at the 132/150 kV system itself will be significantly impacted when undergrounding the lines in the 132/150 kV system. Additionally, the harmonic propagation from the 400 kV to the 132/150 kV system might increases.

9 Future Work

In this chapter, future work suggestions based on the studies made in this report are proposed and discussed.

In Figure 2.4 it was shown that with unbalanced simulations, the resonance frequencies for lower order harmonics could be different between phases. This shows that the inter-sequence couplings can have an significant impact on the results. Therefore, to obtain knowledge about the impact on the inter-sequence coupling when changing line types could be of interest. In such a study, bonding of UGCs and transposition of OHLs should be included. Hence, unbalanced simulations would be interesting in future studies.

In several analyses in this report, the off-diagonal impedance proved to be beneficial, compared to the harmonic penetration method. Therefore, the off-diagonal impedance could in future studies have great value, as it can give the voltage relation between every bus, even with multiple harmonic current injections. In theory, the off-diagonal impedance could be calculated between every busbar in the system, in order to find the correlations. The correlations could then be used in design decisions in order to predict how system changes will affect the harmonic propagation.

An exploratory study of mitigation was done in this report to obtain the optimal filter location, when the harmonic current source was connected in different busses. Here it was found, that the optimal filter location in most cases was in the bus, where the largest impedance was observed before a filter was implemented. This could be investigated further utilising the off-diagonal impedances in the system which would provide information for inter-harmonic orders as well. The filter locations on the different voltage levels should be investigated further. Here it should be examined, why it in this specific case study seems that the filter location on the LV-side is superior to the filter on the HV-side. Additionally, several harmonic current sources could be connected in the system at the same time. With multiple harmonic current sources, the off-diagonal impedance could be a useful tool to determine where the impedance would be largest. The optimal filter location is an optimisation problem with several parameters. Furthermore, as a filter is cheaper on lower voltage levels, a cost benefit analysis should be made where realistic filter sizes should be used.

Bibliography

[1] Cigré JWG C4/B4.38. Network modelling for harmonic studies. Technical report, Cigré, 2019.

[2] Energinet. Technical Issues Related to New Transmission Lines in Denmark. Technical report, Energinet, 2018.

[3] Energinet. *Kabelhandlingsplan, 132-150 kV.* https://energinet.dk/-/media/Energinet/Projekter-KTR-HFV/Dokumenter/Netplanlaegning/Kabelhandlingsplan-132-150-kV---marts-2009.pdf?la=da, 2009. Visited 12-02-2020.

[4] Forsynings-og Klimaministeriet Energi. *Aftale om afskaffelse af PSO-afgiften.* https://efkm.dk/media/7912/elementer-i-aftale-om-pso.pdf, 2016. Visited 12-02-2020.

[5] Kommissarius ved Statens Ekspropriationer i Jylland. *400/150 kV jordkabel ved Vejle Ådal, besigtigelses- og ekspropriationsforretningen den 26. august 2015.* http://www.kommissarius.dk/content/400150-kv-jordkabel-ved-vejle-%C3%A5dal-besigtigelses-og-ekspropriationsforretningen-den-26-augus, 2015. Visited 12-02-2020.

[6] Forsynings-og Klimaministeriet Energi. *Markant færre master og luftledninger i Syd- og Vestjylland.* https://kefm.dk/aktuelt/nyheder/2018/dec/markant-faerre-master-og-luftledninger-i-syd-og-vestjylland/, 2018. Visited 07-02-2020.

[7] Energinet. *Transmission System Data.* https://en.energinet.dk/-/media/9160AAB5C484432399767220B78DE44D.jpg?la=en&hash=%5C%5C%5C%5C292D303A1536D9A1D3AC406A8717BA2A5219A13F. Visited 12-02-2020.

[8] Meeting with Energinet 10/02/2020.

[9] Chris Skovgaard Hansen and Kristian Didriksen Lund. Harmonic Modelling & Analysis of a Cable Based Transmission System. 2016.

[10] Christian Frank Flytkjær. Power system component harmonic modelling, October 2018.

[11] IEC. Electromagnetic compatibility (emc) - part 3-6: Limits - assessment of emission limits for the connection of distorting installations to mv, hv and ehv power systems. Standard, The International Electrotechnical Commission, Geneva, 2008.

[12] J Arrillaga and N. R. Watson. *Power System Harmonics*, chapter 1,2,3,4,6. John Wiley & Sons, Ltd, 2nd edition, 2004.

[13] Ph. D. Surya Santoso, Mark F. McGranaghan, Roger C. Dugan, and H. Wayne Beaty. *Electrical Power Systems Quality, Third Edition.* McGraw-Hill Education, New York, 2012.

[14] Zia Emin, C Jensen, and Łukasz Kocewiak. Amplification of harmonic background distortion in wind power plants with long high voltage connections. In *Cigré SESSION PAPERS AND PROCEEDINGS* - $C4-112-2016$, 08 2016.

[15] Sergio Herraiz, Luis Sainz, and Jordi Clua. Review of Harmonic Load Flow Formulations. 18(3):1079–1087, 2003.

[16] J. C. DAS. *Power System Harmonics and Passive Filter Designs*, chapter 6,15. John Wiley & Sons, Ltd, 2015.

[17] Ewald F. Fuchs Mohammed A. S. Masoum. *Power Quality in Power Systems and Electrical Machines*, chapter 9. Elsevier Inc., 2nd edition, 2015.

[18] Filipe Faria da Silva and Claus Leth Bak. *Electromagnetic transients in power cables*, chapter 3. Springer, 2013.

[19] Morten Vadstrup and Troels Jakobsen. *Filter Position Optimisation in Transmission System using Homotopy Analysis Method.* `https://projekter.aau.dk/projekter/files/306567870/EPSH4_1032_Filter_Position_Optimisation_in_Transmission_System_using_Homotopy_Analysis_Method.pdf`, 2019.

[20] S. Vørtz. *Elektriske fordelingsanlæg*, chapter 4 & 5. 1990.

[21] Oscar Lennerhag. A POWER SYSTEM MODEL FOR RESONANCE STUDIES. (June):3–6, 2019.

[22] P.B. Holst F. Faria da Silva, C. L. Bak. Study of Harmonics in Cable-based Transmission Networks. (C4-108):12–13, 2012.

[23] Eli Maria Stenseth and Jakob Harder Poulsen. HARMONIC AMPLIFCATION AND MITIGATION IN A MODERN MESHED TRANSMISSION SYSTEM. 2019.

[24] Systime. *Ellipsen.* `https://mata3stx.systime.dk/?id=645`, 2020. Visited 25-05-2020.

[25] Mack Grady. Understanding Power System Harmonics. Technical report, Dept. of Electrical & Computer Engineering University of Texas at Austin, 2012.

[26] DIgSILENT Powerfactory. *Example for Resonance Studies*, 2020.

[27] DIgSILENT Powerfactory. *Technical Reference - Harmonic Filter*, 2020.

Line Parameters in Radial System A

In this appendix, the utilised parameters in the radial system analyses from [21] are presented.

A.1 Overhead Lines

The OHL conductor types A and B are described in the modelling of the *Example grid* by Oscar Lennerhag in [21]. Additionally, the tower dimensions, conductor type, shield wires etc. is described in [21]. The resistance, inductance and capacitance of each line are calculated in PowerFactory using a geometry based line model. The parameters are calculated based on the tower type geometry and the shield wire types. Tower type geometry A is utilised in both Line 1 and 2 in the radial system and is shown in Figure A.1. The shield wire types are also identical in Line 1 and 2 in the radial system and each contains two type A. The parameters of the shield wires are given in Table A.2. The parameters required for the conductor in PowerFactory are the Geometrical Mean Radius (GMR), the DC-resistance and the bundle spacing. The GMR of the conductors are calculated from the conductor diameter, d, as seen in Equation A.1.

$$GMR = 0.772 \cdot \frac{d}{2} \tag{A.1}$$

The conductor diameters, DC-resistances and bundle-spacing are given in Table A.1.

Table A.1: Parameters of conductor types for OHL. [21]

Type	**d [mm]**	**Strands (outer/core)**	**Strand d [mm]**	**DC-resistance [Ω]**	**Sub-conductors**	**Sub-conductor spacing [cm]**
A	39.24	61	4.36	0.0337	2	60
B	36.18	61	4.02	0.0396	3	45
D	31.68	54/7	3.52/3.52	0.0551	1	N/A

Table A.2: Parameters of shield wire types. [21]

Type	**Diameter [mm]**	**Strands [Al/Fe]**	**Strand diameter [mm]**	**DC-resistance [Ω]**
A	20.10	12/7	4.02/4.02	0.1890

In Figure A.1 the tower type used in the radial system i shown. In Figure A.2 the 130 kV type used in the radial system i shown.

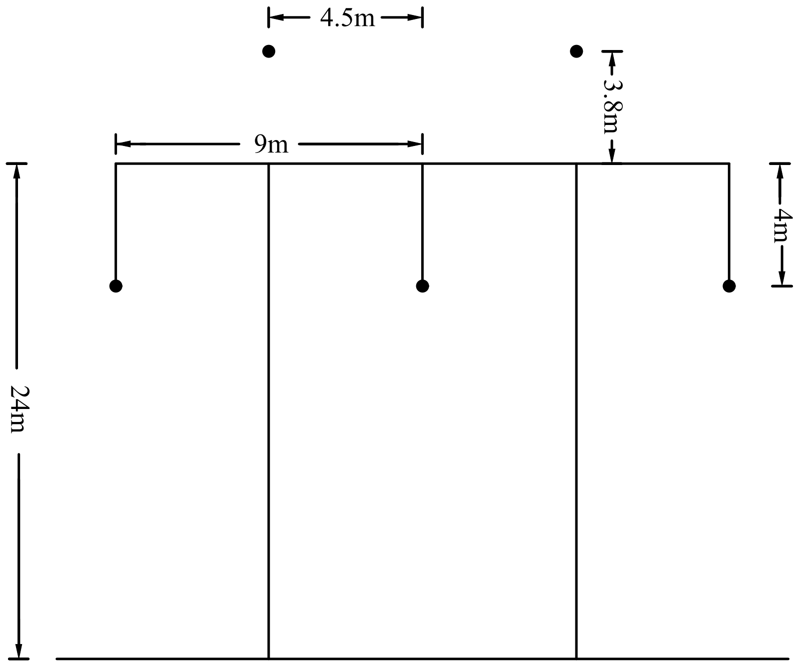

Figure A.1: Tower type A for 400 kV. [21]

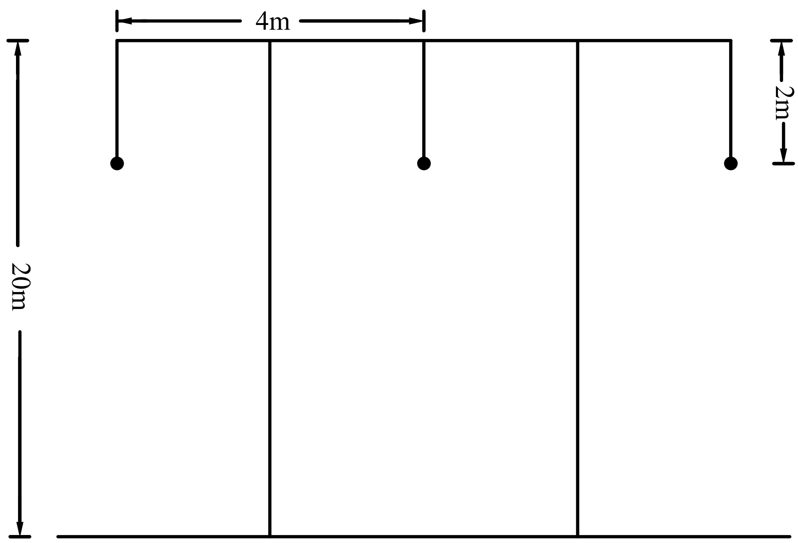

Figure A.2: Tower type D for 130 kV. [21]

A.2 Underground Cables

The UGC parameters for the 400 kV cable from the Example grid is shown in Table A.3.

Table A.3: UGC parameters for 400 kV cables. (*) Including water blocking tape. [21]

	2500 mm^2 Cu
Cable usage	Ground
Core diameter [mm]	63
Semi-conductive layer thickness [mm]	1.7
Insulation thickness	26
Semi-conductive layer thickness [mm]*	2.7
Screen thickness [mm]	2.05
Oversheath thickness [mm]*	7.0
DC-resistance of conductor at 20°C [Ω/km]	0.0072
DC-resistance of screen at 20°C [Ω/km]	0.0932
Relative permittivity of insulation	2.5
Relative permittivity of oversheath	2.4

Implementing the parameters from Table A.3 in PowerFactory, the electrical parameters of the Cu cable can be seen in Table A.4.

Table A.4: Electrical parameters of a 2500 mm^2 Cu cable when arranged in a trefoil.

Conductor Type	**Resistance [Ω/km]**	**Inductance [mH/km]**	**Capacitance [μF/km]**	**Conductance [μS/km]**
2500 mm^2 Cu	0.0126	0.3170	0.2111	1.5109

Radial System B

In this appendix, the radial system with and without the external grid will be analysed using nominal π-models to explain the system behavior. Additionally, the changes occurring in the frequency scan by the implementation of different voltage levels will be analysed.

B.1 Radial System without Grid

The impedance characteristic of a frequency scan from Bus 1, 5 and 7, from the system in Figure 3.2(c), is shown in Figure B.1. The simulations here are made utilising tower type models of the OHLs in PowerFactory as this is the case in the original *Example grid*.

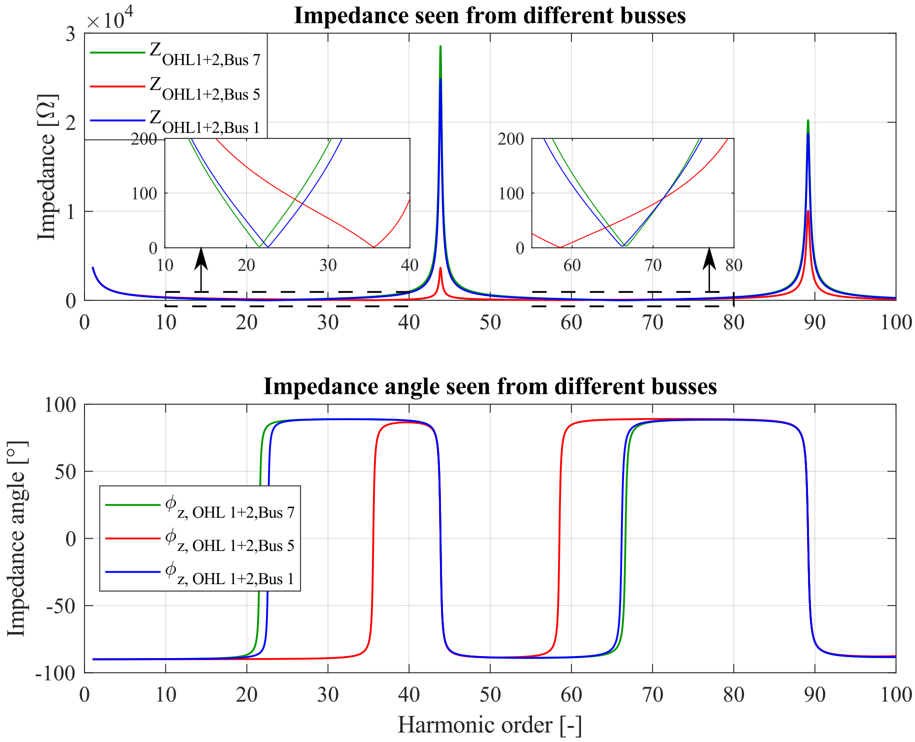

Figure B.1: Impedance magnitudes and phase angles as a function of the harmonic order, seen from Bus 1, 5 and 7, for the radial system in open circuit.

From Figure B.1, it is visible that the parallel resonance frequencies, are the same, whether the frequency scan is made from Bus 1, 5 or 7. To explain this, OHL 1 and 2 are considered as nominal π-models, as shown in Figure B.2. The resistance has an impact on the magnitude of the impedance at the resonance frequencies but no influence on which harmonic order the resonance frequencies occur. Therefore, the resistance is not included in the analysis. Additionally, nominal π-models introduce an error in the resonance frequency. However, as nominal π-models are easy to analyse, this modelling approach can be used as a proof of concept.

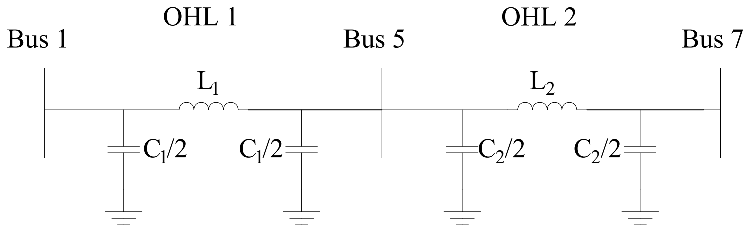

Figure B.2: Radial system in open circuit with OHLs as nominal π-model.

At the parallel resonances seen from Bus 7, $C_2/2$ is in parallel with the rest of the system. Therefore, parallel resonances occurs when $j/(\omega C_2/2)$ is equal to the reactance of the rest of the system, as shown in Equation B.1.

$$\frac{j}{\omega C_2/2} = \frac{(j \cdot \omega L_1 - \frac{j}{\omega C_1/2}) \cdot (\frac{-j}{\omega (C_1+C_2)/2})}{(j \cdot \omega L_1 - \frac{j}{\omega C_1/2}) + (\frac{-j}{\omega (C_1+C_2)/2})} + j \cdot \omega L_2 \qquad \textit{Seen from Bus } 7 \tag{B.1}$$

For the parallel resonances seen from Bus 1, $C_1/2$ is in parallel with the rest of the system. Therefore, the reactance at the parallel resonances appears as shown in Equation B.2.

$$\frac{j}{\omega C_1/2} = \frac{(j \cdot \omega L_2 - \frac{j}{\omega C_2/2}) \cdot (\frac{-j}{\omega (C_1+C_2)/2})}{(j \cdot \omega L_2 - \frac{j}{\omega C_2/2}) + (\frac{-j}{\omega (C_1+C_2)/2})} + j \cdot \omega L_1 \qquad \textit{Seen from Bus } 1 \tag{B.2}$$

The parallel resonances seen from Bus 5 has OHL 1 in parallel with OHL 2. Therefore, the parallel resonances appears when $X_{OHL1} = -X_{OHL2}$, as given by Equation B.3.

$$\frac{(j \cdot \omega L_1 - \frac{j}{\omega C_1/2}) \cdot (\frac{-j}{\omega C_1/2})}{(j \cdot \omega L_1 - \frac{j}{\omega C_1/2}) + (\frac{-j}{\omega C_1/2})} = -\frac{(j \cdot \omega L_2 - \frac{j}{\omega C_2/2}) \cdot (\frac{-j}{\omega C_2/2})}{(j \cdot \omega L_2 - \frac{j}{\omega C_2/2}) + (\frac{-j}{\omega C_2/2})} \; \textit{Seen from Bus } 5 \tag{B.3}$$

Solving for ω in either Equation B.1, B.2 or B.3, the same result is obtained. This result is shown in Equation B.4.

$$\omega_{0,parallel} = \frac{\sqrt{C_1 C_2 L_1 L_2 (C_1 + C_2)(C_1^2 L_1 + 2L_1 C_1 C_2 + 2C_1 C_2 L_2 + C_2^2 L_2 \pm \sqrt{y})}}{C_1 C_2 L_1 L_2 (C_1 + C_2)} \tag{B.4}$$

Where y is given in Equation B.5.

$$\begin{aligned} y =& C_1^4 L_1^2 + 4C_1^3 C_2 L_1^2 - 4C_1^3 C_2 L_1 L_2 + 4C_1^2 C_2^2 L_1^2 - 6C_1^2 C_2^2 L_1 L_2 + \\ & 4C_1^2 C_2^2 L_2^2 - 4C_1 C_2^3 L_1 L_2 + 4C_1 C_2^3 L_2^2 + C_2^4 L_2^2 \end{aligned} \tag{B.5}$$

This shows that the occurrence of the parallel resonance frequencies are independent of which bus the system is observed from.

An analysis regarding the series resonance frequencies can likewise be made utilising the nominal π-model shown in Figure B.2. From this analysis, it can be explained, why the series resonance frequencies seen from Bus 1 and 7 are not identical as shown in Figure B.1.

Seen from Bus 7, L_2 is in series with $C_2/2$, $C_1/2$, L_1 and $C_1/2$, and therefore, the series resonances appears when the reactance of these components are zero as shown in Equation B.6.

$$0 = \frac{(j \cdot \omega L_1 - \frac{j}{\omega C_1/2}) \cdot (\frac{-j}{\omega(C_1+C_2)/2})}{(j \cdot \omega L_1 - \frac{j}{\omega C_1/2}) + (\frac{-j}{\omega(C_1+C_2)/2})} + j \cdot \omega L_2 \qquad \textit{Seen from Bus } 7 \tag{B.6}$$

Seen from Bus 1, L_1 is in series with $C_1/2$, $C_2/2$, L_2 and $C_2/2$, and therefore, the series resonance appears when the reactance of these components are zero as shown in Equation B.7.

$$0 = \frac{(j \cdot \omega L_2 - \frac{j}{\omega C_2/2}) \cdot (\frac{-j}{\omega(C_1+C_2)/2})}{(j \cdot \omega L_2 - \frac{j}{\omega C_2/2}) + (\frac{-j}{\omega(C_1+C_2)/2})} + j \cdot \omega L_1 \qquad \textit{Seen from Bus } 1 \tag{B.7}$$

Seen from Bus 5, the series resonance frequencies are equal to the series resonance points of the individual OHLs, as explained in Section 3.2.

From Equations B.6 and B.7 it can be seen that they are not equal. Seen from Bus 7, $C_2/2$ is not part of the series resonance and seen from Bus 1, $C_1/2$ is not part of the series resonance. Hence, the series resonance frequencies seen from Bus 1 and 7 are not identical, since OHL 1 and 2 are different.

B.2 Radial System with External Grid

In the analysis of the radial system including the external grid, as shown in Figure 3.1, the impedance characteristic seen from Bus 1, 5 and 7 are as shown in Figure B.3. The simulation is made using tower type models representing the OHLs as this is the case in the *Example grid*.

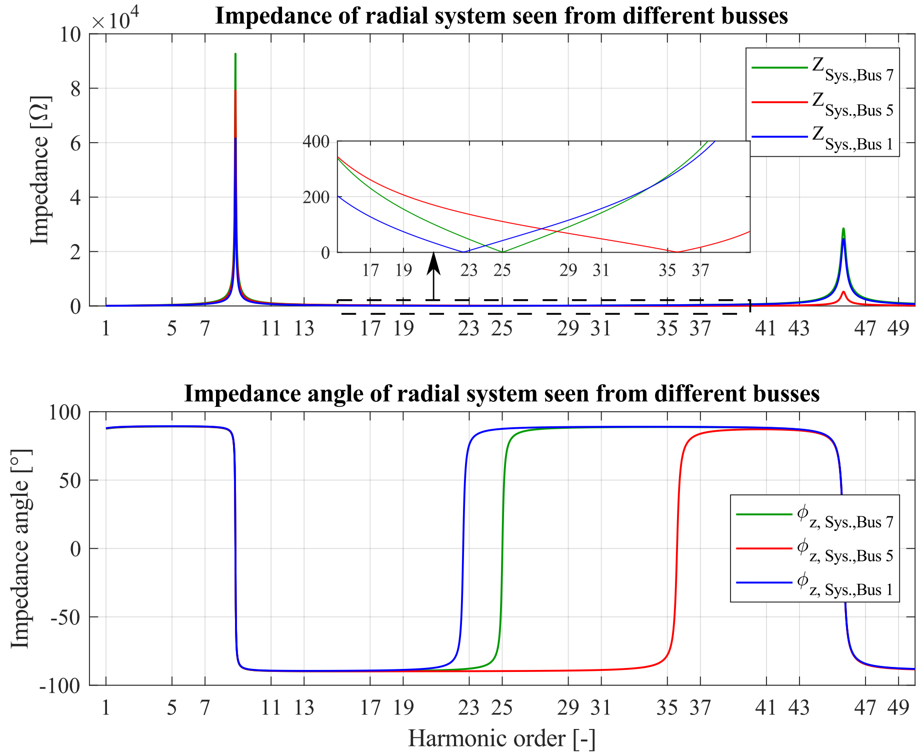

Figure B.3: Impedance magnitudes and phase angles of radial system as a function of the harmonic order seen from Bus 1, 5 and 7.

From Figure B.3, it is visible that the parallel resonance frequencies are the same, whether the frequency scan is made from Bus 1, 5 or 7. To explain this, the OHLs are considered as nominal π-models, as shown in Figure B.4.

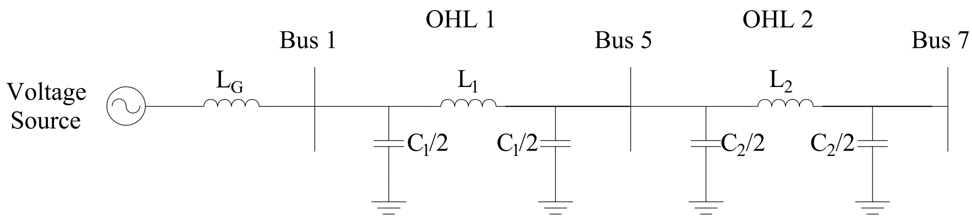

Figure B.4: Radial system with OHLs as nominal π-model.

For the parallel resonances seen from Bus 7, $C_2/2$ is in parallel with the rest of the system. Therefore, the parallel resonances occurs when $j/(\omega C_2/2)$ is equal to the reactance of the rest of the system, as given by Equation B.8.

$$\frac{j}{\omega C_2/2} = \frac{\left(\frac{j\omega L_G \cdot \frac{-j}{\omega C_1/2}}{j\omega L_G + \frac{-j}{\omega C_1/2}} + j \cdot \omega L_1\right) \cdot \left(\frac{-j}{\omega (C_1+C_2)/2}\right)}{\left(\frac{j\omega L_G \cdot \frac{-j}{\omega C_1/2}}{j\omega L_G + \frac{-j}{\omega C_1/2}} + j \cdot \omega L_1\right) + \left(\frac{-j}{\omega (C_1+C_2)/2}\right)} + j \cdot \omega L_2 \qquad \textit{Seen from Bus 7} \tag{B.8}$$

Seen from Bus 1, $-\frac{j\omega L_G \cdot (-j/(\omega C_1/2))}{j\omega L_G - j/(\omega C_1/2)}$ is in parallel with the rest of the system, which is given by Equation B.9.

$$-\frac{j\omega L_G \cdot -\frac{j}{\omega C_1/2}}{j\omega L_G - \frac{j}{\omega C_1/2}} = \frac{(j \cdot \omega L_2 - \frac{j}{\omega C_2/2}) \cdot (\frac{-j}{\omega(C_1+C_2)/2})}{(j \cdot \omega L_2 - \frac{j}{\omega C_2/2}) + (\frac{-j}{\omega(C_1+C_2)/2})} + j \cdot \omega L_1 \quad Seen\ from\ Bus\ 1 \tag{B.9}$$

The parallel resonances seen from Bus 5 are obtained when the reactance of OHL 2 is equal to the reactance of OHL 1 in series with the grid, but with opposite sign. This is shown in Equation B.10.

$$\frac{\left(\frac{j\omega L_G \cdot \frac{-j}{\omega C_1/2}}{j\omega L_G - \frac{j}{\omega C_1/2}} + j\omega L_1\right) \cdot (\frac{-j}{\omega C_1/2})}{\frac{j\omega L_G \cdot \frac{-j}{\omega C_1/2}}{j\omega L_G - \frac{j}{\omega C_1/2}} + j\omega L_1 - \frac{j}{\omega C_1/2}} = -\frac{(j \cdot \omega L_2 - \frac{j}{\omega C_2/2}) \cdot (\frac{-j}{\omega C_2/2})}{(j \cdot \omega L_2 - \frac{j}{\omega C_2/2}) + (\frac{-j}{\omega C_2/2})} \quad Seen\ from\ Bus\ 5 \tag{B.10}$$

By isolating for ω in either Equation B.8, B.9 or B.10 a long complex equation is obtained. Utilising the actual values and isolating for ω, the exact same parallel resonance frequencies are obtained, independent of the bus from where it is observed. The parallel resonance obtained are at harmonic orders: 9.5, 40.4 and 70.8.

To compare the series resonances of the radial system with and without the grid, the impedance seen from Bus 1 and 7, with and without the external grid is made and shown in Figure B.5. The simulations are made using tower type models of the OHLs.

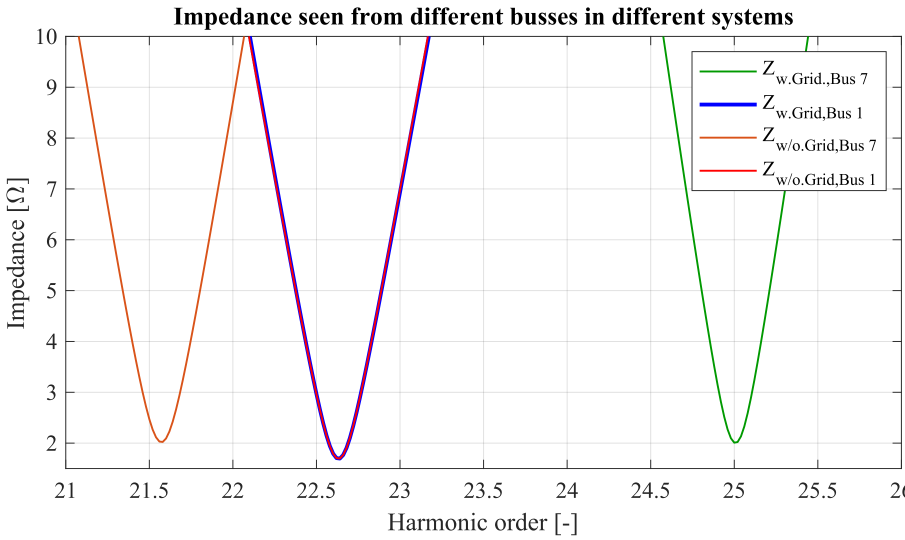

Figure B.5: Impedances as a function of the harmonic order seen from Bus 1 and 7, for the radial system with and without grid.

Here it can be seen that the series resonance is the same seen from Bus 1 with and without the grid. However, seen from Bus 7, the series resonance is shifted to a higher order harmonic when the grid is included. This can be explained by utilising the circuit with the nominal π-models representing the OHLs, as shown in Figure B.4.

Seen from Bus 1, L_1 is in series with $C_1/2$, $C_2/2$, L_2 and $C_2/2$, and therefore, the series resonance appears when the reactance of these components are zero as shown in Equation

B.11.

$$0 = \frac{(j \cdot \omega L_2 - \frac{j}{\omega C_2/2}) \cdot (\frac{-j}{\omega(C_1+C_2)/2})}{(j \cdot \omega L_2 - \frac{j}{\omega C_2/2}) + (\frac{-j}{\omega(C_1+C_2)/2})} + j \cdot \omega L_1 \qquad Seen\ from\ Bus\ 1 \tag{B.11}$$

Equation B.11 is equal to Equation B.7, which was valid for the open circuit model. Therefore, the series resonance frequencies seen from Bus 1, is independent of the grid impedance.

Seen from Bus 7, L_2 is in series with $C_2/2$, $C_1/2$, L_1, $C_1/2$ and L_G, and therefore, the series resonances appears when the reactance of these components are zero as shown in Equation B.12.

$$0 = \frac{\left(\frac{j\omega L_G \cdot \frac{-j}{\omega C_1/2}}{j\omega L_G + \frac{-j}{\omega C_1/2}} + j \cdot \omega L_1\right) \cdot (\frac{-j}{\omega(C_1+C_2)/2})}{\left(\frac{j\omega L_G \cdot \frac{-j}{\omega C_1/2}}{j\omega L_G + \frac{-j}{\omega C_1/2}} + j \cdot \omega L_1\right) + (\frac{-j}{\omega(C_1+C_2)/2})} + j \cdot \omega L_2 \qquad Seen\ from\ Bus\ 7 \tag{B.12}$$

From Equations B.11 and B.12 it can be seen that they have some differences. Seen from Bus 7, $C_2/2$ is not part of the series resonance and seen from Bus 1, $C_1/2$ and L_G is not part of the series resonance. Hence, the series resonance seen from Bus 1 is independent of the grid, while the series resonance seen from Bus 7 is.

B.3 Radial System with Transformer

To analyse the radial system with a transformer, the system is analysed with a transformer without resistance and reactance, referred as a lossless transformer. The system with a lossless 410/145 kV transformer is compared to a system with a lossless 410/410 kV transformer. In both systems, the exact same grid and line parameters are used, to make them comparable. The system with the 410/410 kV lossless transformer is equivalent to the system analysed in Section B.2, as the transformer does not introduce any impedance.

The impedance characteristics seen from Bus 7 for both the system with the 410/410 kV and the 410/145 kV lossless transformer are shown in Figure B.6. The simulations are made using tower type models of the OHLs as in the *Example grid*.

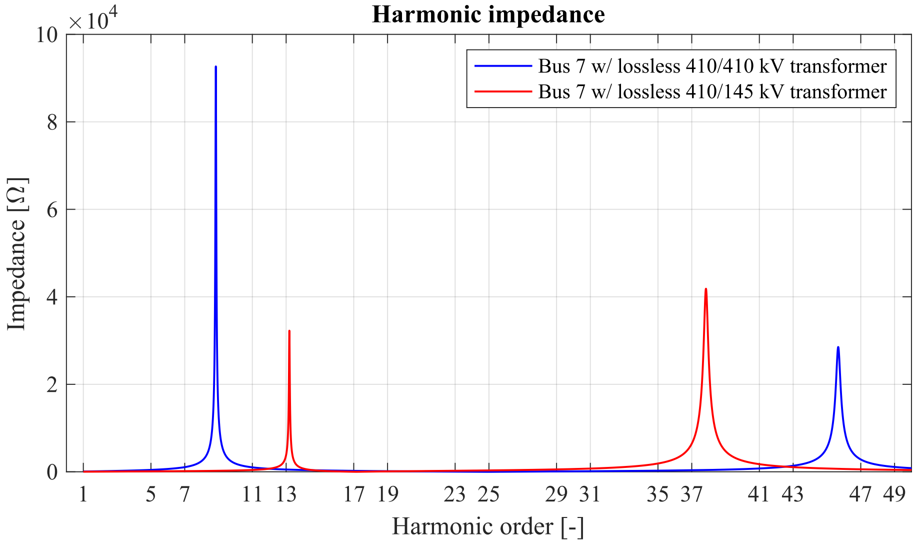

Figure B.6: Impedance magnitudes and phase angles as a function of the harmonic order seen from Bus 7, for the radial system with a 410/410 kV and a 410/145 kV lossless transformer.

From Figure B.6, it is visible that the first parallel resonance frequency has shifted upward and the second has shifted downward for the system with 410/145 kV transformer. Since the transformers are lossless, the shifts occur only due to the different voltage levels in the 410/145 kV transformer system. To analyse why the parallel resonance peaks are shifted, the systems are analysed using nominal π-models for the OHLs. Additionally, in Chapter 4.1 it is explained, that the frequency scan observed from the 145 kV side sees the impedance on the 410 kV side a factor eight lower. Therefore, the two radial transformer systems with nominal π-models are as shown in Figure B.7.

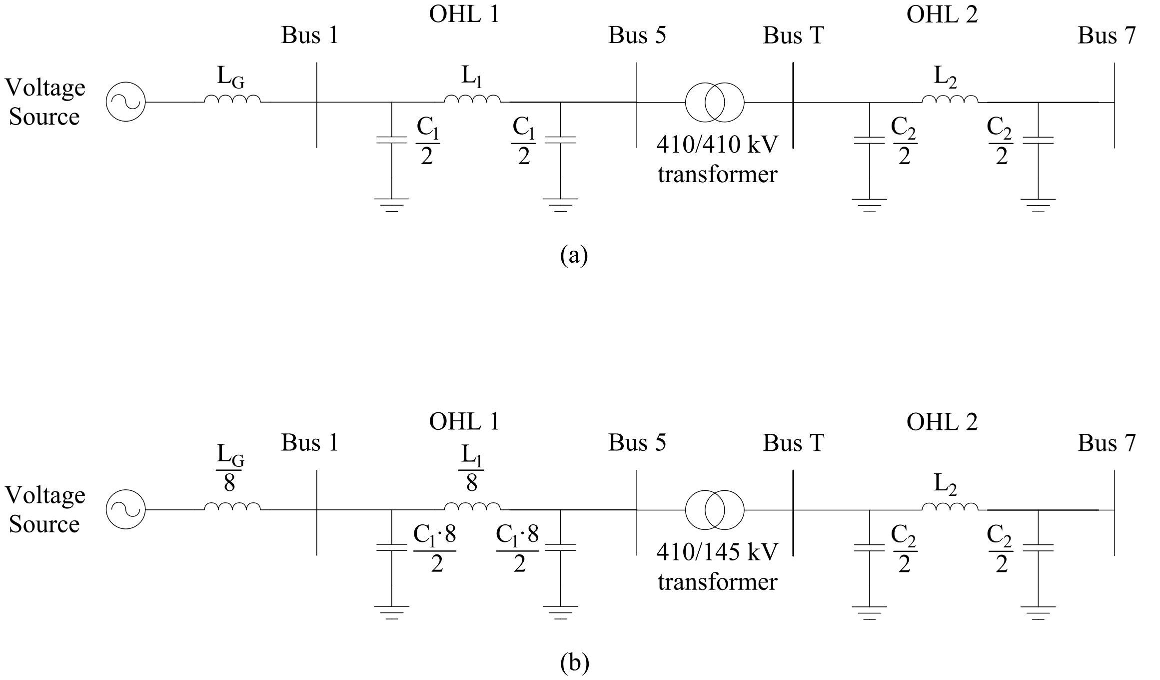

Figure B.7: Radial system with OHLs as nominal π-model and lossless transformers. The first plot (a) is a 410/410 kV system and the second plot (b) is a 410/145 kV system observed from the 145 kV side.

Regarding the parallel resonances seen from Bus 7, $C_2/2$ is in parallel with the rest of the system. Therefore, the parallel resonances occurs when $j/(\omega C_2/2)$ is equal to the reactance of the rest of the system. For the 410/410 kV system, the equation is as presented previously in Equation B.8. For the 410/145 kV system, the impedances on the HV side are divided by a factor of eight, as shown in Equation B.13.

$$\frac{j}{\omega C_2/2} = \frac{\left(\frac{j\omega\frac{L_G}{8}\cdot\frac{-j}{\omega C_1\cdot 8/2}}{j\omega\frac{L_G}{8}+\frac{-j}{\omega C_1\cdot 8/2}} + j\cdot\omega\frac{L_1}{8}\right)\cdot\left(\frac{-j}{\omega(C_1\cdot 8+C_2)/2}\right)}{\left(\frac{j\omega\frac{L_G}{8}\cdot\frac{-j}{\omega C_1\cdot 8/2}}{j\omega\frac{L_G}{8}+\frac{-j}{\omega C_1\cdot 8/2}} + j\cdot\omega\frac{L_1}{8}\right)+\left(\frac{-j}{\omega(C_1\cdot 8+C_2)/2}\right)} + j\cdot\omega L_2 \qquad \textit{Seen from Bus 7} \tag{B.13}$$

Solving for ω in these equations gives a long and complex equation. However, by looking at Equation B.4 for parallel resonance frequencies in the system without the external grid, it is clear that the inductance and capacitance have a different influence on the resonance frequencies. Hence, the factor eight does not simply even out.

Additionally, the calculations of the first and second parallel resonance frequencies are not identical. Therefore, the resonance frequencies cannot be calculated using the classic formula for resonance: $\frac{1}{\sqrt{LC}}$. Nonetheless, the formula $\frac{1}{\sqrt{LC}}$ can still be used as a guideline.

To visualise the effect of the per unit conversion factor, a, the two parallel resonance points in Figure B.6 are analysed for different factors of a. The analysis will be made on a circuit with nominal π-models and with a varying per unit conversion factor as shown in Figure B.8. A conversion factor of 8, corresponds to the HV side being 410 kV and the LV side being 145 kV. A conversion factor of 1, corresponds to the HV side being 145 kV and the LV side likewise.

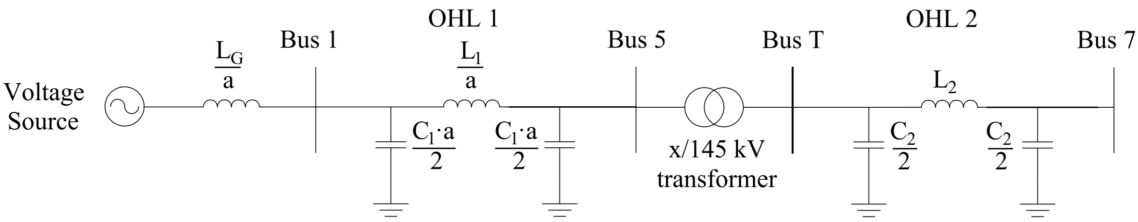

Figure B.8: Radial system with OHLs as nominal π-model and lossless transformers for system with 145 kV and varying per unit conversion factor.

Using Equation B.13 with the specific conversion factor of eight replaced with the per unit conversion factor, a, the first two parallel resonance frequencies can be calculated. By varying the per unit conversion factor from 0.25 to 8.5, the first and second parallel resonance frequencies shifts as shown in Figure B.9.

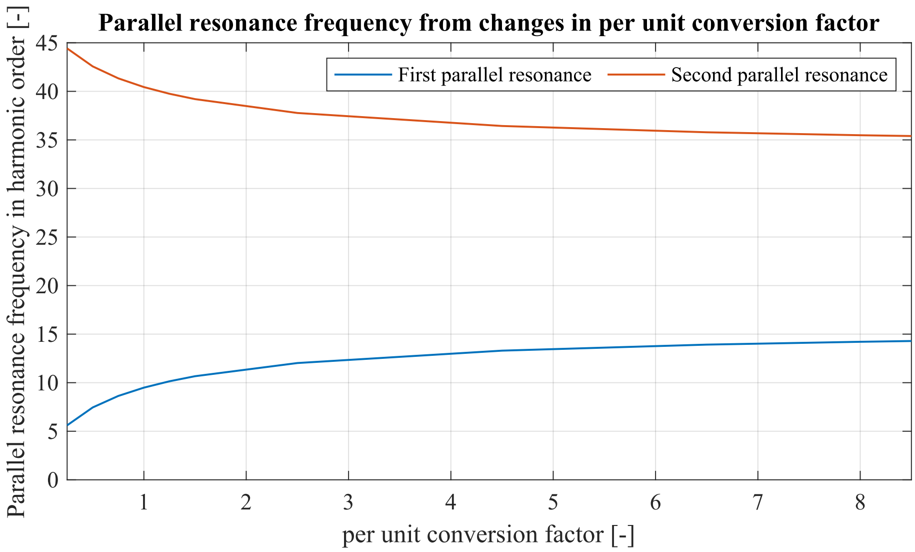

Figure B.9: The first and second parallel resonance frequencies in the radial system with a lossless transformer, with a varying per unit conversion factor.

From Figure B.9, it can be seen that the resonance frequency of the first parallel resonance peak is increasing and the second is decreasing, with an increasing conversion factor. This shows that the two resonance points are changed differently with a varying per unit conversion factor.

Meshed System C

C.1 PowerFactory Model of Meshed System

The *Example grid* developed by Oscar Lennerhag, is implemented as part of PowerFactory's library. The details of the implementation in PowerFactory is described in [26]. The PowerFactory model of the *Example grid* is shown in Figure C.1.

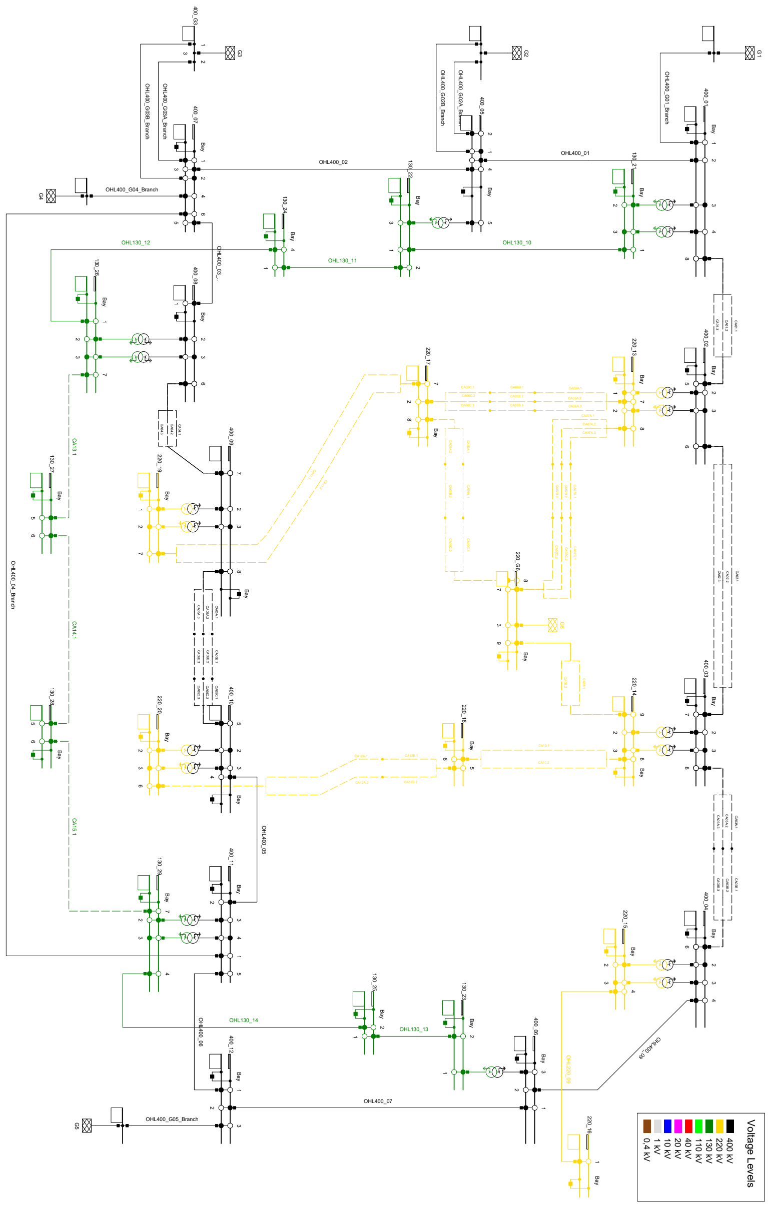

Figure C.1: Overview of the original meshed system in PowerFactory. [26]

C.2 System Modelling

In this section additional system parameters and an analysis regarding the harmonic current source angles are presented.

C.2.1 Urban Network Parameters

The urban equivalent loads are connected through two 135/11 kV transformers at each 130 kV bus. The max load of the equivalent loads L1 - L9 together with the transformer MVA is shown in Table C.1.

Table C.1: Equivalent max load of the urban networks and the corresponding transformer rating. [21]

Load	Max load [MW]	Transformer rating [MVA]
L1	150	2 x 100
L2	70	2 x 50
L3	250	2 x 175
L4	150	2 x 100
L5	100	2 x 70
L6	350	2 x 245
L7	100	2 x 70
L8	100	2 x 70
L9	300	2 x 210

C.3 Harmonic Source Analysis

In the previous harmonic propagation studies in the radial, the harmonic sources were injecting with an angle of 0°. In this section, the influence of the harmonic current source on the voltage angle is analysed. The harmonic current source injects 1 pu at the harmonics of interest. The harmonic voltage magnitudes and angles are measured in Bus 7, while the harmonic current source is connected in different busses in the system. In Figure C.2, the harmonic voltage magnitude and angle is measured in Bus 7, when connecting the harmonic current source in Bus 7, 1, 4, 12, 21, 26 or 29.

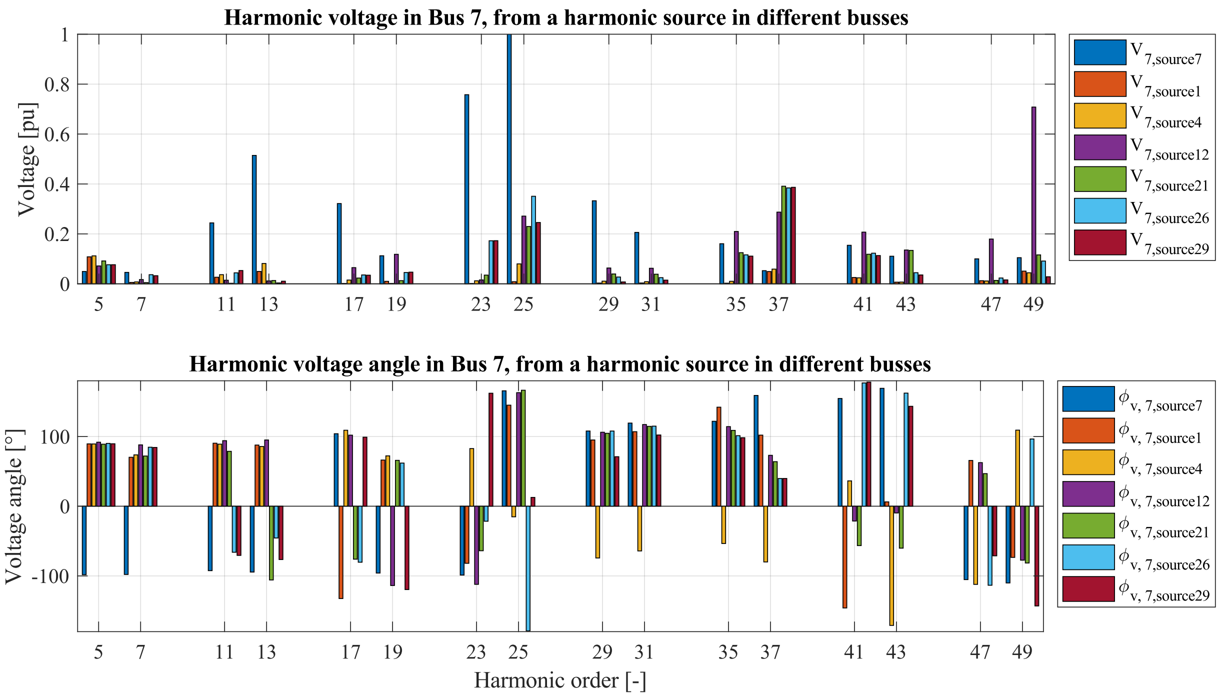

Figure C.2: Harmonic voltage magnitude and angle in Bus 7 when connecting the harmonic current source in Bus 7, 1, 4, 12, 21, 26 or 29.

In the radial system in Section 3.5, a tendency was observed that the harmonic voltage had the same polarity for lower orders and opposite polarity for higher order harmonic voltages, when the currents was injected in different busses. From Figure C.2 this tendency can no longer be observed. This is the case since, no tendency in whether the angles are positive or negative can be observed in the bottom plot.

C.4 Additional Impedance Analysis

This section will showcase additional studies performed regarding the impedance analysis.

C.4.1 Case 4: Influence of Transformer Impedance

The impedance characteristic of Bus 11 at 400 kV, when the lines at the 400 kV system are changed, with and without transformer impedance can be seen in Figure C.3.

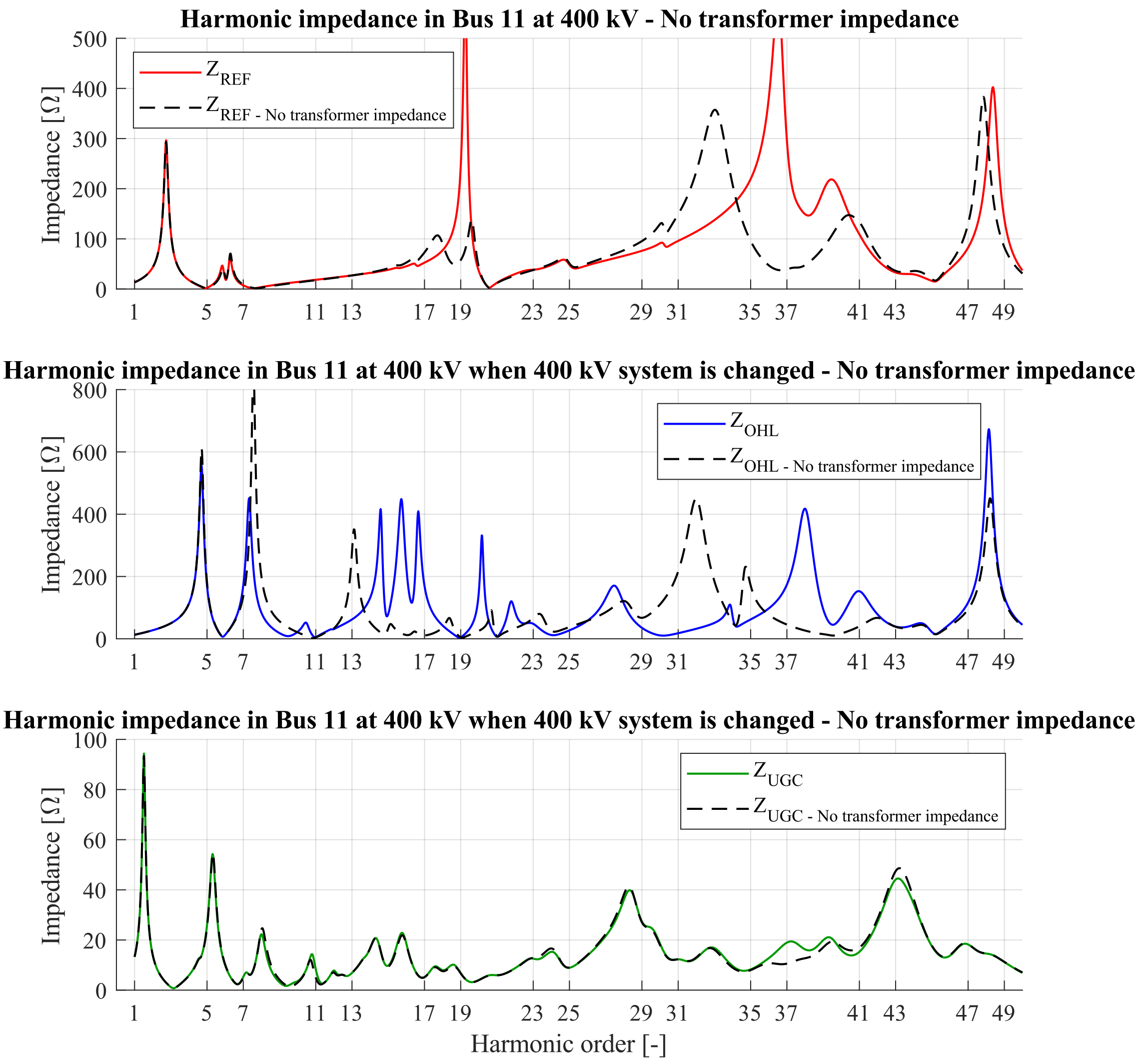

Figure C.3: Comparison of harmonic impedance in Bus 11 at 400 kV, when the 400 kV lines are changed, with and without transformer impedance.

As seen in Figure C.3 the main differences with and without transformer impedance are with regards to the impedance magnitudes. The largest difference in impedance magnitude is present for the OHL case, then the reference case, while the UGC cases are barely affected. Additionally, the resonance frequencies has also changed significantly for the OHL and reference case. This is due to the harmonic propagation flowing to the path of least impedance. Hence, when implementing UGCs at 400 kV, the path of least impedance is in the 400 kV system and the removal of transformer impedance does not change this.

The impedance characteristic of Bus 29 at 400 kV, when the lines at the 400 kV system are changed, with and without transformer impedance can be seen in Figure C.4.

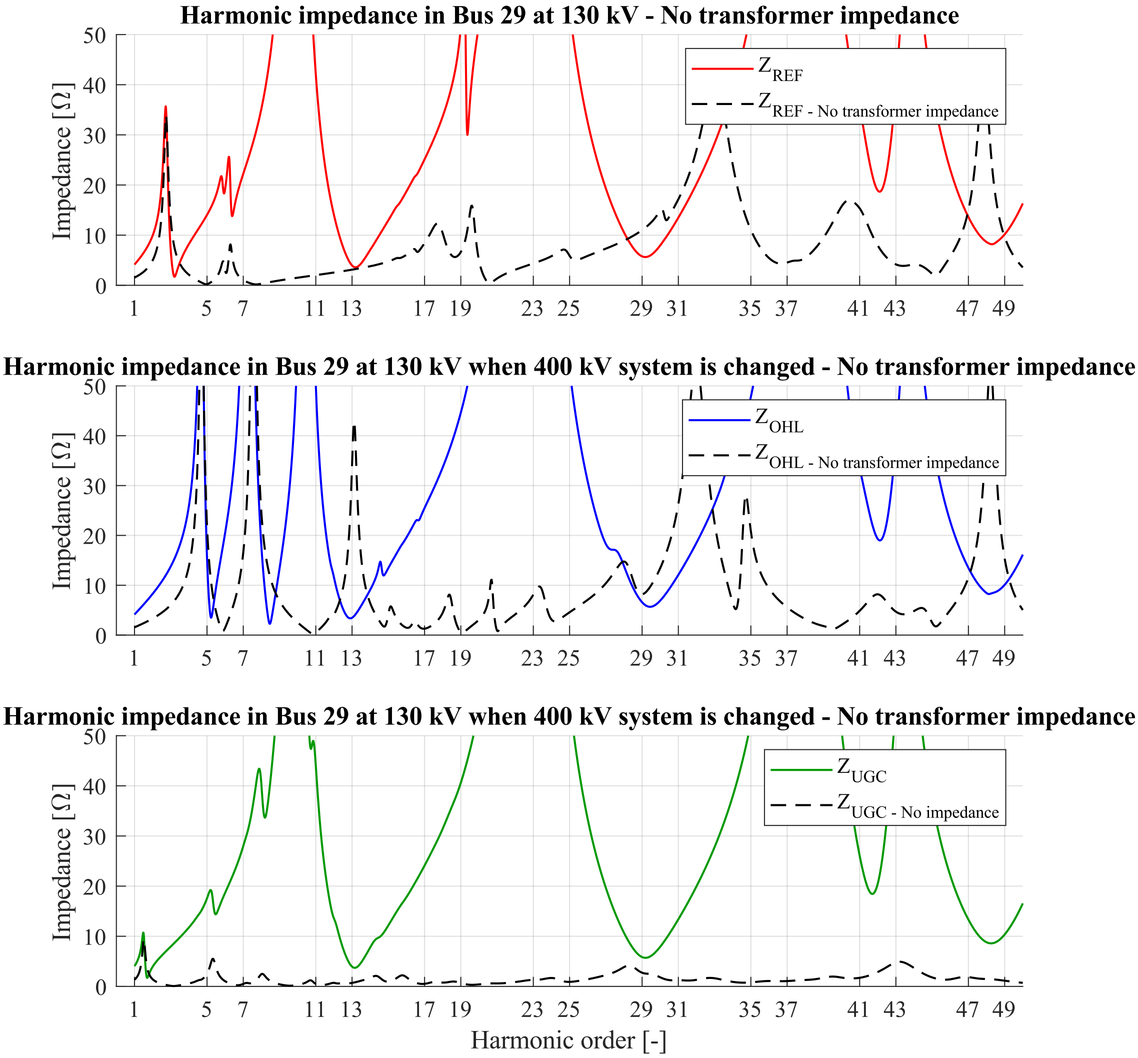

Figure C.4: Comparison of harmonic impedance in Bus 29 at 130 kV, when the 400 kV lines are changed, with and without transformer impedance.

As seen in Figure C.4 the largest differences are observed for the UGC case. This is due to the harmonic current would rather propagate to the 400 kV system, when the 400 kV system is changed to UGCs.

C.4.2 Case 5: Longer Lines at LV System

The impedance characteristic comparison with and without longer lines at the LV-system in Bus 11 at 400 kV can be seen in Figure C.5.

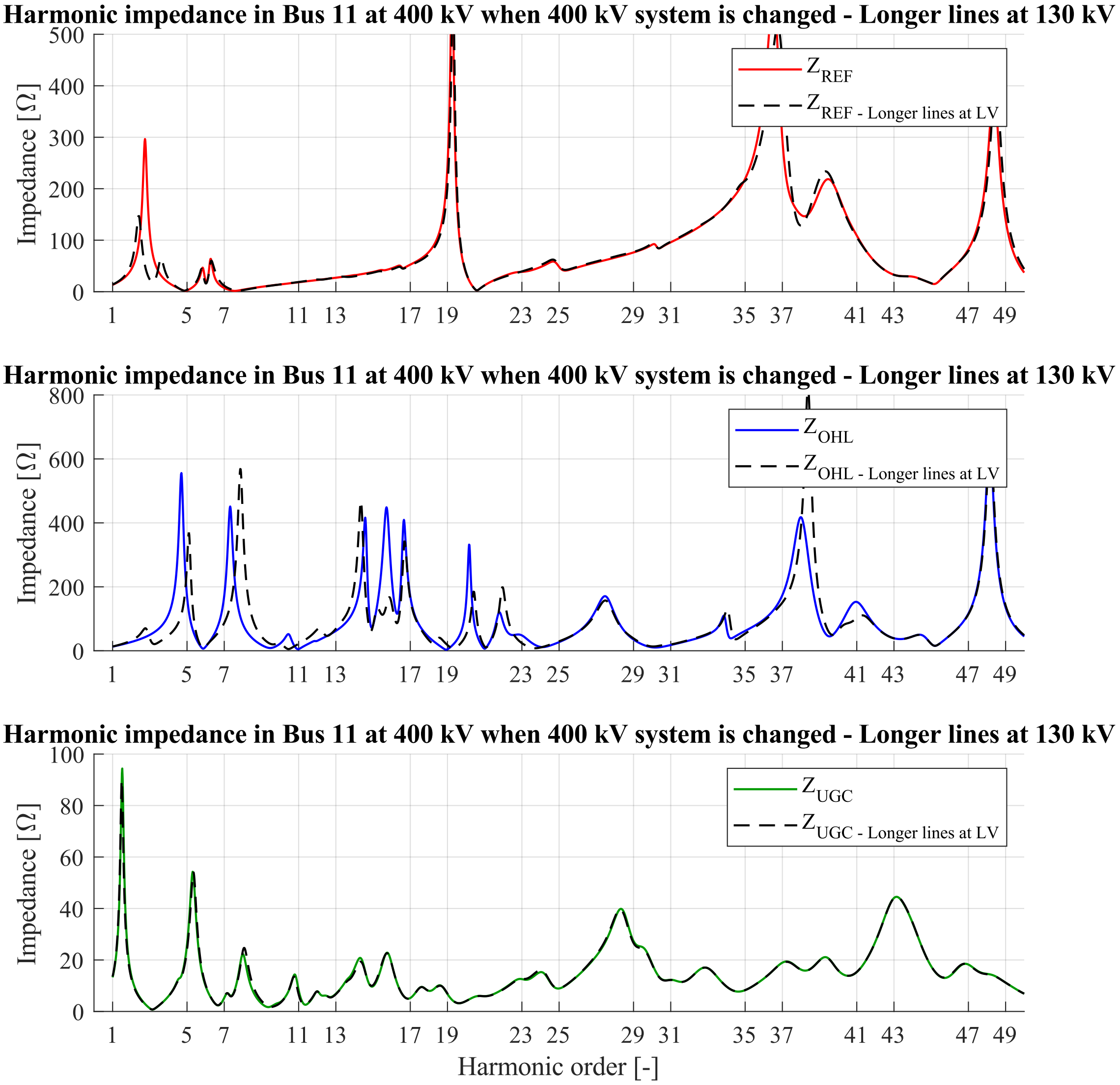

Figure C.5: Comparison of harmonic impedance in Bus 11 at 400 kV, when the 400 kV lines are changed, with and without longer lines at the 130 kV system.

As seen in Figure C.5, when the lines in the 400 kV system are replaced by UGCs, the impedance characteristic is not affected. This can be explained from the path of least impedance, which still is at the 400 kV system. When the lines in the 400 kV system are replaced by OHLs, small differences in the impedance characteristic can be seen, mainly in terms of the harmonic impedance magnitudes.

C.5 Comparison of Frequency Scan and Harmonic Penetration Method

In Section 3.5, it was analysed if the harmonic penetration and frequency scan methods could be compared in the radial system.

The harmonic current source is placed in Bus 7, and the voltage is measured in Bus 5. Here, the impedance seen from Bus 5 times the injected current and the measured harmonic voltage in Bus 5 should not be identical. However, the same analysis in the radial system did show, that the characteristics of the two voltages were following each other. Additionally, as shown in the analysis of the radial system, the off-diagonal impedance from Bus 7 to Bus 5, Z_{7-to-5}, multiplied by the injected harmonic current in Bus 7, I_7, is compared to the voltage measured in Bus 5 from the harmonic penetration method. The results from these two analyses are shown in Figure C.6.

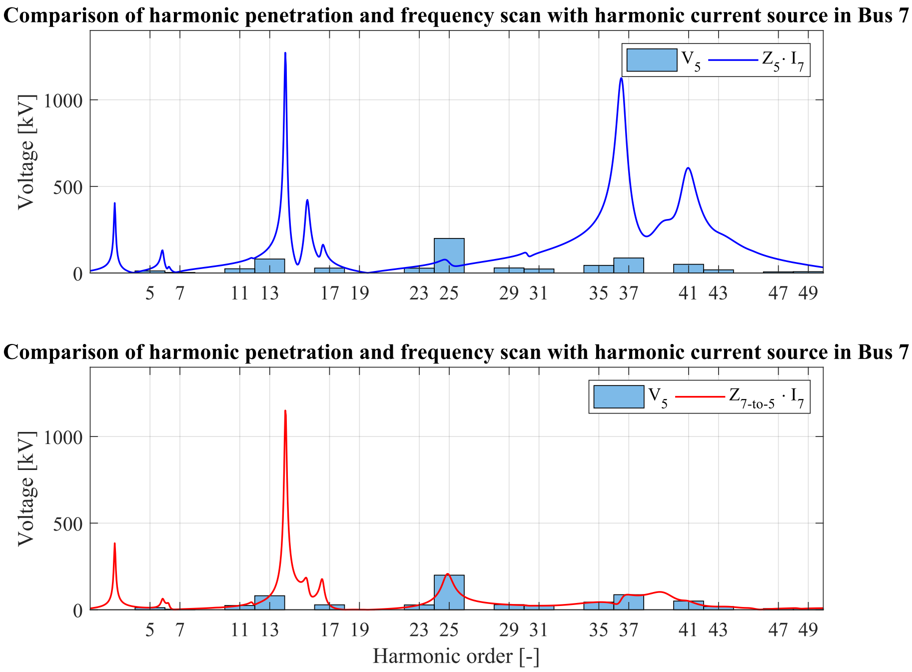

Figure C.6: Harmonic voltages in Bus 5 obtained from a harmonic penetration with a harmonic current source in Bus 7 compared to harmonic voltages obtained from the frequency scan method in Bus 5 and the off-diagonal impedance from Bus 7 to Bus 5.

From the top plot in Figure C.6 it can be concluded that the measured voltage in Bus 5 does not have the same tendency as the calculated voltage from the frequency scan as the case was in the radial system. Utilising the off-diagonal impedance between the busses, the two voltages are identical for the harmonic orders injected by the harmonic current source as in the radial system.

It is also analysed whether the off-diagonal impedance from the frequency scan can be used to determine the harmonic voltage in a bus far away. Therefore, the harmonic current source is connected in Bus 21 at the 130 kV level, injecting 1 pu current. The harmonic voltage is measured utilising the harmonic penetration in Bus 12 on the 400 kV side, which is located on the other side of the meshed system compared to Bus 21. The off-diagonal impedance from Bus 21 to 12, $Z_{21-to-12}$ is multiplied by the injected current in Bus 21 in order to determine the voltage $V_{21-to-12}$. The comparison of the off-diagonal impedance from the frequency scan and the harmonic penetration in Bus 12 can be seen in Figure C.7.

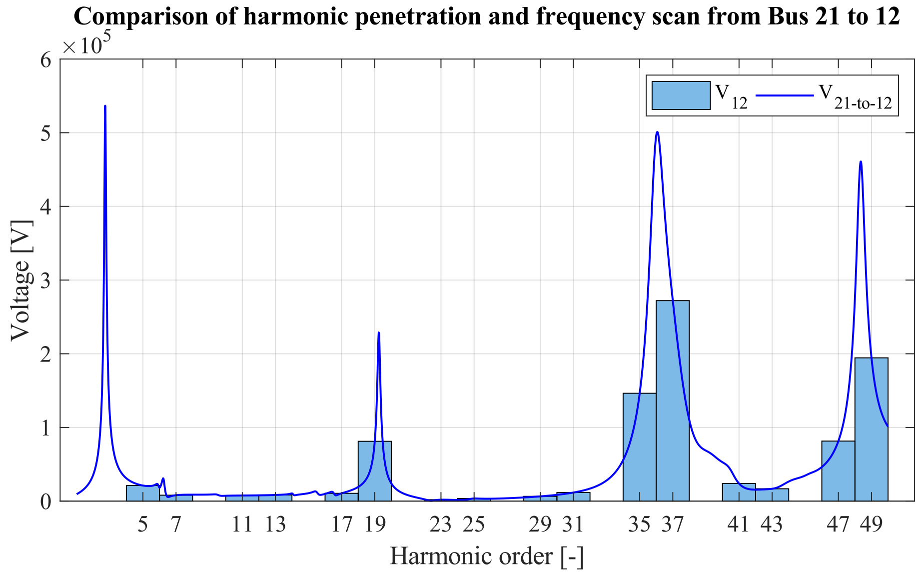

Figure C.7: Harmonic voltages in Bus 12 obtained from a harmonic penetration with a harmonic current source in Bus 21 compared to harmonic voltages obtained from the off-diagonal impedance from Bus 21 to Bus 12 multiplied by the injected current.

From Figure C.7, it is visible that the off-diagonal impedance from the frequency scan can be used for busses far from each other in a meshed system in order to determine the harmonic voltage in a bus different from the bus of injection. The advantage of utilising the off-diagonal impedance from the frequency scan compared to harmonic penetration is that the inter harmonic voltages can directly be calculated from the impedance characteristic. Hence, the off-diagonal impedance between every bus can help identify resonances in a meshed system.

C.6 Propagation of Harmonic Voltages through a Transformer

In Section 5.3.3 it was shown that the harmonic voltages was damped for the harmonic orders of interest from the LV- to the HV-side of the transformer T1. It was also shown that if changes occurred in the system, the characteristic could change, and an amplification could occur at the low order of harmonics, at the harmonic of injection. Therefore, it is tested, how the characteristic is changed, when all the UGCs in 400 kV system is replaced with OHLs. In Figure C.8, the relation between the harmonic voltage on the HV- and LV-side is shown for each harmonic order, from injecting harmonic currents in Bus 21 in the system with OHLs in the 400 kV system.

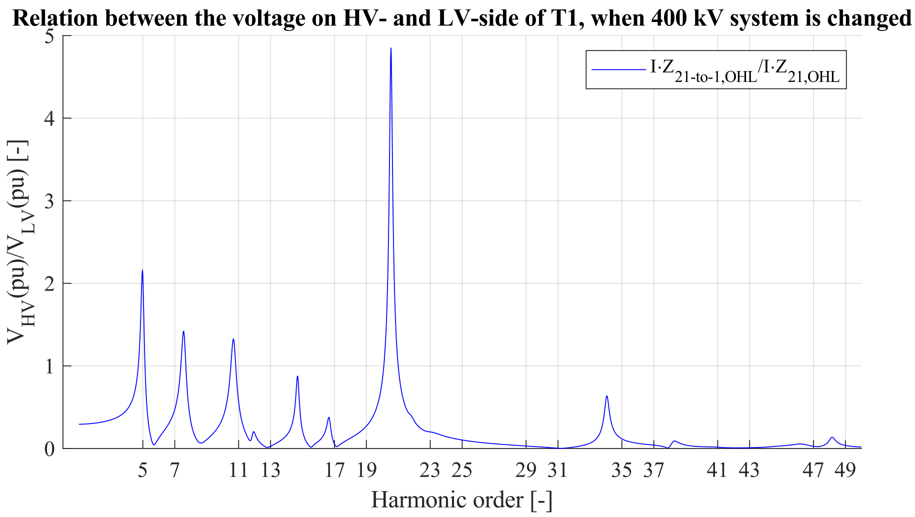

Figure C.8: Relation between the voltage on HV- and LV-side of T1 for the harmonic orders of interest, when 400 kV system has purely OHLs.

From Figure C.8 it can be seen that the impedance characteristic is changed. The voltage on the HV-side is more than twice the voltage on the LV-side for the 5^{th} harmonic order. This occurs as the 5^{th} harmonic order is at a peak now. Therefore, an amplification of harmonic voltages through the transformer occurs.

C.7 Harmonic Voltages in Meshed System

To analyse the harmonic voltage propagation in the busses in the meshed system, the harmonic current source is connected in Bus 21, and the harmonic voltages are measured in the busses in the system. In Figure C.9 the harmonic voltages for the specified harmonic orders are shown for the reference system. In Figure C.10 and C.11 the harmonic voltages are shown for the system, where the 130 kV system consist of OHLs or UGCs respectively.

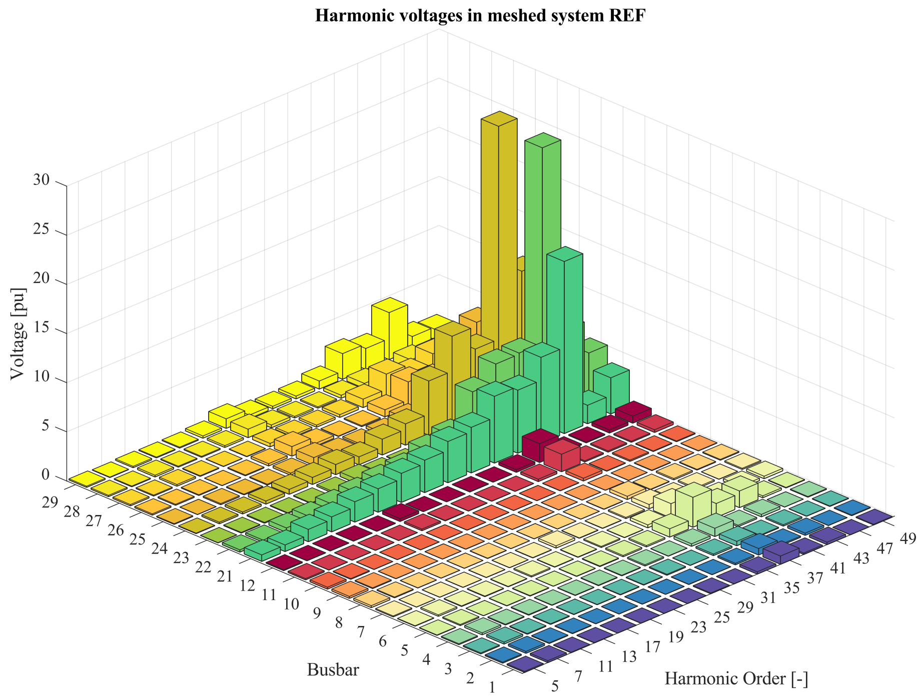

Figure C.9: Harmonic voltages for each bus in the meshed system for every harmonic order for the reference case, with harmonic current injected in Bus 21.

From Figure C.9 it can be seen that the harmonic voltages in general are largest in Bus 21, which is the bus of injection. Additionally, it can be seen that the harmonic voltages are larger on the busses on 130 kV (21 to 29), compared to the busses on 400 kV (1 to 12)

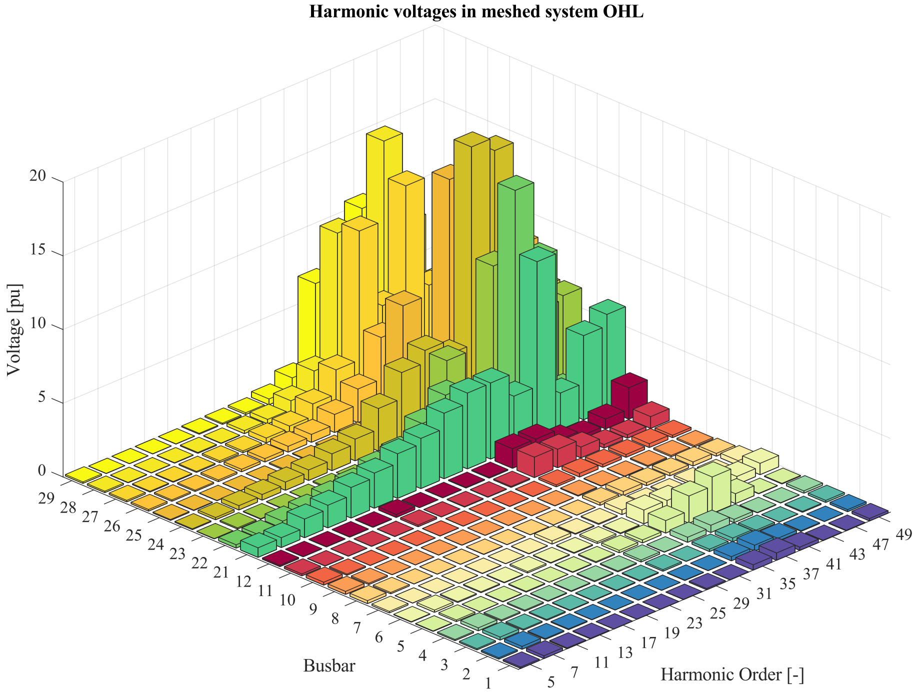

Figure C.10: Harmonic voltages for each bus in the meshed system for every harmonic order for the OHL case, with harmonic current injected in Bus 21.

From Figure C.10 it can be seen that harmonic voltage of the high harmonic orders have increased compared to the reference case in Figure C.9. This occurs as the impedance of the high order harmonics increases for the OHL case compared to the REF case, as was shown in Figure 5.3.

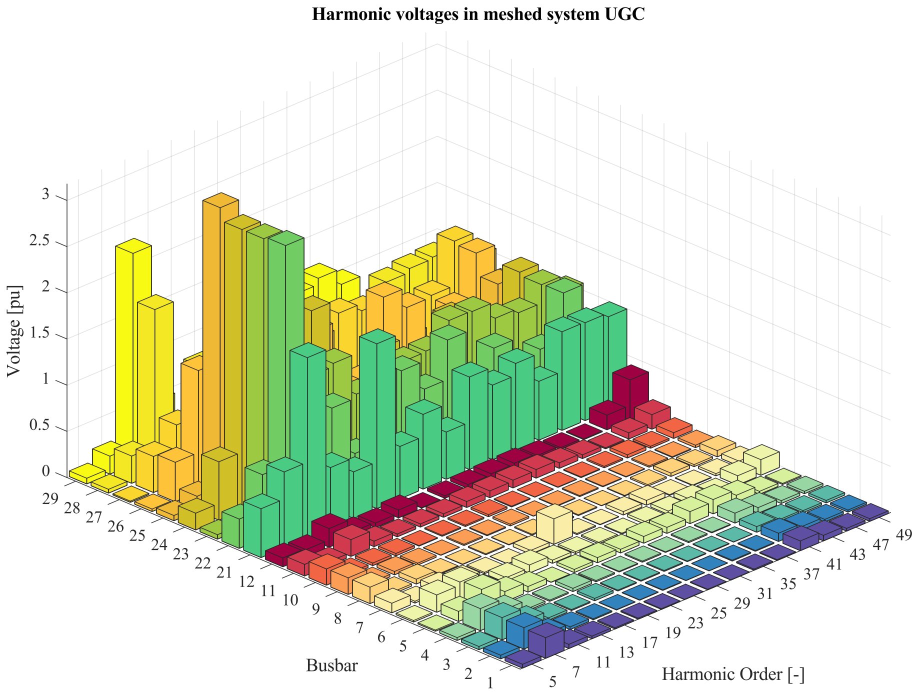

Figure C.11: Harmonic voltages for each bus in the meshed system for every harmonic order for the UGC case, with harmonic current injected in Bus 21.

From Figure C.11 it can be seen that the harmonic voltages have decreased for the high order of harmonics, compared to the REF case in Figure C.9. Additionally, the harmonic voltages have increased for the low order harmonics, compared to the REF case. These effects can be explained from the introduction of UGCs, that lowers the impedance of the system, and shift the parallel resonance frequencies to lower harmonic orders, as seen in Figure 5.3.

Harmonic Mitigation D

In this appendix, the harmonic voltage decrease for every bus in the system with a filter in every bus injected is shown. The harmonic current is injected in Bus 6. The harmonic voltage decrease in the HV-side busses are shown in Figure D.1.

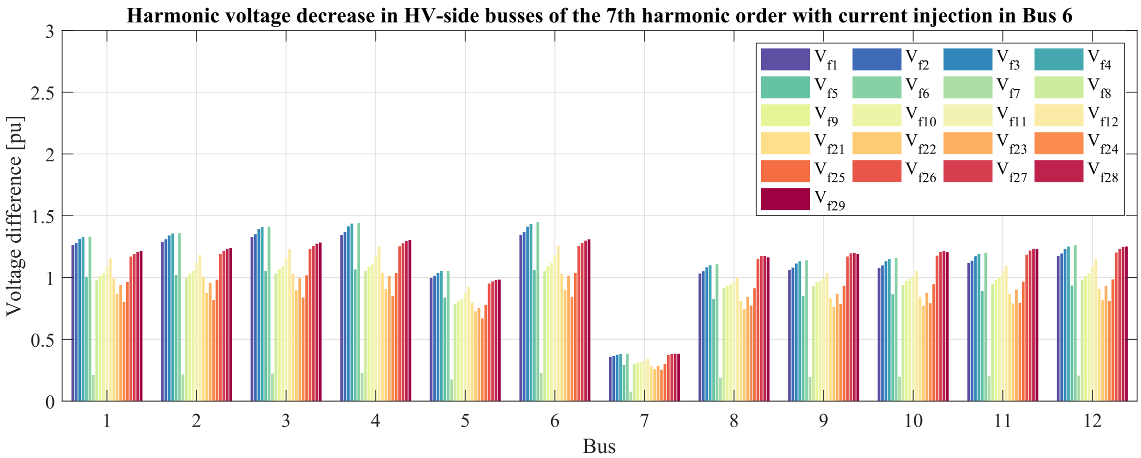

Figure D.1: Harmonic voltage decrease in the HV-side busses in the system without a filter compared to having a filter in either of the busses in the system. The harmonic current is injected in Bus 6.

The harmonic voltage decrease in the LV-side busses with harmonic current injected in Bus 6 are shown in Figure D.2.

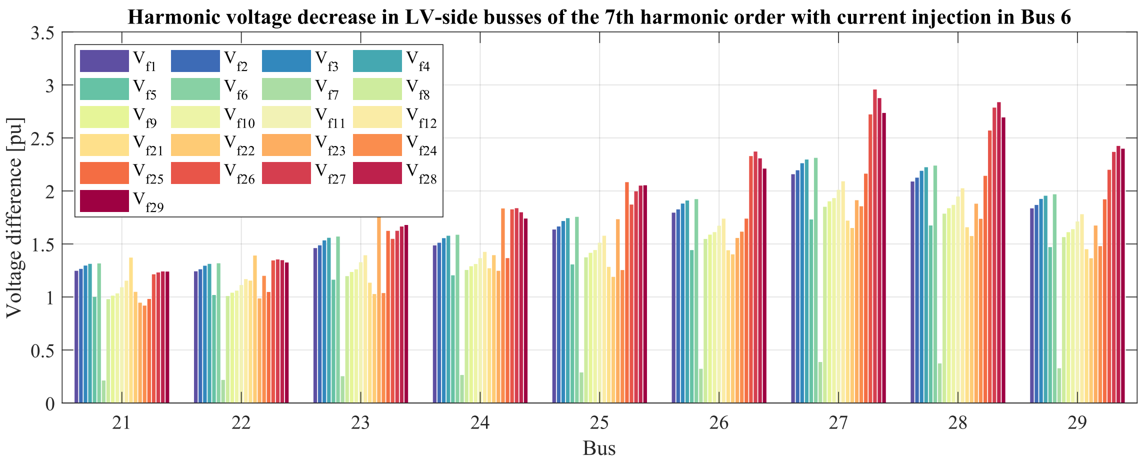

Figure D.2: Harmonic voltage decrease in the LV-side busses in the system without a filter compared to having a filter in either of the busses in the system. The harmonic current is injected in Bus 6.

The harmonic voltage decrease in the HV-side busses when a harmonic current is injected in Bus 27 are shown in Figure D.3.

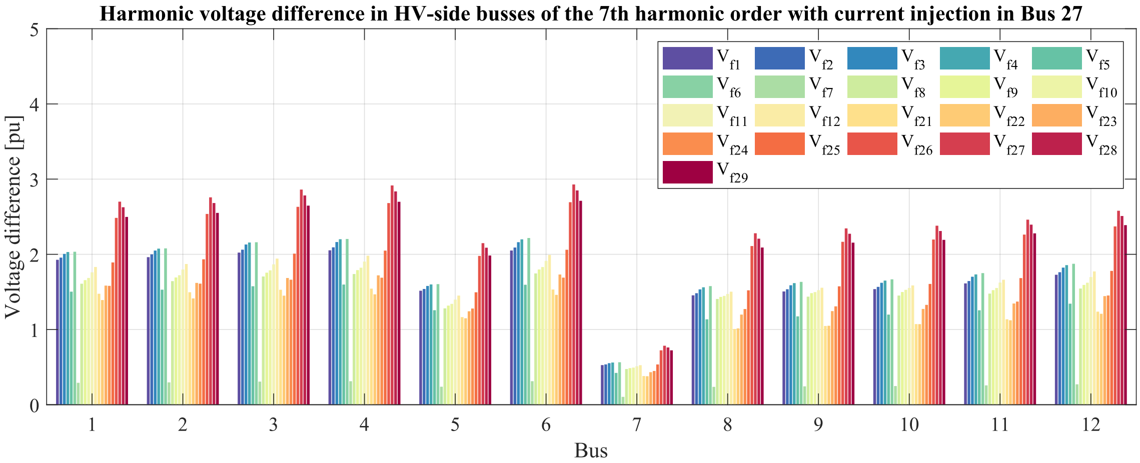

Figure D.3: Harmonic voltage decrease in the HV-side busses in the system without a filter compared to having a filter in either of the busses in the system. The harmonic current is injected in Bus 27.

The harmonic voltage decrease in the LV-side busses with harmonic current injected in Bus 27 are shown in Figure D.4.

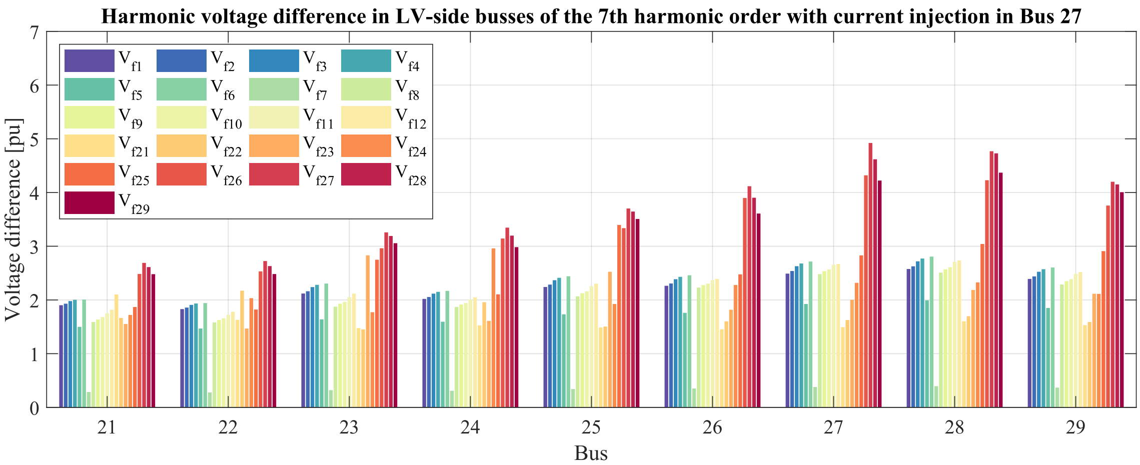

Figure D.4: Harmonic voltage decrease in the LV-side busses in the system without a filter compared to having a filter in either of the busses in the system. The harmonic current is injected in Bus 6.